Posttranscriptional Chemical Labeling of RNA *in vitro* and in Cells by Using Bioorthogonal Azide-Alkyne Cycloaddition Reactions

A thesis

Submitted in partial fulfillment of the requirements

For the degree of

Doctor of Philosophy

By

Anupam A. Sawant

Reg. No. 20093032

INDIAN INSTITUTE OF SCIENCE EDUCATION
AND RESEARCH PUNE

2016

This dissertation is dedicated to
my family and grandparents

INDIAN INSTITUTE OF SCIENCE EDUCATION AND RESEARCH (IISER), PUNE
(An Autonomous Institution, Ministry of Human Resource Development, Govt. of India)
Dr. Homi Bhabha Road, Pashan, Pune–411 008

Dr. Seergazhi. G. Srivatsan
Associate Professor, Chemistry

Dr. Seergazhi G. Srivatsan
Associate Professor, Chemistry
Indian Institute of Science Education and Research, Pune

CERTIFICATE

Certified that the work incorporated in the thesis entitled *"**Posttranscriptional Chemical Labeling of RNA in vitro and in Cells by Using Bioorthogonal Azide-Alkyne Cycloaddition Reactions**"* submitted by Mr. Anupam A. Sawant was carried out by the candidate under my supervision. The work presented here or any part of it has not been included in any other thesis submitted previously for the award of any degree or diploma from any other University or Institution.

Date: March 1, 2016
Place: Pune

Dr. Seergazhi G. Srivatsan

Tel.: +91-20-2590 8086 Fax: +91-20-2590 8186 E-mail: srivatsan@iiserpune.ac.in

DECLARATION

I declare that this written submission represents my ideas in my own words and where others ideas have included; I have adequately cited and referenced the original sources. I also declare that I have adhered to all principles of academic honesty and integrity and have not misrepresented or fabricated or falsified any idea/data/fact/source in my submission. I understand that violation of the above will be cause for disciplinary action by the institute and can also evoke penal action from the sources which have thus not been properly cited or from whom proper permission has not been taken when needed.

The work reported in this thesis is the original work done by me under the guidance of Dr. S. G. Srivatsan.

Date: March 1, 2016
Place: Pune

Mr. Anupam A. Sawant
Reg. No. 20093032

Acknowledgements

I am extremely grateful to my research advisor, Dr. S. G. Srivatsan. He is an exceptionally dedicated research mentor, and I feel privileged to have an opportunity to work under his guidance. He has shown endless support, encouragement, and patience in developing my potential as a PhD student. He holds himself and his students to the highest standards of achievement. Above all, I admire his creativity and passion for designing and performing experiments. These aspects of his character have constantly inspired me to give my best.

I am extremely grateful to Prof. K. N. Ganesh (Director, IISER Pune) for providing the excellent research facilities. Furthermore, I would like to acknowledge my doctoral research advisory committee members Dr. Partha Hazra and Dr. Shivprasad Patil for their critical assessment through RAC meetings. I am blessed to have worked with many wonderful colleagues. I thank my labmates Dr. Maroti, Arun, Harita, Pooja, Shweta, Siddharth, Pramod, Ashok, Sudeshna, Pragya, Jerrin, Dr. Cornelia, Sangemesh and Manisha for their support and sharing some of the most memorable moments during my life at IISER. I sincerely thank my talented collaborator Prof. Sanjeev Galande and his lab members, Ashwin, Rahul, Soumitra, Praveena, Rini, Mouli, Manu, Santosh kaka, Vipradas sir for giving me the opportunity to pursue my graduate work in their lab. I would like to extend my gratitude to all faculty members and research scholars of IISER Pune for their constant support and encouragement. It is my prime duty to acknowledge Council of Scientific and Industrial Research (CSIR) India for my graduate research fellowship.

Finally, I owe perhaps my deepest gratitude to my family, who supported me in every way possible and gave me the unconditional love I needed to achieve my dreams and never once doubted that this moment would come.

Anupam A. Sawant

Chapter 2 is reprint of: **Sawant, A. A**., Mukherjee, P. P., Jangid, R. K., Galande, S. and Srivatsan, S. G. Clickable UTP Analog for the Posttranscriptional Chemical Labeling and Imaging of RNA. *Org. Biomol. Chem.*, 2016 (under revision).
The dissertation author is the main author and researcher for this work.

Chapter 3A is reprint of: **Sawant, A. A**., Mukherjee, P. P., Jangid, R. K., Galande, S. and Srivatsan, S. G. Clickable UTP Analog for the Posttranscriptional Chemical Labeling and Imaging of RNA. *Org. Biomol. Chem.*, 2016 (under revision).
The dissertation author is the main author and researcher for this work.

Chapter 3B is a reprint of: **Sawant, A. A**., Tanpure, A. A., Mukherjee, P. P., Athavale, S., Kelkar, A., Galande, S. and Srivatsan, S. G. A versatile toolbox for posttranscriptional chemical labeling and Imaging of RNA. *Nucl. Acids Res.*, **44**, e16 (2016).
The dissertation author is one of the main authors and researcher for this work.

Chapter 4 is a reprint of: **Sawant, A. A**., Mukherjee, P. P., Jangid, R. K., Galande, S. and Srivatsan, S. G. Clickable UTP Analog for the Posttranscriptional Chemical Labeling and Imaging of RNA. *Org. Biomol. Chem.*, 2016 (under revision).
Sawant, A. A., Tanpure, A. A., Mukherjee, P. P., Athavale, S., Kelkar, A., Galande, S. and Srivatsan, S. G. A versatile toolbox for posttranscriptional chemical labeling and Imaging of RNA. *Nucl. Acids Res.*, **44**, e16 (2016).
The dissertation author is the main authors and researcher for this work.

Table of content

Chapter 2. Alkyne-modified UTP analogs as bioorthogonal chemical label for the *in vitro* posttranscriptional functionalization of RNA by using azide-alkyne cycloaddition reaction

Chapter 3. Clickable UTP Analogs for the Posttranscriptional Chemical Imaging of RNA

Chapter 3A. Imaging cellular RNA transcripts using an alkyne-modified UTP analog

Chapter 3B. Imaging cellular RNA transcripts using an azide-modified UTP analog

Chapter 4. Alkyne and azide-labeled RNA transcripts as potential candidates for *in vitro* selection of nucleic acid aptamers

Abbreviations

ε	molar extinction coefficient
μg	microgram
μL	microliter
μM	micro molar
AMdU	5-(azidomethyl)-2'-deoxyuridine
2-AP	2-aminopurine
4-sU	4-thiouridine
A	adenine
Abs	absorption
Ac	acetyl
ACN	acetonitrile
AMP	adenosine monophosphate
ATP	adenosine triphosphate
BARAC	biarylazacyclooctynone
BSA	bovine serum albumin
BrU	5-Bromouridine
Bz	benzoyl
C	cytosine
CD	circular dichroism
CIAP	calf intestinal alkaline phosphatase
CMP	cytidine monophosphate
Cu	copper
CuAAC	copper(I)-catalyzed alkyne-azide cycloaddition
$CuSO_4$	copper sulphate
DA	Diels-Alder
DAPI	4',6-diamidino-2-phenylindole
DCC	*N*, *N'*-dicyclohexylcarbodiimide
DEAE	diethylaminoethyl
DFHBI	3,5-difluoro-4-hydroxybenzylidene imidazolinone
DIFO	difluorinated cyclooctyne
DIBO	biarylazacyclooctynone
DIS	dimerization initiation site
DMAP	4-Dimethylaminopyridine
DMEM	Dulbecco's Modified Eagle Medium
DMSO	N, N-dimethyl sulfoxide
DMF	Dimethylformamide
DMT	dimethoxytrityl
DNA	deoxyribonucleic acid
DOTAP	*N*-[1-(2,3-Dioleoyloxy)propyl]-*N*,*N*,*N*-trimethylammonium methylsulfate
ds	double stranded
DTT	dithiothreitol
EDC	1-ethyl-3-(3-dimethylaminopropyl)carbodiimide

EDTA	ethylenediaminetetraacetic acid
em	emission
EPR	electron paramagnetic resonance
EST	expressed sequence tag
EdU	5'-ethynyl deoxyuridine
EU	5'-ethynyl uridine
FBS	fetal bovine serum
FI	fluorescence intensity
FISH	fluorescence *in situ* hybridization
FRET	förster resonance energy transfer
G	guanine
GFP	green fluorescent protein
GTP	guanosine triphosphate
HPA	hydroxylpiccolinic acid
HPLC	High performance liquid chromatography
HBS	HEPES buffered saline
IEDDA	Inverse-electron demand Diels-Alder
IR	infrared
in vitro	outside living organism
in vivo	inside living organism
5-IU	5-Iodouridine
LSM	laser scanning microscope
MALDI-TOF	matrix assisted laser desorption ionisation-time
max	maximum
MeOH	methanol
$(MeO)_3PO$	trimethyl phosphate
mg	milligram
MHz	megahertz
mM	milimolar
mW	miliwatt
ng	nanogram
nmol	nanomolar
nm	nanometer
NMP	*N*-methyl-2-pyrrolidone
NMR	nuclear magnetic resonance
mRNA	messenger RNA
mM	milimolar
MTT	3-(4, 5-dimethylthiazol-2-yl)-2,5-diphenyltetrazolium bromide
NHS	*N*-hydroxysuccinimide
NTPs	nucleoside triphosphates
ON	oligonucleotide
PAGE	polyacrylamide gel electrophoresis
PBS	phosphate buffered saline
PCR	polymerase chain reaction
Pd	palladium

$POCl_3$	phosphorus oxychloride
ppm	parts per million
rel	relative
R_f	retention factor
RNA	ribonucleic acid
rRNA	ribosomal RNA
RuAAC	ruthenium-catalyzed azide–alkyne cycloaddition
SAGE	serial analysis of gene expression
SELEX	systematic evolution of ligands by exponential enrichment
siRNA	Small interfering RNA
SPAAC	strain-promoted alkyne-azide cycloadditions
SRS	stimulated Raman scattering
ss	single stranded
T	thymine
tRNA	transfer RNA
TBDMS	*tert*-butyldimethylsilyl
TBTA	tris(benzyltriazolyl)methyl amine
TEAA	triethylammonium acetate
TEAB	triethylammonium bicarbonate
TEG	triethylene glycol
THF	tetrahydrofuron
THPTA	tris-(3-hydroxypropyl triazolylmethyl)amine
TLC	thin layer chromatography
T_m	thermal melting
TOM	triisopropylsilyloxymethy
U	uridine
Tris	tris (hydroxymethyl) amino methane
UMP	uridine monophosphate
UTP	uridine triphosphate
UV	ultraviolet
VdU	5-vinyl-2'-deoxyuridine
WC	Watson-Crick

Synopsis

Posttranscriptional Chemical Labeling of RNA *In Vitro* and in Cells by Using Bioorthogonal Azide-Alkyne Cycloaddition Reactions

Background and Aim: Ribonucleic acid (RNA) performs several essential cellular functions, which include storage and transfer genetic information, catalysis, and regulation of gene expression.[1,2] Although chemically less diverse than protein, RNA expands its functional repertoire by adopting diverse secondary and tertiary structures, thereby providing scaffolds for specific recognition of proteins, nucleic acids and small molecule metabolites.[3-5] RNA molecules, which play important roles in disease states (e.g., cancer, HIV, bacterial infection) are being rigorously evaluated as targets for the discovery of small molecules of therapeutic potential.[6] Consequently, several biophysical tools have been and are being developed in order to understand the fundamentals of RNA structure and function both *in vitro* and in cells.

The majority of biophysical investigations of RNA rely on techniques, namely, fluorescence, electrophoresis, nuclear magnetic resonance (NMR), X-ray crystallography and microscopy.[7] Needless to say; these techniques utilize appropriately labeled RNA molecules, which are traditionally synthesized by solid-phase oligonucleotide synthesis and enzymatic methods. While solid-phase oligonucleotide synthesis protocol is the method of choice for generating site-specifically labeled RNA oligonucleotides for a variety of applications, enzymatic synthesis of long and modified RNA molecules is also possible by transcription reaction. However, in several instance the modified substrates are not compatible under the stringent solid-phase oligonucleotide synthesis conditions and are not good substrates for enzymatic incorporation.[8] Therefore, there is a significant demand for the development of new strategies to modify nucleic acids *in vitro* and in cells with functionalities that cannot be straight forwardly introduced by these two methods.

The aim of this doctoral thesis is to develop robust and modular chemical functionalization methodology that would allow the labeling of RNA *in vitro* and in cells with biophysical probes for variety applications. Here, we have utilized the versatility of bioorthogonal reactions namely azide-alkyne cycloaddition reaction, which has been widely

utilized in the study of glycan, protein and DNA, to develop a simple and practical posttranscriptional chemical functionalization method to label RNA *in vitro* and in cells.[9-11] In simple steps we have synthesized alkyne-modified UTP analogs, which enabled the effective incorporation of alkyne functionalities into RNA (i) *in vitro* by using T7 RNA polymerase and (ii) in cells by using endogenous RNA polymerases. The alkyne-modified transcripts are conveniently labeled posttranscriptionally by copper (I)-catalyzed azide-alkyne cycloaddition (CuAAC) reactions with a variety of biophysical probes. Further, we have incorporated azide functionality into cellular RNA transcripts by using one of the azide-modified UTP analogs, which was earlier developed in our group for *in vitro* posttranscriptional chemical modification of RNA. The specific labeling of cellular RNA with azide and alkyne groups followed by click reactions further enabled the visualization of newly transcribing RNA in fixed and live cells by fluorescence microscopy. It is expected that this new methodology and important observations reported in this thesis will provide new opportunities to advance our fundamental understanding of RNA structure, proliferation and function.

The thesis is organized as follows:

Chapter 1: Bioorthogonal chemistry as a tool to functionalize nucleic acids

In this chapter a concise overview of the methods that have been conventionally used to label and study nucleic acids *in vitro* and in cells is provided. Further, we provide a detailed discussion on the development and use of bioorthogonal chemical reactions as tools to label nucleic acids. The limitations of presently available RNA labeling techniques and the inspiration for the present research work are also detailed in this chapter.

Chapter 2: Alkyne-modified UTP analogs as a bioorthogonal chemical label for the *in vitro* posttranscriptional functionalization of RNA by using azide-alkyne cycloaddition reaction

Postsynthetic modification of biomolecules such as protein, glycan and DNA by click reactions has been well explored. However, postsynthetic functionalization of RNA is not straight forward as methods developed for DNA do not always apply for RNA due to its inherent instability.[12] Incorporation of structurally non-invasive and reactive alkyne functionality into RNA is an important prerequisite for postsynthetic labeling of RNA by using azide-alkyne cycloaddition reaction. In addition, the alkyne intrinsically possesses unique stretching vibrations (1800 to

2800 cm^{-1}) which reside in Raman silent region of cell. Therefore, incorporation of alkyne group into RNA will provide additional spectroscopic handle to study RNA structure *in vitro* as well as in cells.[13] Although, solid-phase oligonucleotide synthesis can be used to label RNA with alkyne functionality, we sought to develop a milder method, namely transcription reaction, to incorporate alkyne functionality into RNA oligonucleotides. Such an endeavour would essentially equip RNA with alkyne functionality, which would allow further functionalization of RNA with biophysical probes by azide-alkyne cycloaddition reaction as well as analysis by Raman spectroscopy.

In this regard, two 5-modified alkyne uridine analogs, 5-ethynyl uridine (EU) and 5-(octadiynyl) uridine (ODU), and their corresponding triphosphate substrates necessary for transcription reaction were synthesized (Figure 1A).[14,15] The efficiency of T7 RNA polymerase to incorporate EUTP and ODUTP into RNA transcripts was investigated by performing *in vitro* transcription reactions in the presence of various DNA templates (Figure 1B).[16] T7 RNA polymerase was found to accept and efficiently incorporate both UTP analogs into RNA near the promoter region and also at multiple sites (Figure 2). Importantly, when reactions were performed in the presence of equimolar concentration of natural and modified UTPs, the enzyme was found to incorporate both natural and modified UTPs reasonably well. Such a property could be exploited in metabolic labeling of cellular RNA with alkyne functionality by endogenous RNA polymerases. Collectively, these experiments demonstrate the utility of *in vitro* transcription reactions to endow non-biogenic alkyne functionality into RNA.

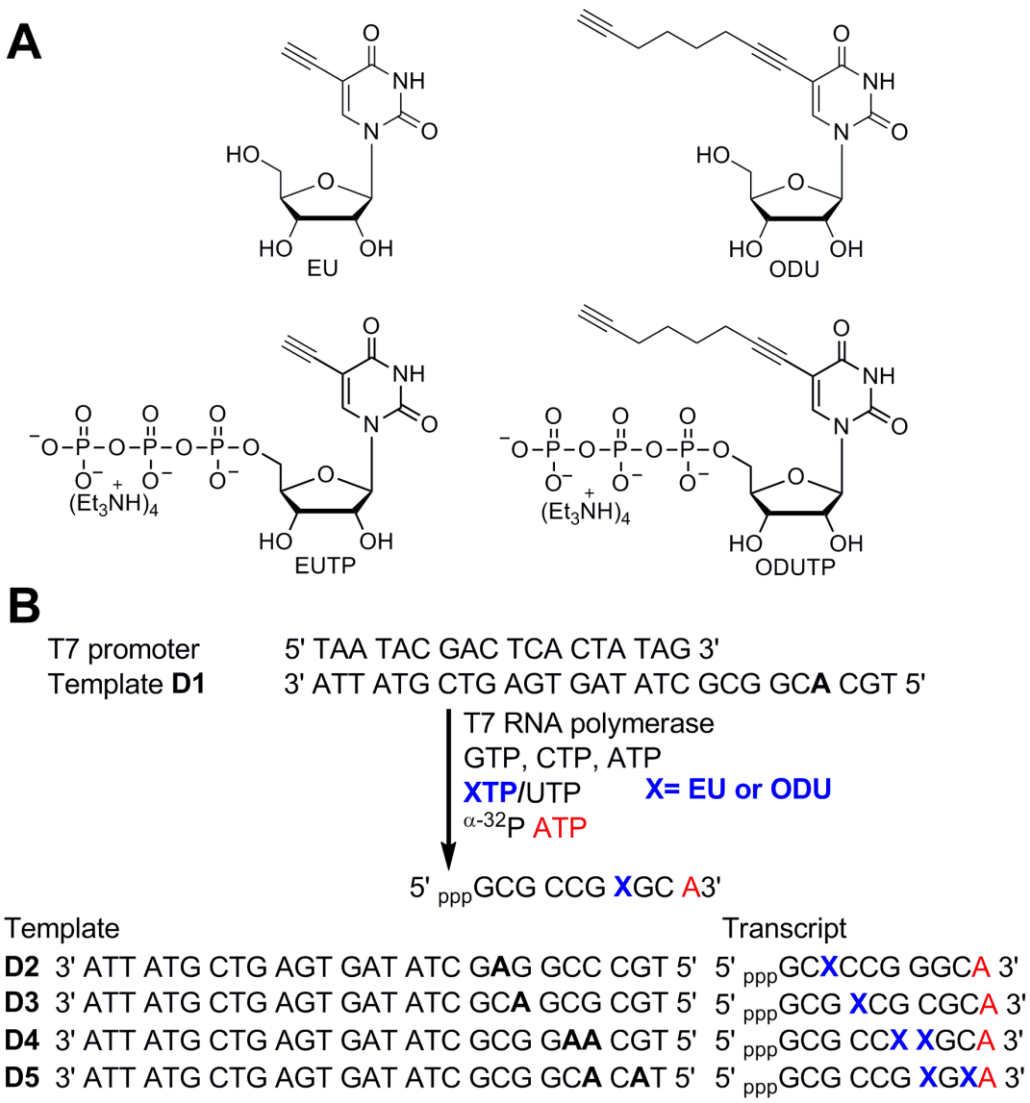

Figure 1. (**A**) Chemical structure of alkyne-modified uridine ribonucleoside analogs EU and ODU. (**B**) Enzymatic incorporation of alkyne-modified UTPs analogs EUTP and OUDTP into RNA using *in vitro* transcription reactions.

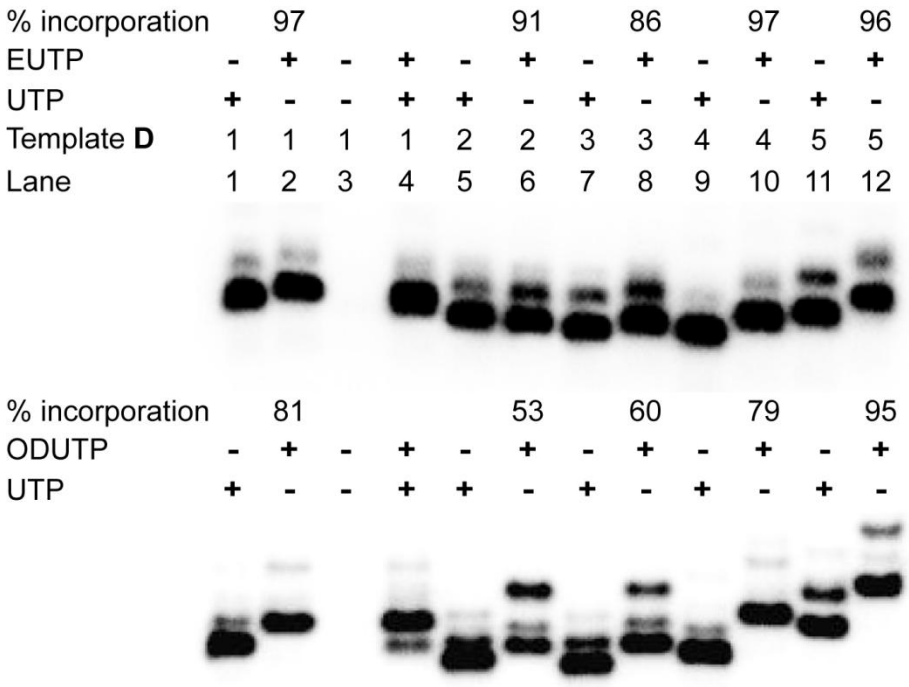

Figure 2. Enzymatic incorporation of EUTP and ODUTP into RNA ONs by T7 RNA polymerase. Transcription reactions were performed with templates **D1**−**D5** in the presence of UTP and or EUTP and ODUTP. % formation of modified full-length transcript is given with respect to the amount of full-length transcript formed in the presence of natural NTPs.

After successfully establishing a milder method to incorporate alkyne functionality into RNA by transcription reaction, we sought to investigate the suitability of alkyne-modified RNA transcripts for posttranscriptional modification by azide-alkyne click reaction with a variety of biophysical probes. For this purpose, azide-modified substrates ranging from fluorescent probes to affinity tags to amino acid and sugar were either synthesized. RNA ONs containing EU and ODU were subjected to click reaction in the presence of a water-soluble Cu (I) stabilizing ligand, tris-(3-hydroxypropyltriazolylmethyl) amine (THPTA), $CuSO_4$ and sodium ascorbate at 37 °C (Figure 3).[17] Click reactions with various azide substrates were completed in 30 min and the degradation under this reaction conditions was found to be very minimum. Typically, a 12 nmole reaction scale resulted in the isolation of 3-8 nmoles of the clicked product after gel electrophoretic purification. Taken together, our results demonstrate that this posttranscriptional chemical labeling methodology would provide an alternate route to access labeled RNA for biophysical analysis.

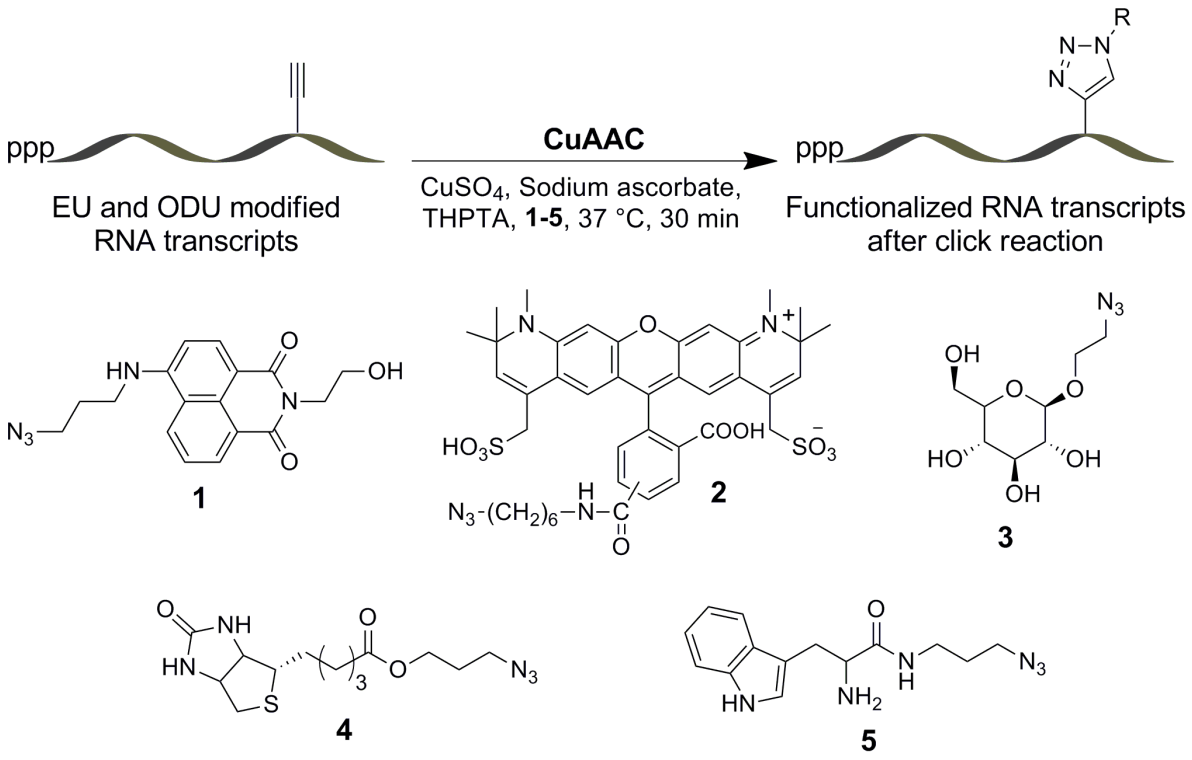

Figure 3. Postsynthetic modification of alkyne-modified RNA ONs containing EU and ODU with a series of azide substrates **1**−**5** using CuAAC reactions.

Chapter 3A: Imaging cellular RNA transcription using an alkyne-modified UTP analog

Cellular RNA levels at any given time depend strongly on highly regulated processes of RNA production, processing and degradation. The metabolic labeling of modified nucleoside analogs such as radioisotope labeled [^{3}H]-uridine, 5-bromouridine, and very recently 4-thiouridine has enabled the detection and enrichment of nascent transcripts in order to monitor RNA dynamics in mammalian cells. Furthermore, UTP analogs of these modified ribonucleosides were also used in the measurement of the frequency of transcription initiation and capture active transcription *in vitro*.[18-20] However, use of radioactivity, antibody staining and competing issue with cellular thiols make these modified analogs less applicable and cumbersome for cellular RNA imaging.

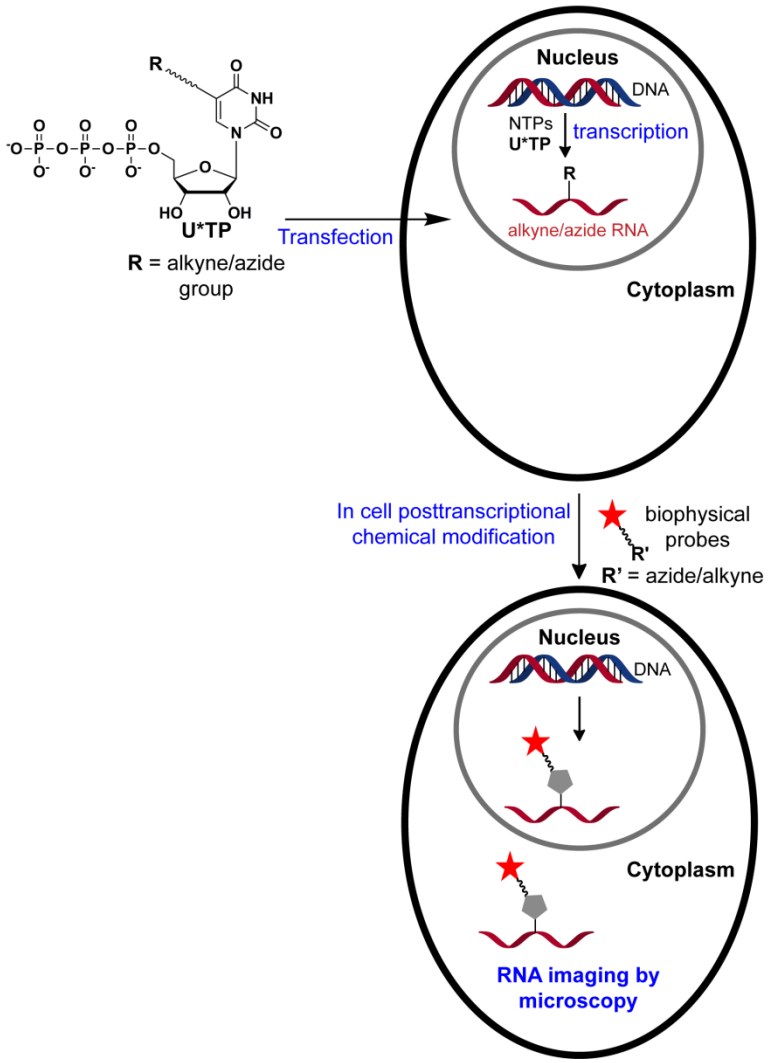

Figure 4: Schematic illustrating the posttranscriptional chemical labeling of RNA transcripts *in vitro* and in cells by using alkyne- and azide-modified UTP analogs.

The metabolic labeling of EU has been established as the first ribonucleoside analog to be compatible with fluorescence imaging of nascent RNA transcripts in cells, tissues and model organisms by click reaction with azide-functionalized fluorescent dyes (Figure 4).[14] Further, to verify the candidature of the novel alkyne-modified ribonucleoside analog ODU to labels cellular RNA, we analyzed the metabolic incorporation of ODU into RNA transcripts in mammalian cells. However, the metabolic labeling of cellular RNA with ODU by ribonucleoside salvage pathway did not work. This failure of cellular RNA labeling by ODU is presumably due to hydrophobic nature of the substrate, which probably does not allow ODU to penetrate cell or allow phosphorylation during the salvage pathway.

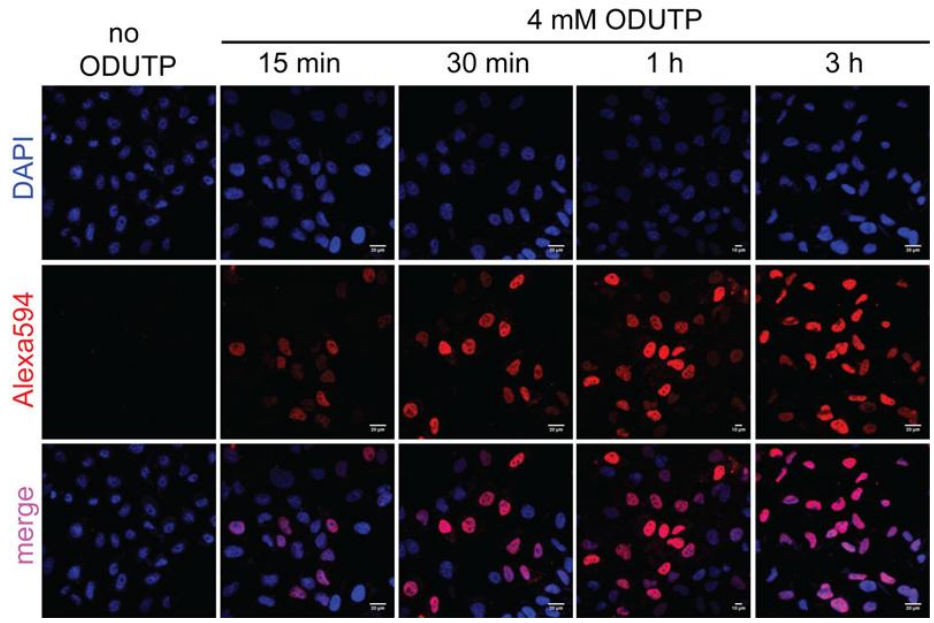

Figure 5. Metabolic incorporation of ODUTP into RNA transcripts as a function of transfection time. HeLa cells were incubated with ODUTP (4 mM) in the presence of a transfecting agent for 15 min to 3 h. The cells were fixed, permeabilized and the ODU-labeling was detected by performing CuAAC reaction with Alexa594-azide.

In order to permit metabolic labeling of new alkyne-modified uridine analogue more practical, HeLa cells were directly transfected with ODUTP.[21] Rewardingly, cells transfected with ODUTP were able to incorporate alkyne modification in newly synthesized RNA transcripts, which were detected by fluorescence microscopy after performing click reaction with Alexa594-azide **2** (Figure 5). We observed a dose dependant increase in nuclear staining indicating incorporation of ODUTP into nascent RNA transcripts. The specific incorporation of alkyne functionality into newly transcribing RNA was confirmed by performing control experiments with hydroxyurea (an inhibitor of replication process), actinomycin D (RNA polymerases inhibitor) and RNase. All these experiments unambiguously confirmed the specific incorporation of alkyne functionality into RNA transcripts by endogenous RNA polymerases. The biosynthetic incorporation of ODUTP into RNA followed by click reaction using azide probes is a valuable method for the detection of nascent RNA transcripts and RNA turnover in cells.

Chapter 3B: Imaging cellular RNA transcription using an azide-modified UTP analog

Azide group, which is a common reactive species in copper (I)-catalyzed azide-alkyne cycloaddition (CuAAC), copper-free strain-promoted azide-alkyne cycloaddition (SPAAC) and azide-phosphine Staudinger ligation reactions cannot be easily incorporated into RNA oligonucleotides by solid-phase oligonucleotide synthesis protocols. This is because, the azide functionality undergoes **a** Staudinger-type reaction with phosphoramidite substrates used in the solid-phase reactions.[22] Notably, while methods are available to metabolically incorporate the versatile azide functional group into glycan, protein and DNA, incorporation of azide groups into cellular RNA has remained elusive until now.[23] Therefore, incorporation of azide into cellular RNA would allow the chemical labeling of RNA in a modular fashion by click and Staudinger reactions. Towards this endeavour, three azide-modified UTP analogs (AMUTP, PAUTP and ATUTP) were tested, which were earlier prepared in our group for incorporation into RNA by *in vitro* transcription reaction (Figure 6). Rewardingly, HeLa cells transfected with 5-azidomethyl UTP (AMUTP) resulted in AMU-labeled RNA transcripts, which were detected by click reactions using fluorescent alkyne probes (Figure 7). Control experiments performed with actinomycin D, hydroxyurea and RNase A also confirmed the specific incorporation of AMUTP into cellular RNA transcripts by endogenous RNA polymerases. Furthermore, specific labeling of RNA with azide group uniquely enabled the (i) visualization of newly transcribing RNA in live cells and (ii) simultaneous imaging of replicating DNA and transcribing RNA in same cells (Figure 8). Our results demonstrate that this modular and practical chemical labeling methodology will provide a new platform to study RNA *in vitro* and in cells (e.g., RNA synthesis, localization and degradation).

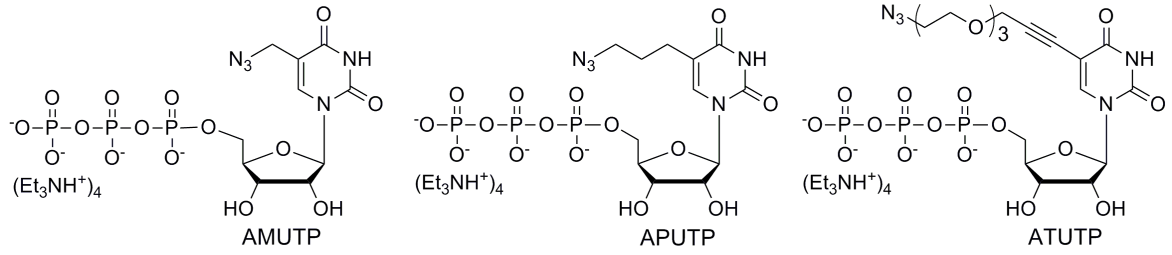

Figure 6. Azide-modified UTPs (AMUTP, PAUTP, TAUTP) for cellar labeling of RNA transcritps, which are detected by click reactions using variety of alkyne probes.

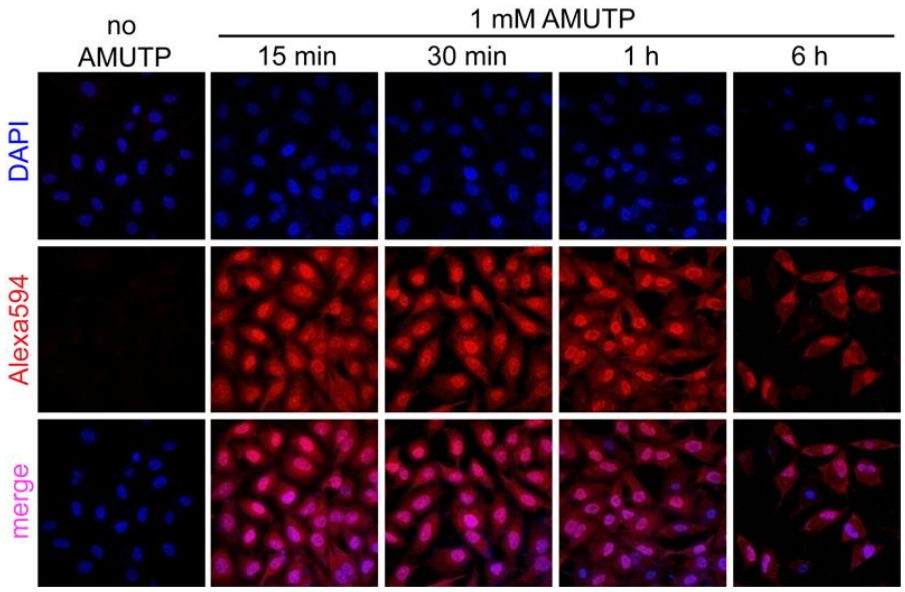

Figure 7. Imaging of cellular RNA transcription using AMUTP. Cultured HeLa cells were transfected with AMUTP (50 μM upto 1 mM) for 1 h using a transfecting agent. The cells were fixed, permeabilized and the AMU-labeling was detected by performing CuAAC reaction with Alexa594-alkyne.

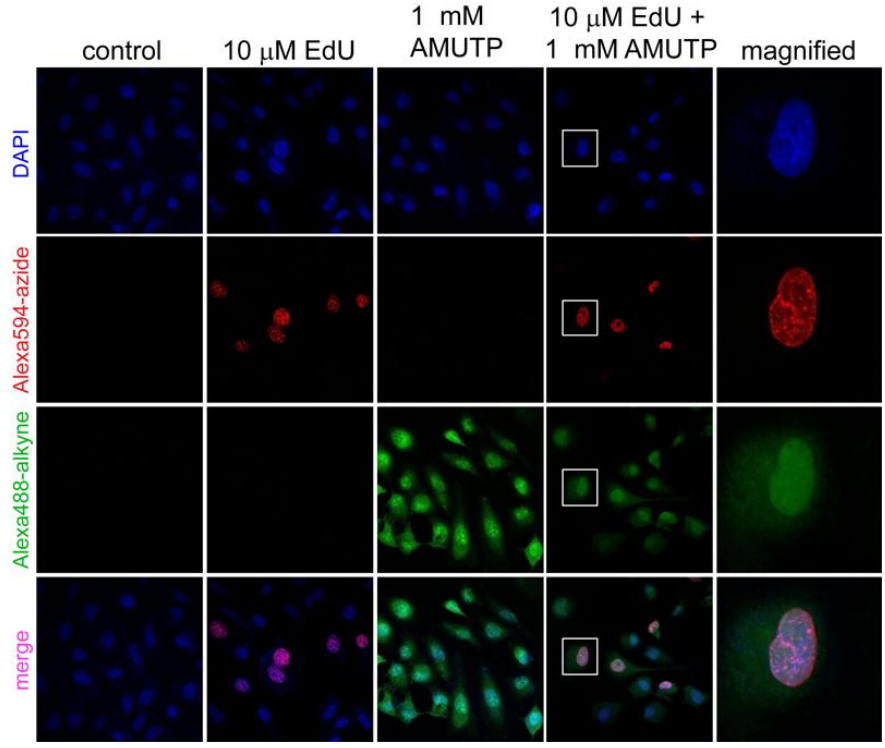

Figure 8. Simultaneous visualization of DNA and RNA synthesis in cells by CuAAC reactions. In separate experiments, HeLa cells were incubated with EdU/AMUTP and a combination of EdU and AMUTP. While EdU labeling in DNA was detected by Click reaction with Alexa594-azide (red), AMU-labeling in RNA was detected by a reaction with Alexa488-alkyne (green). Bottom panel is a merge of all three channels (blue, red and green). Boxed cell has been magnified.

Chapter 4: Alkyne and azide-labeled RNA transcripts as potential candidates for *in vitro* selection of nucleic acid aptamers

In vitro selection using oligonucleotide libraries containing modified nucleosides has resulted in the isolation of robust aptamers with improved stability and binding properties.[24] In order for a modified nucleotide to be suitable for *in vitro* selection protocols, it is important that it meets the following requirements: (i) modified nucleotide triphosphate must be compatible to incorporation into RNA by a RNA polymerase with high fidelity and (ii) modified transcripts must be compatible to reverse transcription to produce cDNA with high fidelity prior to PCR amplification.[25] For this purpose, a biologically relevant RNA (nearly 1 kb) was transcribed by *in vitro* transcription reactions using PCR amplified DNA template in presence of UTP or modified UTPs (Figure 9). Subsequently, these transcribed RNA were subjected to reverse transcription reactions. The resultant cDNA was further amplified by using PCR reaction conditions. The sequencing of the dsDNA obtained from modified RNA containing alkyne and azide functionalities revealed that reverse transcription and amplification proceed with high fidelity. The compatibility of these modified nucleotides to transcription, reverse transcription followed by PCR amplification and again transcription**,** highlights the potential use of these alkyne and azide-modified UTP analogs in expanding the structural and functional diversity of RNA library used in the *in vitro* selection of RNA.

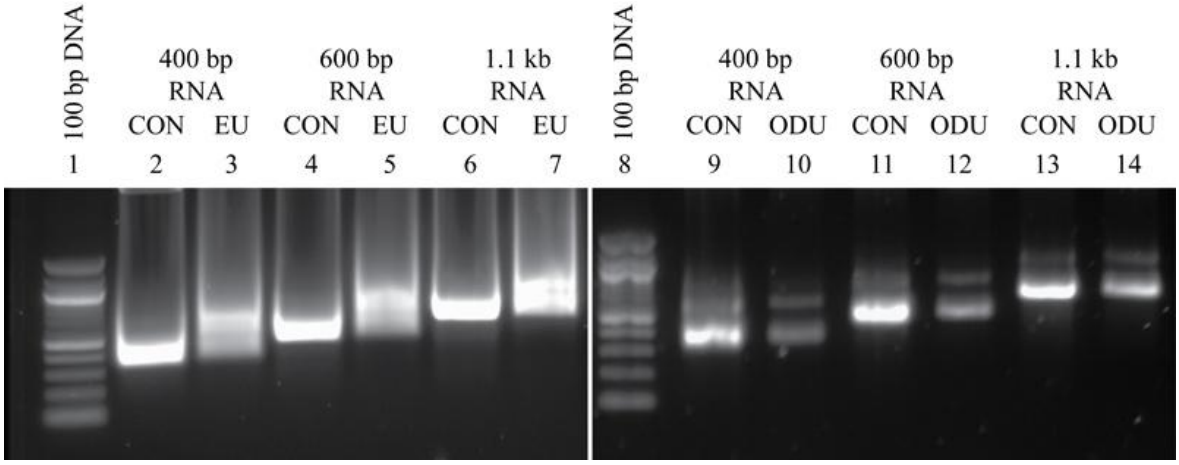

Figure 9. Representative agarose gel for *in vitro* transcription reactions with UTP and modified UTP (EUTP and ODUTP) with linearized plasmid DNA of varying length.

References:

1. Gilbert, W. The RNA world. *Nature* **319**, 618 (1986).
2. Eddy, S. Non-coding RNA genes and the modern RNA world. *Nature Reviews Genetics* **2**, 919–929 (2001).
3. He, L. and Hannon, G. J. Micro RNAs: Small RNAs with a big role in gene regulation. *Nature Reviews Genetics* **5**, 522–531 (2004).
4. Jabri, E. Non-coding RNA: Small, but in control. *Nature Reviews Molecular Cell Biology* **6**, 361 (2005).
5. Serganov, A. and Patel, D. J. Ribozymes, riboswitches and beyond: Regulation of gene expression without proteins. *Nature Reviews Genetics* **8**, 776–790 (2007).
6. Cooper, T. A., Wan, L. and Dreyfuss, G. RNA and Disease. *Cell* **136**, 777–793 (2009).
7. Wachowius, F. and Hçbartner, C. Chemical RNA modifications for studies of RNA structure and dynamics. *ChemBioChem*, **11**, 469–480 (2010).
8. Beaucage, S. L. and Reese, C. B. Recent advances in the chemical synthesis of RNA. *Curr. Protoc. Nucleic Acid Chem.*, Unit 2.16 (2009).
9. Kolb, H. C., Finn, M. G. and Sharpless, K. B. Click chemistry: Diverse chemical function from a few good reactions. *Angew. Chem. Int. Ed.*, **40**, 2004–2021 (2001).
10. Prescher, J. A. and Bertozzi, C. R. Chemistry in living systems. *Nature Chemical Biology*, **1**, 13–21(2005).
11. Grammel, M. and Hang, H.C. Chemical reporters for biological discovery. *Nature Chemical Biology*, **9**, 475–484 (2013).
12. El-Sagheer, A. H. and Brown, T. Click chemistry with DNA. *Chem. Soc. Rev.*, **39**, 1388–1405 (2010).
13. Wei, L. Live-cell imaging of alkyne tagged small biomolecules by stimulated Raman scattering. Nature Methods, **11**, 410–414 (2014).
14. Jao, C.Y. and Salic, A. Exploring RNA transcription and turnover in vivo by using click chemistry. *PNAS*, **105**, 15779-15784 (2008).
15. Seela, F., Sirivolu, V. R. and Padmaja, C. Modification of DNA with octadiynyl side chains: Synthesis, base pairing, and formation of fluorescent coumarin dye conjugates of four nucleobases by the alkyne-azide "Click" reaction. *Bioconjugate Chem.*, **19**, 211–224 (2008).
16. Rao, H., Tanpure, A. A., Sawant, A. A. and Srivatsan, S. G. Enzymatic incorporation of an azide-modified UTP analog into oligoribonucleotides for post-transcriptional chemical functionalization. *Nature Protocols*, **7**, 1097–1112 (2012).
17. Rao, H., Sawant, A. A., Tanpure, A. A. and Srivatsan, S. G. Posttranscriptional chemical functionalization of azide-modified oligoribonucleotides by bioorthogonal click and Staudinger reactions. *Chem. Commun.*, **48**, 498–500 (2012).
18. Uddin, M. *et al.* Radio autographic visualization of differences in the pattern of [3H] uridine and [3H] orotic acid incorporation into the RNA of migrating columnar cells in the rat small intestine. *J Cell Biol.*, **98**, 1619–1629 (1984).
19. Cmarko, D. *et al.* Ultrastructural analysis of transcription and splicing in the cell nucleus after bromo-UTP microinjection. *Mol Biol Cell*, **10**, 211–223 (1999).
20. Rabani, M. *et al*. Metabolic labeling of RNA uncovers principles of RNA production and degradation dynamics in mammalian cells. *Nature Biotechnology* **29**, 436–442 (2011).

21. Haukenes, G. *et al.* Labeling of RNA transcripts of eukaryotic cells in culture with BrUTP using a liposome transfection reagent (DOTAP). *BioTechniques*, **22**, 308–312 (1997).
22. Wada, T. *et al.* Synthesis and properties of 2-azidodeoxyadenosine and its incorporation into oligodeoxynucleotides. *Tetrahedron Lett*. **42**, 9215–9219 (2001).
23. Neef, A. B. and Luedtke, N. W. An azide-modified nucleoside for metabolic labeling of DNA. *ChemBioChem*, **15**, 789–793 (2014).
24. Kuwahara, M. and Sugimoto, N. Molecular evolution of functional nucleic acids with chemical modifications. *Molecules*, **15**, 5423–5444 (2010).
25. Kato, Y. *et.al.* New NTP analogs: The synthesis of 4-thioUTP and 4-thioCTP and their utility for SELEX. *Nucleic Acids Research*, **33**, 2942–2951 (2005).

List of Publications

1. Srivatsan, S. G. and **Sawant, A. A.** Fluorescent ribonucleoside analogues as probes for investigating RNA structure and function. *Pure Appl. Chem.*, **1**, 213–232 (2011).
2. Rao, H., **Sawant**, **A. A.,** Tanpure, A. A. and Srivatsan, S. G. Posttranscriptional chemical functionalization of azide-modified oligoribonucleotides by bioorthogonal click and Staudinger reactions *Chem. Commun.*, **48**, 498–500 (2012).
3. Rao, H., Tanpure, A. A. **Sawant**, **A. A.** and Srivatsan, S. G. Enzymatic incorporation of an azide-modified UTP analog into oligoribonucleotides for post-transcriptional chemical functionalization. *Nat. Protocols*, **7**, 1097–1112 (2012).
4. **Sawant**, **A. A.,** Tanpure, A. A., Mukherjee, P. P., Athavale, S., Kelkar, A., Galande, S. and Srivatsan, S. G. A versatile toolbox for posttranscriptional chemical labeling and imaging of RNA. *Nucl. Acids Res.*, **44**, e16 (2016).
5. **Sawant**, **A. A.,** Mukherjee, P. P., Jangid, R. K., Galande, S. and Srivatsan, S. G. Clickable UTP Analog for the Posttranscriptional Chemical Labeling and Imaging of RNA. *Org. Biomol. Chem*., 2016 (manuscript under revision).

Patent

1. Tanpure, A. A., **Sawant, A. A**., Galande, S. and Srivatsan, S. G. Novel azide-modified UTP analogs for posttranscriptional chemical functionalization and imaging of RNA. *Indian Patent Application No.1555/MUM/2015* (2015).

Chapter 1

Bioorthogonal chemistry as a tool to functionalize nucleic acids

1.1 Introduction

1.1.1 Significance of chemical functionalization of RNA

In contemporary biology RNA displays a vast variety of cellular functions wherein it stores genetic information (retrovirus),[1] regulates gene expression in bacteria (riboswitches),[2] silences gene in eukaryotes (RNA interference),[3] and catalyze reactions (ribozymes)[4] (Figure 1). RNA essentially elucidates these functions by interacting with nucleic acids, proteins and small molecule metabolites. The functional diversity exhibited by RNA has been attributed to its propensity to self-assemble into complex secondary and tertiary structures upon binding to its cognate target (Figure 2).[5,6] Consequently, several biophysical methods have been developed to advance the basic understanding of the conformational changes that happen during RNA–protein, RNA–nucleic acid, and RNA–small molecule interactions. Many such biophysical tools have been utilized in devising practical assays to study the structure and function of RNA *in vitro* and in cells. The majority of biophysical techniques are based on fluorescence, nuclear magnetic resonance (NMR), electron paramagnetic resonance (EPR), X-ray crystallography and microscopy. In particular, fluorescence-based methods provide effective systems for examining RNA structure and dynamics, often in real time and with great sensitivity. These biophysical techniques require fluorescent probes, NMR and EPR active label such as ^{13}C, ^{15}N, ^{2}H, ^{19}F and nitroxide radicals, heavy atoms such as selenium, and halides for X-ray analysis.[7-10] Unfortunately, no intrinsic reporters are present in RNA which can be utilized for practical applications using biophysical techniques mentioned above. Therefore, chemical modification of RNA has become indispensible in the study of its structure and function and in the development of nucleic acid-based diagnostic and therapeutic tools.[11,12]

There are two main strategies available to generate labelled RNA. Solid-phase RNA synthesis is a popular route to generate short modified RNA.[13,14] In this strategy incorporation of label i.e. modified phosphoramidite into RNA oligonucleotide (ON) can be accomplished within few synthetic cycles and purification steps. Chemical incompatibility of certain modified phosphoramidite substrates under synthesis conditions, and possible low yields during stepwise incorporation of modified substrate are the major bottlenecks in the chemical synthesis of labeled RNA. In addition, high density functionalization of long RNA strands for possible applications in hybridization experiments is a challenging task as coupling yields progressively decrease with increasing RNA chain length. Alternatively, *in vitro* transcription

reaction using RNA polymerases can be employed to synthesize long and high density functionalized RNA transcripts.[15] However, there are two major drawbacks encountered in this strategy. Firstly, the acceptance of the unnatural ribonucleoside triphosphate analogs carrying the desired functional labels is often restricted and unpredictable. Secondly, there is no control over the site of incorporation of the label into RNA ONs. Latter problem can be somewhat addressed by incorporating modifications into RNA by using unnatural base-pairing scheme.[16-18]

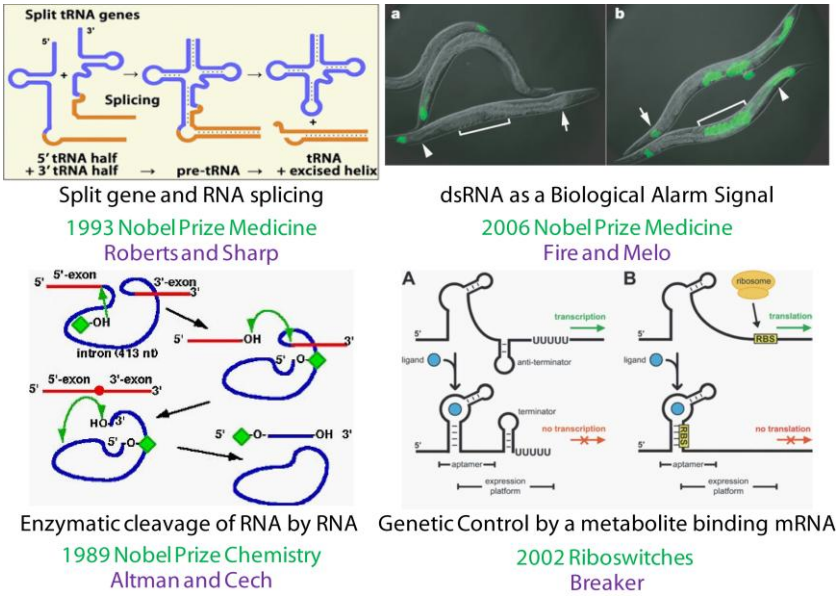

Figure 1. RNA controls biology by performing vast variety of functions in cells.

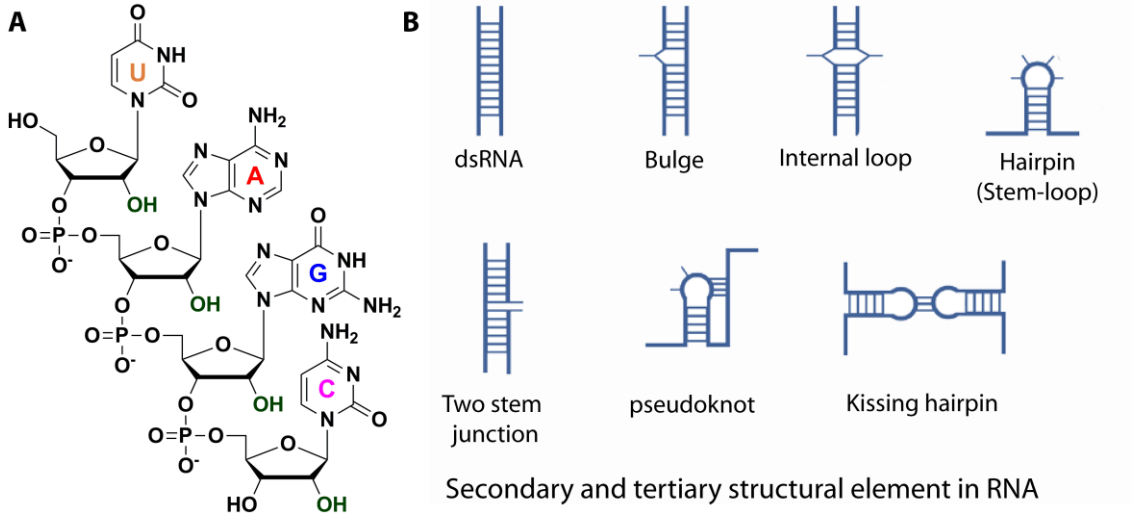

Figure 2. (**A**) Molecular composition of RNA molecule. (**B**) Representative examples of secondary and tertiary structures adopted by RNA.

In recent years, postsynthetic modification approaches has been developed to overcome these limitations. This strategy allows flexible conjugation of different functional

molecules to the pre-modified RNA ON by employing bioorthogonal chemical reactions.[19-22] In the following sections a concise overview of methods that have been conventionally used to label and study nucleic acids *in vitro* and in cells is provided. Further, a detailed discussion on the development and use of bioorthogonal chemical reactions as tools to label nucleic acids is also provided. Finally, current challenges in labeling RNA in cells and the motivation for the study reported in this thesis is elaborated.

1.1.2 Methods to study RNA *in vitro*

Typically, *in vitro* based biophysical RNA labeling techniques such as fluorescence, electrophoresis, circular dichroism (CD), calorimetry, nuclear magnetic resonance (NMR), electron paramagnetic resonance (EPR), X-ray crystallography rely on site-specifically modified RNA molecules.[12] All techniques have their own pros and cons regarding the utility in studying RNA structure and function. Notably fluorescence spectroscopy has an edge over most of the techniques due to its accessibility and versatility in providing information in real time with great sensitivity.[23-27] Nucleic acids are practically non-emissive, and hence, incorporation of extrinsic fluorophores is a prerequisite for fluorescence based assays of RNA.[28,29] Applications such as fluorescence resonance energy transfer (FRET) involve 5' and 3' end labeling of RNA molecule with donor (e.g., Cy3) and acceptor (e.g., Cy5) like fluorophores. FRET systems have been widely utilized in understanding complex folding processes in RNA motif and in elucidation of various RNA-RNA and RNA-protein interactions.[30-36] Although, highly useful in monitoring the global conformational changes, such labels are bulky and cannot be satisfactorily used to study conformational changes that occur at the nucleotide level as they would perturb the native RNA structure. To circumvent this problem minimally invasive base modified fluorescent nucleoside analogs have been employed to study RNA structure, function and dynamics.[37] Microenvironment sensitive fluorescent nucleobase analogs such as 2-aminopurine (2-AP, **1)**,[38-47] 5-furan-uridine (**2)**,[48] fused thieno[3,4-d]pyrimidino analog (**3)**,[49] 5-benzofuran uridine (**4**)[50] have been used in the investigation of small molecules and proteins binding to therapeutically relevant RNA motifs and in the monitoring of RNA conformational changes at the nucleotide level (Figure 3A).

Similarly, incorporation of modified nucleosides doped with stable isotopes such as ^{13}C, ^{15}N, ^{2}H, ^{19}F and chemically inert paramagnetic nitroxide radicals into RNA has provided tools to study small RNA by NMR and EPR spectroscopy, respectively (Figure 3B and 3C). These site-specifically modified RNA molecules harbouring NMR or paramagnetic spin

labels afford the study of RNA-ligand, RNA-metal ion binding dynamics of small RNA motifs in solution state.[51-59] In addition, X-ray crystallography offers a distinct advantage to study 3 dimensional (3D) structures of RNA motifs in solid state. Chemically modified RNA molecules containing appropriate nucleoside derivatives composed of halogen or selenium atom enable 3D structure determination of RNA (Figure 3D) Notably, crystals derived from covalently modified RNA with selenium atom serve as better alternative compared to halogen-containing nucleosides.[60-64] This is due to superior properties of selenium atom, which is light insensitive unlike halogens (bromine and iodine) and can be aptly utilized in single-wavelength and multi-wavelength anomalous dispersion phasing experiments to determine 3D structure of nucleic acids. Understanding of active site in functional RNA motif such as Diels–Alder ribozyme and HIV-1 genomic RNA dimerization initiation site (DIS) constructs has been greatly assisted by applying X-ray crystallographic techniques.[65-67]

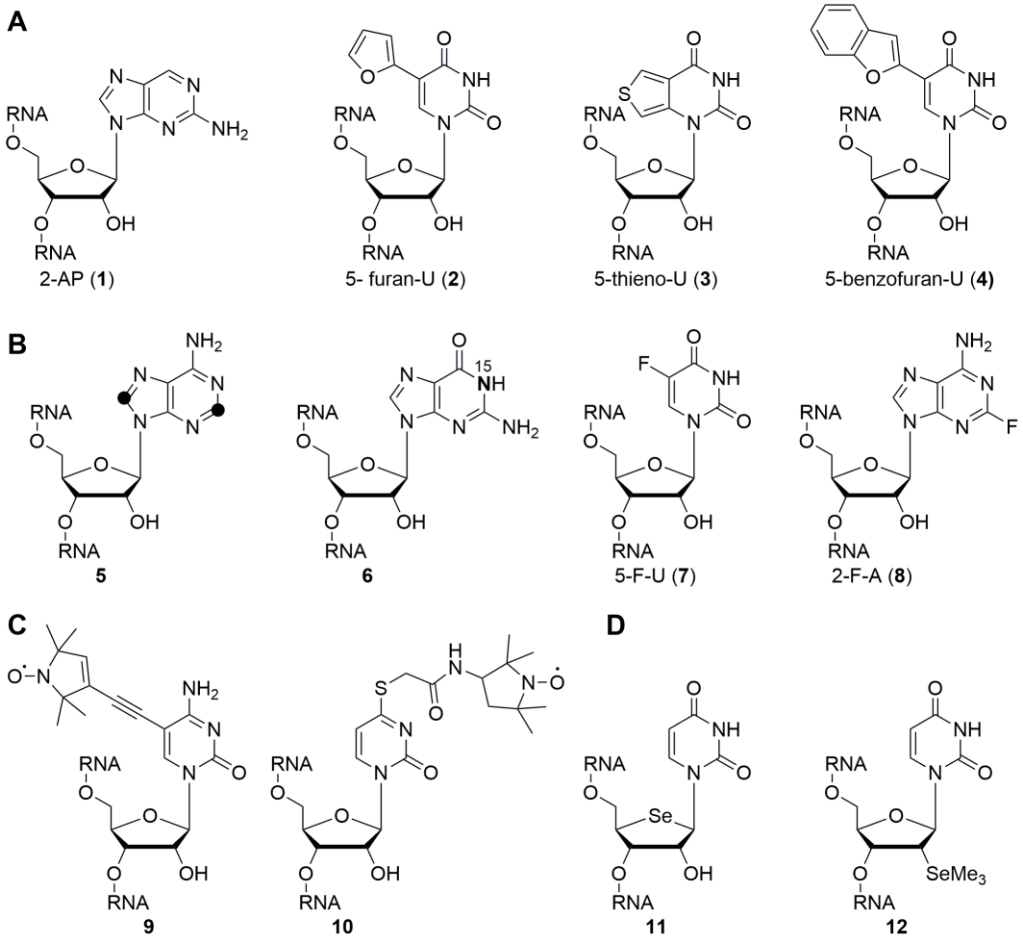

Figure 3. Representative examples of base-modified nucleoside analogs used in biophysical analysis of RNA by (**A**) fluorescence (**B**) NMR (**C**) EPR (**D**) X-ray crystallography.

The amount of information we have gained on RNA using these techniques is arguably undeniable. However, the majority of these biophysical tools are applicable to *in vitro* systems only. Therefore, much of the recent interest in the RNA probe development is dedicated towards developing robust tools that would allow the investigation of RNA structure, dynamics and function *in vitro* and in cellular settings.

1.1.3 Methods to study RNA in cells

Cell behaviour under normal or disease state highly depends on the synthesis, maturation, transport, function and degradation of RNA molecules.[68] Therefore, various methods have been developed to study RNA processing and regulation in cells. Techniques such as polymerase chain reaction (PCR), Northern blotting, expressed sequence tag (EST), and serial analysis of gene expression (SAGE) provide invaluable information about the regulatory RNA sequences from cell lysates.[69-72] However, information about spatial and temporal RNA distribution is frequently lost.[68] The fluorescence based non-covalent labeling using commercially available SYTORNAselect dyes are used for visualizing whole RNA in cells.[73] In addition, fluorescence *in situ* hybridization (FISH) based antisense technique where gene specific RNA sequences modified with fluorescent reporter (fluorescein, rhodamine, Alexa and cyanine dye) have been appropriately utilized for in-cell RNA detection (Figure 4A). These modified oligomers act as hybridization probes and their sequence is complementary to the target RNA present endogenously.[75-79] However, low stability of ON probes in cellular environment and background signal due non-specific interaction limit the utility of this technique.

Few of the drawbacks of FISH technique were circumvented by using "switch on" probes named as molecular beacons. This technique was formularized using a hairpin shaped oligomer modified at the end with fluorophore-quencher pair (Figure 4B). Interestingly, non-fluorescent beacon will give "switch on" signal only upon binding to specific target RNA.[78] In recent years, nanoparticle assisted fluorescent labels (nanoflares) are utilised to target RNA in cells. Assembly of nanoparticles and probes allows efficient delivery and trigger release of antisense probe in presence of complementary target RNA.[79]

In recent times, RNA selection protocols have benefited the discovery of RNA motifs which show fluorescence emitting properties upon binding to small molecules. Jaffrey and coworkers exploited this in developing aptamer based fluorescence detection of specific RNA targets in live cells (Figure 4C). The tRNA based motifs were named as Spinach, Spinach2,

Broccoli showed binding with 3,5-difluoro-4-hydroxybenzylidene imidazolinone (DFHBI) which results in green florescence similar to green fluorescent protein (GFP).[80-85] Further development resulted in the evolution of sulforhodamine and malachite green binding aptamers for *in vivo* RNA imaging. Singer group recently developed an approach based on genetic encoding of RNA using fluorescent protein.[86-91] Their strategy based on coexpression of fluorescent protein in cell where they selectively bind to hairpin motifs introduced into the 3' untranslated region of the target RNA present in same cell (Figure 4D). Although, these technique looked promising until recent reports revealed degradation can induce nonspecific localization of signals.[92]

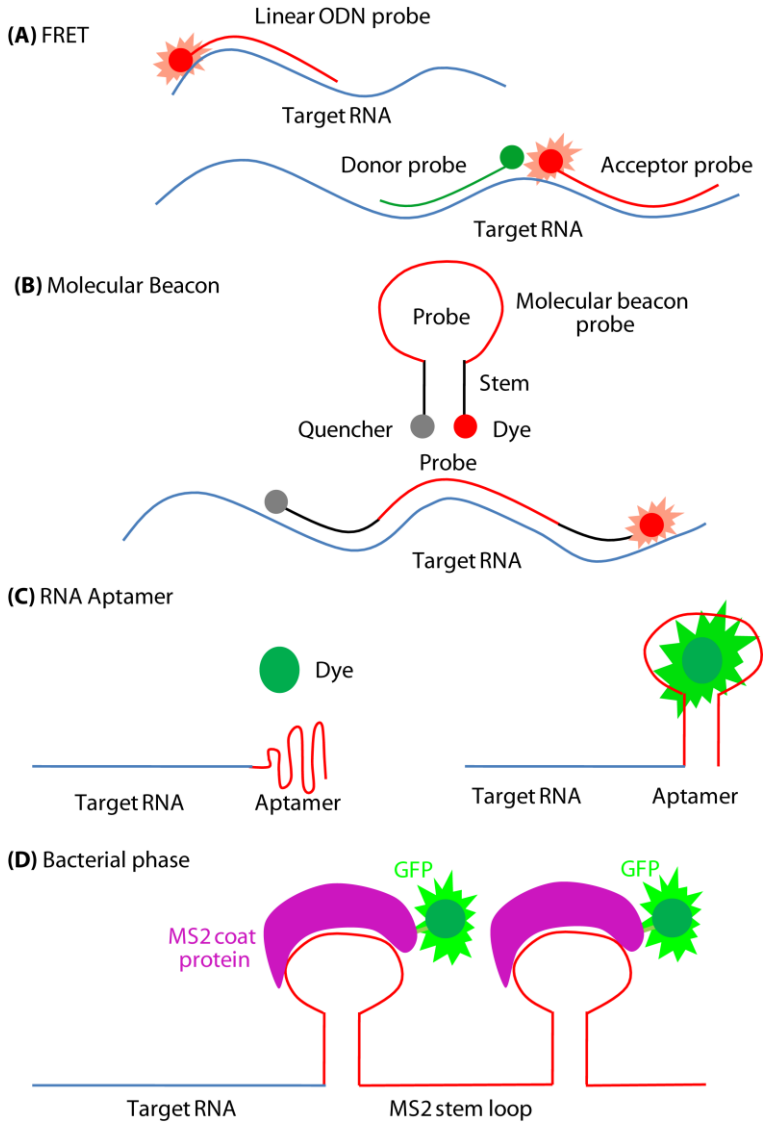

Figure 4. Depicting methods to visualize RNA in live and in fixed cells. (**A** and **B**) fluorescence *in situ* hybridization (FISH) based technique use antisense ON sequences modified with fluorescent reporters. (**C** and **D**) Aptamer and vector based techniques utilize RNA motif that bind to fluorescent reporters.

1.2 Synthetic strategies to generate labeled RNA

1.2.1 Chemical synthesis of functionalized RNA

Solid-phase RNA synthesizers allows synthesis of large quantities of unmodified and modified RNA ONs (Figure 5).[93-95] The primary 5'-hydroxyl group of pentose sugar is commonly protected by using an acid-labile DMT (4,4'dimethoxytrityl) group,[96] while secondary 2'-hydroxy group present in ribonucleoside is protected with a fluoride labile TBDMS (t-butyldimethylsilyl) group or with TOM (tri-iso-propylsilyloxymethyl) group.[97-99] The exocyclic amino groups present in purines (A and G) and Pyrimidines (C) are protected in orthogonal fashion with Bz (benzoyl) protection, isobutyryl group and Ac (acetyl) group (Figure 6).[100-104] Most commonly, internal labeling of RNA is achieved by using phosphoramidites modified at the 2' position. The labels are either directly linked to the 2' oxygen of the nucleotide or by a carbamate moiety as linker. 2' amide modified attachment was used for attachment of several aromatic residues. Further internal modification can be achieved using base modified phosphoramidites. The 5-C modified pyrimidine derivatives and 7 or 8-C modified purines amidites are commonly used.

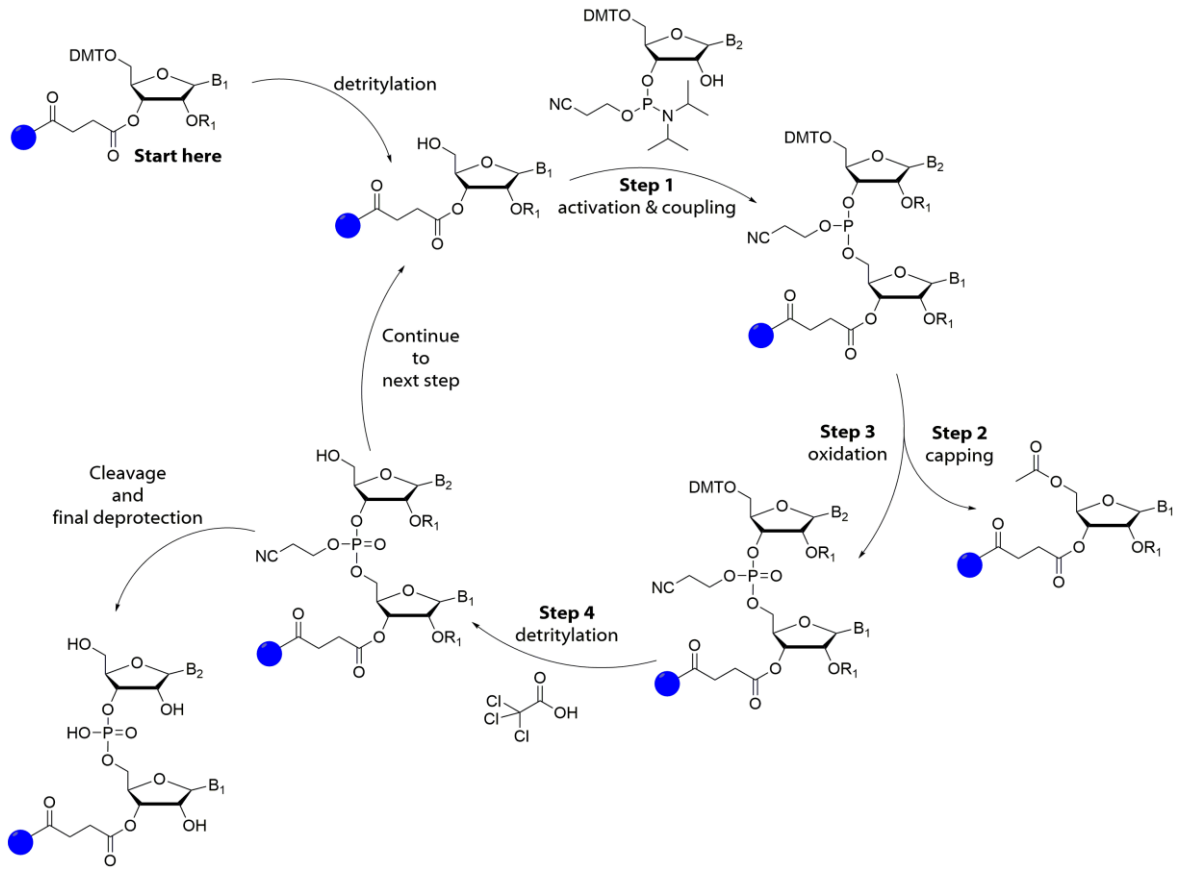

Figure 5. Solid-phase synthesis of RNA (ON) by using phosphoramidites building blocks.

Depending on the label the conformational and thermodynamic stability of the resulting modified RNA is evaluated with respect to native unmodified RNA by CD and thermal melting studies. Despite the success of solid-phase synthesis in generating labeled RNA ONs, several modified phosphoramidites show poor stability under synthesis condition and or exhibit poor coupling efficiency. For example in certain cases standard phosphoramidites are rapidly oxidized, which can be circumvented partially by using H-phosphonates (longer coupling times required) based approaches. Multi-labeling or the generation of long RNA strands is difficult due to progressive reduction coupling efficiency.[105]

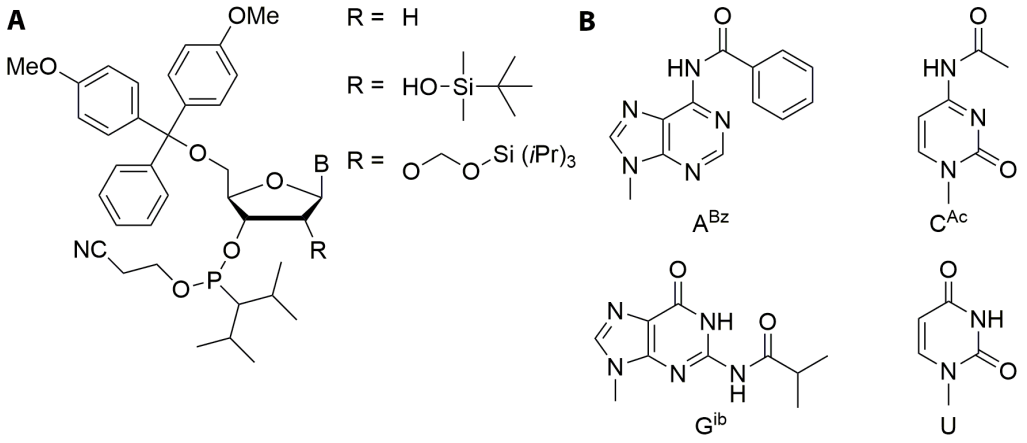

Figure 6. Different protecting sites in nucleoside such as (**A**) ribose (**B**) nucleobase are protected to obtain the desired phosporamedite substrate for solid-phase ON synthesis.

1.2.2 Enzymatic synthesis of functionalized RNA

T4 RNA ligase processes single-stranded RNA and catalyzes 5' to 3' nucleotide attachments in RNA. T4 RNA ligase is primarily used for labeling the 3' end of RNA with appropriately modified nucleoside 3',5'-bisphosphate.[106,107] Stringent ligation protocols are required to achieve effective ligation. Moreover, drawbacks like poor stability of ligation products and incorrect ligation of RNA strands does not encourage the use of enzymatic ligation method for large scale RNA synthesis.[108] *In vitro* transcription reactions catalyzed by T3, T7 and SP6 RNA polymerases are effectively utilized for the incorporation of one or even multiple nucleotide analogs into RNA (Figure 7).[109-111] For that instance acceptance of modified triphosphates by these RNA polymerase is of paramount importance.[112,113] Generally, C-5 modified pyrimidines[48-50] and C-7 modified deazapurines triphosphates are often tolerated,[114] whereas C-8 modified purines triphosphates are only rarely utilized.[115]

Very recently, researchers have shifted towards the use of chemo-enzymatic approach to synthesize modified RNA molecules. This is an improvised enzymatic approach, which

allows modification of RNA by using unnatural substrates and their respective co-enzymes. RNA-specific enzymes such as poly(A) polymerases, terminal uridylyl transferase, methyl transferase are wisely utilized in 3' and 5' end labeling of RNA transcripts.[116-119] Additionally, chemically engineered derivatives of methyltransferases allow labeling of RNA at 5' terminal.[120,121] Importantly, methyltransferases which target particular class of RNA (mRNA, tRNA) holds an advantage over regular RNA polymerases because they allow site-specific modification of target RNA sequences. High density functionalization of RNA might be essential for generation of efficient RNA aptamers, ribozymes and better RNA sequencing technologies. For such application transcription reactions would be useful as high density modifications can be achieved with reasonable efficiency.

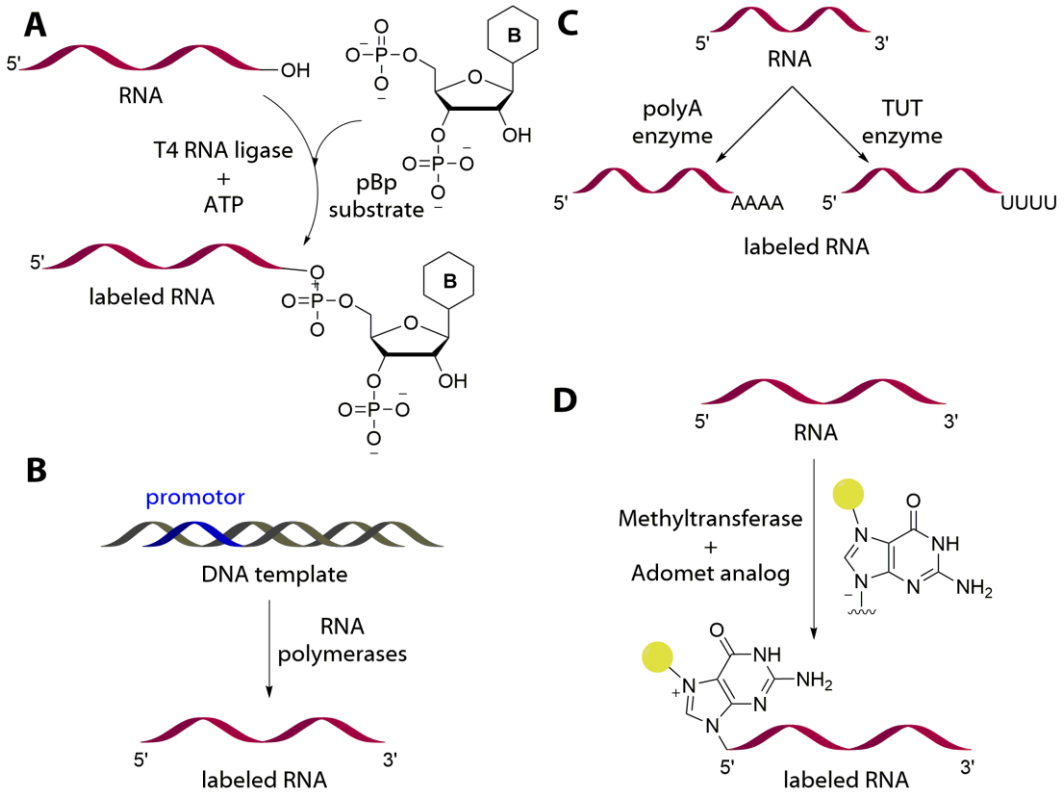

Figure 7. Enzymatic synthesis of RNA by using (**A**) ligation (**B**) transcription (**C**) polyadenylation and uridylation (**D**) transferase enzymes.

1.2.3 Chemical functionalization of RNA by postsynthetic modification strategy

Posttranscriptional labeling of RNA can be accomplished in two steps; in the first step modified nucleoside containing small reactive functionality is introduced during solid phase or enzymatic reactions (Figure 8). The incorporation of small reactive functionality is often useful as they would have better coupling efficiency under the chemical synthesis conditions. In addition, they are better accepted by RNA polymerases as unnatural substrate compared to

complex and potentially bulky probes. In the subsequent step a chemoselective reaction is carried out between reactive functionality incorporated into RNA and cognate label or functional group.

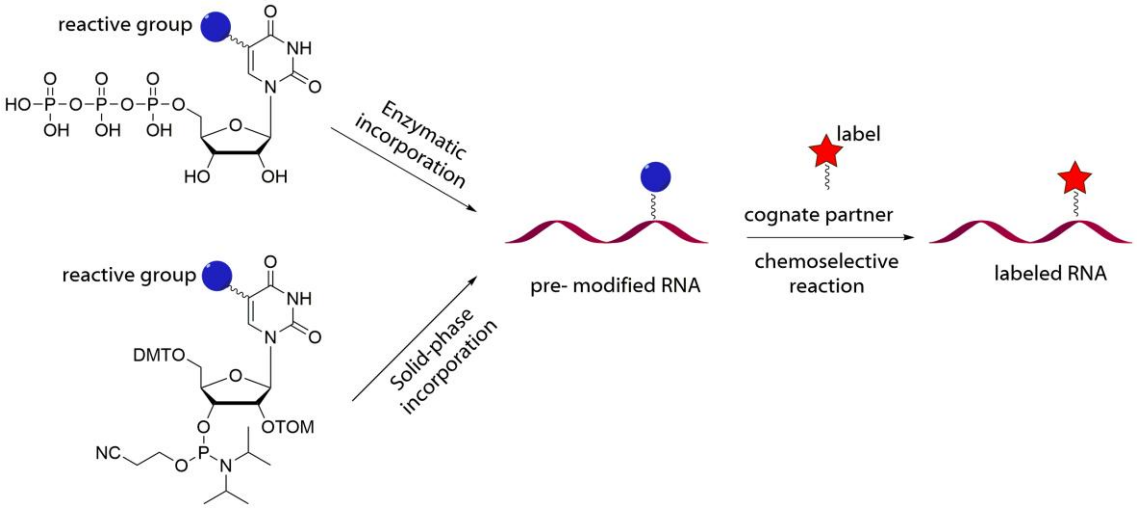

Figure 8. General concept of postsynthetic RNA labeling.

In early years, postsynthetic RNA labeling was accomplished by coupling reaction between reactive amine incorporated into RNA and activated carboxylic acids or derivatives.[122,123] Unfortunately, acid–amine coupling reactions are pH sensitive; at lower pH amines becomes unreactive due to protonation while higher pH leads to hydrolysis of the activated carboxylic acids. Similar to amines, thiols have also been utilized in nucleic acid labeling.[124,125] In this case they are reacted with α-haloacetyls, maleimides or activated disulfides. However, disulfides have a propensity to undergo reduction prior to desirable conjugation reaction, which reduces the applicability of thiol for bioconjugation of RNA. Therefore, RNA labeling with complex and reactive labels using amine and thiols is often limited. The presence of intrinsic reactive functionalities like amines, alcohols needs considerable attention to achieve chemoselectivity as they can potentially interfere during the course of reaction. In addition, to use postsynthetic strategy for biomolecule labeling following criteria must be fulfilled (i) reaction partners involved in reaction must remain inert toward native functionalities present in the biomolecules (ii) ideally labeling reaction should be kinetically fast at room temperature giving high yield without any byproducts or degradation of RNA over the course of reaction. Postsynthetic chemical functionalization of RNA ON remains a challenging task and development of non-toxic and biocompatible chemical reaction conditions are highly desirable for RNA labeling inside live cells.

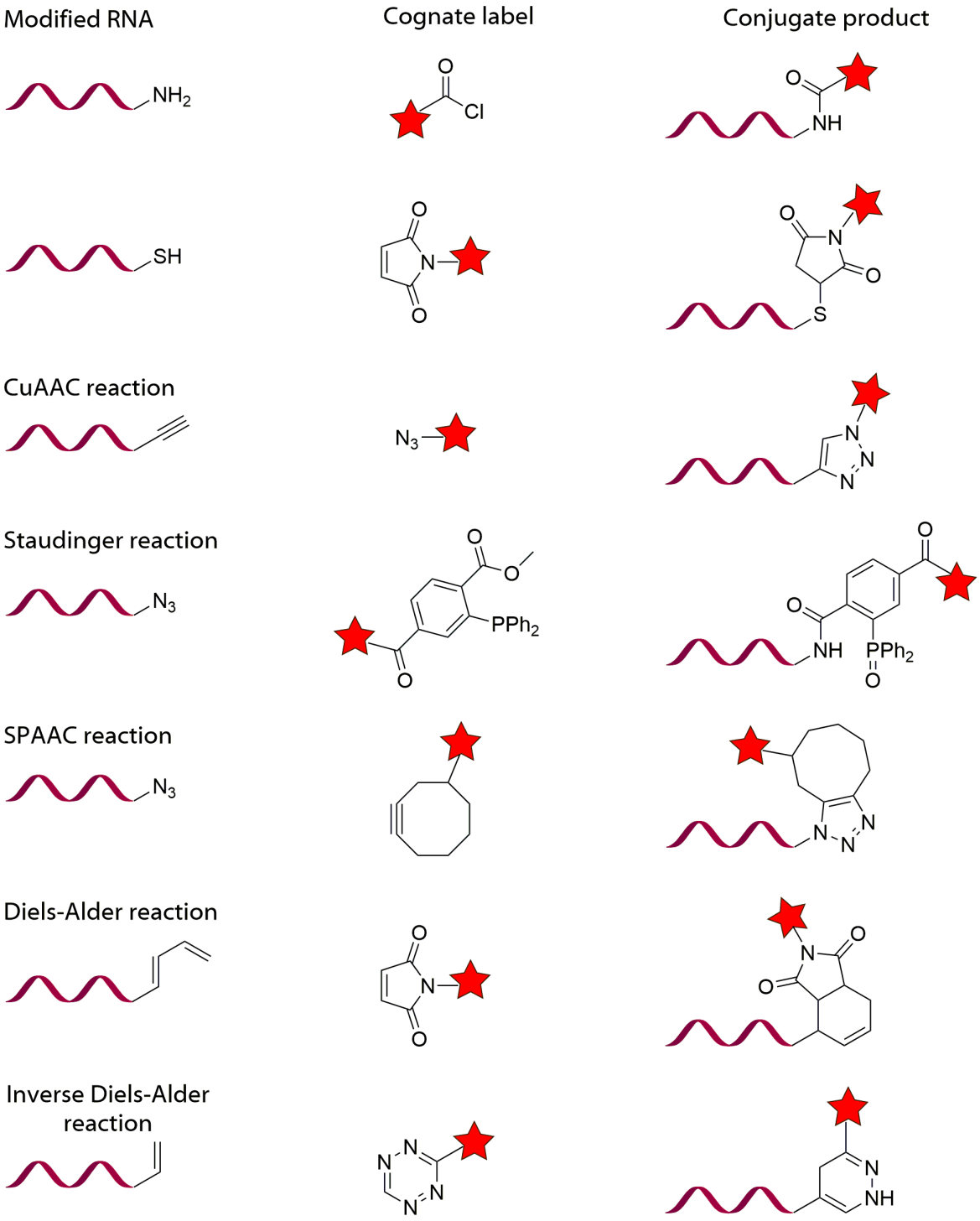

Figure 9. List of chemical reactions that can be utilized for postsynthetic labeling of RNA.

1.3 Introduction to bioorthogonal click reactions

The discovery of click reaction by Sharpless and Meldal in 2001 addressed most of the requirements for a reaction to be bioorthogonal. However, development of click reaction for *in vivo* labeling of biomolecules required considerable optimization due to toxicity of reaction partners, catalysts and the kinetics of the reaction. Traditionally, monoclonal antibodies are extensively used for biomolecule labeling in cells. The binding of antibodies to their respective antigens depends upon biomolecular diffusion rate constants that approach the limit (ca. 109 $M^{-1}s^{-1}$).[126] As a result, effective target binding is observed with reasonable rate at low working concentrations. Bimolecular click reaction follows typical second order rate constants and unfortunately, second-order chemical reactions have lower magnitude of rate constant. Therefore, cycloaddition reactions need to performed at relatively high concentrations (often high µM to mM) to compensate slower reaction kinetics. In bioorthogonal labeling inside cell, water-solubility of the labeling reagent is an additional parameter that needs to be taken into consideration. In the following section click reaction conditions which are employed for the postsynthetic chemical modification of nucleic acids are discussed.

1.3.1 Staudinger ligation

The Staudinger ligation reaction is a modified version of Staudinger reduction reaction.[127] The first step of ligation proceeds with reduction of an azide by a phosphine via an iminophosphorane intermediate. In the subsequent step an intramolecular acetylation of the iminophosphorane takes place (Figure 10). Therefore, stable amide bond is formed during conjugation of azide and phosphine. The utility of Staudinger ligation in bioconjugation was first shown by Bertozzi in 2001 and consequently coined the term bioorthogonal chemistry.[128] Azide shows high intrinsic reactivity towards phosphine and orthogonal to nearly all functional groups present in biomolecules. However, the phosphines are bulkier which cause low water solubility and susceptibility to oxidation prior to the ligation reaction. Despite this phosphine moiety shows bioorthogonalilty to almost all biofunctional groups and thus work selectively for *in vivo* labeling of cell surface azido glycoconjugates with biotin. Subsequently, Staudinger ligation became a general reaction for bioorthogonal labeling of peptides, proteins, carbohydrates and DNA.[129-135] Further, Bertozzi and coworker investigated the mechanism and kinetics of Staudinger ligation. They observed that Staudinger ligation follows second order rate kinetic with rate constant of 2.5×10^{-3} $M^{-1}s^{-1}$.

The solvent effect was also observed on kinetic of reaction where highly polar and protic solvents increase the rate of reaction. Solvents like methanol and DMSO enhance the rate constant upto 3.6×10^{-3} $M^{-1}s^{-1}$.[136]

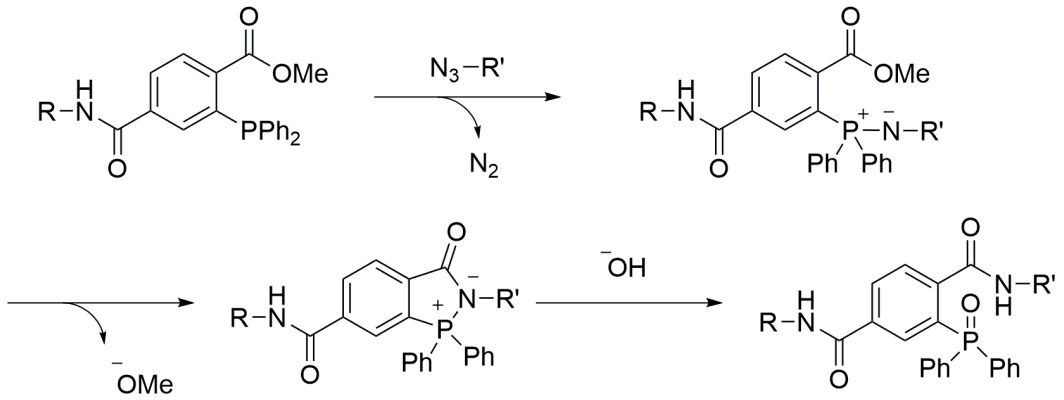

Figure 10. Simplified reaction mechanism of the Staudinger ligation. R: biomolecule and R': label

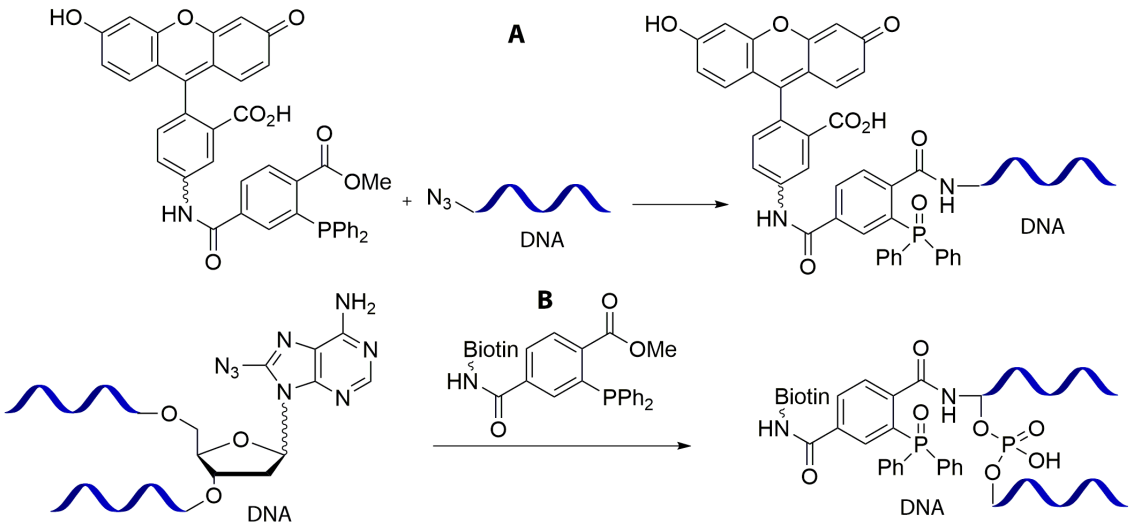

Figure 11. (**A**) 5' end labeling and (**B**) internal labeling of DNA by Staudinger ligation reactions.

The labeling of DNA and RNA by Staudinger ligations is challenging task mainly due to incompatibility of azide and triphenylphosphine groups in phosphoramidite synthesis chemistry. Despite the synthetic challenges couple of example of Staudinger liagtion on DNA set the tone for postsynthetic labeling of nucleic acids. In the first example, azide group was incorporated into DNA postsynthetically by using an azido-activated ester.[137] In the following step, selective reaction is carried out with fluorescein modified with triphenylphosphine reagent. 12 h of incubation at RT resulted in 90% conversion of the ligated product (Figure 11). In other example, chemoenzymatic approach allows labeling of DNA at N-6 position of deoxyadenosine by using azide cosubstrate and DNA methyltransferase (Figure 11). Subsequent Staudinger ligation allowed the conjugation of biotin or phenanthroline substrate

within 14 h at 40 °C.[138] Later Marx group showed utility of Staudinger ligation for labeling DNA ONs. They successfully synthesized and incorporated series of azide-modified deoxynucleotide analogs into DNA, which was then modified postsynthetically using triphenylphosphine containing affinity and fluorescent labels.[139] Additionally, several groups have used Staudinger reactions for templated probe release and to study various aspect of nucleic acid functions (Figure 12). It is important to note that bulky triphenyl phosphine remains as part of ligation product after Staudinger ligation and has few drawbacks. Especially, steric hindrances disturb the native structure which potentially prevents high density labeling of biomolecule by using Staudinger ligation.

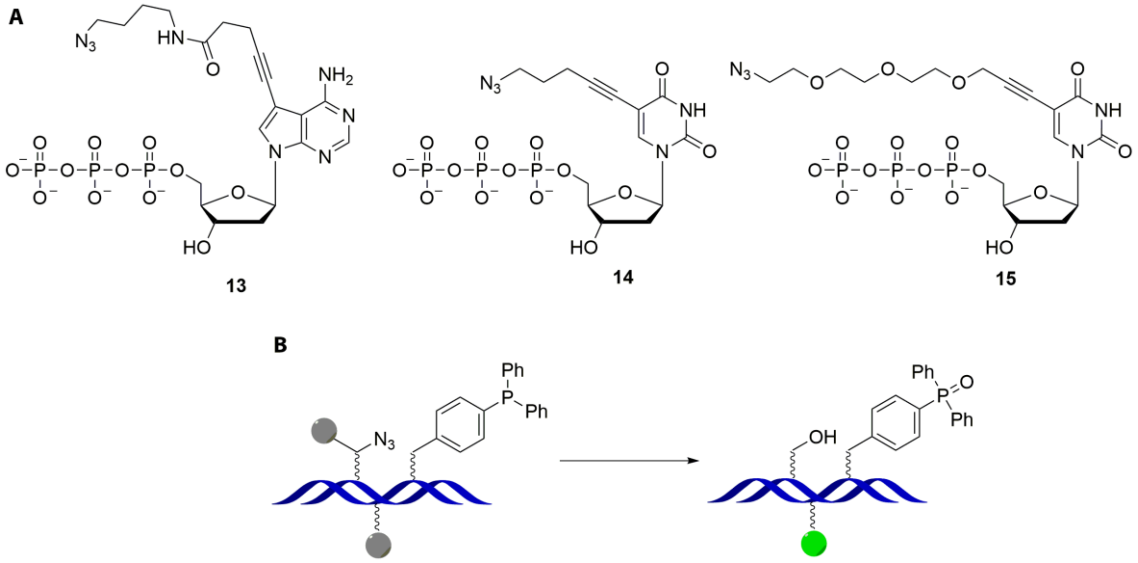

Figure 12. (**A**) Enzymatic incorporation of azide group into DNA for Staudinger ligation. (**B**) Staudinger ligation reactions are effectively use for templated release of fluorophore.

1.3.2 Copper-catalyzed azide-alkyne cycloaddition (CuAAC) reaction

The azide group exhibit high reactivity and chemoselectivity towards alkynes in a [2 + 3] dipolar cycloaddition reaction (Figure 13A). The thermal reaction between azide and alkyne forms stable triazole reported for the first time by Huisgen.[140] The conventional cycloaddition reaction is far away from being developed into bioorthogonal reaction due to its slow kinetics and harsh reaction conditions. However, Sharpless and Meldal independently reported a notable variant of the Huisgen 1,3-dipolar cycloaddition in 2001.[141,142] This cycloaddition reaction between azide and terminal alkyne was dramatically accelerated by using Cu(I) as a catalyst in aqueous solution to afford 1,4-regioisomer of 1,2,3-triazole as the sole product (Figure 13B). Both azides and alkynes are bioorthogonal and therefore soon recognized as useful handle for bioconjugation.[143,144] After their discovery this reaction was renamed as

copper-catalyzed alkyne-azide cycloaddition (CuAAC) or click reaction. Mechanism and outcome of the cycloaddition reaction is drastically altered by copper catalyst (Figure 14).[145] The use of copper catalyst enhance the rate of CuAAC reaction by the factor of 10^7 compare to conventional [2 + 3] dipolar cycloaddition reaction,[146] making it conveniently fast at room temperature.

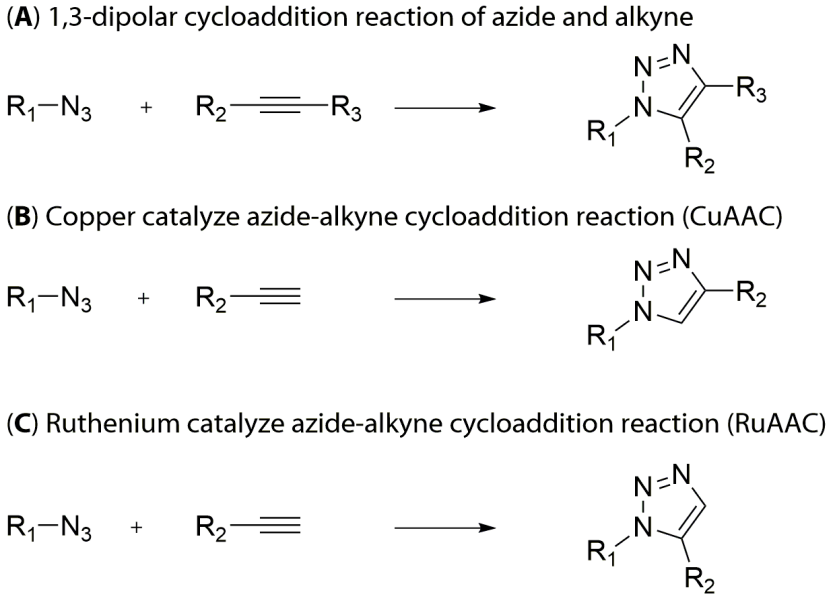

Figure 13. Thermal cycloaddition of azides and alkynes results in mixtures of both 1,4-and 1,5-regioisomers (**A**) CuAAC produces only 1,4-disubstituted-1,2,3-triazoles (**B**). The RuAAC reaction proceeds with both terminal and internal alkynes and gives 1,5-disubstituted 1,2,3-triazoles.

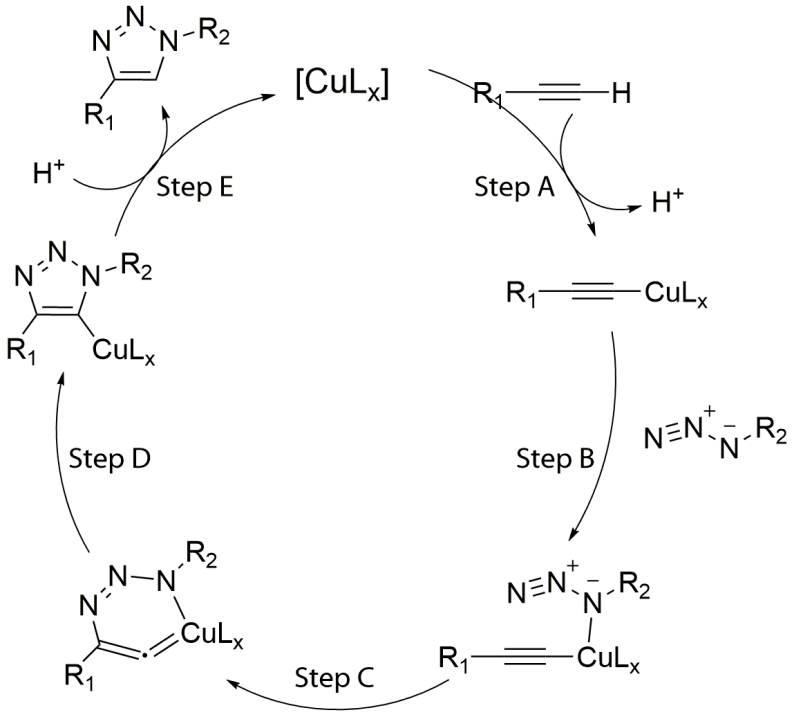

Figure 14. Proposed mechanism of catalytic cycle in CuAAC reaction.

Copper serve as a reliable catalyst for the formation 1,4-regiospecific product during azide–alkyne cycloaddition. Interestingly, ruthenium cyclopentadienyl complexes were found to catalyze the formation of the 1,5-disubstituted triazole from cycloaddition between azides and terminal as well as internal alkynes (Figure 13C). Mechanistic distinction in ruthenium-catalyzed azide–alkyne cycloaddition (RuAAC) with CuAAC is that electron back donation is observed from ruthenium centre into the pie system.[147] Although, RuAAC shows excellent functional group compatibility, the sensitivity of reaction to the solvents and the steric demands of the azide substituents restrict the potential of RuAAC in comparison to CuAAC reactions. Different Cu(I) sources such as copper(I) halides and coordination complexes such as $[Cu(CH_3CN)_4]PF_6$ and $[Cu(CH_3CN)_4]OTf$ can be directly utilized in the reaction.[148] However, formation of polynuclear acetylide complexes may interfere with the catalytic cycle and overall productivity of reaction. Alternatively, CuAAC reaction can be performed in aqueous solvents using water soluble Cu(II) salts such as $CuSO_4$. The reactive Cu(I) ions can be generated *in situ* in the presence of reducing agent. Ascorbate, a mild reductant, was used by Fokin and coworkers, which can be used in combination with a Cu(II) salt in aqueous solvents.[149]

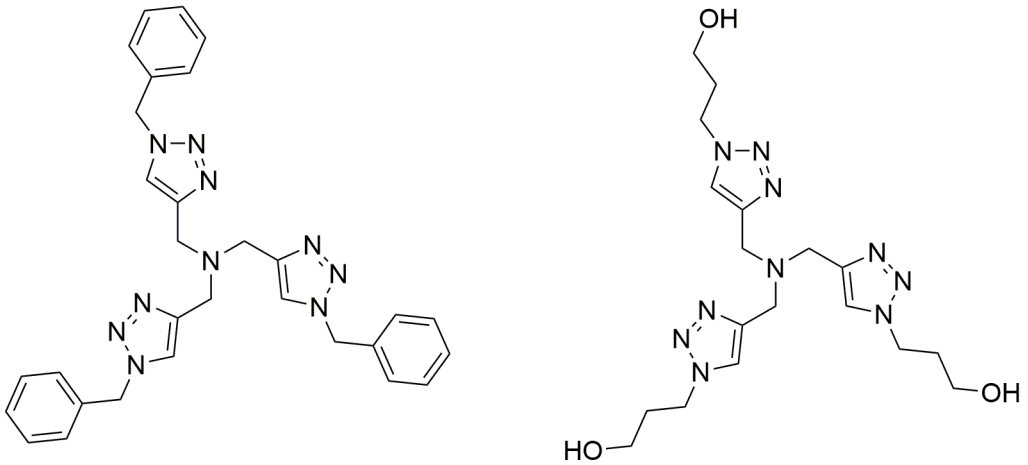

(**A**) Tris(benzyltriazolyl)methyl amine (TBTA) (**B**) Tris(3-hydroxypropyltriazolylmethyl)- amine (THPTA)

Figure 15. CuAAC-accelerating ligands of choice: (**A**) Tris(benzyltriazolyl)methyl amine (TBTA) suitable in non polar solvents. (**B**) Tris(3-hydroxypropyltriazolylmethyl)- amine (THPTA) extensively used in aqueous solvents.

Over the years CuAAC reaction was optimized for reaction conditions and kinetics. During this development it was observed that CuAAC reaction between azide and alkyne rarely form any side product therefore step like workup or purification of the product can be bypassed or avoided. Most importantly, both azides and alkynes are found to tolerant towards

other functionalities and therefore thought to be employed in bioconjugation of nucleic acids. Despite the scope of CuAAC reaction postsynthetic labeling of nucleic acid was delayed by the fact that Cu(I) ions are unstable and easily oxidize to Cu(II) which impose stringency to experimental conditions. The redox conversion of Cu(I) to Cu(II) results in the oxidative damage of nucleic acids.

The demand of effective chemical bioconjugation of biomolecules such as nucleic acids necessitated the development of Cu(I) stabilizing ligands. The ideal ligands should work under milder condition without affecting the rate, chemoselectivity or biocompatibility of the reaction. Tris(benzyltriazolyl)methyl amine (TBTA, Figure 15A) served as an alternative solution to the bioconjugation problem.[150] The ligand was found to effectively stabilize the Cu(I) oxidation state in aqueous-organic solvent combination with significant acceleration in reaction rate. TBTA was widely adopted for bioconjugation of proteins, glycan, and lipids, however poor solubility of TBTA in water prompted the development of more polar analogs such as Tris(3-hydroxypropyltriazolylmethyl)-amine (THPTA, Figure 15B) and its variants.[151] Subsequently, a combinatorial approach led to the identification of the ligand component which are water-soluble and enhance the CuAAC reactions under dilute aqueous conditions.

After these developments in CuAAC reaction the utility of cycloaddition reaction for nucleic acid labeling was first demonstrated in DNA by Seo *et al* in 2003.[152] In their experiment azide modified DNA was reacted with fluorescein alkyne in the absence of copper catalyst. Nearly 90% of labeled DNA was recovered after the reaction (3 days at 80 ^{o}C). The use of copper as a catalyst allows complete conversion of DNA within 2 h at room temperatrure. However, DNA damage was observed due to stand break.[153,154] Alternatively, highly reactive terminal alkyne has been specifically incorporated into DNA and smoothly conjugated with different azide building blocks (Figure 16A). Carell group developed an 5-octadi(1,7)ynyl deoxyuridine analog which can be incorporated into DNA and further postsyntheic labeling was achieved by using CuAAC reaction with an azide-modified carbohydrate, coumarin azide or fluorescein azide.[155] In addition, postsyntheic modification of DNA in a modular fashion was achieved with different protecting groups (TMS and TIPS) for the alkyne moiety. Orthogonal protection of alkyne allows DNA labeling with different probes (Figure 16B). The labeling is obtained on solid support with an unprotected alkyne and subsequent deprotection of TMS and TIPS led to three-in-one DNA labeling. Thereafter, terminal alkyne has been attached to the DNA using alkyne modified phosphoramidites,

triphosphates for DNA conjugation by CuAAC reaction.[156,157] The complete conversion in labeling reaction is achieved within hours at room temperature.

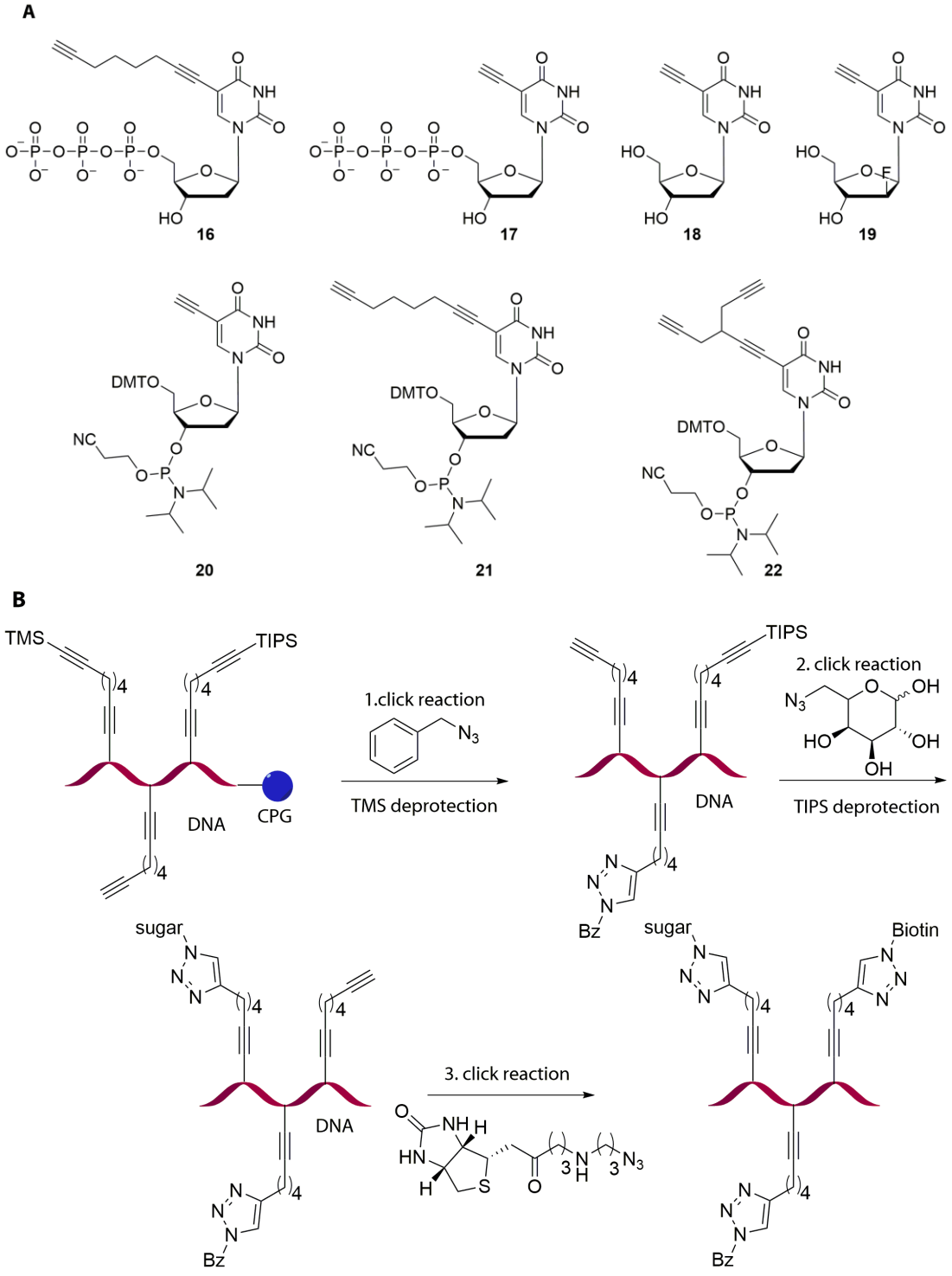

Figure 16. (**A**) alkyne-modified nucleoside analogs that can be incorporated into DNA by solid-phase or enzymatic reactions. (**B**) A classical example of multiplex labeling of DNA by using CuAAC reaction. In this strategy orthogonally protected alkyne-modified nucleoside analogs were incorporated into DNA by solid-phase and subsequently label with various azide labels by CuAAC reactions.

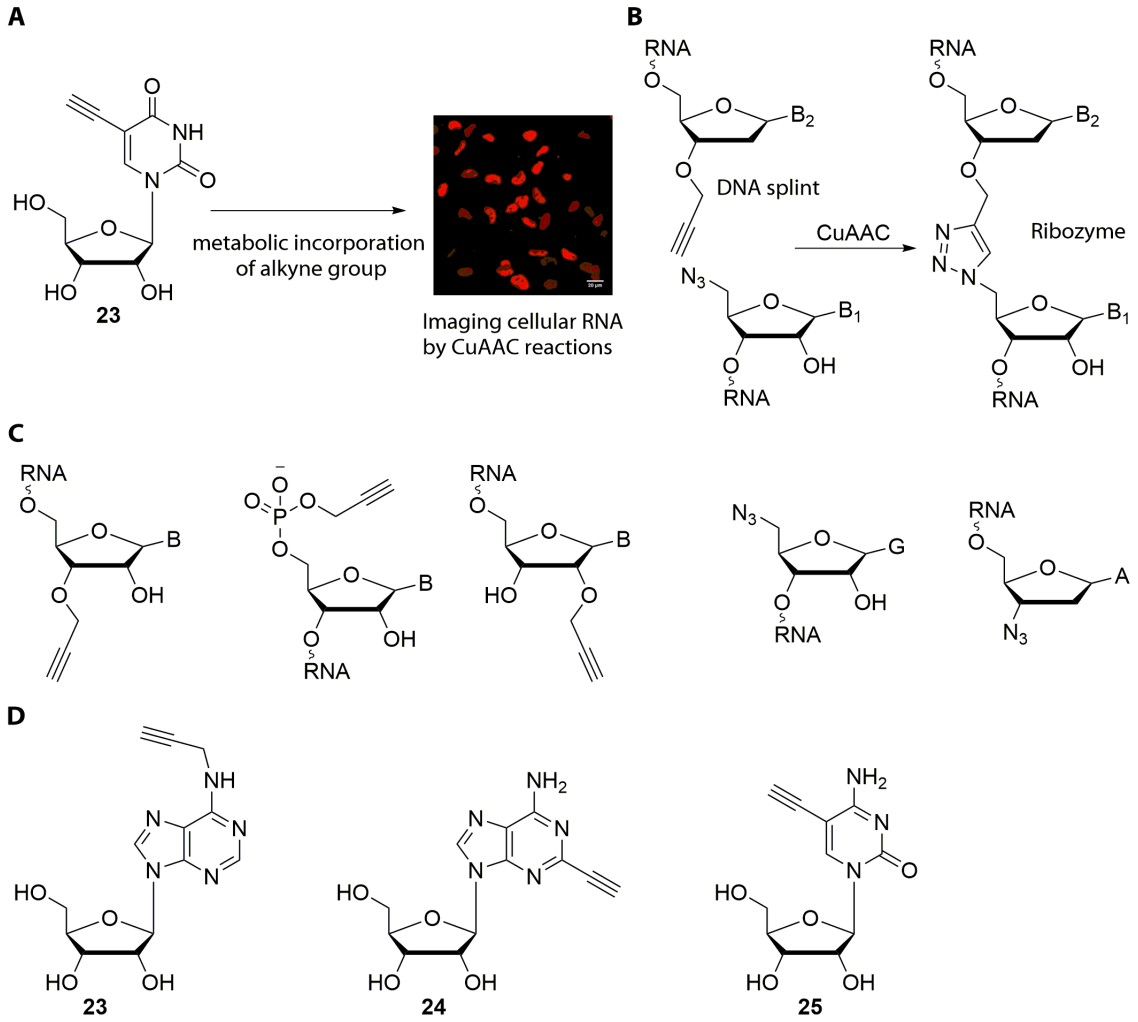

Figure 17. Early development of CuAAC reactions for labeling RNA by using alkyne and azide modified nucleotide analogs.(**A**) Salic reported RNA imaging using metabolic incorporation of **23** followed by CuAAC reaction with fluorescent azide. (**B**) Brown group utilized CuAAC reaction to generate active ribozyme. (**C**) Das group showed postsyntheic modification of alkyne and azide mofided RNA by click reaction. (**D**) alkyne-modified ribonucleosides utilized for biosynthetic incorporation of alkyne and imaging of cellular RNA.

Recently, terminal alkyne analogs **18** and **19** have been effectively utilized for metabolic labeling and imaging of cellular DNA by CuAAC reactions.[158,159] After successfully establishing DNA labeling protocol by CuAAC reactions various groups tested the compatibility of RNA labeling using click reactions. Recently, Brown and coworker extended CuAAC labeling strategy for RNA labeling.[160] They elegantly utilized click chemistry to ligate DNA and RNA to generate functional ribozyme (Figure 17B). Simultaneously, Paredes and Das systematically optimized reaction conditions for *in vitro* bioconjugation of RNA.[161] They successfully showed that click chemistry can be used on naked RNA with no modification on 2'-hydroxyl groups. They also demonstrated RNA

labeling in presence of Cu(I) catalyst wherein degradation of RNA was prevented by using water soluble Cu(I) stabilizing ligand (Figure 17C). Despite this the use of toxic Cu (I) in CuAAC reactions obstructs the use of copper-based click reactions in live cell labeling and imaging. Salic group in 2008 reported the cellular labeling and imaging of alkyne modified RNA transcript in cells by using CuAAC reactions.[162] In their experiment, cellular RNA transcripts metabolically incorporated with 5-ethynyluridine (EU) were imaged by CuAAC reaction with various fluorescent azides in fixed cells (Figure 17A). Further, various groups utilized biosynthetic incorporation of alkyne modified ribonucleoside analogs (**23-25**) into RNA and monitored RNA synthesis and polyadenylation process in cells using CuAAC reactions with azide fluorophores (Figure 17D).[163-165]

1.3.3. Strain-promoted azide alkyne cycloaddition reaction

Bertozzi group developed strained cyclooctynes, which could chemoselectively react with azide functionality like terminal alkynes but in the absence of a copper catalyst. Subsequently, this reaction was named as strain-promoted alkyne-azide cycloaddition (SPAAC) or copper-free click reaction (Figure 18A). Later, Bertozzi group elegantly showed the utility of SPAAC reaction for bioconjugation of proteins and cell surface glycans not only in living cells but also in animals models.[166,167] Albeit, successful use of SPAAC reactions in cell surface labeling, poor water solubility of cyclooctynes limits their applications in bioconjugation of nucleic acids inside cellular environment. Chemical substitution on the cyclooctynes has partially improved their solubility but substituents also affect the rate of the SPAAC reactions (Figure 18B).

To address this problem Bertozzi and coworkers systematically studied various substitutions pattern on cyclooctynes and their kinetics and found that difluorinated cyclooctyne (DIFO) had better reactivity.[168] Boons *et al.* also developed biarylazacyclooctynone (DIBO) system by fusing two benzene rings to cyclooctyne.[169] Interestingly, they observed that the kinetic of bimolecular rate constant was nearly three times higher compare to unsubstituted cyclooctyne. Concurrently, Group of van Delft and coworkers introduced an amide bond into the ring to improve the reactivity of simple cycloctyne (BARAC).[170] Their group also introduced bicyclo[6.1.0]nonyne, a cyclooctyne analog (Figure 18B) for SPAAC, which possessed high reactivity toward azide. Importantly, these analogs can be relatively easily synthesized with moderate yields.[171]

Brown and coworkers showed the use of SPAAC reaction for templated DNA strand ligation in presence of chemically synthesized azide and dibenzocyclooctyne modified DNA strands.[172] Later, Taton and coworkers showed incorporation of cyclooctyne group into DNA by PCR reaction followed by SPAAC reactions with fluorescent azides.[173] Very recently, Luedtke group developed a method to label and image newly replicating DNA in live cells. They utilized 5-(azidomethyl)-2'-deoxyuridine (AMdU) for metabolic incorporation of an azide groups in cellular DNA, which enabled the detection of DNA by SPAAC reaction with BCN-AlexaFluor in cells.[174]

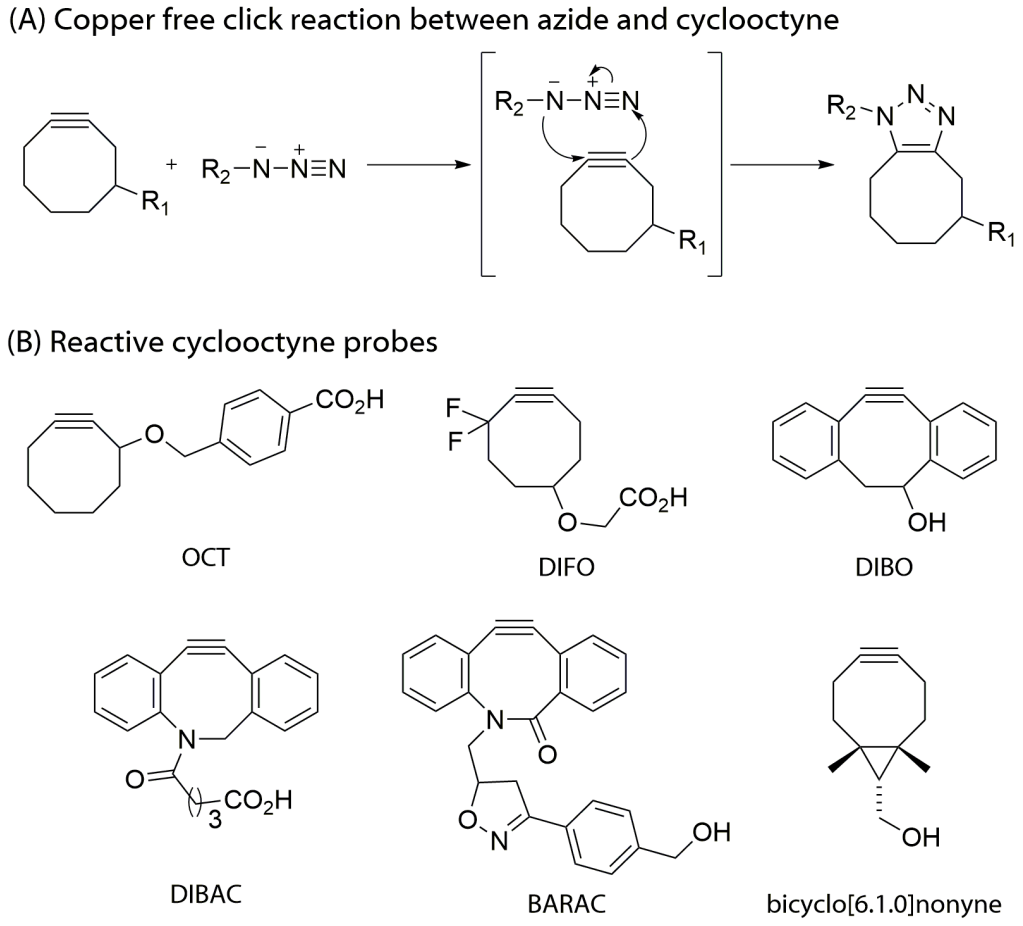

Figure 18. (**A**) Proposed mechanism of copper-free click reaction. (**B**) Various generations of reactive cyclooctyne probes.

RNA labeling by using SPAAC reaction mainly rely on chemo-enzymatic incorporation of azide group into RNA (Figure 19D). Jäschke's group reported a labeling approach in which the RNA of interest was modified at its 3' end by a poly(A) polymerase with an azido-derivatized nucleotide (**34**).[175] The azide was later conjugated via SPAAC reactions. On a similar line of thought Rentmeister's group demonstrated the site-specific

labeling of 5'-capped RNAs by using bioorthogonal chemistry. Their experimental data demonstrated the use of chemically engineered trimethylguanosine synthase to transfer a terminal azido moiety to the guanosine residue (**33)** in mRNA, which could be further modified using SPAAC reactions.[176] In addition to this Micura group showed a rare example of incorporation of 3'-terminal 2'-*O*-(2-azidoethyl) group (**32**) into RNA by using solid support for automated RNA synthesis (Figure 19D). Their strategy allowed the efficient labeling of siRNA using cyclooctyne fluorescent dyes.[177]

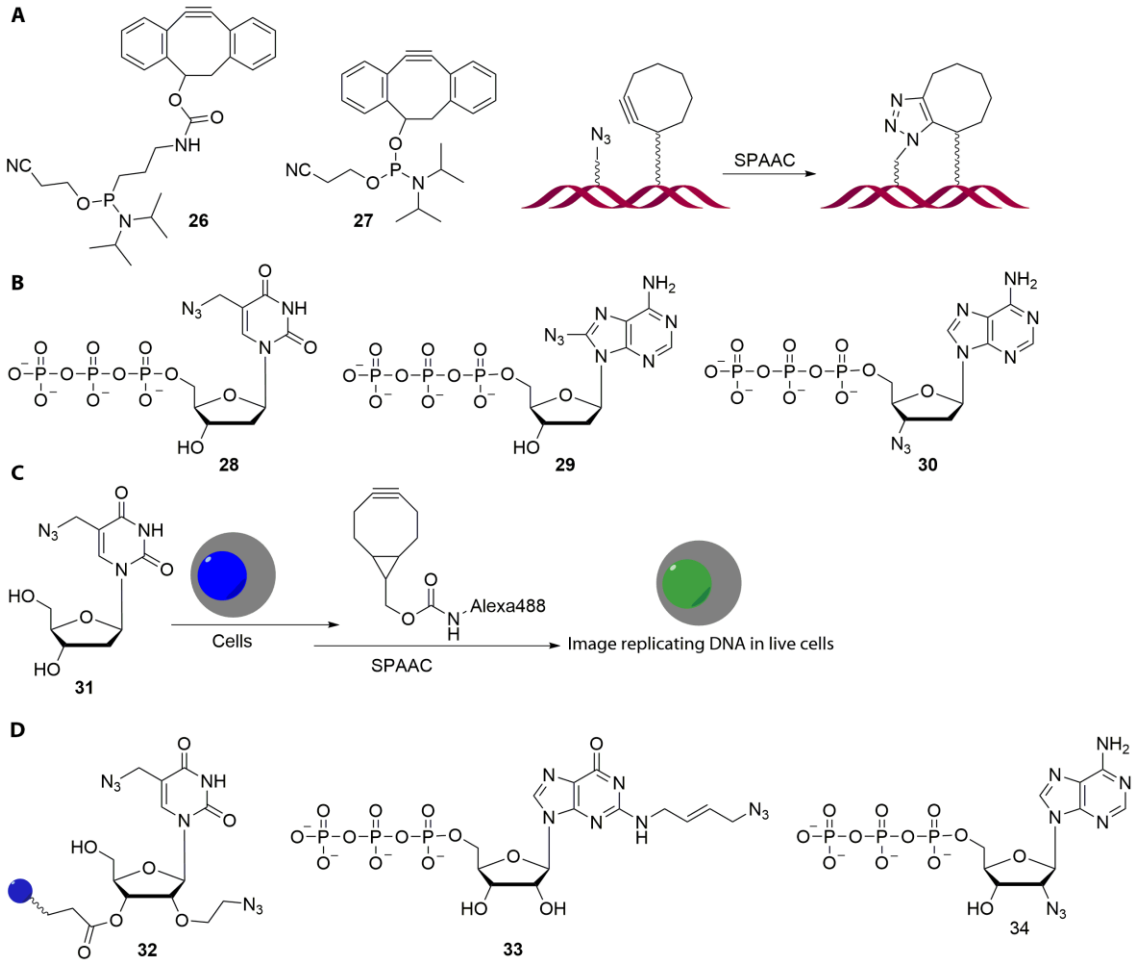

Figure 19. DNA and RNA labeling by using SPAAC reaction (**A**) Brown and Taton groups incorporated cyclooctyne probe into DNA by solid-phase synthesis. (**B**) Jaschke group utilized PCR reaction to label DNA with azide group for subsequent labeling by SPAAC. (**C**) Luedtke group showed DNA labeling and imaging in live cell by utilizing metabolic reporter **31** and BCN-Alexa488. (**D**) RNA labeling with azide performed by using solid-phase and chemoenzymatic methods.

1.3.4 Diels Alder reaction

[4+2] cycloaddition or Diels-Alder (DA) reaction in aqueous buffer in the presence of an appropriate dienophile and diene has been utilized in the labeling of biomacromolecules.[178,179] Typically, maleimide derivatives serve as good dienophile labels as

they can be easily synthesized and are highly reactive under mild reaction conditions. The strained ring system and electron deficient double bond provides enhanced reactivity during ligation reaction with dienes.[180] Despite their reactivity, maleimides show nonspecific reaction with thiols and other nucleophiles, which compromise their utility in bioorthogonal labeling. On the contrary, electron rich and bioorthogonal diene have been incorporated into DNA (e.g. anthracene, hexadiene, cyclohexadiene and furan).[181-183] Eaton group showed the utility of nucleic acid bioconjugation by using DA reaction. They demonstrated the ribozyme-catalyzed DA reaction between DNA modified at 5' end with hexadiene and biotin maleimide (Figure 20B).[184] Dienes such as cyclohexadiene and acyclic hexadiene have been incorporated into DNA using solid-phase synthesis and subsequently labeled using DA reaction with different maleimide functionalized labels. The reaction conditions have been optimized for pH, temperature and label concentrations which led to quantitative conjugation with reaction times ranging from min to hours for more complex functional groups.

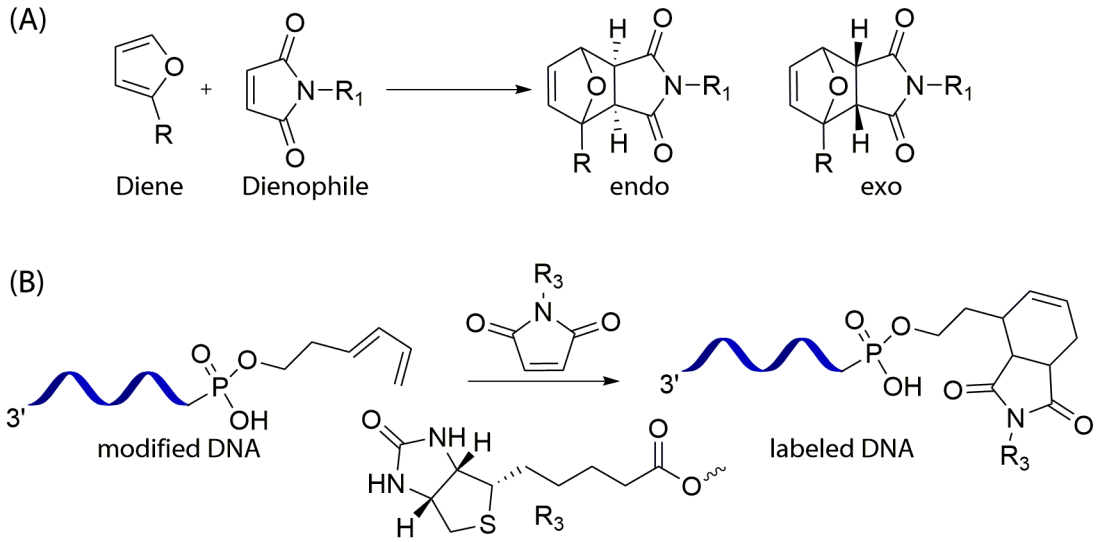

Figure 20. (**A**) DA cycloaddition reaction between an electron rich diene (furan) and dienophile (maleimide). R, R_1: residues to conjugate labels. (**B**) DA reaction between DNA modified at 5' end with hexadiene and biotin maleimide.

1.3.5 Inverse electron-demand Diels–Alder reaction

In 90s Sauer group first reported inverse electron-demand Diels–Alder (IEDDA) reaction between a tetrazine and alkene, which was termed as tetrazine ligation.[185-187] Tetrazine ligation is the variant of DA reaction in which strained alkenes have been used with tetrazines in inverse-electron demand fashion. The ligation reaction proceeds with the formation of cycloadduct in the initial step. In second step retro DA reaction takes place to produce dihydropyridizine with elimination of nitrogen (Figure 21).

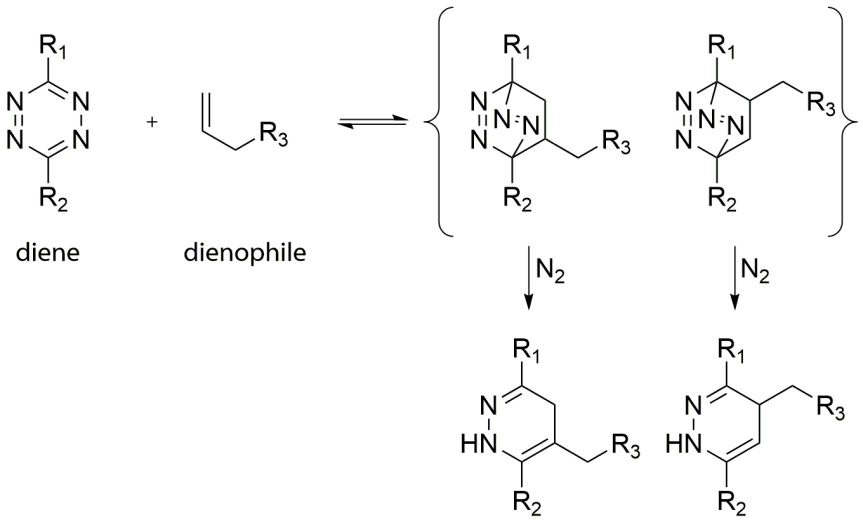

Figure 21. The Diels-Alder-Reaction with inverse electron demand (DARinv) is shown. R_1 and R_2 functional groups decrease electron density on diene. While R_3 group present on dienophile will enhance electron densitiy in the dienophile.

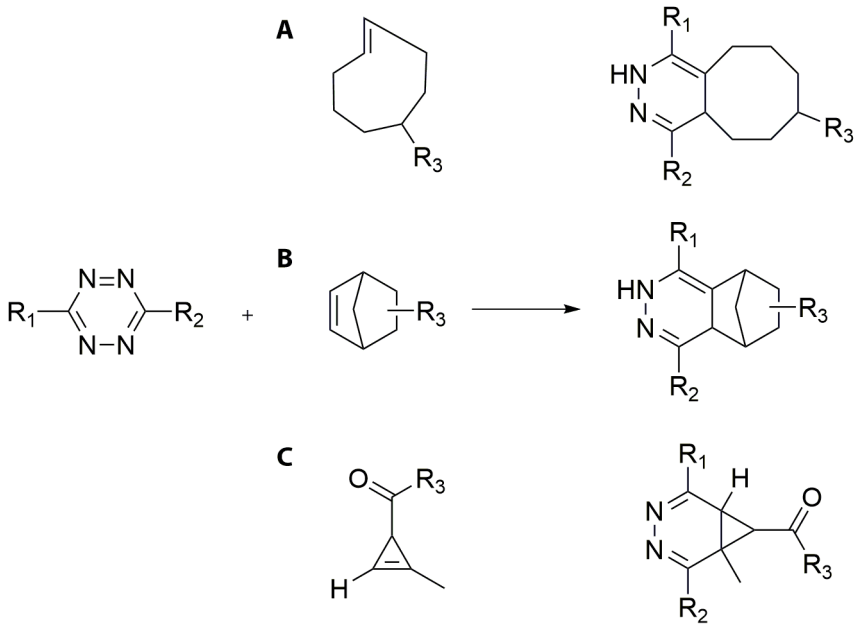

Figure 22. Tetrazine ligation reactions between tetrazine and (**A**) trans-cyclooctene, (**B**) norbornene (**C**) cyclopropene.

The utility of tetrazine ligations for bioorthogonal chemistry was first demonstrated independently by Fox and Hilderbrand in 2008 (Figure 22). They showed the rapid ligation of trans-cyclooctene[188] and norbornene[189] with tetrazine in water with a second-order rate constant of ~2000 $M^{-1}\times s^{-1}$. In addition, the ligation reaction allowed successful live cell imaging with a fluorescent tertazine.[190,191] The major drawback of tetrazine ligation is the use of bulky trans-cyclooctene and norbornene systems. To overcome this obstacle Prescher[192] and Devaraj[193] groups independently investigated the potential of cyclopropene in tetrazine

ligation. (Figure 22C) However, the cyclopropene are highly unstable reactive group, which has tendency to undergo polymerization. Although the rate of the reaction was lower (~0.1–13 $M^{-1} \cdot s^{-1}$) cyclopropenes have been used in the bioconjugation of proteins and metabolic labeling of glycans.[192,194]

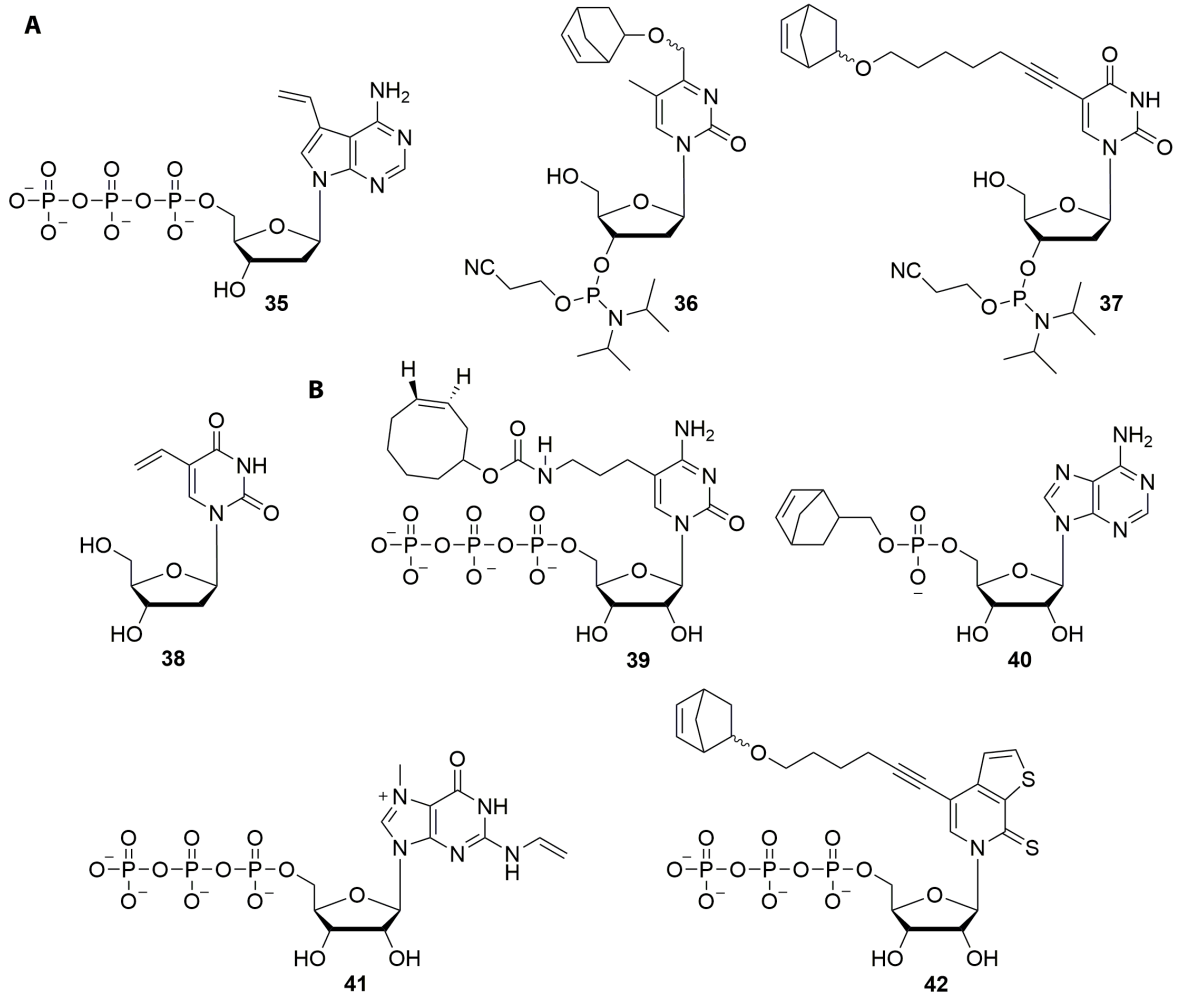

Figure 23. Labeling of nucleic acids by IEDDA reaction. (**A**) Vinyl and trans-cyclooctene substrates for labeling of DNA by enzymatic and chemical synthesis. (**B**) Modified NTP analogs for enzymatic and chemo-enzymatic labeling of RNA.

Very recently, the inverse electron-demand Diels–Alder reaction also turned out to be suitable for nucleic acid labeling (Figure 23).[195] Early reports of IEDDA reaction as a bioorthogonal reaction for the selective and efficient modification of DNA came from Marx and Jäschke group. Marx and coworkers incorporated vinyl functionality (**35**) into DNA enzymatically and performed postsynthetic modification by using a tetrazine substrate.[196] Jäschke group explored the potential of IEDDA reaction for postsynthetic modification of both DNA and RNA. Jäschke and coworker showed incorporation of norbornene dienophiles

(**36** and **37**) into DNA by solid-phase synthesis protocol followed by conjugation with water-soluble tetrazines.[197] In addition, their group explored the usefulness of inverse electron-demand Diels–Alder reactions for postsynthetic RNA labeling. They showed incorporation of norbornene group into RNA by transcription reaction in presence of dienophile (**40**). Further, norbornene modified transcripts were reacted with tetrazine peptides to generated RNA–peptide conjugates. In the same report, they showed chemical synthesis of RNA using modified norbornene phosphoramidite followed by successfully conjugation with tetrazine tagged biotin and fluorescent label. Recently, Rentmeister and coworkers illustrated chemoenzymatic transfer of a vinyl group (**41**) to mRNA at the 5' end cap which allowed mRNA labeling using IEDDA reactions.[198] Luedtke and Kath-Schorr groups demonstrated the efficacy of IEDDA reaction to label and image DNA and RNA in cells. Luedtke showed metabolic incorporation of 5-vinyl-2'-deoxyuridine (VdU, **38**) into DNA, which allowed the imaging of nascent DNA by performing IEDDA reaction with a fluorescent tetrazine.[199] Kath-Schorr successfully reported *in vitro* labeling of norbornene modification (**42**) into RNA, and this norbornene-modified RNA was selectively imaged inside cells by using IEDDA reaction.[200] However, the bulky nature of tetrazine and instability of strained trans-cyclooctene and cyclooctyne dienophile limits the implementation of IEDDA reaction. Moreover, reactive and biocompatible tetrazines are difficult to synthesize and are very expensive. Nevertheless, improved synthetic routes for the preparation of more reactive tetrazine precursors would expand the scope of tetrazine ligation reaction.

1.4 Motivation and outline of the thesis

Solid-phase chemical and enzymatic synthesis protocols for generating labeled RNA ONs are sufficient for most *in vitro* applications. However, in several instance the modified substrates are not compatible under the stringent solid-phase synthesis conditions and are not good substrates for enzymatic incorporation. Alternative, bioorthogonal chemical reactions has recently evolved as a valuable method to label nucleic acids for diagnostic and therapeutic applications. While these bioorthogonal reactions are more compatible for labeling DNA, postsynthetic modification of RNA is not easy as protocols developed for DNA modification do not necessarily work for RNA due to its inherent instability. Therefore, there is a significant demand for the development of robust and practical strategies that will be suitable for labeling RNA both *in vitro* and in cells.

The aim of this doctoral thesis is to develop robust and modular chemical functionalization methodology that would allow the labeling of RNA *in vitro* and in cells with biophysical probes for variety applications. Here, we have utilized the versatility of bioorthogonal reactions namely azide-alkyne cycloaddition reaction, which has been widely utilized in the study of glycan, protein and DNA, to develop a simple and practical posttranscriptional chemical functionalization method to label RNA *in vitro* and in cells. In simple steps we have synthesized alkyne-modified UTP analogs, which enabled the effective incorporation of alkyne functionalities into RNA (i) *in vitro* by using T7 RNA polymerase and (ii) in cells by using endogenous RNA polymerases. The alkyne-modified transcripts are conveniently labeled posttranscriptionally by copper (I)-catalyzed azide-alkyne cycloaddition (CuAAC) reactions with a variety of biophysical probes. Further, we have incorporated azide functionality into cellular RNA transcripts by using one of the azide-modified UTP analogs, which was earlier developed in our group for *in vitro* posttranscriptional chemical modification of RNA. The specific labeling of cellular RNA with azide and alkyne groups followed by click reactions further enabled the visualization of newly transcribing RNA in fixed and live cells by fluorescence microscopy. It is expected that this new methodology and important observations reported in this thesis will provide new opportunities to advance our fundamental understanding of RNA structure, proliferation and function.

1.5 References

1. Ahlquist, P. RNA-dependent RNA polymerases, viruses, and RNA silencing. *Science*, **296**, 1270–1273 (2002).
2. Nahvi, A., Sudarsan, N., Ebert, M. S., Zou, X., Brown, K. L. and Breaker, R. R. Genetic control by a metabolite binding mRNA. *Chem. Biol*., **9**, 1043–1049 (2002).
3. Timmons, L., Tabara, H., Mello, C. C. and Fire, A. Z. Inducible Systemic RNA Silencing in Caenorhabditis elegans. *Mol. Biol. Cell*, **14**, 2972–2983 (2003).
4. Altman, S., Baer, M., Guerrier-Takada, C. and Vioque, A. Enzymatic cleavage of RNA by RNA. *Trends Biochem. Sci*., **11**, 515–518 (1986).
5. Tinoco Jr, I. and Bustamante, C. How RNA folds. *J. Mol. Biol*., **293**, 271–281 (1999).
6. Hermann, T. and Patel, D. J. RNA bulges as architectural and recognition motifs. *Structure*, **8**, 47–54 (2000).
7. Asseline, U. Development and applications of fluorescent oligonucleotides. *Curr. Org. Chem*., **10**, 491–518 (2006).
8. Piton, N., Mu, Y., Stock, G., Prisner, T. F., Schiemann, O. and Engels, J. W. Base-specific spin-labeling of RNA for structure determination. *Nucl. Acids Res*., **35**, 3128–3143 (2007).
9. Qin, P. Z., Hideg, K., Feigon, J. and W. L. Hubbell, Monitoring RNA base structure and dynamics using site-directed spin labeling. *Biochemistry*, **42**, 6772–6783 (2003).

10. Olieric, V. *et al.* A fast selenium derivatization strategy for crystallization and phasing of RNA structures. *RNA*, **15**, 707–715 (2009).
11. Corey, D. R. Chemical modification: the key to clinical application of RNA interference. *J. Clin. Invest.*, **117,** 3615−3622 (2007).
12. Wachowius, F. and Höbartner, C. Chemical RNA modifications for studies of RNA structure and dynamics. *ChemBioChem*, **11,** 469−480 (2010).
13. Khorana, H. G. Nucleic acid synthesis. *Pure Appl. Chem*., **17**, 349–381 (1968).
14. Gait, M. J. An introduction to modern methods of DNA synthesis. In: Oligonucleotide Synthesis: A Practical Approach. Gait, M. J., ed. 1984. Washington, D.C.: IRL Press Ltd.
15. Milligan, J. F., Groebe, D. R., Witherell, G. W. and Uhlenbeck, O. C. Oligoribonucleotide synthesis using T7 RNA polymerase and synthetic DNA templates. *Nucl. Acids Res*., **15**, 8783–8798 (1987).
16. Piccirilli J. A., Krauch T., Moroney S. E. and Benner S. A.Enzymatic incorporation of a new base pair into DNA and RNA extends the genetic alphabet. *Nature*, **343**, 33–37 (1990).
17. M. Kimoto, Y. Hikida, and I. Hirao, Site-Specific Functional Labeling of Nucleic Acids by *In vitro* Replication and Transcription using Unnatural Base Pair Systems. *Israel J. Chem*., **53**, 450–468 (2013).
18. Ohtsuki, T., Kimoto, M., Ishikawa, M., Mitsui, T., Hirao, I. and Yokoyama, S. Unnatural base pairs for specific transcription. *Proc. Natl. Acad. Sci. USA*, **98**, 4922–4925 (2001).
19. Defrancq, E., Singh, Y. and Spinelli, N. Chemical Strategies for Oligonucleotide-Conjugates Synthesis. *Curr. Org. Chem*., **12**, 263–290 (2008).
20. Best, M. D. Click chemistry and bioorthogonal reactions: unprecedented selectivity in the labeling of biological molecules. *Biochemistry*, **48**, 6571–6584 (2009).
21. Weisbrod, S. H. and Marx, A. Novel strategies for the site-specific covalent labeling of nucleic acids. *Chem. Commun*., 5675–5685 (2008).
22. Paredes, E., Evans, M. and Das, S. R. RNA labeling, conjugation and ligation. *Methods*, **54**, 251–259 (2011).
23. Bevilacqua, P. C. and Turner, D. H. Use of fluorescence spectroscopy to elucidate RNA folding pathways. *Curr. Protoc. Nucl. Acid Chem*., Unit 11.8, (2002).
24. Walter, N. G. Probing RNA structural dynamics and function by fluorescence resonance energy transfer (FRET). *Curr. Protoc. Nucl. Acid Chem*., Unit 11.10 (2003).
25. Zhao, R. and Rueda, D. RNA folding dynamics by single-molecule fluorescence resonance energy transfer. *Methods*, **49**, 112–117 (2009).
26. Zhao, L. and Xia, T. Probing RNA conformational dynamics and heterogeneity using femtosecond time-resolved fluorescence spectroscopy. *Methods*, **49**, 128–135 (2009).
27. Hengesbach, M., Kobitski, A., Voigts-Hoffmann, F., Frauer, C., Nienhaus, G. U. and Helm, M. *Curr. Protoc. Nucl. Acid Chem*., Unit 11.12 (2008).
28. Pecourt, J. M. L., Peon, J. and Kohler, B. Ultrafast internal conversion of electronically excited RNA and DNA nucleosides in water. *J. Am. Chem. Soc*., **122**, 9348–9349 (2000).
29. E. Nir, K. Kleinermanns, L. and Grace, M. S. de Vries. On the Photochemistry of purine nucleobases. *J. Phys. Chem. A*, **105**, 5106–5110 (2001).
30. Cornish, P. V. and Ha, T. A survey of single-molecule techniques in chemical biology. *ACS Chem. Biol*., **2**, 53–61 (2007).
31. Karunatilaka, K. S. and Rueda, D. Single-molecule fluorescence studies of RNA: A decade's progress. *Chem. Phys. Lett*., **476**, 1–10 (2009).
32. Aleman, E. A., Lamichhane, R. and Rueda, D. Exploring RNA folding one molecule at a time. *Curr. Opin. Chem. Biol*., **12**, 647–654 (2008).

33. Ditzler, M. A., Aleman, E. A., Rueda, D. and Walter, N. G. Focus on function: single molecule RNA enzymology. *Biopolymers*, **87**, 302–316 (2007).
34. Stone, M. D., Mihalusova, M., O'Connor, C. M., Prathapam, R., Collins, K. and Zhuang, X. Stepwise protein-mediated RNA folding directs assembly of telomerase ribonucleoprotein. *Nature*, **446**, 458–561 (2007).
35. Steiner, M., Karunatilaka, K. S., Sigel,R. K. and Rueda, D. Single-molecule studies of group II intron ribozymes. *Proc. Natl. Acad. Sci. USA*, **105**, 13853–13858 (2008).
36. Guo, Z., Karunatilaka, K. S. and Rueda, D. Single-molecule analysis of protein-free U2-U6 snRNAs. *Nat. Struct. Mol. Biol*., **16**, 1154–1159 (2009).
37. Rist, M. J. and Marino, J. P. Fluorescent nucleotide base analogs as probes of nucleic acid structure, dynamics and interactions *Curr. Org. Chem*., **6**, 775–793 (2002).
38 Ward, D. C., Reich, E. and Stryer, L. Fluorescence studies of nucleotides and polynucleotides. I. Formycin, 2-aminopurine riboside, 2,6-diaminopurine riboside, and their derivatives. *J. Biol. Chem*., **244**, 1228–1237 (1969).
39. Menger, M., Tuschl, T., Eckstein, F. and Pçrschke, D. Mg(2+)-dependent conformational changes in the hammerhead ribozyme. *Biochemistry*, **35**, 14710–14716 (1996).
40. Kirk, S. R., Luedtke, N. W. and Tor, Y. 2-Aminopurine as a real-time probe of enzymatic cleavage and inhibition of hammerhead ribozymes. *Bioorg. Med. Chem.*, **9**, 2295–2301 (2001).
41. DeJong, E. S., Chang, C. E., Gilson, M. K. and Marino, J. P. Proflavine acts as a Rev inhibitor by targeting the high-affinity Rev binding site of the Rev responsive element of HIV-1. *Biochemistry*, **42**, 8035–8046 (2003).
42. Bradrick, T. D. and Marino, J. P. Ligand-induced changes in 2-aminopurine fluorescence as a probe for small molecule binding to HIV-1 TAR RNA. *RNA*, **10**, 1459–1468 (2004).
43. Mihailescu, M. R. and Marino, J. P. A proton-coupled dynamic conformational switch in the HIV-1 dimerization initiation site kissing complex. *Proc. Natl. Acad. Sci. USA*, **101**, 1189–1194 (2004).
44. Lago, H., Parrott, A. M., Moss, T., Stonehouse, N. J., and Stockley, P. G. Probing the kinetics of formation of the bacteriophage MS2 translational operator complex: identification of a protein conformer unable to bind RNA. *J. Mol. Biol.*, **305**, 1131–1144 (2001).
45. Liang, B., Kahen, E. J., Calvin, K., J., Zhou, M., Blanco, and Li, H. Long-distance placement of substrate RNA by H/ACA proteins. *RNA*, **14**, 2086–2094 (2008).
46. Kaul, M., Barbieri, C. M. and Pilch, D. S. Fluorescence-based approach for detecting and characterizing antibiotic-induced conformational changes in ribosomal RNA: comparing aminoglycoside binding to prokaryotic and eukaryotic ribosomal RNA sequences. *J. Am. Chem. Soc*., **126**, 3447–3453 (2004).
47. Shandrick, S. *et al*. Monitoring molecular recognition of the ribosomal decoding site. *Angew. Chem. Int. Ed.*, **43**, 3177–3182 (2004).
48. Srivatsan, S. G. and Tor, Y. Fluorescent pyrimidine ribonucleotide: synthesis, enzymatic incorporation, and utilization. *J. Am. Chem. Soc*., **129**, 2044–2053 (2007).
49. S. G. Srivatsan, and Y. Tor, Enzymatic incorporation of emissive pyrimidine ribonucleotides. *Chem. Asian J*., **4**, 419–427 (2009).
50. Tanpure, A. A. and Srivatsan, S. G. Conformation-sensitive nucleoside analogues as topology-specific fluorescence turn-on probes for DNA and RNA G-quadruplexes. *Nucl. Acids Res.*, **43**, e149 (2015).
51. Schultheisz, H. L., Szymczyna, B. R., Scott, L. G. and Williamson, J. R. Pathway engineered enzymatic de novo purine nucleotide synthesis. *ACS Chem. Biol*., **3**, 499–511 (2008).

52. Wenter, P. and Pitsch, S. Synthesis of Selectively 15N-Labeled 2′-O-{[(Triisopropylsilyl)oxy]methyl}(tom)-Protected Ribonucleoside Phosphoramidites and Their Incorporation into a Bistable 32Mer RNA Sequence. *Helv. Chim. Acta*, **86**, 3955–3974 (2003).
53. Wenter, P., Bodenhausen, G., Dittmer, J. and Pitsch, S. Kinetics of RNA refolding in dynamic equilibrium by 1H-detected 15N exchange NMR spectroscopy. *J. Am. Chem. Soc*., **128**, 7579–7587 (2006).
54. Kreutz, C. and Micura, R. Modified Nucleosides in Biochemistry Biotechnology and Medicine (Ed.: P. Herdewijn), Wiley-VCH, Weinheim, 3 (2008).
55. Suydam, I. T. and Strobel, S. A. Fluorine substituted adenosines as probes of nucleobase protonation in functional RNAs. *J. Am. Chem. Soc*., **130**, 13639–13648 (2008).
56. Qin, P. Z., Hideg, K., Feigon, J. and W. L. Hubbell, Monitoring RNA base structure and dynamics using site-directed spin labeling. *Biochemistry*, **42**, 6772–6783 (2003).
57. Ramos, A. and Varani, G. A new method to detect long-range protein−RNA contacts: NMR detection of electron−proton relaxation induced by nitroxide spin-labeled RNA. *J. Am. Chem. Soc*., **120**, 10992–10993 (1998).
58. Piton, N., Mu, Y., Stock, G., Prisner, T. F., Schiemann,O. and Engels, J. W. Base-specific spin-labeling of RNA for structure determination. *Nucl. Acids Res*., **35**, 3128–3143 (2007).
59. Piton, N., Schiemann, O., Mu, Y., Stock, G., Prisner, T. and Engels, J. W. Synthesis of spin-labeled RNAs for long range distance measurements by peldor. *Nucleosides Nucleotides Nucleic Acids*, **24**, 771–775 (2005).
60. Ennifar, E., Carpentier, P., Ferrer, J. L., Walter, P. and Dumas, P. X-ray-induced debromination of nucleic acids at the Br K absorption edge and implications for MAD phasing. *Acta Crystallogr. Sect. D Biol. Crystallogr*., **58**, 1262–1268 (2002).
61. Puffer, B., Moroder, H., Aigner, M. and Micura, R. 2'-Methylseleno-modified oligoribonucleotides for X-ray crystallography synthesized by the ACE RNA solid-phase approach. *Nucl. Acids Res*., **36**, 970–983 (2008).
62. Olieric, V. *et al.* A fast selenium derivatization strategy for crystallization and phasing of RNA structures. *RNA*, **15**, 707–715 (2009).
63. Inagaki, Y., Minakawa, N. and Matsuda, A. Synthesis and properties of oligonucleotides containing 4'-selenoribonucleosides. *Nucl. Acids Symp. Ser*., 329–330 (2008).
64. Watts, J. K., Johnston, B. D., Jayakanthan, K., Wahba, A. S., Pinto, B. M. and Damha, M. J. Synthesis and biophysical characterization of oligonucleotides containing a 4'-selenonucleotide. *J. Am. Chem. Soc*., **130**, 8578–8579 (2008).
65. Puffer, B., Moroder, H., Aigner, M. and Micura, R. 2'-Methylseleno-modified oligoribonucleotides for X-ray crystallography synthesized by the ACE RNA solid-phase approach. *Nucl. Acids Res*., **36**, 970–983 (2008).
66. Olieric, V. *et al.* A fast selenium derivatization strategy for crystallization and phasing of RNA structures. *RNA*, **15**, 707–715 (2009).
67. Inagaki, Y., Minakawa, N. and Matsuda,A. Synthesis and properties of oligonucleotides containing 4'-selenoribonucleosides. *Nucl. Acids Symp. Ser*., 329–330 (2008).
68. Dölken, L. *et al.* High-resolution gene expression profiling for simultaneous kinetic parameter analysis of RNA synthesis and decay. *RNA*, **14**, 1959–1972 (1972).
69. Brady, G., Barbara, M. and Iscove, N. N. Representative *in vitro* cDNA amplification from individual hemopoietic cells and colonies. *Methods Mol. Cell. Biol*., **2**, 17–25 (1990).
70. Van Gelder, R. N. *et al.* Amplified RNA synthesized from limited quantities of heterogeneous cDNA. *Proc. Natl. Acad. Sci. USA*, **87**, 1663–1667 (1990).

71. Velculescu, V. E., Zhang, L., Vogelstein, B. and Kinzler, K. W. Serial analysis of gene expression. *Science*, **270**, 484–487 (1995).
72. Nagaraj, S. H., Gasser, R. B. and Ranganathan, S. A hitchhiker's guide to expressed sequence tag (EST) analysis. *Brief Bioinform.*, **8**, 6–21 (2007).
73. Li, Q., Kim, Y., Namm, J., Kulkarni, A., Rosania, G. R., Ahn, Y.-H. and Chang, Y.-T. RNA-selective, live cell imaging probes for studying nuclear structure and function. *Chem. Biol.*, **13**, 615–623 (2006).
74. Lawrence, J. B. and Singer, R. H. Intracellular localization of messenger RNAs for cytoskeletal proteins. *Cell*, **45**, 407–415 (1986).
75. Tyagi, S. and Kramer, F. R. Molecular beacons: probes that fluoresce upon hybridization. *Nat. Biotechnol*., **14**, 303–308 (1996).
76. Kummer, S., Knoll, A., Socher, E., Bethge, L., Herrmann, A. and Seitz, O. Fluorescence imaging of influenza H1N1 mRNA in living infected cells using single-chromophore FIT-PNA. *Angew. Chem. Int. Ed. Engl*., **50**, 1931–1934 (2011).
77. Hovelmann, F., Gaspar, I., Ephrussi, A. and Seitz, O. Brightness enhanced DNA FIT-probes for wash-free RNA imaging in tissue. *J. Am. Chem. Soc*., **135**, 19025–19032 (2013).
78. Bratu, D. P., Cha, B. J., Mhlanga, M. M., Kramer, F. R. and Tyagi, S. Visualizing the distribution and transport of mRNAs in living cells. *Proc. Natl. Acad. Sci. USA*, **100**, 13308–13313 (2003).
79. Briley, W. E. Bondy, M. H. Randeria, P. S., Dupper, T. J. and Mirkin, C. A. Quantification and real-time tracking of RNA in live cells using Sticky-flares. *Proc. Natl. Acad. Sci. USA*, **112**, 9591–9595 (2015).
80. Paige, J. S., Wu, K.Y. and Jaffrey, S. R. RNA mimics of green fluorescent protein. *Science*, **333**, 642–646 (2011).
81. Strack, R. L., Disney, M. D. and Jaffrey, S. R. A superfolding Spinach2 reveals the dynamic nature of trinucleotide repeat-containing RNA. *Nat. Methods*, **10**, 1219–1224 (2013).
82. Filonov, G. S., Moon, J. D., Svensen, N. and Jaffrey, S. R. Broccoli: rapid selection of an RNA mimic of green fluorescent protein by fluorescence-based selection and directed evolution. *J. Am. Chem. Soc*., **136**, 16299–16308 (2014).
83. Sunbul, M. and Jaschke, A. Contact-mediated quenching for RNA imaging in bacteria with a fluorophore-binding aptamer. *Angew. Chem. Int. Ed. Engl*., **52**, 13401–13404 (2013).
84. Kolpashchikov, D. M. Binary malachite green aptamer for fluorescent detection of nucleic acids. *J. Am. Chem. Soc.*, **127**, 12442–12443 (2005).
85. Dolgosheina, E. V. RNA mango aptamer-fluorophore: a bright, high-affinity complex for RNA labeling and tracking. *ACS Chem. Biol*., **9**, 2412–2420 (2014).
86. Bertrand, E., Chartrand, P., Schaefer, M., Shenoy, S. M., Singer, R. H. and Long, R. M. Localization of ASH1 mRNA particles in living yeast. *Mol. Cell*, **2**, 437–445 (1998).
87. Park, H.Y. *et al.* Visualization of dynamics of single endogenous mRNA labeled in live mouse. *Science*, **343**, 422–424 (2014).
88. Rackham, O. and Brown, C. M. Visualization of RNA-protein interactions in living cells: FMRP and IMP1 interact on mRNAs. *EMBO J.*, **23**, 3346–3355 (2004).
89. Valencia-Burton, M., McCullough, R. M., Cantor, C. R. and Broude, N. E. RNA visualization in live bacterial cells using fluorescent protein complementation. *Nat. Methods*, **4**, 421–427 (2007).
90. Valencia-Burton, M. *et al.* Spatiotemporal patterns and transcription kinetics of induced RNA in single bacterial cells. *Proc. Natl. Acad. Sci. USA*, **106**, 16399–16404 (2009).

91. Kellermann, S. J., Rath, A. K. and Rentmeister, A. Tetramolecular fluorescence complementation for detection of specific RNAs *in vitro*. *ChemBioChem*, **14**, 200–204 (2013).
92. Garcia, J. F. and Parker, R. MS2 coat proteins bound to yeast mRNAs block 5' to 3' degradation and trap mRNA decay products: implications for the localization of mRNAs by MS2-MCP system. *RNA*, **21**, 1393–1395 (2015).
93. Usman, N. and Cedergren, R. Exploiting the chemical synthesis of RNA. *Trends Biochem. Sci*., **17**, 334–339 (1992).
94. Beaucage, S. L. and Reese, C. B. Recent advances in the chemical synthesis of RNA. *Curr. Protoc. Nucl. Acid Chem*., Unit 2.16, 1–35 (2009).
95. Chow, C. S. Mahto, S. K. and Lamichhane, T. N. Combined approaches to site-specific modification of RNA. *ACS Chem. Biol*., **3**, 30–37 (2008).
96. Beaucage, S. L. Solid-phase synthesis of siRNA oligonucleotides. *Curr. Opin. Drug Discovery Dev*., **11**, 203–216 (2008).
97. Usman, N., Ogilvie, K. K., Jiang, M. Y. and Cedergren, R. J. Automated chemical synthesis of long oligoribonucleotides using 2'-O-silylated ribonucleoside 3'-O-phosphoramidites on a controlled-pore glass support: Synthesis of a 43-nucleotide sequence similar to the 3'-half molecule of an *Escherichia coli* Formylmethionine tRNA. *J. Am. Chem. Soc.*, **109**, 7845–7854 (1987).
98. Pitsch, S., Weiss, P. A., Jenny, L., Stutz, A. and Wu, X. Reliable chemical synthesis of oligoribonucleotides (RNA) with 2′-O-[(Triisopropylsilyl)oxy]methyl(2′-O-tom)-protected phosphoramidites. *Helv. Chim. Acta*, **84**, 3773–3795 (2001).
99. Scaringe, S. A., Wincott, F. E. and Caruthers, M. H. Novel RNA synthesis method using 5'-O-silyl-2'-O-orthoester protecting groups. *J. Am. Chem. Soc*., **120**, 11820–11821 (1998).
100. McBride, L. J., Kierzek, R., Beaucage,S. L. and Caruthers, M. H. Amidine protecting groups for oligonucleotide synthesis. *J. Am. Chem. Soc.*, **108**, 2040–2048 (1986).
101. Schulhof, J. C. Molko, D. and Teoule, R. The final deprotection step in oligonucleotide synthesis is reduced to a mild and rapid ammonia treatment by using labile base-protecting groups. *Nucl. Acids Res*., **15**, 397–416 (1987).
102. Reddy, M. P., Hanna, N. B. and Farooqui, F. Ultrafast cleavage and deprotection of oligonucleotides synthesis and use of C-*Ac* derivatives. *Nucleosides & Nucleotides*, **16**, 1589–1598 (1997).
103. McMinn, D. L. and Greenberg, M. M. Synthesis of oligonucleotides containing 3'-alkyl amines using N-isobutyryl protected deoxyadenosine phosphoramidite. *Tet. Lett*., **38**, 3123–3126 (1997).
104. Zhu, Q., Delaney, M. O. and Greenberg, M. M. Observation and elimination of N-acetylation of oligonucleotides prepared using fast-deprotecting phosphoramidites and ultra-mild deprotection. *Bioorg. Med. Chem. Lett*., **11**, 1105–1107 (2001).
105. Blackburn, G. M., Gait, M. J., Loakes, D. and Williams, D. M. *Nucleic Acids in Chemistry and Biology* **2006**, *3rd edition*, RSC publications.
106. Barrio, J. R., Barrio, M. C., Leonard, N. J., England, T. E. and Uhlenbeck, O. C. Synthesis of modified nucleoside 3',5'-bisphosphates and their incorporation into oligoribonucleotides with T4 RNA ligase. *Biochemistry*, **17**, 2077–2081 (1978).
107. Gumport, R. I. and Uhlenbeck, O. C. T4 RNA ligase as a nucleic acid synthesis and modification reagent. *Gene Amplif. Anal*., **2**, 313–345 (1981).
108. Purtha, W. E., Coppins, R. L., Smalley, M. K. and Silverman, S. K. General deoxyribozyme-catalyzed synthesis of native 3'-5' RNA linkages. *J. Am. Chem. Soc*., **127**, 13124–13125 (2005).

109. Melton, D. A., Krieg, P. A., Rebagliati, M. R., Maniatis, T., Zinn, K. and Green, M. R. Efficient *in vitro* synthesis of biologically active RNA and RNA hybridization probes from plasmids containing a bacteriophage SP6 promoter. *Nucl. Acids Res*., **12**, 7035–7056 (1984).
110. Jorgensen, E. D., Durbin, R. K., Risman, S. S. and McAllister, W. T. Specific contacts between the bacteriophage T3, T7, and SP6 RNA polymerases and their promoters. *J. Biol. Chem*., **266**, 645–651 (1991).
111. Arnaud-Barbe, N., Cheynet-Sauvion, V., Oriol, G., Mandrand, B. and Mallet, F. Transcription of RNA templates by T7 RNA polymerase. *Nucl. Acids Res*., **26**, 3550–3554 (1998).
112. Caton-Williams J., Lin, L., Smith, M. and Huang, Z. Convenient synthesis of nucleoside 5'-triphosphates for RNA transcription. *Chem. Commun*., **47**, 8142–8144 (2011).
113. Hollenstein, M. Nucleoside triphosphates building blocks for the modification of nucleic acids. *Molecules*, **17**, 13569–13591 (2012).
114. Da Costa, C. P., Fedor, M. J. and Scott, L. G. 8-Azaguanine reporter of purine ionization states in structured RNAs. *J. Am. Chem. Soc*., **129**, 3426–3432 (2007).
115. Chawla, M., Credendino, R., Oliva, R. and Cavallo, L. Structural and energetic impact of non-natural 7-deaza-8-azaadenine and its 7-substituted derivatives on H-bonding potential with uracil in RNA molecules. *J. Phys. Chem. B*., **119**, 12982–12989 (2015).
116. Motorin, Y., Burhenne, J., Teimer, R., Koynov, K., Willnow, S., Weinhold, E. and Helm, M. Expanding the chemical scope of RNA:methyltransferases to site-specific alkynylation of RNA for click labeling. *Nucl. Acids Res*., **39**, 1943–1952 (2011).
117. Onizuka, K., Shibata, A., Taniguchi, Y. and Sasaki, S. Pin-point chemical modification of RNA with diverse molecules through the functionality transfer reaction and the copper-catalyzed azide-alkyne cycloaddition reaction. *Chem. Commun*., **47**, 5004–5006 (2011).
118. Tomkuviene, M., d'Orval, B. C., Cerniauskas, I., Weinhold E. and Klimasauskas, S. Programmable sequence-specific click-labeling of RNA using archaeal box C/D RNP methyltransferases. *Nucl. Acids Res.*, **40**, 6765–6773 (2012).
119. Winz, M. L., Samanta, A., Benzinger, D. and Jäschke, A. Site-specific terminal and internal labeling of RNA by poly(A) polymerase tailing and copper-catalyzed or copper-free strain-promoted click chemistry. *Nucl. Acids Res*., **40**, e78 (2012).
120. Schulz, D., Holstein, J. M. and Rentmeister, A. A chemo-enzymatic approach for site-specific modification of the RNA cap. *Angew. Chem. Int. Ed.*, **52**, 7874–7878 (2013).
121. Holstein, J. M., Schulz, D. and Rentmeister, A. Bioorthogonal site-specific labeling of the 5'-cap structure in eukaryotic mRNAs. *Chem. Commun*., **50**, 4478–4481 (2014).
122. Jones, D. S. *et al.* Immuno specific reduction of antioligonucleotide antibody-forming cells with a tetrakis-oligonucleotide conjugate (LJP 394), a therapeutic candidate for the treatment of *Lupus Nephritis*. *J. Med. Chem*., **38**, 2138–2144 (1995).
123. Jin, S., Miduturu, C. V., McKinney, D. C., and Silverman, S. K. Synthesis of amine- and thiol-modified nucleoside phosphoramidites for site-specific introduction of biophysical probes into RNA. *J. Org. Chem.*, **70**, 4284–4299 (2005).
124. Ghosh, S. S., Kao, P. M., McCue, A. W. and Chappelle, H. L. Use of maleimide-thiol coupling chemistry for efficient syntheses of oligonucleotide-enzyme conjugate hybridization probes. *Bioconjugate Chem*., **1**, 71–76 (1990).
125. Blackburn, G. M., Gait, M. J., Loakes, D. and Williams, D. M. Nucleic Acids in Chemistry and Biology, RSC, UK, 3rd ed., 2006.
126. Voss, E. W. Kinetic measurements of molecular interactions by spectrofluorometry. *J. Mol. Recognit*., **6**, 51–58 (1993).

127. Staudinger, H. and Meyer, J. Über neue organische Phosphorverbindungen III. Phosphinmethylenderivate und Phosphinimine. *Helv. Chim. Acta*, **2**, 635–646 (1919).
128. Saxon, E. and Bertozzi, C. R. Cell surface engineering by a modified Staudinger reaction. *Science*, **287**, 2007–2010 (2000).
129. Laughlin, S. T. and Bertozzi, C. R. Metabolic labeling of glycans with azido sugars and subsequent glycan-profiling and visualization via Staudinger ligation. *Nat. Protoc*., **2**, 2930–2944 (2007).
130. Reddie, K. G., Seo, Y. H., Muse, W. B., Leonard, S. E. and Carroll, K. S. A chemical approach for detecting sulfenic acid-modified proteins in living cells. *Mol. Biosyst*., **4**, 521–531 (2008).
131. Stabler, C. L., Sun, X.-L., Cui, W., Wilson, J. T., Haller, C. A. and Chaikof, E. L. Surface re-engineering of pancreatic islets with recombinant azido-thrombomodulin. *Bioconjugate Chem*., **18**, 1713–1715 (2007).
132. Verdoes, M. *et al*. Azido-BODIPY acid reveals quantitative Staudinger-Bertozzi ligation in two-step activity-based proteasome profiling. *Chembiochem*, **9**, 1735–1738 (2008).
133. Yanagisawa, T., Ishii, R., Fukunaga, R., Kobayashi, T., Sakamoto, K. and Yokoyama, S. Multistep engineering of pyrrolysyl-tRNA synthetase to genetically encode N(epsilon)-(o-azidobenzyloxycarbonyl) lysine for site-specific protein modification. *Chem. Biol*., **15**, 1187–1197 (2008).
134. Comstock, L. R. and Rajski**,** S. R. Methyltransferase-directed DNA strand scission. *J. Am. Chem. Soc*., **127**, 14136–14137 (2005).
135. Wang, C. C. Y., Seo, T. S., Li, Z., Ruparel, H. and Ju, J. Site-specific fluorescent labeling of DNA using Staudinger ligation. *Bioconjugate Chem*., **14**, 697–701 (2003).
136. Lin, F. L., Hoyt, H. M., Van Halbeek, H., Bergman, R. G. and Bertozzi, C. R. Mechanistic investigation of the staudinger ligation. *J. Am. Chem. Soc.*, **127**, 2686–2695 (2005).
137. Wang, C. C. Y., Seo, T. S., Li, Z., Ruparel, H. and Ju, J. Site-specific fluorescent labeling of DNA using Staudinger ligation. *Bioconjugate Chem*., **14**, 697–701 (2003).
138. Comstock, L. R. and Rajski, S. R. Methyltransferase-directed DNA strand scission. *J. Am. Chem. Soc*., **127**, 14136–14137 (2005).
139. Weisbrod, S. H., Baccaro, A. and Marx, A. DNA conjugation by Staudinger ligation. *Nucl. Acids Symp. Ser*., **52**, 383–384(2008).
140. Huisgen, R. 1,3-Dipolar cycloadditions; past and future. *Angew. Chem. Int. Ed. Engl*., **2**, 565–598 (1963).
141. Rostovtsev, V. V., Green, L. G., Fokin, V. V., and Sharpless, K. B. A stepwise huisgen cycloaddition process: copper(I)-catalyzed regioselective "ligation" of azides and terminal alkynes. *Angew. Chem. Int. Ed. Engl*., **41**, 2596–2599 (2002).
142. Tornøe, C. W., Christensen, C. and Meldal, M. Peptidotriazoles on solid phase: [1,2,3]-triazoles by regiospecific copper(i)-catalyzed 1,3-dipolar cycloadditions of terminal alkynes to azides. *J. Org. Chem*., **67**, 3057–3064 (2002).
143. Moses, J. E. and Moorhouse, A. D. The growing applications of click chemistry. *Chem. Soc. Rev*., **36**, 1249–1262 (2007).
144. Breinbauer, R. and Köhn, M. Azide-alkyne coupling: a powerful reaction for bioconjugate chemistry. *Chembiochem*, **4**, 1147–1149 (2003).
145. Rodionov, V. O., Fokin, V. V. and Finn, M. G. Mechanism of the ligand-free Cu(I)-catalyzed azide–alkyne cycloaddition reaction. *Angew. Chem., Int. Ed*., **44**, 2210–2215 (2005).

146.Himo, F., Lovell, T., Hilgraf, R., Rostovtsev, V. V., Noodleman, L., Sharpless, K. B. and Fokin, V. V. Copper(I)-catalyzed synthesis of azoles. DFT study predicts unprecedented reactivity and intermediates. *J. Am. Chem. Soc*., **127**, 210–216 (2005).
147.Zhang, L., Chen, X., Xue, P., Sun, H. H., Williams, I. D., Sharpless, K. B., Fokin, V. V. and Jia, G. Ruthenium-catalyzed cycloaddition of alkynes and organic azides. *J. Am. Chem. Soc*., **127**, 15998–15999 (2005).
148.Meldal, M. and Tornoe, C.W. Cu-catalyzed azide-alkyne cycloaddition. *Chem. Rev*., **108**, 2952–3015 (2008).
149.Hein, J. E., Tripp, J. C., Krasnova, L. B., Sharpless, K. B. and Fokin, V. V. Copper(I)-catalyzed cycloaddition of organic azides and 1-iodoalkynes. *Angew. Chem., Int. Ed*., **48**, 8018–8021 (2009).
150.Chan, T. R., Hilgraf, R., Sharpless, K. B. and Fokin, V. V. Polytriazoles as copper(I)-stabilizing ligands in catalysis. *Org. Lett*., **6**, 2853–2855 (2004).
151.Hong, V., Presolski, S. I., Ma, C. and Finn, M. G. Analysis and optimization of copper-catalyzed azide-alkyne cycloaddition for bioconjugation. *Angew. Chem., Int. Ed*., **48**, 9879–9883 (2009).
152.Seo, T. S., Li, Z., Ruparel, H. and Ju, J. Click chemistry to construct fluorescent oligonucleotides for DNA sequencing. *J. Org. Chem*., **68**, 609–612 (2003).
153.Burrows, C. J. and Muller, J. G. Oxidative nucleobase modifications leading to strand scission. *Chem. Rev*., **98**, 1109–1152 (1998).
154.Weller, R. L. and Rajski, S. R. DNA methyltransferase-moderated click chemistry. *Org. Lett*., **7**, 2141–2144 (2005).
155.Gramlich, P. M. E., Warncke, S., Gierlich, J. and Carell, T. Click-click-click: single to triple modification of DNA. *Angew. Chem. Int. Ed. Engl*., **47**, 3442–3444 (2008).
156.Gierlich, J., Burley, G. A., Gramlich, P. M. E., Hammond, D. M. and Carell, T. Click chemistry as a reliable method for the high-density postsynthetic functionalization of alkyne-modified DNA. *Org. Lett*., **8**, 3639–3642 (2006).
157.Gramlich, P. M. E., Wirges, C. T., Gierlich, J. and Carell, T. Synthesis of modified DNA by PCR with alkyne-bearing purines followed by a click reaction. *Org. Lett*., **10**, 249–251 (2008).
158.Salic, A. and Mitchison, T. J. A chemical method for fast and sensitive detection of DNA synthesis *in vivo*. *Proc. Natl. Acad. Sci. USA*, **105**, 2415–2420 (2008).
159.Neef, A. B. and Luedtke, N. W. Dynamic metabolic labeling of DNA *in vivo* with arabinosyl nucleosides. *Proc. Natl. Acad. Sci. USA*, **108**, 20404–20409 (2011).
160.El-Sagheer, A. H. and Brown, T. New strategy for the synthesis of chemically modified RNA constructs exemplified by hairpin and hammerhead ribozymes. *Proc. Natl. Acad. Sci. USA*, **107**, 15329– 15334 (2010).
161.Paredes, E., Evans, M. and Das, S. R. RNA labeling, conjugation and ligation. *Methods*, **54**, 251–259 (2011).
162.Jao, C. Y. and Salic, A. Exploring RNA transcription and turnover *in vivo* by using click chemistry. *Proc. Natl. Acad. Sci. USA*, **105**, 15779–15784 (2008).
163.Grammel, M., Hang, H. and Conrad, N. Chemical reporters for monitoring RNA synthesis and poly(A) tail dynamics. *ChemBioChem*, **13**, 1112–1115 (2012).
164.Qua, D., Zhou, L., Wanga, W., Wang, Z., Wang, G., Chi, W. and Zhang, B. 5-Ethynylcytidine as a new agent for detecting RNA synthesis in live cells by "click" chemistry. *Anal. Biochem*., **434**, 128–135 (2013).
165.Curanovic, D., Cohen, M., Singh, I., Slagle, C. E., Leslie, C. S. and Jaffrey, S. R. Global profiling of stimulus-induced polyadenylation in cells using a poly(A) trap. *Nat. Chem. Biol*., **9**, 671–673 (2013).

166. Agard, N. J., Prescher, J. A. and Bertozzi, C. R. A strain-promoted [3+2] azide-alkyne cycloaddition for covalent modification of biomolecules in living systems. *J. Am. Chem. Soc.*, **126**, 15046–15047 (2004).
167. Baskin, J. M. *et al.* Copper-free click chemistry for dynamic *in vivo* imaging. *Proc. Natl. Acad. Sci. USA*, **104**, 16793–16797 (2007).
168. Codelli, J. A., Baskin, J. M., Agard, N. J. and Bertozzi, C.R. Second-generation difluorinated cyclooctynes for copper-free click chemistry. *J. Am. Chem. Soc.*, **130**, 11486–11493 (2008).
169. Ning, X., Guo, J., Wolfert, M. A. and Boons, G. J. Visualizing metabolically labeled glycoconjugates of living cells by copper-free and fast huisgen cycloadditions. *Angew. Chem. Int. Ed.*, **47**, 2253–2255 (2008).
170. Debets, M. F., van Berkel, S. S., Schoffelen, S., Rutjes, F. P., van Hest, J. C. and van Delft, F. L. Aza-dibenzocyclooctynes for fast and efficient enzyme PEGylation via copper-free (3+2) cycloaddition. *Chem. Commun.*, **46**, 97–99 (2010).
171. Dommerholt, J. *et al.* Readily accessbile bicyclononynes for bioorthogonal labeling and three-dimensional imaging of living cells. *Angew. Chem. Int. Ed.*, **49**, 9422–9425 (2010).
172. Shelbourne, M., Chen, X., Brown, T. and El-Sagheer, A. H. Fast copper-free click DNA ligation by the ring-strain promoted alkyne-azide cycloaddition reaction. *Chem. Commun*., **47**, 6257–6259 (2011).
173. Marks, I. S., Kang, J. S., Jones, B. T., Landmark, K. J., Cleland, A. J. and Taton, T. A. Strain-promoted "click" chemistry for terminal labeling of DNA. *Bioconjugate Chem.*, **22**, 1259–1263 (2011).
174. Neef, A. B. and Luedtke, N. W. An azide-modified nucleoside for metabolic labeling of DNA. *ChemBioChem*, **15,** 789−793 (2014).
175. Winz, M. L., Samanta, A., Benzinger, D. and Jäschke, A. Site-specific terminal and internal labeling of RNA by poly(A) polymerase tailing and copper-catalyzed or copper-free strain-promoted click chemistry.*Nucl. Acids Res*., **40**, e78 (2012).
176. Holstein, J. M., Schulz, D. and Rentmeister, A. Bioorthogonal site-specific labeling of the 5'-cap structure in eukaryotic mRNAs. *Chem. Commun*., **50**, 4478–4481 (2014).
177. Santner, T., Hartl, M., Bister, K. and Micura, R. Efficient access to 3'-terminal azide-modified RNA for inverse click-labeling patterns. *Bioconjugate Chem*., **25**, 188−195 (2014).
178. Pozsgay, V., Vieira, N. E. and Yergey, A. A Method for Bioconjugation of carbohydrates using Diels−Alder cycloaddition. *Org. Lett.*, **4**, 3191–3194 (2002).
179. Jouanno, L. A. *et al.* Kondrat'eva Ligation: Diels–Alder-based irreversible reaction for bioconjugation. *J. Org. Chem.*, **79**, 10353–10366 (2014).
180. Dewar, M. J. S., Olivella, S. and Stewart, J. J. P. Mechanism of the Diels-Alder reaction: reactions of butadiene with ethylene and cyanoethylenes. *J. Am. Chem. Soc*., **108**, 5771–5779 (1986).
181. Seelig, B. and Jäschke, A. A small catalytic RNA motif with Diels-Alderase activity. *Chem. Biol*., **6**, 167–176 (1999).
182. Borsenberger, V. and Howorka, S. Diene-modified nucleotides for the Diels-Alder-mediated functional tagging of DNA. *Nucl. Acids. Res*., **37**, 1477–1485 (2009).
183. Tona, R. and Häner, R. Functionalisation of a diene-modified hairpin mimic via the Diels-Alder reaction. *Chem. Commun*., 1908–1909 (2004).
184. Tarasow, T. M., Tarasow,S. L. and Eaton, B. E. RNA-catalysed carbon-carbon bond formation. *Nature*, **389**, 54–57 (1997).
185. Balcar, J., Chrisam, G., Huber, F. X. and Sauer, J. Reaktivität von stick stoff-heterocyclen genenüber cyclooctin als dienophil. *Tet. Lett.*, **24**, 1481–1484 (1983).

186. Thalhammer, F., Wallfahrer, U. and Sauer, J. Reaktivität einfacher offenkettiger und cyclischer dienophile bei diels-alder-reaktionen mit inversem elektronenbedarf. *Tet. Lett.*, **31**, 6851–6854 (1990).
187. Sauer, J., Heldmann, D. K., Hetzenegger, J., Krauthan, J., Sichert, H. and Schuster, J. 1,2,4,5-tetrazine: Synthesis and reactivity in [4+2] cycloadditions. *Eur. J. Org. Chem.*, **1998**, 2885–2896 (1998).
188. Blackman, M. L., Royzen, M. and Fox, J. M. Tetrazine ligation: Fast bioconjugation based on inverse-electron-demand diels-alder reactivity. *J. Am. Chem. Soc.*, **130**, 13518–13519 (2008).
189. Devaraj, N. K., Weissleder, R. and Hilderbrand, S. A. Tetrazine-based cycloadditions: Application to pretargeted live cell imaging. *Bioconjugate Chem.*, **19**, 2297–2299 (2008).
190. Devaraj, N. K., Hilderbrand, S., Upadhyay, R., Mazitschek, R. and Weissleder, R. Bioorthogonal turn-on probes for imaging small molecules inside living cells. *Angew. Chem. Int. Ed.*, **49**, 2869–2872 (2010).
191. Patterson, D. M., Nazarova, L. A., Xie, B., Kamber, D. N. and Prescher, J. A. Functionalized cyclopropenes as bioorthogonal chemical reporters. *J. Am. Chem. Soc.*, **134**, 18638–18643 (2012).
192. Yang, J., Seckute, J., Cole, C. M. and Devaraj, N. K. Live-cell imaging of cyclopropene tags with fluorogenic tetrazine cycloadditions. *Angew. Chem. Int. Ed.*, **51**, 7476–7479 (2012).
193. Lang, K., Davis, L., Torres-Kolbus, J., Chou, C., Deiters, A. and Chin, J. W. Genetically encoded norbornene directs site-specific cellular protein labeling via a rapid bioorthogonal reaction. *Nat. Chem.*, **4**, 298–304 (2012).
194. Šečkutė, J., Yang, J. and Devaraj, N. K. Rapid oligonucleotide-templated fluorogenic tetrazine ligations. *Nucl. Acids Res.*, **41**, e148 (2013).
195. Bußkamp, H., Batroff, E., Niederwieser, A., Abdel-Rahman, O. S., Winter, R. F., Wittmann, V. and Marx, A. Efficient labeling of enzymatically synthesized vinyl-modified DNA by an inverse-electron-demand Diels-Alder reaction. *Chem. Commun.*, **50**, 10827–10829 (2014).
196. Schoch, J., Wiessler, M. and Jäschke, A. Post-synthetic modification of DNA by inverse-electron-demand Diels-Alder reaction. *J. Am. Chem. Soc*., **132**, 8846–8847 (2010).
197. Winz, M. L., Linder, E. C., Andre, T., Becker J. and Jäschke, A. Nucleotidyl transferase assisted DNA labeling with different click chemistries. *Nucl. Acids Res*., **43**, e110 (2015).
198. Holstein, J. M. Stummer, D. and Rentmeister, A. Enzymatic modification of 5′-capped RNA with a 4-vinylbenzyl group provides a platform for photoclick and inverse electron-demand Diels–Alder reaction. *Chem. Sci*., **6**, 1362–1369 (2015).
199. Rieder, U. and Luedtke, N. W. Alkene–Tetrazine ligation for imaging cellular DNA. *Angew. Chem. Int. Ed*., **53,** 9168−9172 (2014).
200. Domnick, C., Eggert, F. and Kath-Schorr, S. Site-specific enzymatic introduction of a norbornene modified unnatural base into RNA and application in post-transcriptional labeling. *Chem. Commun.*, **51**, 8253–8256 (2015).

Chapter 2

Alkyne-modified UTP analogs as bioorthogonal chemical label for the *in vitro* posttranscriptional functionalization of RNA by using azide-alkyne cycloaddition reaction

2.1 Introduction

Chemical functionalization strategy based on bioorthogonal reactions has emerged as a valuable tool in nucleic acid diagnosis and in nucleic acid-based nanotechnological applications.[1-7] Typically, this method involves a two-step procedure in which a precursor containing a reactive functionality is incorporated into the oligonucleotide (ON) by either chemical or enzymatic means and a chemoselective reaction is carried out between the labeled ON and its cognate reactive counterpart to afford the desired functionalized ON. The examples of bioorthogonal reactions used in the labeling of nucleic acids include Staudinger ligation,[8-15] copper-catalyzed azide-alkyne cycloaddition (CuAAC),[16-25] strain-promoted azide-alkyne cycloaddition (SPAAC)[26-31] and inverse electron demand Diels-Alder reactions.[32-38] Among these reactions, azide-alkyne cycloaddition reaction has been widely used as this reaction is very specific and reasonably fast.[39-41] Moreover, the incorporation of these small reactive groups minimally perturbs the native structure of the ONs.[42] While much of the initial efforts were focused on optimizing the conditions for postsynthetic modification of DNA, recently, the focus has shifted towards applying this methodology to label RNA for various applications.[43,44]

Two main strategies have so far been employed to label RNA postsynthetically by azide-alkyne cycloaddition reaction, and they are: (i) direct incorporation of reactive functionalities by solid-phase ON synthesis protocol or polymerase enzymes using appropriate substrates[45-49] and (ii) chemo-enzymatic incorporation of reactive functionalities into ONs using transferase enzymes, which show promiscuity in substrate selectivity.[50-55] The bioconjugation is then performed with cognate reactive partner by using CuAAC or SPAAC reaction. Although the azide group can participate in a broad range of bioorthogonal reactions, its incorporation into ONs is not straight forward because the azides are not stable under phosphoramidite ON synthesis conditions.[56] Nevertheless, few methods have been developed to introduce azide groups by using 3'-terminal azide-modified resin support and by azide displacement reaction on the solid-support.[57-60] Recently, our group developed a small set of azide-containing UTP analogs, which are effectively incorporated into RNA ONs by T7 RNA polymerase. The azide-labeled RNAs can be readily functionalized posttranscriptionally by using Staudinger ligation, CuAAC and SPAAC reactions.[61,62] In another example, site-specific posttranscriptional click functionalization of RNA has been

achieved by incorporating azide group site-specifically into RNA by transcription reaction in the presence of an unnatural nucleotide base pair.[63]

Unlike azides, alkynes are more stable and can be readily incorporated into ONs by using terminal alkyne-modified phosphoramidites and nucleotides.[43,44] Following the incorporation of alkyne moieties the bioconjugation is performed with biophysical azide-tags in the presence of Cu(II) salt, ascorbic acid and a Cu(I) stabilizing ligand (e.g., tris(hydroxypropyltriazolyl)methylamine, THPTA), which protects the nucleic acid from oxidative damage.

Interestingly, alkynes exhibit characteristic strong Raman scattering in the range of 2100–2250 cm^{-1} with high contrast, which apparently falls in the Raman-silent region of the cells (1800–2800 cm^{-1}).[64,65] Bioconjugates made of this unique bioorthogonal vibrational frequency tag has been recently utilized in the detection of biomacromolecules including nucleic acids in cells by means of Raman spectroscopy.[66-68] In another example, a clickable alkyne nucleoside has been aptly utilized in expanding the chemical space of nucleic acid libraries in generating nucleobase-modified DNA aptamers with excellent recognition properties.[69] Encouraged by these useful chemical and spectroscopic features of the alkyne functionality, we sought to expand its functional repertoire by developing new alkyne-modified ribonucleoside analogs, which could be suitable for (i) high density functionalization of RNA transcripts, (ii) selection of robust RNA aptamers, and (iii) metabolic labeling and imaging of cellular RNA by using click reaction and Raman spectroscopy. Such tools are particularly desirable as alkyne-bearing ribonucleoside analogs suitable for both cell-free and in cells analysis of RNA is scarce.

In this chapter, we describe the synthesis of a new alkyne-modified UTP analog, 5-(1,7-octadinyl)uridine triphosphate (ODUTP). Further, we tested the enzymatic incorporation of ODUTP and 5-ethynyl uridine triphosphate (EUTP) into RNA transcripts by using T7 RNA polymerase. Additionally, the alkyne-modified RNA transcripts containing (EU and ODU) are readily functionalized posttranscriptionally by using CuAAC reaction with a variety of azide substrates ranging from fluorescent probe to affinity tag to amino acid and sugar. Furthermore, literature precedence and our preliminary spectroscopic analysis provide evidence that ODU label could be potentially suitable for dual imaging of RNA by click chemistry as well as by Raman spectroscopy.

2.2 Result and Discussion

2.2.1 Synthesis of alkyne-modified ribonucleosides and respective triphosphates analogs

The prerequisite of labeling RNA by Click reaction demands incorporation of sterically undemanding and potentially reactive alkyne functionality into RNA. In order to utilized *in vitro* transcription reactions to incorporate the alkyne moiety into a RNA ON, we synthesized alkyne-modified UTP analogs **5** and **6** as precursors from their corresponding ribonucleosides **3** and **4** (Scheme 1). The alkyne-modified ribonucleoside **4** (ODU) was synthesized using analogous literature procedure known for deoxyribonucleoside analog.[19] The synthesis of alkyne-modified triphosphates **6** was accomplish by performing a one pot two step reaction on ribonucleoside **4** using freshly distilled $POCl_3$ and bistributylammonium pyrophosphate in trimethylphosphate. The synthesis of ribonucleoside **3** (EU) was already reported.[70] The alkyne-modified triphosphates **5** and **6** were extensively purified using DEAE-sephadex and reverse phase chromatography prior to *in vitro* transcription reactions.

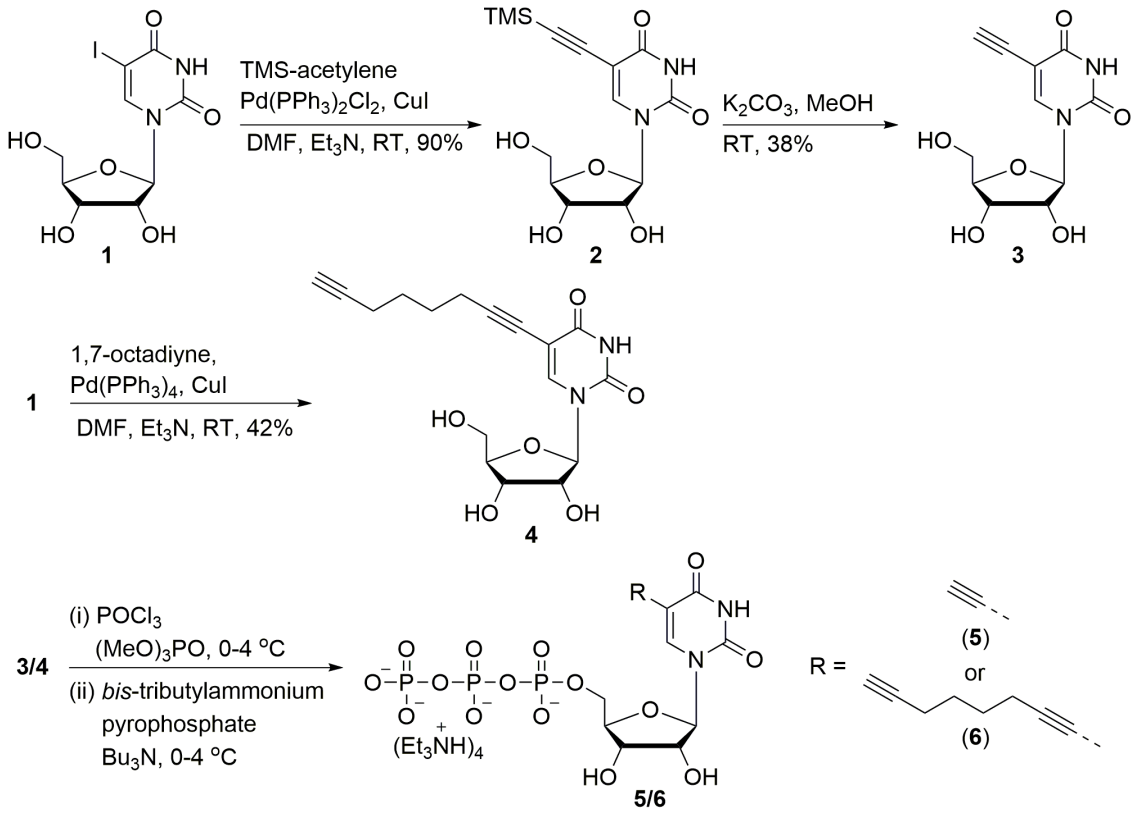

Scheme 1. Synthesis of alkyne-modified UTP analogs **5** and **6** from their corresponding ribonucleosides **3** and **4** respectively.

2.2.2 Enzymatic incorporation alkyne-modified EUTP (5) and ODUTP (6)

The efficacy and scope of *in vitro* transcription reaction in generating EU- and ODU-labeled RNA was assessed by performing reactions in the presence of T7 RNA polymerase and various DNA templates (**D1**–**D5**). The templates contained one or two dA residues in the coding region to guide the incorporation of monophosphate of EU and ODU into RNA transcripts (Figure 1). Further, the templates also contained a single dT nucleoside at the 5'-end of the coding region of each template. Transcription reactions performed in the presence of GTP, CTP, α-^{32}P ATP and UTP/**5**/**6** were analyzed by denaturing polyacrylamide gel electrophoresis (PAGE). Under this reaction condition, only the full-length RNA transcript formed in a successful reaction will contain an α-^{32}P adenosine radiolabel at the 3'-end. Hence, upon phosphor imaging full-length RNA transcripts would be detected and truncated transcripts resulting from failed reactions would remain undetected.

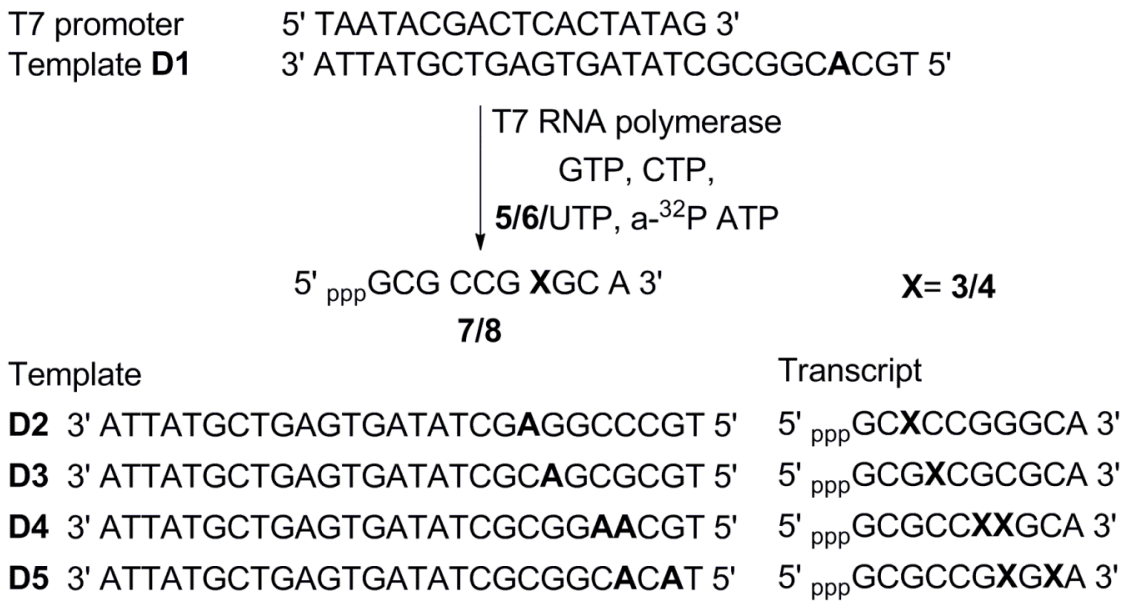

Figure 1. Incorporation of EUTP **5** and ODUTP **6** into RNA ONs by *in vitro* transcription reactions. Incorporation of **5** and **6** in the presence of DNA template **D1** will produce RNA transcripts **7** and **8**, containing EU and ODU respectively. Transcripts resulting from **D2–D5** are also shown.

Transcription reaction with EUTP/ODUTP and template **D1** resulted in the formation of EU- and ODU-labeled RNA transcripts **7** and **8** in very good yield as compared to a control reaction with natural UTP (Figure 2, lane 2). Noticeable reduction in the mobility of alkyne-modified RNA ON **7** and **8** further indicated the incorporation of the heavier nucleotide during transcription reaction (Figure 2, compare lanes 1 and 2). Further, full-length transcript was not formed in a control reaction carried out in the absence of UTP and **5**/**6**, which ruled out any misincorporation by RNA polymerase during transcription reactions

(Figure 2, lane 3). The competitive incorporation of natural UTP versus modified UTP by the enzyme was assessed by doing a reaction in the presence of 1:1 concentration of UTP and **5**/**6**. Interestingly, the RNA polymerase incorporated both EUTP and ODUTP with comparable efficiency in presence of UTP (Figure 2, lane 4). Reactions with other DNA templates (**D2**–**D5**) showed that RNA ONs containing alkyne modification at one or two sites could be generated in moderate to very good yields (Figure 2, lanes 6, 8, 10 and 12). Along with full-length transcripts, faint bands corresponding to random non-coded incorporation products (e.g., N+1 and N+2) were also formed. Such transcription products are often formed in reactions catalyzed by T7 RNA polymerase.[71]

RNA ON **7** and **8** was subjected to further analysis to confirm the presence of EU/ODU labels in the RNA transcript. Mass analysis of **7**/**8** (Figure 3) and HPLC analysis of enzymatic digestion products of **7** (Figure 4) and **8** (Figure 5) unambiguously ascertained the presence of EU- and ODU- labels in the full-length RNA transcript (Table 1). Moreover, UV-thermal melting analysis of duplexes made of ODU-labeled RNA and control unmodified RNA revealed that ODU slightly destabilized the duplex (Figure 6 and 7).

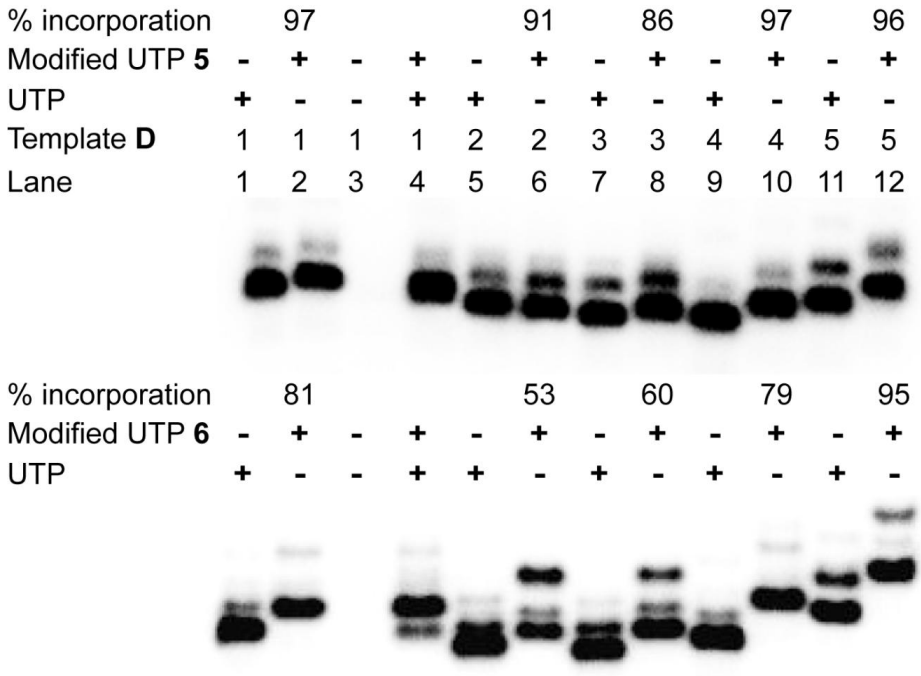

Figure 2. Transcription reactions were performed with templates **D1**−**D5** and T7 polymerase in the presence of UTP and or modified UTPs **5** and **6**. % formation of modified full-length transcript is given with respect to the amount of full-length transcript formed in the presence of natural NTPs.

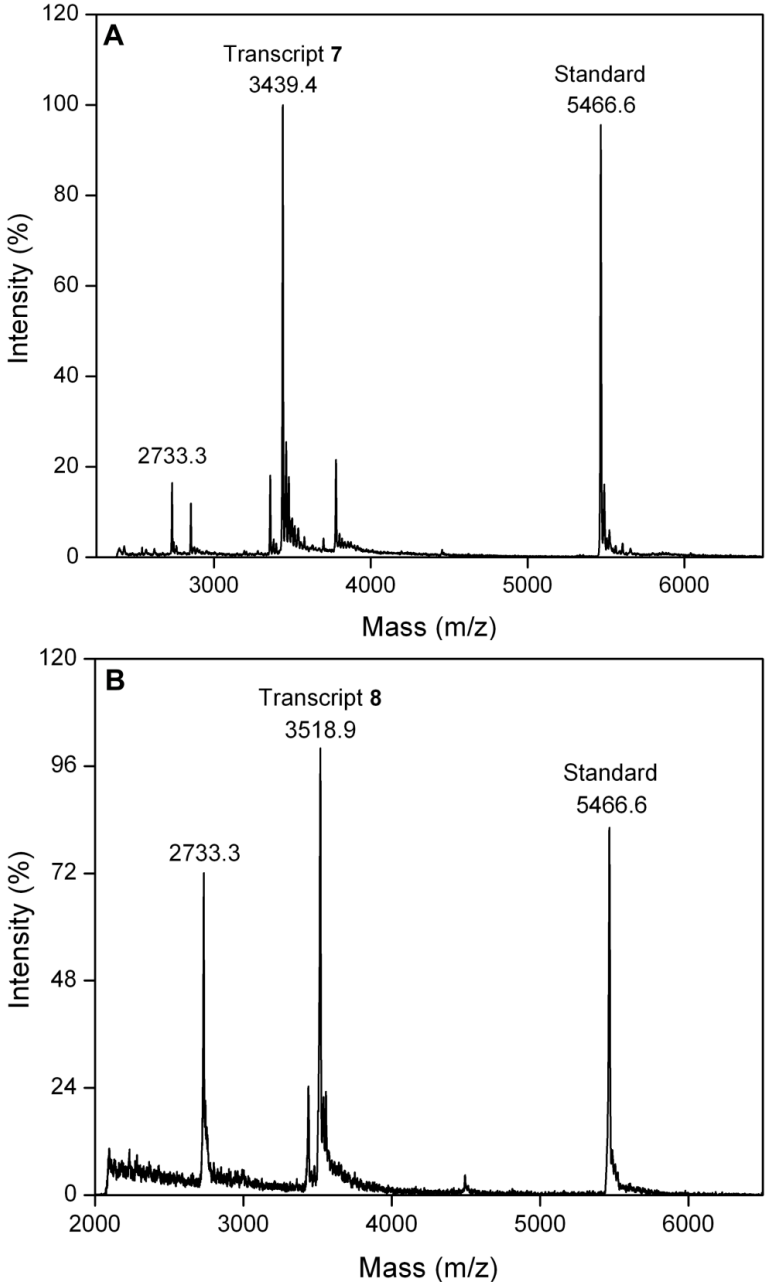

Figure 3 MALDI-TOF mass spectrum of alkyne-modified RNA transcripts **7** and **8** calibrated relative to the +1 and +2 ion of an internal 18-mer DNA oligonucleotide standard (m/z for +1 and +2 ion are 5466.6 and 2733.3, respectively). (**A**) Calcd. For **7**: 3438.9 [M]; found: 3439.4; (**B**) Calcd. For **8**: 3519.2 [M]; found: 3518.9.

Table 1 ε_{260}, isolated yield and MALDI-TOF mass data of alkyne-modified RNA transcripts obtained from large-scale transcription reactions with template **D1**.

RNA Transcript	ε_{260} ($M^{-1}cm^{-1}$)	Isolated yield (nmol)[a]	Calcd. mass	Observed mass
7	85040	18	3438.9	3439.4
8	84680	15	3519.2	3518.9

[a] Yield from large-scale transcription reactions (250 μL volume reaction).

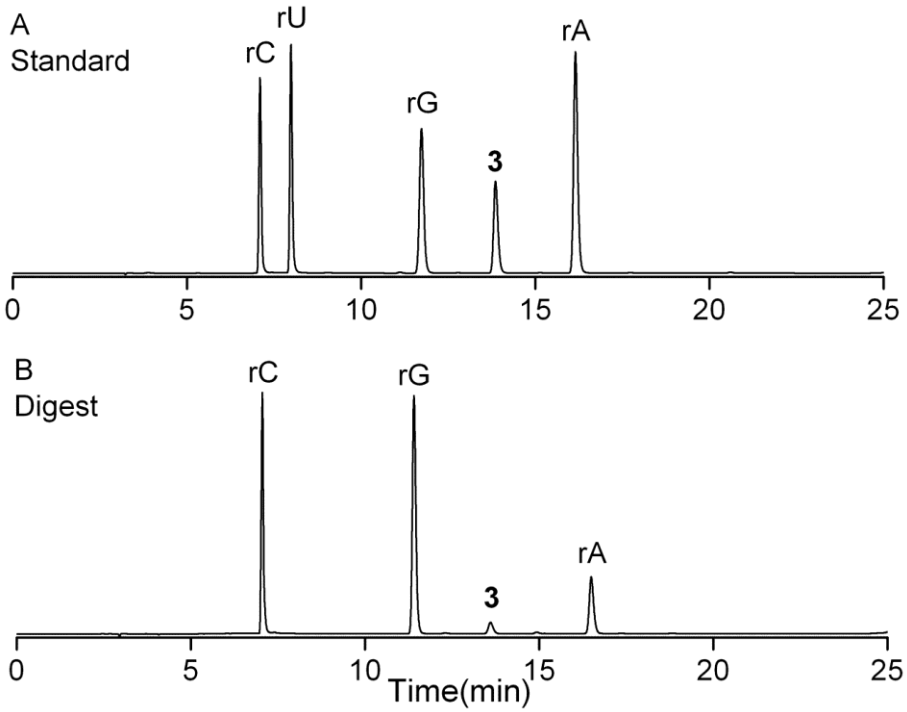

Figure 4. HPLC chromatogram of ribonucleoside products obtained from an enzymatic digestion of RNA transcript 7 at 260 nm. (top) A standard mix of natural ribonucleosides and 3. (B) RNA ON 7 digests. Mobile phase A: 100 mM TEAA (pH 7.5); mobile phase B: acetonitrile. Flow rate: 1 mL/min. Gradient: 0−10% B in 20 min and 10−100% B in 10 min.

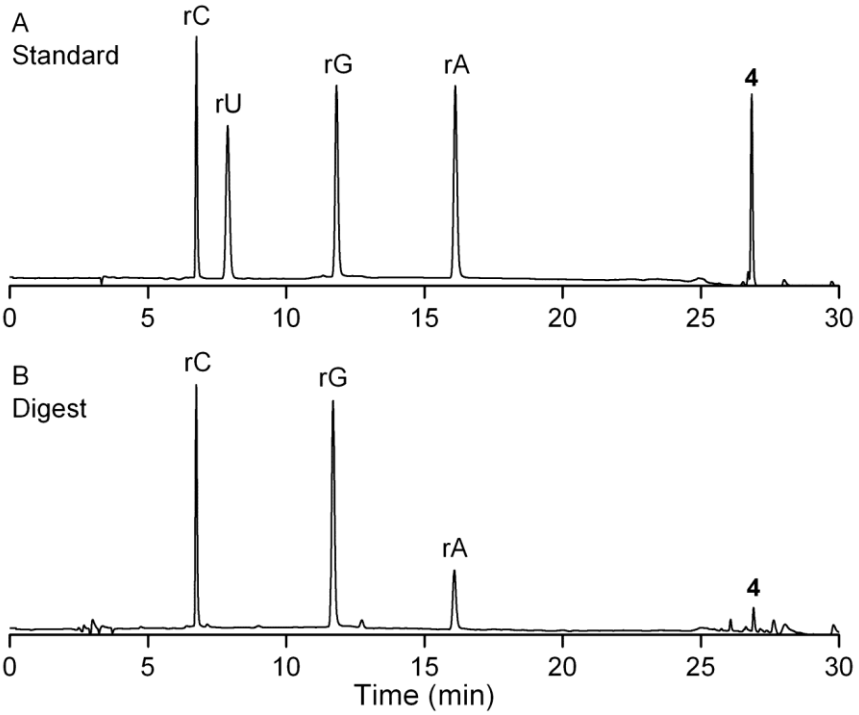

Figure 5. HPLC chromatogram of ribonucleoside products obtained from an enzymatic digestion of RNA transcript 8 at 260 nm. (A) A standard mix of natural ribonucleosides and 4. (B) RNA ON 8 digests. Mobile phase A: 100 mM TEAA (pH 7.5); mobile phase B: acetonitrile. Flow rate: 1 mL/min. Gradient: 0−10% B in 20 min and 10−100% B in 10 min.

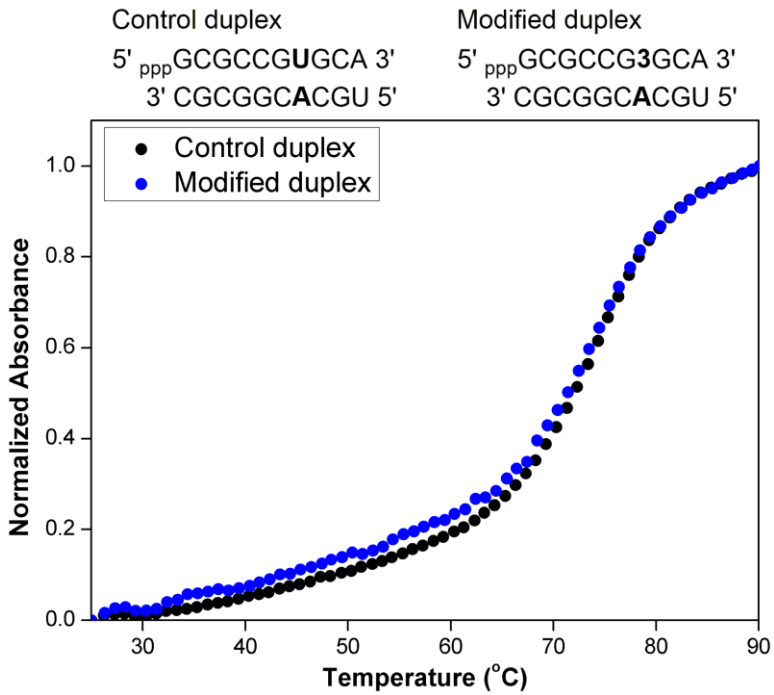

Figure 6. UV-thermal melting of control unmodified duplex (black, 1 µM) and EU-modified duplex (blue, 1 µM) in 20 mM cacodylate buffer (pH 7.1, 500 mM NaCl, 0.5 mM EDTA). Duplexes were formed by heating a 1:1 mixture of the ONs at 90 °C for 3 min and cooling the solutions slowly to room temperature. T_m for control duplex was 75.8 ± 0.2 °C and modified duplexes was 75.1 ± 0.5°C.

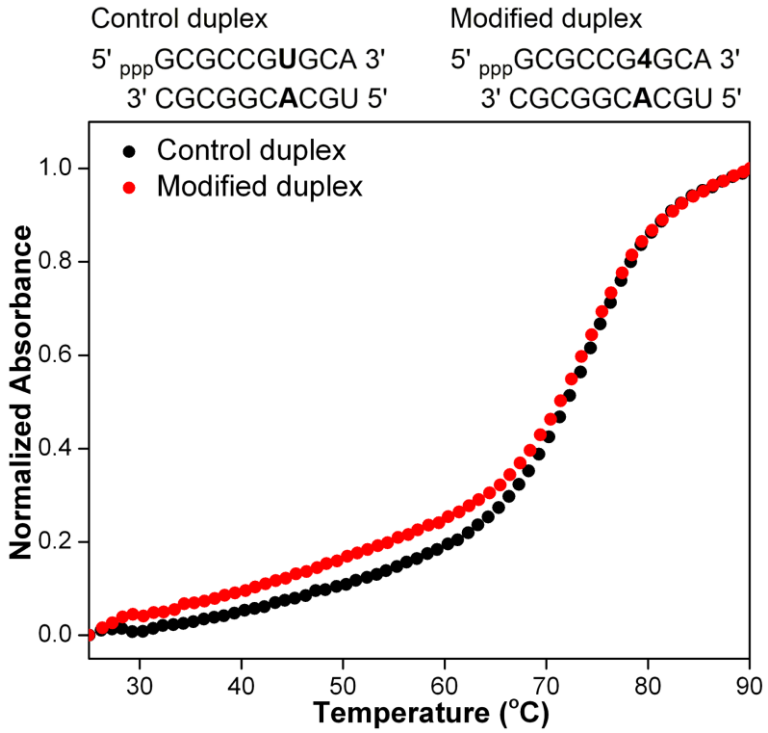

Figure 7. UV-thermal melting of control unmodified duplex (black, 1 µM) and ODU-modified duplex (red, 1 µM) in 20 mM cacodylate buffer (pH 7.1, 500 mM NaCl, 0.5 mM EDTA). Duplexes were formed by heating a 1:1 mixture of the ONs at 90 °C for 3 min and cooling the solutions slowly to room temperature. T_m for control duplex was 76.0 ± 0.7 °C and modified duplexes was 75.4 ± 0.5 °C.

2.2.4 Posttranscriptional chemical functionalization of RNA ONs 7 and 8

The alkyne-modified RNA ONs **7** and **8** were subjected to posttranscriptional chemical modification by click reaction using series of azide substrates such as fluorescent, affinity,[72] sugar[73] and amino acid tag **9−13** (Figure 8). The reaction was carried out in the presence of water-soluble Cu (I) stabilizing ligand, tris-(3-hydroxypropyltriazolylmethyl) amine (THPTA), $CuSO_4$ (as a copper source) and sodium ascorbate (as a reducing agent) at 37 °C for 30 min. The use of water-soluble Cu (I) stabilizing ligand accelerates the click reaction and additionally protects the RNA from degradation during the course of reaction. After completion of click reactions, the corresponding click products were purified by PAGE and analyzed by MALDI-TOF mass analysis. We found that click reactions with RNA ON **8** gave very good isolable yield of the click products after PAGE purification compared to RNA ON **7** (Scheme 2, Table 2). This is presumably due to longer linker present in transcript **8** which is more accessible for cycloaddition reaction with azide counterparts. These results demonstrate the robustness and suitability of click reactions for the postsynthetic labeling of alkyne-modified RNAs. These labeled RNA can be utilised as biophysical probes in diverse biological assays.

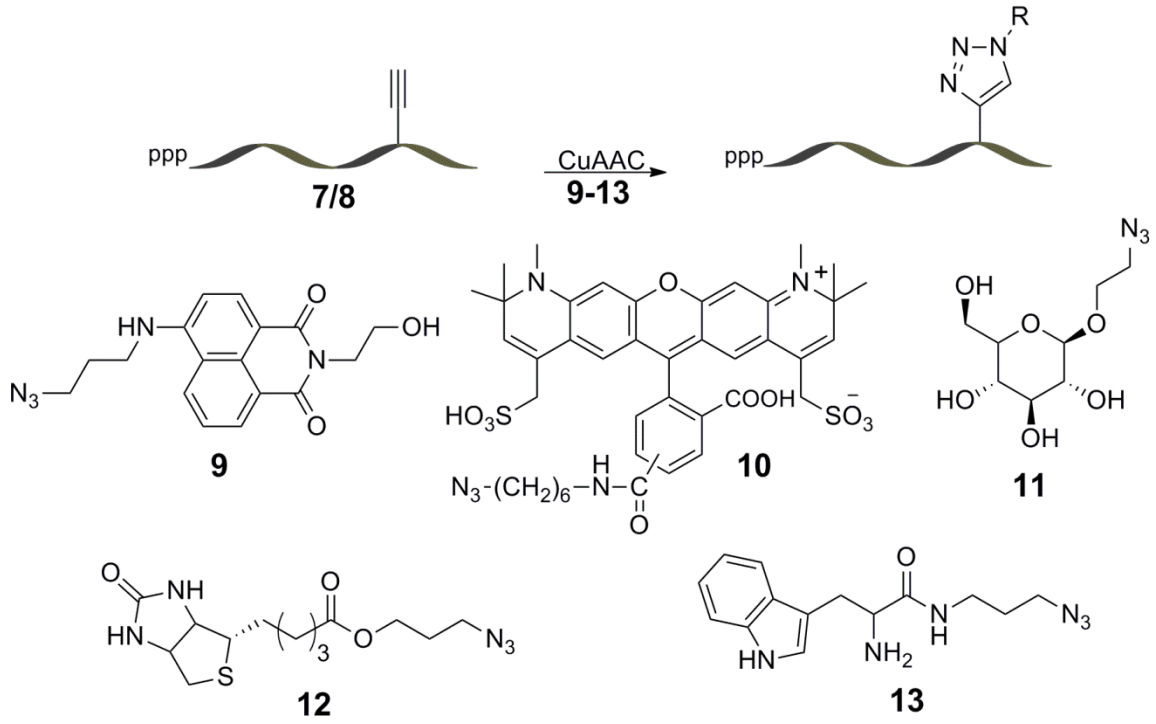

Figure 8. CuAAC reactions with alkyne-modified RNA ONs **7** and **8** with series of azides substrates **9−13** containing flourecent, affinity, sugar and amino acid tags.

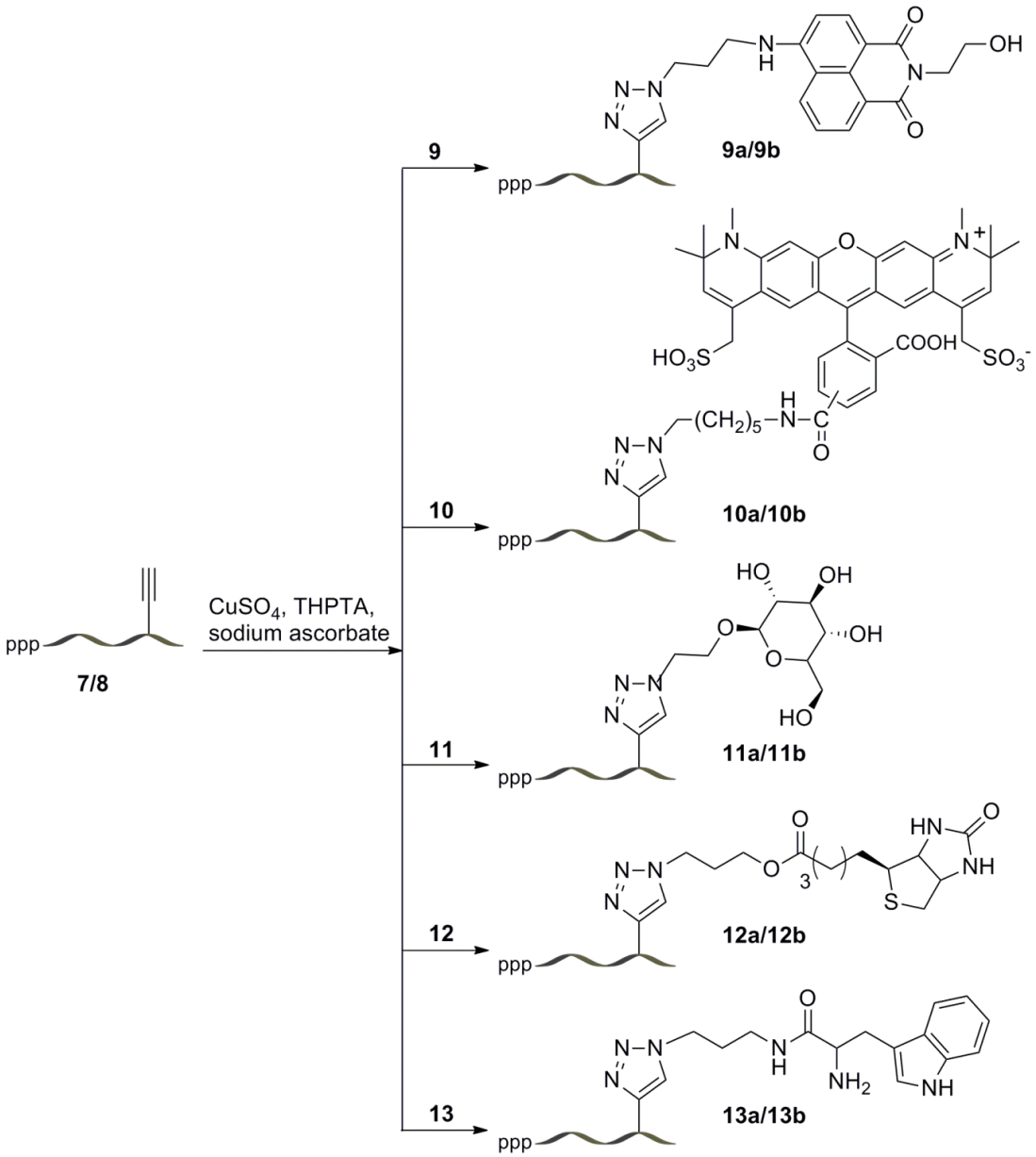

Scheme 2. Posttranscriptional chemical functionalization of alkyne-modified RNA transcripts **7**–**8** by CuAAC reaction using azide substrates **9**–**13**.

Table 2. Yield and mass data of posttranscriptionally functionalized RNA ONs **7** and **8**

Entry	RNA ON	Substrate	Product	Yield (nmol)	Isolated Yield[a] %	MALDI-TOF mass analysis of products (m/z)	
						Calculated mass	Observed mass
1	**7**	**9**	**9a**	6	50	3778.3	3778.5
2	**7**	**10**	**10a**	7	58	4286.9	4286.2
3	**7**	**11**	**11a**	3	25	3688.2	3688.2
4	**7**	**12**	**12a**	3	25	3766.8	3766.5
5	**7**	**13**	**13a**	4.5	38	3725.3	3725.7
6	**8**	**9**	**9b**	7.8	65	3858.6	3858.3
7	**8**	**10**	**10b**	8.2	68	4367.0	4368.3
8	**8**	**11**	**11b**	4	33	3768.8	3768.2
9	**8**	**12**	**12b**	6.3	52	3846.8	3846.4
10	**8**	**13**	**13b**	4	33	3806.1	3805.3

[a] All reactions were performed on 12 nmol scale of modified RNA ONs. Yields reported are with respect to the RNA products isolated after PAGE purification.

2.2.4 Raman analysis of 5-octadinyl-modified uridine (ODU)

Alkyne-modified nucleosides (EdU and EU) analogs exhibit characteristic Raman shifts (~2122 cm^{-1}), which appear in the Raman-silent region of the cells.[66-68] This unique Raman signature and metabolic incorporation of EdU and EU into DNA and RNA, respectively, has enabled the imaging of the synthesis of DNA and RNA in cells by using stimulated Raman scattering (SRS) microscopy. Based on these observations we wanted to test if ODU, which contains an internal and terminal alkyne group, could serve as a useful label for RNA study by Raman spectroscopy. Raman spectrum of EU and ODU was recorded on a confocal Raman microscope using 633 nm laser with 2 $mW/\mu m^2$ power. A solution of EU (1 mM) and ODU (1 mM) was drop casted on a quartz support and the laser output was focused on the sample. EU containing a terminal alkyne exhibited strong Raman shift at 2112 cm^{-1}, which was in good agreement with the literature reports (Figure 9).[66-68] Importantly, ODU displayed two Raman shifts–one relatively weak at 2106 cm^{-1} and second strong at 2240 cm^{-1} (Figure 9). It has been observed that the Raman intensity and shift depends on the substitution pattern. For example, attaching an alkyne group to aromatic rings enhances the

Raman intensity of the alkyne as compared to alkyl substituent. In terms of Raman shift, terminal alkynes are detected at lower wavenumbers (2080–2120 cm^{-1}) as compared to internal alkynes (2200 cm^{-1} and higher). Consistent with the literature reports the intensity and shift exhibited by ODU points out that the 2106 cm^{-1} peak corresponds to terminal alkyne and the 2240 cm^{-1} peak corresponds to internal alkyne. Although EU and ODUTP can be incorporated specifically into cellular RNA, ODU has an added advantage as ODU-modified RNA will contain two Raman scattering alkyne labels. When subjected to click staining, only the terminal alkyne would undergo reaction leaving the internal alkyne intact. Hence, both click chemistry (using terminal alkyne) and Raman spectroscopy (using internal alkyne) could be potentially used simultaneously to image RNA synthesis in cells.

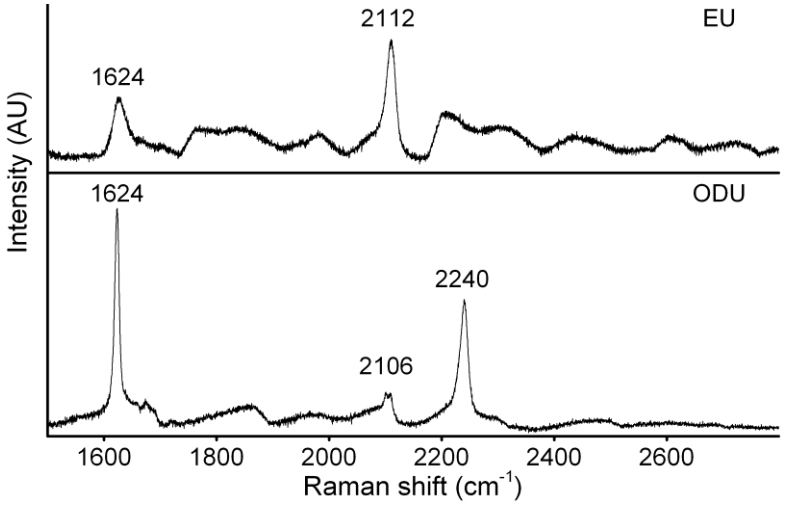

Figure 9. Raman spectrum of EU (top) and ODU (bottom). The samples were excited using 633 nm laser with a power of 2 $mW/\mu m^2$.

2.3 Conclusion

In summary, we have developed a new alkyne-modified UTP analog (ODUTP), which contains a clickable moiety and a Raman active label. We also tested enzymatic incorporation of EUTP and ODUTP into short RNA transcripts having one or two incorporations. We found that EUTP and ODUTP both served as good substrates for T7 RNA polymerase in *in vitro* transcription reaction and further, EU-and ODU-labeled RNA transcript were conveniently functionalized posttranscriptionally by using CuAAC reaction with a variety of substrates that include fluorescent probe, affinity tag, amino acid and sugar residues. Taken together, compatibility to enzymatic manipulations and posttranscriptional chemical modification, and preliminary Raman spectroscopic analysis underscore the usefulness of EU and ODU label as an efficient tool for the investigation of RNA *in vitro* settings.

2.4 Experimental Section

2.4.1 Materials

Uridine, 5-iodouridine, tetrakis(triphenylphosphine) palladium (0), 1,7-octadiyne, copper(I) iodide, formaldehyde, 4-bromo-1,8-naphthalic anhydride, sodium azide, sodium ascorbate, $CuSO_4$, biotin, DEAE Sephadex A-25 resin, triton X-100, actinomycin D, hydroyurea and snake venom phosphodiesterase I were obtained from Sigma-Aldrich. $POCl_3$ was purchased from Across Organics and freshly distilled prior to use. Fluorescent dyes Alexa594-azide **10**, and calf intestinal alkaline phosphatase (CIAP) were acquired from Invitrogen. Biotin azide (**11**) and sugar azide (**12**) were synthesized as per our earlier reports. Radiolabeled α-^{32}P ATP (2000 Ci/mmol) was purchased from the Board of Radiation and Isotope Technology, Government of India. T7 RNA polymerase, ribonuclease inhibitor (RiboLock), NTPs, RNase A and RNase T1 were obtained from Fermentas Life Science. DNA oligonucleotides were purchased from Integrated DNA Technologies, Inc., purified by gel electrophoresis under denaturing condition and desalted using Sep-Pak Classic C18 cartridges (Waters Corporation). Chemicals for preparing all buffer solutions were purchased from Sigma-Aldrich (BioUltra grade). Autoclaved water was used in all biochemical reactions and HPLC analysis.

2.4.2 Instrumentation

NMR spectra were recorded on a 400 MHz Jeol ECS-400. All MALDI-MS measurements were recorded on an Applied Biosystems 4800 Plus MALDI TOF/TOF analyzer, Micro Mass ESI-TOF and Water Synapt G2 High Defination mass spectrometer. Absorption spectra were recorded on PerkinElmer, Lambda 45 UV-Vis and Shimadzu UV-2600 spectrophotometers. Reversed-phase flash chromatographic (C18 Redi*SepRf* column) purifications were carried out using Teledyne ISCO, Combi Flash *Rf* RP-HPLC analyses were performed using Agilent Technologies 1260 Infinity and Dionex ICS 3000. Phosphorimages were recorded on a Typhoon Trio+, GE-Healthcare phosphorimager.

2.4.3 Synthesis of alkyne-modified urdine triphospahte analogs

2.4.3.1 Synthesis of 5-ethynyl uridine (EU) 3

5-ethynyl uridine **3** was prepared in two steps by following a reported literature procedure. In first step intermediate **2** was prepared by reacting 5-iodouridine **1** (1.008 g, 2.70 mmol, 1.0 equiv), TMS- acetylene (1.75 mL, 12.62 mmol, 4.7 equiv), CuI (0.052 g, 0.27 mmol, 0.1 equiv) and Pd [$(PPh_3)_2$ Cl_2] (0.043 g, 0.061 mmol, 0.022 equiv) in anhydrous 15 mL solution containing DMF 10 ml and 5 mL triethylamine. The reaction mixture then stirred at RT for 4 h. The reaction mixture was evaporated to get the crude residue which was further purified by column chromatography (0−10% MeOH in $CHCl_3$) to yield TMS protected ethynyl uridine **2** as pale brown solid (0.83 g, 90%). In second step, TMS deportation is carried out by reacting **2** (0.820 g, 2.41 mmol, 1.0 equiv) and K_2CO_3 (0.666 g, 4.82 mmol, 2.0 equiv) in 25 mL anhydrous methanol at RT for 45 min. Reaction mixture was diluted with MeOH/DCM (1:1, 25 mL) followed by the addition of Dowex resin (1×8 100-200 mesh, H+ form, 1.010 g) and continued the stirring for 30 min. Resin was filtered and washed with MeOH/DCM (1:1, 25 mL). Combined filtrate was evaporated and crude residue was purified by reversed-phase flash column chromatography (C18 RediSepRf, 0–50% acetonitrile in water system to yield product **3** as off-white solid (0.23 g, 38%). TLC ($CHCl_3$: MeOH = 80:20) *Rf* = 0.65; ^{1}H NMR (400 MHz, *d6*-DMSO): δ= 8.26 (s, 1H), 5.74 (d, *J* = 4.6 Hz, 1H), 4.00 (m, *J* = 9.6, 4.9 Hz, 3H), 3.87 – 3.81 (m, 1H), 3.66 (dd, *J* = 12.0, 2.8 Hz, 1H), 3.56 (dd, *J* = 12.0, 2.7 Hz, 1H); ^{13}C NMR (101 MHz, *d6*-DMSO): δ= 163.95 (s), 151.22 (s), 144.36 (s), 97.59 (s), 88.55 (s), 84.61 (s), 82.93 (s), 77.43 (s), 73.97 (s), 69.39 (s), 60.35 (s). MALDI-TOF: (m/z) calculated mass for $C_{11}H_{12}N_2NaO_6$ $[M+Na]^+$ = 291.21, found = 291.22; ε 260 = 3740 $M^{-1}cm^{-1}$, 287= 9920 $M^{-1}cm^{-1}$

2.4.3.2 Synthesis of 5-ethynyl uridine-5'-triphosphate 5 (EUTP)

To an ice cold solution of ribonucleoside **3** (97 mg, 0.36 mmol, 1.0 equiv) and proton sponge (154 mg, 0.72 mmol, 2.0 equiv) in trimethyl phosphate (1.2 mL) was slowly added freshly distilled $POCl_3$ (67 µL, 0.72 mmol, 2.0 equiv). The reaction mixture was stirred for 4 h at ~4 °C. A solution of bis-tributylammonium pyrophosphate (0.5 M in DMF, 3.6 mL, 1.81 mmol, 5.0 equiv) and tributylamine (0.85 mL, 3.62 mmol, 10.0 equiv) was rapidly added under ice cold condition. The reaction was quenched after 30 min with 1 M triethylammonium bicarbonate buffer (TEAB, pH 7.6, 15 mL) and was extracted with ethyl acetate (2×10 mL). The aqueous layer was evaporated and the residue was purified first on DEAE sephadex-A25

anion exchange column (10 mM–1 M TEAB buffer, pH 7.6) followed by reversed-phase flash column chromatography (C18 RediSepRf, 0–40% acetonitrile in 100 mM triethylammonium acetate buffer, pH 7.5, 50 min). Appropriate fractions were lyophilized to afford the desired triphosphate product **5** as a tetratriethylammonium salt (30 mg, 9%). ^{1}H NMR (400 MHz, D_2O): δ = 8.22 (s, 1H), 5.95 (d, *J* = 4.8 Hz, 1H), 4.38 (d, *J* = 4.9 Hz, 2H), 4.25 (d, *J* = 4.8 Hz, 3H), 3.60 (s, 1H); ^{31}P NMR (162 MHz, D_2O) δ = -8.76 (s), -10.84 (s), -22.08 (s); HRMS: (m/z) Calculated for $C_{11}H_{14}N_2O_{15}P_3$ $[M-H]^-$ = 506.9613, found = 506.9603.

2.4.3.3 Synthesis of 5-(octa-1,7-diynyl) uridine 4 (ODU)

Ribonucleoside **4** was prepared by following an analogous procedure reported for the synthesis of 2'-deoxyribonucleoside analog.19 A mixture of 5-iodouridine **1** (1.055 g, 2.85 mmol, 1.0 equiv), 1,7-octadiyne (3.8 mL, 28.63 mmol, 10.0 equiv), CuI (0.117 g, 0.61 mmol, 0.2 equiv) and tetrakis(triphenylphosphine) palladium(0) (0.355 g, 0.31 mmol, 0.1 equiv) was taken in anhydrous DMF (15 ml). Triethylamine (0.8 mL, 5.70 mmol, 2.0 equiv) was slowly added to the above solution and stirred at RT for 6 h. Reaction mixture was diluted with MeOH/DCM (1:1, 30 mL) followed by the addition of Dowex resin (1×8 100–200 mesh, H^+ form, 1 g) and continued the stirring for 1 h. Resin was filtered and washed with MeOH/DCM (1:1, 50 mL). Combined filtrate was evaporated and crude residue was purified by silica gel column chromatography (0−10% MeOH in $CHCl_3$) to yield product **4** as off-white solid (0.42 g, 42%). TLC ($CHCl_3$: MeOH = 80:20) R_f = 0.42; ^{1}H NMR (400 MHz, *d6*-DMSO): δ = 11.59 (s, 1H), 8.19 (s, 1H), 5.74 (d, J = 5.0 Hz, 1H), 5.41 (d, J = 5.4 Hz, 1H), 5.19 (t, J = 4.8 Hz, 1H), 5.08 (d, J = 5.2 Hz, 1H), 4.03 (dd, J = 10.2, J = 5.1 Hz, 1H), 3.96 (dd, J = 9.5, J = 4.7 Hz, 1H), 3.84 (d, J = 3.4 Hz, 1H), 3.68–3.63 (m, 1H), 3.58–3.53 (m, 1H), 2.77 (t, J = 2.4 Hz, 1H), 2.37 (t, J = 6.2 Hz, 2H), 2.19 (d, J = 2.4 Hz, 2H), 1.56 (t, J = 3.0 Hz, 4H); ^{13}C NMR (100 MHz, *d6*-DMSO): δ (ppm) 161.8, 149.8, 142.9, 99.1, 93.0, 88.1, 84.9, 84.3, 73.8, 73.0, 71.5, 69.6, 60.5, 27.3, 27.1, 18.3, 17.3; HRMS: (m/z) Calculated for $C_{17}H_{21}N_2O_6$ $[M+H]^+$ = 349.1400, found = 349.1405; ε_{260} = 3380 $M^{-1}cm^{-1}$, ε_{292} = 10520 $M^{-1}cm^{-1}$

2.4.3.4 Synthesis of 5-(octa-1,7-diynyl) uridine-5'-triphosphate 6 (ODUTP)

To an ice cold solution of alkyne-modified ribonucleoside **4** (93 mg, 0.27 mmol, 1.0 equiv) in trimethyl phosphate (1.2 mL) was slowly added freshly distilled $POCl_3$ (37 μL, 0.40 mmol, 1.5 equiv). The reaction mixture was stirred for 5 h at ~4 °C. A solution of *bis*-tributylammonium pyrophosphate (0.5 M in DMF, 2.75 mL, 5.1 equiv) and tributylamine

(0.65 mL, 2.75 mmol, 10 equiv) was rapidly added under ice cold condition. The reaction was quenched after 30 min with 1 M triethylammonium bicarbonate buffer (TEAB, pH 7.6, 15 mL) and was extracted with ethyl acetate (2×10 mL). The aqueous layer was evaporated and the residue was purified first on DEAE sephadex-A25 anion exchange column (10 mM–1 M TEAB buffer, pH 7.6) followed by reversed-phase flash column chromatography (C18 RediSep*Rf*, 0–40% acetonitrile in 100 mM triethylammonium acetate buffer, pH 7.5, 50 min). Appropriate fractions were lyophilized to afford the desired triphosphate product **6** as a tetratriethylammonium salt (42 mg, 16%). ^{1}H NMR (400 MHz, D_2O): δ (ppm) 8.00 (s, 1H), 5.91 (d, J = 4.5 Hz, 1H), 4.38 (br, 2H), 4.23 (br, 3H), 2.43 (t, J = 6.4 Hz, 2H), 2.38 (t, J = 2.4 Hz, 1H), 2.24 (d, J = 2.4 Hz, 2H), 1.65 (br, 4H); ^{13}C NMR (100 MHz, D_2O) δ (ppm) 164.5, 150.7, 143.3, 100.6, 96.4, 88.6, 85.9, 83.3, 73.3, 70.9, 69.5, 65.1, 27.1, 26.9, 23.4, 18.3, 17.2; ^{31}P NMR (162 MHz, D_2O) δ (ppm) 7.91 (br), 10.73 (br) 21.93 (br); HRMS: (m/z) Calculated for $C_{17}H_{22}N_2O_{15}P_3$ $[M-H]^+$= 587.0233, found = 587.0337.

2.4.4. Synthesis of azide counterparts

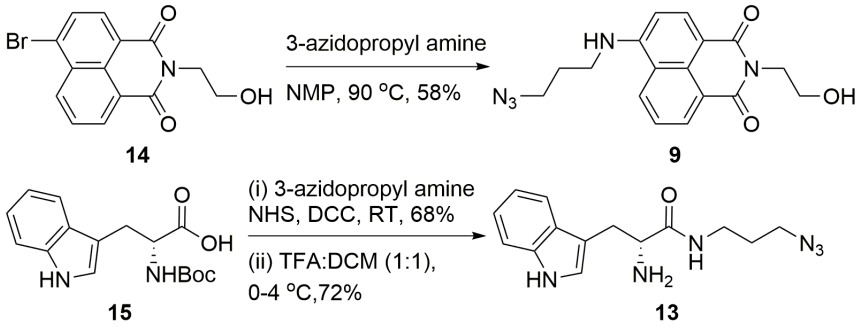

Scheme 4 Synthesis of azide substrates **9** and **13** for CuAAC reactions, NMP = *N*-methyl-2-pyrrolidone, NHS = *N*-hydroxysuccinimide, DCC = *N*, *N'*-dicyclohexylcarbodiimide.

2.4.4.1 Synthesis of 4-(3-azidopropyl) amino)-N-(2-hydroxyethyl)-1, 8-naphthalimide (9)

A mixture of **14**[74] (0.210 g, 0.66 mmol, 1.0 equiv) and 3-azidopropyl amine (0.275 g, 2.72 mmol, 4.1 equiv) in NMP (15 mL) was heated at 90 °C for 12 h. Reaction mixture was diluted by adding 50 mL of dichloromethane and washed with ice cold water (2×25 mL). Organic layer was dried over sodium sulphate and evaporated, and the resulting crude product was purified by column chromatography (0−10% MeOH in $CHCl_3$) to yield bright yellow solid product **9**. (0.13 g, 58%) TLC ($CHCl_3$:MeOH = 80:10) *Rf*= 0.22; ^{1}H NMR (400 MHz, d_6-DMSO): δ(ppm) 8.67 (d, J= 8.0 Hz, 1H), 8.40 (d, J= 6.8 Hz, 1H), 8.24 (d, J= 8.2 Hz, 1H), 7.89–7.58 (m, 2H), 6.77 (d, J= 8.2 Hz, 1H), 4.79 (s, 1H), 4.11 (s, 2H), 3.62–3.32 (m, 6H), 2.03–1.88 (m, 2H); ^{13}C NMR (100 MHz, d_6-DMSO): δ (ppm) 163.9, 163.0, 150.4,

134.2, 130.6, 129.4, 128.6, 124.3, 122.0, 120.2, 108.0, 103.8, 58.0, 48.6, 41.4, 27.2.); HRMS: (m/z) Calculated for $C_{17}H_{18}N_5O_3$ $[M+1]^+$ = 340.1331, found = 340.1410.

2.4.4.2 Synthesis of 3-azidopropyl-biotin (11)

Glucosyl azide **11** was prepared in two steps using reported procedure: In first step acetylated 2-bromo-ethyl-D-glucoside (1.020 g, 2.24 mmol, 1 equiv) and sodium azide (0.29 g, 4.48 mmol, 2.0 equiv) were allowed to react in 5 ml DMF for 4 h at 80^{o}C. After completion of reaction 100 mL brine solution was added to reaction mixture and product was extracted in ether (2 × 30 mL). Combined organic extract then evaporated to dryness and yellow crude residue is then purified by column chromatography ($CHCl_3$:MeOH, 95:5) to afford acetylated 2-azido-ethyl-D-glucoside as a white solid (800 mg, 85%). In second step acetylated 2-azido-ethyl-D-glucoside (300 mg, 0.72 mmol, 1 equiv) was deprotected using sodium methoxide (163 mg, 3.1 mmol, 4.2 equiv) in 2 mL methanol at RT for 2 h. reaction was neutralised by adding amberlite resin. Resin was washed using (2 × 5 mL) methanol and filtrate was evaporated to get crude product. The crude product was further purified by column chromatograpghy (60-120 silica, CHCl3:MeOH, 90: 10) to afford colourless oil of 2-azido-ethyl-D-glucoside **11** (142 mg, 79%). 1H NMR (400 MHz, D_2O): δ = 4.49 (d, *J* = 7.9 Hz, 1H), 4.10 – 3.99 (m, 1H), 3.95 – 3.88 (m, 1H), 3.87 – 3.78 (m, 1H), 3.74 – 3.68 (m, 1H), 3.56 (m, *J* = 10.0, 4.8 Hz, 2H), 3.51 – 3.42 (m, 2H), 3.41 – 3.34 (m, 1H), 3.28 (dd, *J* = 9.3, 8.0 Hz, 1H)$^{\cdot}$; MALDI-TOF: (m/z) Calculated $C_8H_{15}KN_3O_6$ $[M+K]^+$= 288.32 found = 288.30.

2.4.4.3 Synthesis of biotin propyl azide (12)

Synthesis of biotin propyl azide **12** was achieved by following reported literature procedure: A solution of biotin (0.15 g, 0.6 mmol, 1.0 equiv) and 3-azido-1-propanol (0.52 g, 5.2 mmol, 8.6 equiv) in DCM (20 mL) was cooled to 0 °C, and EDC•HCl (0.57 g, 3.0 mmol, 5.0 equiv) and DMAP (0.007 g, 0.06 mmol, 0.1 equiv) were sequentially added. The solution was stirred at 0 °C for 2 h, then at ambient temperature overnight. The reaction mixture was washed with DCM (2 × 1 mL) and volatile was removed under reduced pressure. the crude product was purified by column chromatography (CH_2Cl_2: MeOH, 90:10) to obtained biotin propyl azide **12** (98 mg, 50%) as a white powder. ^{1}H NMR (400 MHz, *d6*-DMSO): δ = 6.40 (d, *J* = 29.6 Hz, 2H), 4.36 – 4.24 (m, 1H), 4.22 – 3.87 (m, 3H), 3.43 – 3.34 (m, 2H), 3.22 – 3.00 (m, 1H), 2.82 (dd, *J* = 12.4, 5.1 Hz, 1H), 2.57 (d, *J* = 12.4 Hz, 1H), 2.31 (t, *J* = 7.4 Hz, 2H), 1.83 (p, *J*

= 6.5 Hz, 2H), 1.69 – 1.24 (m, 6H); MALDI-TOF: (m/z) Calculated for $C_{13}H_{21}N_5NaO_3S$ $[M+Na]^+$= 350.39 found = 350.46.

2.4.4.4 Synthesis of N-(3-azidopropyl)-tryptophan (13)

N-Boc-protected tryptophan **15** (0.251 g, 0.82 mmol, 1.0 equiv) and N-hydroxysuccinimide (0.141 g, 1.23 mmol, 1.5 equiv) were dissolved in anhydrous DMF (1 mL). Resultant reaction mixture was stirred at 0 °C for 15 min and DCC (0.168 g, 0.82 mmol, 1.0 equiv) was added and stirred at RT for 24 h. Reaction mixture was diluted with dichloromethane (20 mL) and filtered through celite pad. Celite pad was washed with dichloromethane (10 mL). The organic layer was washed with saturated sodium carbonate (20 mL) followed by 1M HCl solution (20 mL). Organic layer was dried over sodium sulphate and the solvent was evaporated. The resulting crude product was purified by column chromatography (0−5% MeOH in $CHCl_3$) to yield Boc-protected azide derivative as a white solid. This product was dissolved in TFA/DCM (1:1, 5 mL) and stirred for 30 min; solvent was evaporated completely and the residue was resuspended in saturated sodium carbonate (100 mL). The product was extracted in ethyl acetate (3×25 mL). The organic extract was dried over sodium sulphate and evaporated, and the resulting crude product was purified by column chromatography (0−10% MeOH in $CHCl_3$) to yield product **13** as a pale yellow viscous oil. (0.053 g, 72%). TLC ($CHCl_3$:MeOH = 90:10) *Rf*= 0.30; ^{1}H NMR (400 MHz, *d6*-DMSO): δ(ppm) 10.89 (s, 1H), 8.03 (s, 1H), 7.56 (d, J= 7.8 Hz, 1H), 7.33 (d, J= 8.1 Hz, 1H), 7.14 (s, 1H), 7.06 (t, J= 7.5 Hz, 1H), 6.97 (t, J= 7.4 Hz, 1H), 3.36 (t, J= 7.0 Hz, 2H), 3.19 (t, J= 6.8 Hz, 2H), 3.09 (t, J= 6.4 Hz, 2H), 2.84 (dd, J= 14.0, J= 7.6 Hz, 1H), 1.60–1.51 (m, 2H), 1.23 (s, 2H); ^{13}C NMR (100 MHz, *d6*-DMSO): δ(ppm) 172.4, 136.2, 127.3, 124.1, 120.9, 118.5, 118.3, 111.4, 109.3, 54.6, 52.0, 48.2, 35.8, 28.2; MALDI-TOF: (m/z) $C_{14}H_{18}N_6ONa$ $[M+Na]^+$= 309.33, found = 309.21.

2.4.5 Enzymatic incorporation of alkyne-modified UTP 5 and 6

2.4.5.1 Transcription reactions with $^{\alpha\text{-}32}$P ATP

The promoter-template duplexes (5 μM) were assembled by heating T7 RNA polymerase consensus promoter DNA sequence and DNA template (**D1–D5**) in TE buffer (10 mM Tris-HCl, 1 mM EDTA, 100 mM NaCl, pH 7.8) at 90 °C for 3 min. The solution was allowed to come to room temperature slowly and then placed on an ice bath for 20 min, and stored at −40 °C. The transcription reactions were carried out at 37 °C in 40 mM Tris-HCl buffer (pH

7.9) containing 250 nM annealed promoter-template duplexes, 10 mM $MgCl_2$, 10 mM NaCl, 10 mM of dithiothreitol (DTT), 2 mM spermidine, 1 U/μL RNase inhibitor (Riboblock), 1 mM GTP, CTP, UTP and or modified UTP **5−6**, 20 μM ATP, 5 μCi $^{\alpha\text{-}32}$P ATP and 3 U/μL T7 RNA in a total volume of 20 μL. The reaction was quenched after 3.5 h by adding 20 μL of loading buffer (7 M urea in 10 mM Tris-HCl, 100 mM EDTA, 0.05% bromophenolblue, pH 8), heated for 3 min at 75 °C followed by cooling the samples on an ice bath. The samples (4 μL) were loaded on a sequencing 18% denaturing polyacrylamide gel and electrophoresed. The radioactive bands were phosphorimaged and then quantified using the GeneTools software from Syngene to determine the relative transcription efficiencies. Percentage incorporation of alkyne-modified ribonucleoside triphosphates **5−6** into full-length transcripts has been reported with respect to transcription efficiency in the presence of natural NTPs. All reactions were performed in duplicate and the errors in yields were ≤5%.

2.4.5.2 Large-scale transcription reactions

Large-scale transcription reactions were performed using DNA template **D1**. Each reaction (250 μL) was performed in the presence of 2 mM GTP, CTP, ATP, and modified UTP **5−6**, 20 mM $MgCl_2$, 0.4 U/μL RNase inhibitor (Riboblock), 300 nM annealed template and 800 units T7 RNA polymerase. After incubating for 12 h at 37 °C, the reaction volume was reduced to 1/3 by speed vac. 50 μL of the loading buffer was added and the sample was loaded on a preparative 20% denaturing polyacrylamide gel. The gel was UV shadowed, appropriate band was cut out, extracted with 0.3 M sodium acetate and desalted using Sep-Pak classic C18 cartridge.

2.4.6 Enzymatic digestion of RNA ONs 7 and 8

~4 nmol of the modified oligoribonucleotide transcripts **7** and **8** were treated with snake venom phosphodiesterase I (0.01 U), calf intestinal alkaline phosphatase (10 μL, 1 U/μL), and RNase A (0.25 μg) in a total volume of 100 μL in 50 mM Tris-HCl buffer (pH 8.5, 40 mM $MgCl_2$, 0.1 mM EDTA) and incubated for 12 h at 37 °C. After this period, RNase T1 (0.2 U/μL) was added, and the samples were incubated for another 4 h at 37 °C. The ribonucleoside mixture obtained from the digest was analyzed by reversed-phase HPLC using Phenomenex-Luna C18 column (250 x 4.6 mm, 5 micron) at 260 nm.

2.4.7 Posttranscriptional modification of RNA ON 7−8 by CuAAC reaction

A solution of THPTA (3 μL, 94 mM), $CuSO_4$ (3 μL, 47 mM) and sodium ascorbate (3 μL, 94 mM) was added to an aqueous solution of alkyne-labeled RNA ON **7** or **8** in water (23μL, 0.54 mM). Stock solutions (7.5 mM) of azide substrates **9−13** were prepared in DMSO. Azide substrates (8 μL, 7.5 mM) were added to individual reaction mix and the final reaction volume was 40 μL. The final concentration of reaction components was the following: THPTA (7.1 mM), $CuSO_4$ (3.5 mM), sodium ascorbate (7.1 mM), RNA ON (0.31 mM, 12 nmol), azide substrates (1.5 mM) and DMSO (20%). The reaction mixtures were incubated at 37 °C for 30 min and purified by PAGE under denaturing conditions. The bands corresponding to clicked products, after UV-shadowing, were cut and extracted in 0.3 M sodium acetate and desalted using Sep-Pak classic C18 cartridge.

2.4.8 Raman analysis of alkyne-modified nucleosides EU and ODU

An aqueous solution (1 mM) of EU or ODU in 10% DMSO was drop casted on a quartz support and dried. The laser (633 nm) output with a power of 2 $mW/\mu m^2$ was focused on the sample using a 60×/0.7 numerical aperture (NA) air immersion objective lens. The confocal slit width of the spectrograph was 200 μm with grating 1800 grooves/mm. The spectrum was recorded on a LabRAM HR 800, HORIBA confocal Raman microscope with an acquisition time of 90 sec.

2.5 References

1. P. M. E. Gramlich, C. T. Wirges, Manetto, A. & Carell, T. Postsynthetic DNA modification through the copper-catalyzed azide-alkyne cycloaddition reaction. *Angew. Chem. Int. Ed.*, **47**, 8350–8358 (2008).
2. Weisbrod, S. H. and Marx, A. Novel strategies for the site-specific covalent labeling of nucleic acids. *Chem. Commun.*, 5675–5685 (2008).
3. El-Sagheer, A.H. and Brown, T. Click chemistry with DNA. *Chem. Soc. Rev*., **39**, 1388–1405 (2010).
4. El-Sagheer, A. H. and Brown, T. Click nucleic acid ligation: applications in biology and nanotechnology. *Acc. Chem. Res*., **45**, 1258–1267 (2012).
5. Uszczyńska, B., Ratajczak, T., Frydrych, E., Maciejewski, H., Figlerowicz, M., Markiewicz, W. T. and Chmielewski, M. K. Application of click chemistry to the production of DNA microarrays. *Lab Chip.,* **12**, 1151–1156 (2012).
6. Merkel, M., Peewasan, K., Arndt, S., Ploschik, D. and Wagenknecht, H-A. Copper-Free Postsynthetic Labeling of Nucleic Acids by Means of Bioorthogonal Reactions. *ChemBioChem*, **16**, 1541–1553 (2015).
7. Routh, A., Head, S. R., Ordoukhanian, P. and Johnson, J. E. ClickSeq: Fragmentation-Free Next-Generation Sequencing via Click Ligation of Adaptors to Stochastically Terminated 3'-Azido cDNAs. *J. Mol. Biol*., **427**, 2610–2616 (2015).

8. Wang, C. C., Seo, T. S., Li, Z., Ruparel, H. and Ju, J. Site-specific fluorescent labeling of DNA using Staudinger ligation. *Bioconjugate Chem.*, **14**, 697–701 (2003).
9. Weisbrod, S. H. and Marx, A. A nucleoside triphosphate for site-specific labeling of DNA by the Staudinger ligation. *Chem. Commun.*, 1828–1830 (2007).
10. Weisbrod, S. H., Baccaro, A. and Marx, A. DNA conjugation by Staudinger ligation. *Nucleic Acids Symp. Ser.*, **52**, 383–384 (2008).
11. Franzini, R. M. and Kool, E. T. *J. Am. Chem. Soc.*, **131**, 16021–16023 (2009).
12. Furukawa, K., Abe, H., Hibino, K., Sako, Y., Tsuneda, S. and Ito, Y. Reduction-triggered fluorescent amplification probe for the detection of endogenous RNAs in living human cells. *Bioconjugate Chem.*, **20**, 1026–1036 (2009).
13. Pianowski, Z., Gorska, K., Oswald, L., Merten, C. A. and Winssinger, N. Imaging of mRNA in live cells using nucleic acid-templated reduction of azidorhodamine probes. *J. Am. Chem. Soc.*, **131**, 6492 –6497 (2009).
14. van Berkel, S. S., van Eldijk, M. B. and van Hest, J. C. M. Staudinger ligation as a method for bioconjugation. *Angew. Chem. Int. Ed.*, **50**, 8806−8827 (2011).
15. Weisbrod, S. H., Baccaro, A. and Marx, A. Site-specific DNA labeling by Staudinger ligation. Methods Mol. Biol., **751**, 195–207 (2011).
16. Seo, T. S., Li, Z., Ruparel, H. and Ju, J. Click chemistry to construct fluorescent oligonucleotides for DNA sequencing. *J. Org. Chem.*, **68**, 609–612 (2003).
17. Gierlich, J., Burley, G. A., Gramlich, P. M., Hammond, D. M. and Carell, T. Click chemistry as a reliable method for the high-density postsynthetic functionalization of alkyne-modified DNA. *Org. Lett.*, **8**, 3639–3642 (2006).
18. Gierlich, J., Gutsmiedl, K., Gramlich, P. M., Schmidt, A., Burley, G.A. and Carell, T. Synthesis of highly modified DNA by a combination of PCR with alkyne-bearing triphosphates and click chemistry. *Chemistry*, **13**, 9486–9494 (2007).
19. Seela, F. and Sirivolu, V. R. Nucleosides and oligonucleotides with diynyl side chains: base pairing and functionalization of 2′-deoxyuridine derivatives by the copper(I)-catalyzed alkyne-azide 'Click' cycloaddition. *Helv. Chim. Acta,* **90**, 535−552 (2007).
20. Salic, A. and Mitchison, T. J. A chemical method for fast and sensitive detection of DNA synthesis in vivo. *Proc. Natl. Acad. Sci. U.S.A.*, **105**, 2415−2420 (2008).
21. Gramlich, P. M. E., Warncke, S., Gierlich, J. and Carell, T. Click-click-click: single to triple modification of DNA. *Angew. Chem. Int. Ed.*, **47**, 3442–3444 (2008).
22. Xu, Y., Suzuki, Y. and Komiyama, M. Click chemistry for the identification of G-quadruplex structures: discovery of a DNA-RNA G-quadruplex. *Angew. Chem Int. Ed.*, **48**, 3281–3284 (2009).
23. Qu, D., Wang, G., Wang, Z., Zhou, L., Chi, W., Cong, S., Ren, X., Liang, P. and Zhang, B. 5-Ethynyl-2'-deoxycytidine as a new agent for DNA labeling: detection of proliferating cells. *Anal. Biochem.*, **417**, 112–121 (2011).
24. Neef, A. B. and Luedtke, N. W. Dynamic metabolic labeling of DNA in vivo with arabinosyl nucleosides *Proc. Natl. Acad. Sci. U.S.A.*, **108**, 20404−20409 (2011).
25. Di Antonio, M., Biffi, G., Mariani, A., Raiber, E., Rodriguez, R. and Balasubramanian, S. Selective RNA versus DNA G-quadruplex targeting by in situ click chemistry. *Angew. Chem. Int. Ed,* **51**, 11073–11078 (2012).
26. Marks, I. S., Kang, J. S., Jones, B. T., Landmark, K. J., Cleland, A. J. and Taton, T. A. Strain-promoted "click" chemistry for terminal labeling of DNA. *Bioconjugate Chem.*, **22**, 1259–1263 (2011).
27. Shelbourne, M., Chen, X., Brown, T. and El-Sagheer, A. H. Fast copper-free click DNA ligation by the ring-strain promoted alkyne-azide cycloaddition reaction. *Chem. Commun.*, **47**, 6257–6259 (2011).

28. Neef, A. B. and Luedtke, N. W. An azide-modified nucleoside for metabolic labeling of DNA. *ChemBioChem*, **15**, 789−793 (2014).
29. Ren, X., El-Sagheer A. H. and Brown, T. Azide and trans-cyclooctene dUTPs: incorporation into DNA probes and fluorescent click-labeling. *Analyst*, **140**, 2671−2678 (2015).
30. Winz, M. L., Linder, E. C., Andre, T., Becker J., and Jäschke, A. Nucleotidyl transferase assisted DNA labeling with different click chemistries. *Nucl. Acids Res*., **43**, e110 (2015).
31. Ren, X., El-Sagheer, A. H. and Brown, T. Efficient enzymatic synthesis and dual-colour fluorescent labeling of DNA probes using long chain azido-dUTP and BCN dyes. *Nucl. Acids Res.,* 2016.
32. Schoch, J., Wiessler, M. and Jäschke, A. Postsynthetic modification of DNA by inverse-electron-demand Diels-Alder reaction. *J. Am. Chem. Soc*., **132**, 8846–8847 (2010).
33. Šečkutė, J., Yang, J. and Devaraj, N. K. Rapid oligonucleotide-templated fluorogenic tetrazine ligations. *Nucl. Acids Res.*, **41**, e148 (2013).
34. Rieder, U. and Luedtke, N. W. Alkene-tetrazine ligation for imaging cellular DNA. *Angew. Chem. Int. Ed.*, **53**, 9168−9172 (2014).
35. Asare-Okai, P. N., Agustin, E., Fabris, D. and Royzen, M. Site-specific fluorescence labeling of RNA using bio-orthogonal reaction of trans-cyclooctene and tetrazine. *Chem. Commun.*, **50**, 7844–7847 (2014).
36. Bußkamp, H., Batroff, E., Niederwieser, A., Abdel-Rahman, O. S., Winter, R. F., Wittmann, V. and Marx, A. Efficient labeling of enzymatically synthesized vinyl-modified DNA by an inverse-electron-demand Diels-Alder reaction. *Chem. Commun.*, **50**, 10827–10829 (2014).
37. Wu, H., Cisneros, B. T., Cole, C. M. and Devaraj, N. K. Bioorthogonal tetrazine-mediated transfer reactions facilitate reaction turnover in nucleic acid-templated detection of microRNA. *J. Am. Chem. Soc.*, **136**, 17942–17945 (2014).
38. Domnick, C., Eggert, F. and Kath-Schorr, S. Site-specific enzymatic introduction of a norbornene modified unnatural base into RNA and application in post-transcriptional labeling. *Chem. Commun.*, **51**, 8253–8256 (2015).
39. Hong, V., Steinmetz, N. F., Manchester, M. and Finn, M. G. Labeling live cells by copper-catalyzed alkyne--azide click chemistry. *Bioconjugate Chem*., **21**, 1912–1916 (2010).
40. Besanceney-Webler, C., Jiang, H., Zheng, T., Feng, L., del Amo, D. S., Wang, W., Klivansky, L. M., Marlow, F. L., Liu, Y. and Wu, P. Increasing the efficacy of bioorthogonal click reactions for bioconjugation: a comparative study. *Angew. Chem. Int. Ed.*, **50**, 8051–8056 (2011).
41. Presolski, S. I., Hong, V. P. and Finn, M. G. Copper-catalyzed azide-alkyne click chemistry for bioconjugation. *Curr. Protoc. Chem. Biol.*, **3**, 153–162 (2011).
42. Phelps, K. J., Ibarra-Soza, J. M., Tran, K., Fisher, A. J. and Beal, P. A. Click modification of RNA at adenosine: structure and reactivity of 7-ethynyl- and 7-triazolyl-8-aza-7-deazaadenosine in RNA. *ACS Chem. Biol.*, **9**, 1780−1787 (2014).
43. El-Sagheer, A. H. and Brown, T. New strategy for the synthesis of chemically modified RNA constructs exemplified by hairpin and hammerhead ribozymes. *Proc Natl Acad Sci USA*., **107**, 15329– 15334 (2010).
44. Paredes, E., Evans, M. and Das, S. R. RNA labeling, conjugation and ligation. *Methods,* **54**, 251–259 (2011).

45. Peacock, H., Maydanovych, O. and Beal, P. A. N(2)-Modified 2-aminopurine ribonucleosides as minor-groove-modulating adenosine replacements in duplex RNA. *Org. Lett.*, **12**, 1044–1047 (2010).
46. Yamada, T. *et al.* Versatile site-specific conjugation of small molecules to siRNA using click chemistry. *J. Org. Chem.*, **76**, 1198–1211 (2011).
47. Paredes, E. and Das, S. R. Click chemistry for rapid labeling and ligation of RNA. *ChemBioChem*., **12**, 125–131 (2011).
48. Ishizuka, T., Kimoto, M., Sato, A. and Hirao, I. Site-specific functionalization of RNA molecules by an unnatural base pair transcription system via click chemistry. *Chem. Commun*., **48**, 10835−10837 (2012).
49. Singh, I., Freeman, C., Madder, A., Vyle, J. S. and Heaney, F. Fast RNA conjugations on solid phase by strain-promoted cycloadditions. *Org. Biomol. Chem.*, **10**, 6633−6639 (2012).
50. Motorin, Y., Burhenne, J., Teimer, R., Koynov, K., Willnow, S., Weinhold, E. and Helm, M. Expanding the chemical scope of RNA:methyltransferases to site-specific alkynylation of RNA for click labeling. *Nucl. Acids Res*., **39**, 1943–1952 (2011).
51. Onizuka, K., Shibata, A., Taniguchi, Y. and Sasaki, S. Pin-point chemical modification of RNA with diverse molecules through the functionality transfer reaction and the copper-catalyzed azide-alkyne cycloaddition reaction. *Chem. Commun*., **47**, 5004–5006 (2011).
52. Tomkuviene, M., d'Orval, B. C., Cerniauskas, I., Weinhold E., and Klimasauskas,S. Programmable sequence-specific click-labeling of RNA using archaeal box C/D RNP methyltransferases. *Nucl. Acids Res.*, **40**, 6765–6773 (2012).
53. Winz, M. L., Samanta, A., Benzinger, D. and Jäschke, A. Site-specific terminal and internal labeling of RNA by poly(A) polymerase tailing and copper-catalyzed or copper-free strain-promoted click chemistry.*Nucl. Acids Res*., **40**, e78 (2012).
54. Schulz, D., Holstein, J. M. and Rentmeister, A. A chemo-enzymatic approach for site-specific modification of the RNA cap. *Angew. Chem. Int. Ed.*, 2013, **52**, 7874–7878.
55. Holstein, J. M., Schulz, D. and Rentmeister, A. Bioorthogonal site-specific labeling of the 5'-cap structure in eukaryotic mRNAs. *Chem. Commun*., **50**, 4478–4481 (2014).
56. Azide group can undergo Staudinger-type reaction with phosphoramidite substrates. Wada, T., Mochizuki, A., Higashiya, S., Tsuruoka, H., Kawahara, S., Ishikawa, M. and Sekine, M. Synthesis and properties of 2-azidodeoxyadenosine and its incorporation into oligodeoxynucleotides *Tet. Lett.*, **42**, 9215–9219 (2001).
57. Kiviniemi, A., Virta, P. and Lönnberg, H. Utilization of intrachain 4'-C-azidomethylthymidine for preparation of oligodeoxyribonucleotide conjugates by click chemistry in solution and on a solid support. *Bioconjugate Chem.*, **19**, 1726-1734 (2008).
58. Pourceau, G., Meyer, A., Vasseur, J.-J. and Morvan, F. Azide solid support for 3'-conjugation of oligonucleotides and their circularization by click chemistry. *J. Org. Chem.*, **74**, 6837–6842 (2009).
59. Qiu, J., El-Sagheer, A. H. and Brown, T. Solid phase click ligation for the synthesis of very long oligonucleotides. *Chem. Commun*., **49**, 6959−6961 (2013).
60. Santner, T., Hartl, M., Bister, K. and Micura, R. Efficient access to 3'-terminal azide-modified RNA for inverse click-labeling patterns. *Bioconjugate Chem*., **25**, 188−195 (2014).
61. Rao, H., Sawant, A. A., Tanpure, A. A. and Srivatsan, S. G. Posttranscriptional chemical functionalization of azide-modified oligoribonucleotides by bioorthogonal click and Staudinger reactions. *Chem. Commun*., **48**, 498–500 (2012).

62. Sawant, A. A., Tanpure, A. A., Mukherjee, P. P., Athavale, S., Kelkar, A., Galande, S. and Srivatsan, S. G. A versatile toolbox for posttranscriptional chemical labeling and imaging of RNA. *Nucl. Acids Res*., (2015) *doi: 10.1093/nar/gkv903.*
63. Someya, T., Ando, A., Kimoto, M. and Hirao, I. Site-specific labeling of RNA by combining genetic alphabet expansion transcription and copper-free click chemistry. *Nucl. Acids Res.*, **43**, 6665–6676 (2015).
64. Yamakoshi, H., Dodo, K., Palonpon, A., Ando, J., Fujita, K., Kawata, S. and Sodeoka, M. Alkyne-tag Raman imaging for visualization of mobile small molecules in live cells. *J. Am. Chem. Soc*., **134**, 20681−20689 (2012).
65. Hong, S., Chen, T., Zhu, Y., Li, A., Huang, Y. and Chen, X. Live-cell stimulated Raman scattering imaging of alkyne-tagged biomolecules. *Angew. Chem. Int. Ed.*, **53**, 5827–5831 (2014).
66. Yamakoshi, H. *et al.* Imaging of EdU, an alkyne-tagged cell proliferation probe, by Raman microscopy. *J. Am. Chem. Soc*., **133**, 6102–6105 (2011).
67. L. Wei, *et al.* Live-cell imaging of alkyne-tagged small biomolecules by stimulated Raman scattering. *Nat. Methods*., **4**, 410–412 (2014).
68. Z. Chen, *et al.* Multicolor live-cell chemical imaging by isotopically edited alkyne vibrational palette. *J. Am. Chem. Soc.*, **136**, 8027–8033 (2014).
69. Tolle, F., Brandle, G. M., Matzner, D. and Mayer, G. A versatile approach towards nucleobase-modified aptamers. *Angew. Chem. Int. Ed*., **54**, 10971–10974 (2015).
70. Jao, C.Y. and Salic, A. Exploring RNA transcription and turnover in vivo by using click chemistry. *Proc. Natl. Acad. Sci. USA*., **105**, 15779–15784 (2008).
71. Milligan, J. F. and Uhlenbeck, O. C. Synthesis of small RNAs using T7 RNA polymerase. *Methods Enzymol*., **180**, 51–62 (1989).
72. Chen, Y., Wu, Y., Henklein, P., Li, X., Hofmann, K. P., Nakanishi, K. and Ernst, O. P. A photo-cross-linking strategy to map sites of protein-protein interactions. *Chem. Eur. J.*, **16**, 7389–7394 (2010).
73. Hotha, S. and Kashyap, S. "Click chemistry" inspired synthesis of pseudo oligosaccharides and amino acid glycoconjugates. *J. Org. Chem.*, **71**, 364−367 (2006).
74. Alexiou, M. S., Tychopoulos, V., Ghorbanian, S., Tyman, J. H. P., Brown, R. G. and Brittain, P. I. The UV–visible absorption and fluorescence of some substituted 1,8-naphthalimides and naphthalic anhydrides. *J. Chem. Soc., Perkin Trans*., **2**, 837–842 (1990).

2.6 Appendix-I: Characterization data of synthesized compounds

^{1}H-NMR of alkyne-modified ribonucleoside **3** in d_6- DMSO

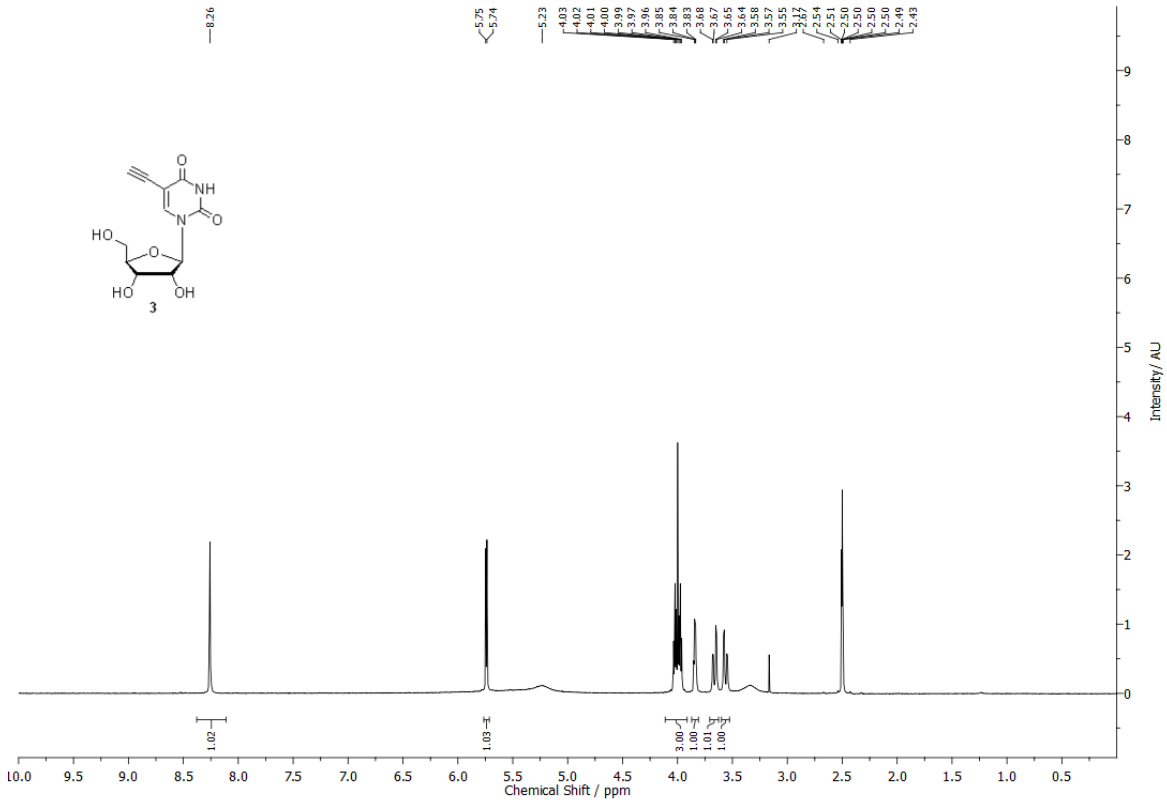

^{13}C-NMR of alkyne-modified ribonucleoside **3** in d_6- DMSO

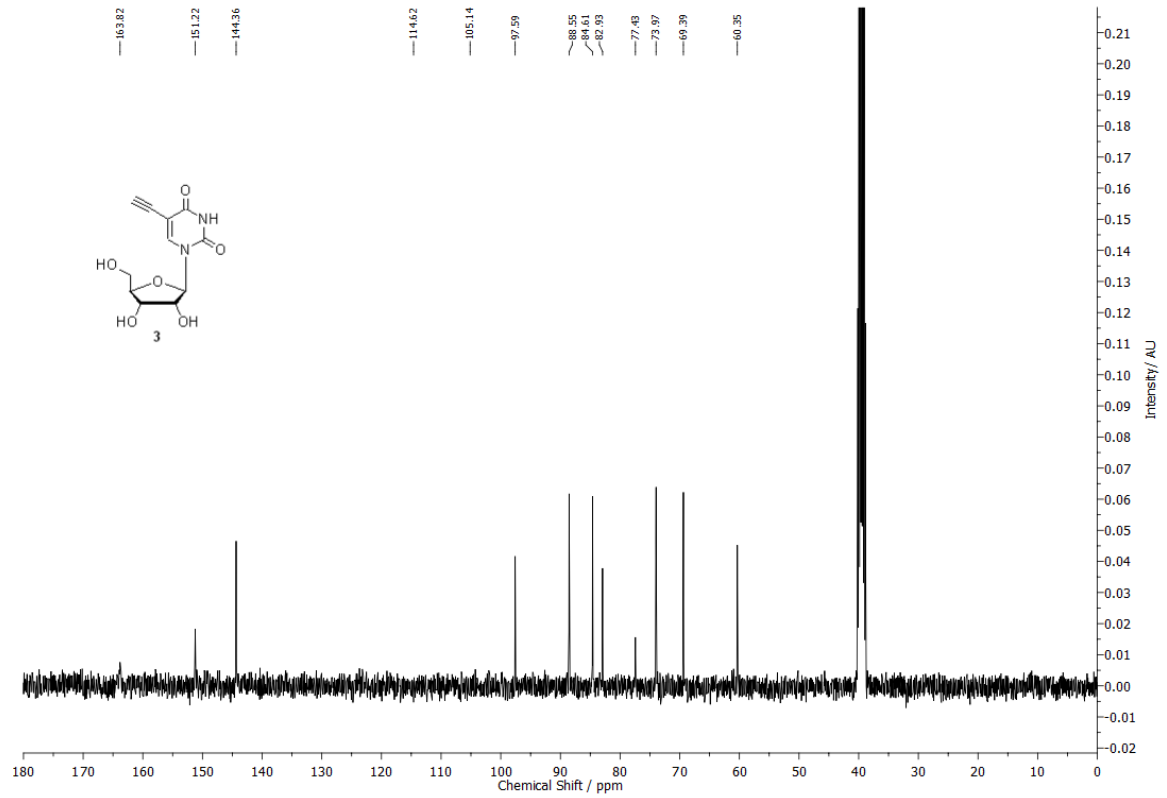

^{1}H-NMR of alkyne-modified ribonucleoside triphosphate **5** in D_2O

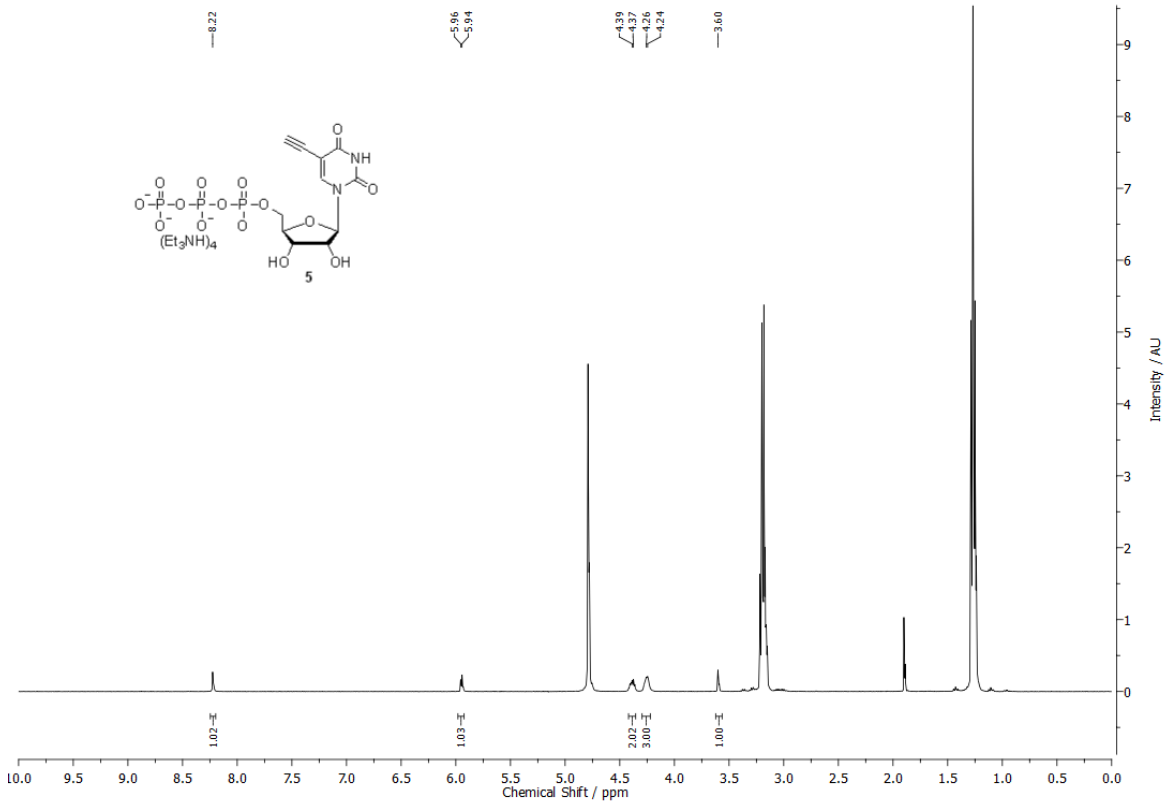

^{31}P-NMR of alkyne-modified ribonucleoside triphosphate **5** in D_2O

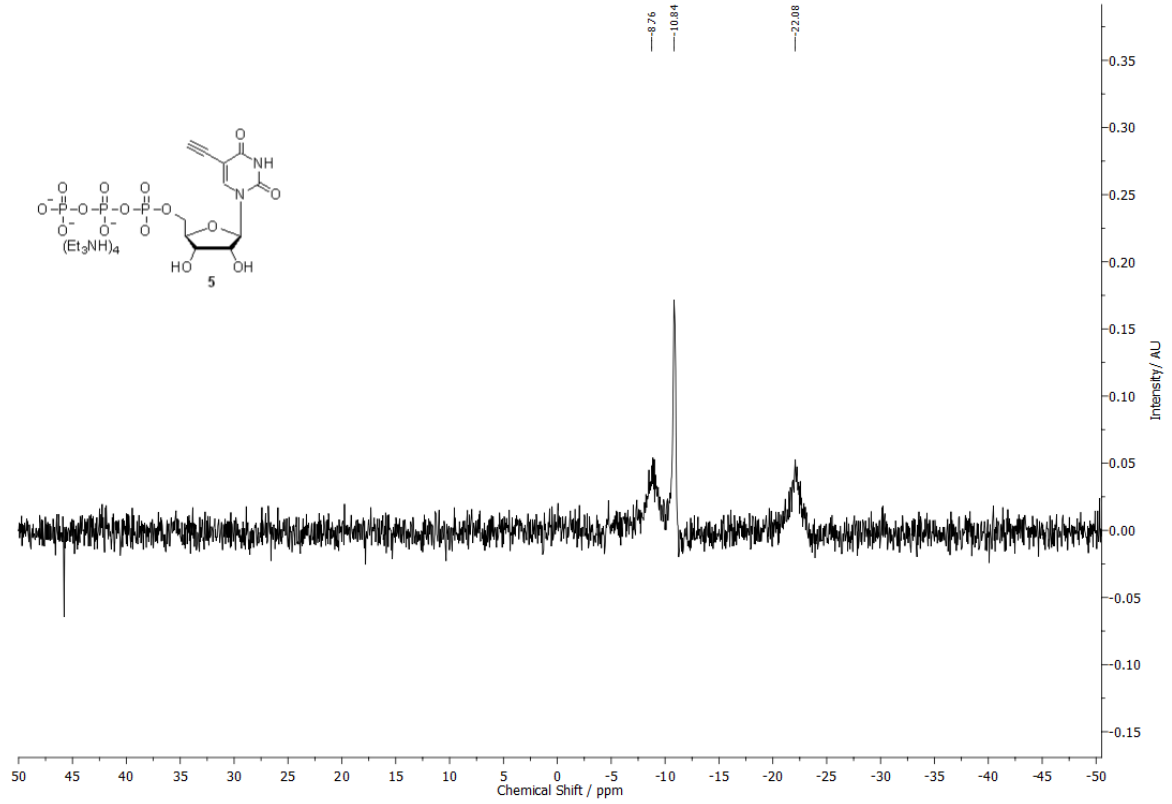

^{1}H-NMR of alkyne-modified ribonucleoside **4** in d_6- DMSO

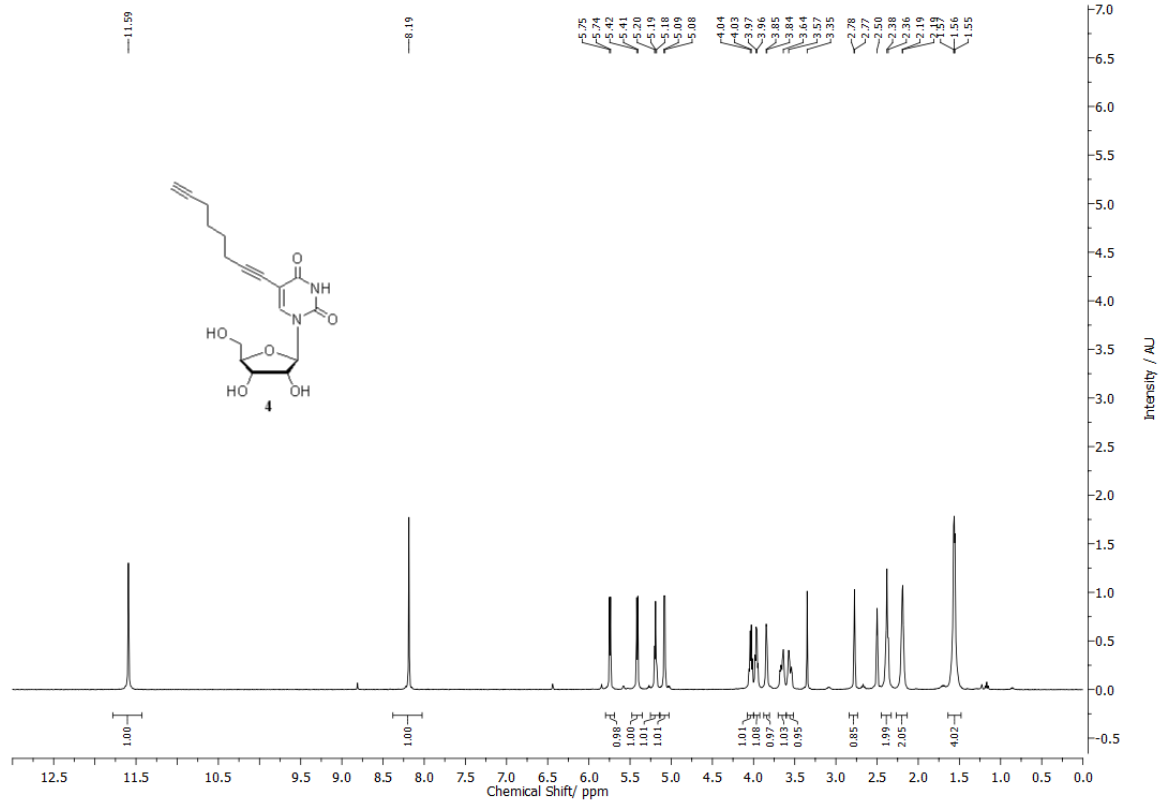

^{13}C-NMR of alkyne-modified ribonucleoside **4** in d_6- DMSO

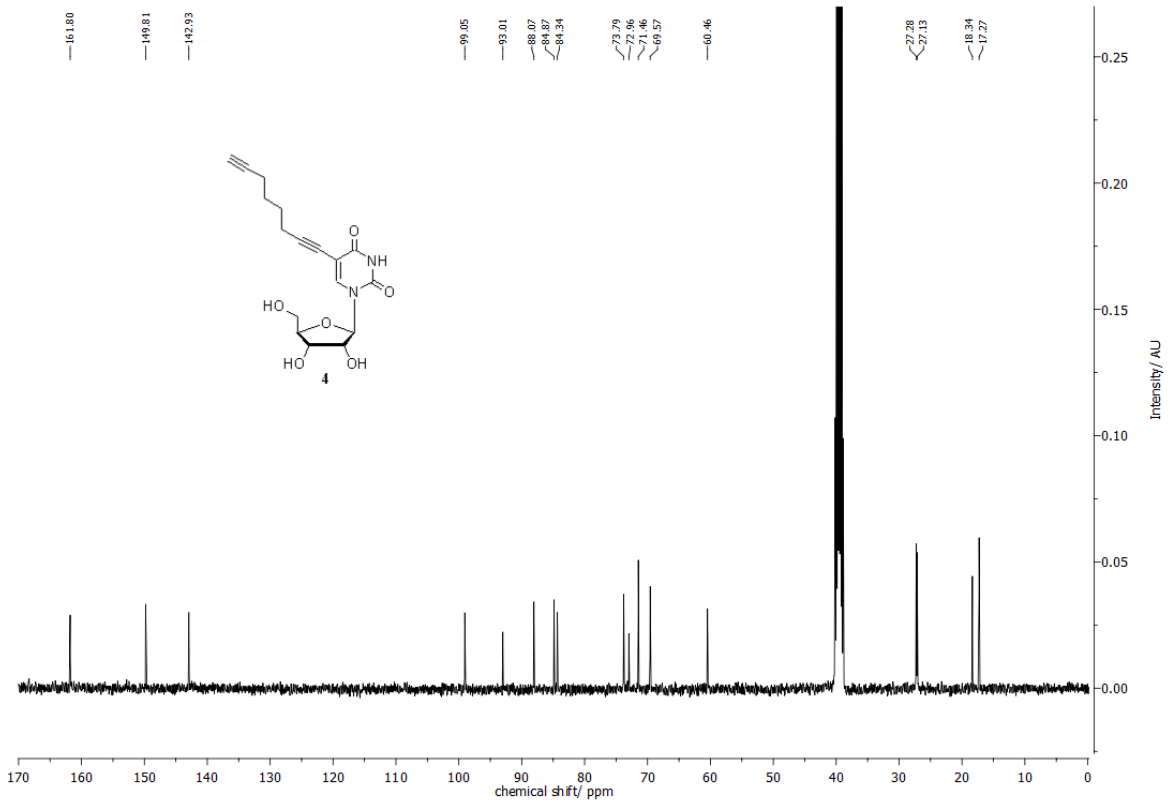

^{1}H-NMR of alkyne-modified ribonucleoside triphosphate **6** in D_2O

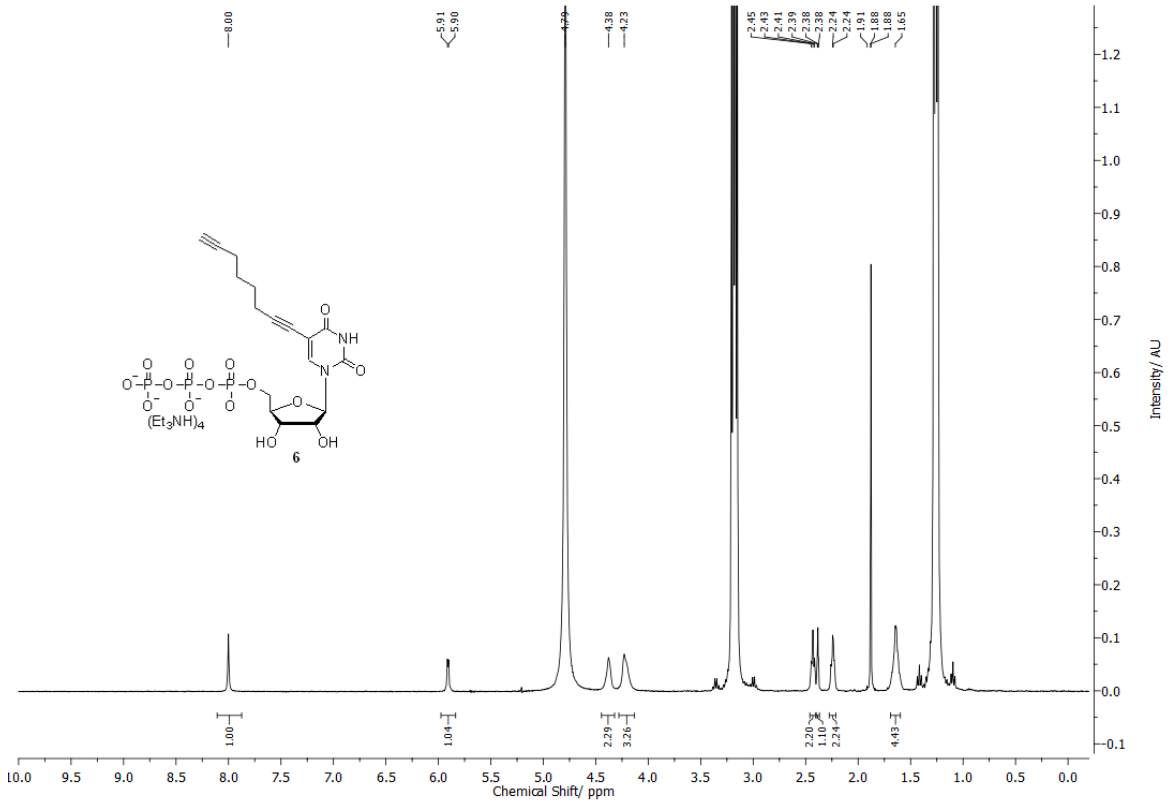

^{13}C-NMR of alkyne-modified ribonucleoside triphosphate **6** in D_2O

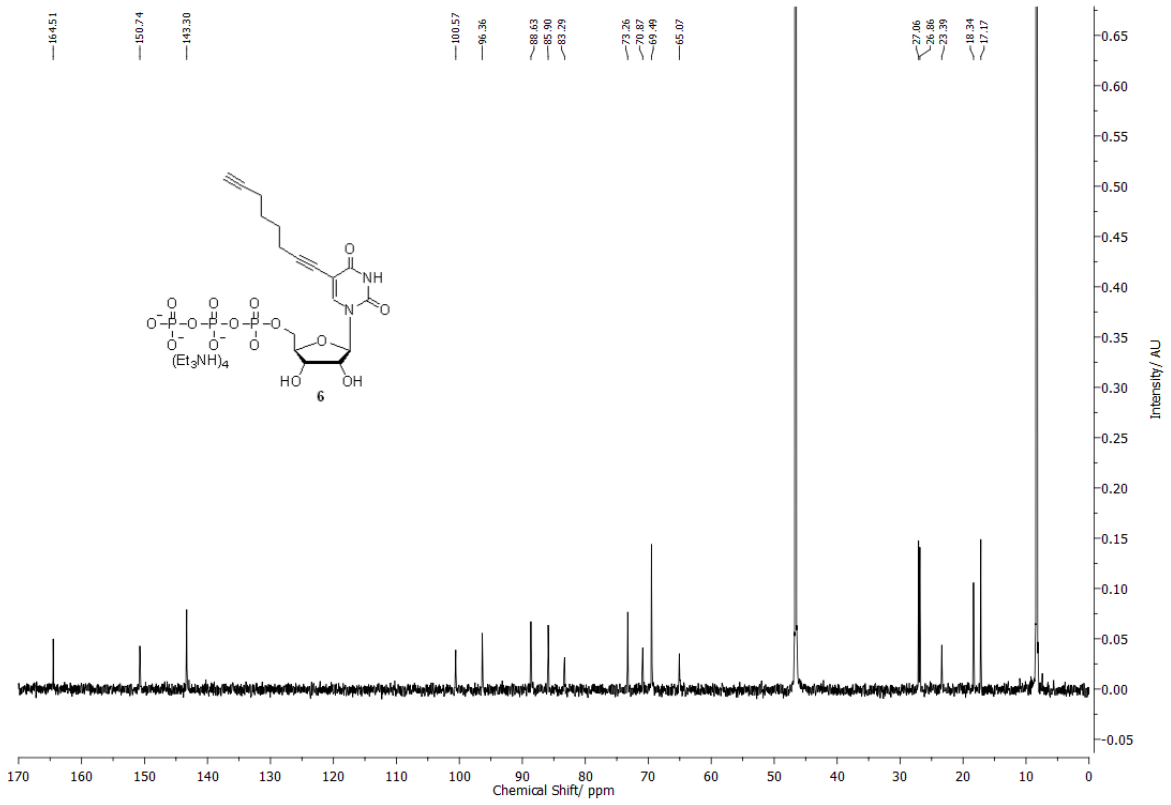

^{31}P-NMR of alkyne-modified ribonucleoside triphosphate **6** in D_2O

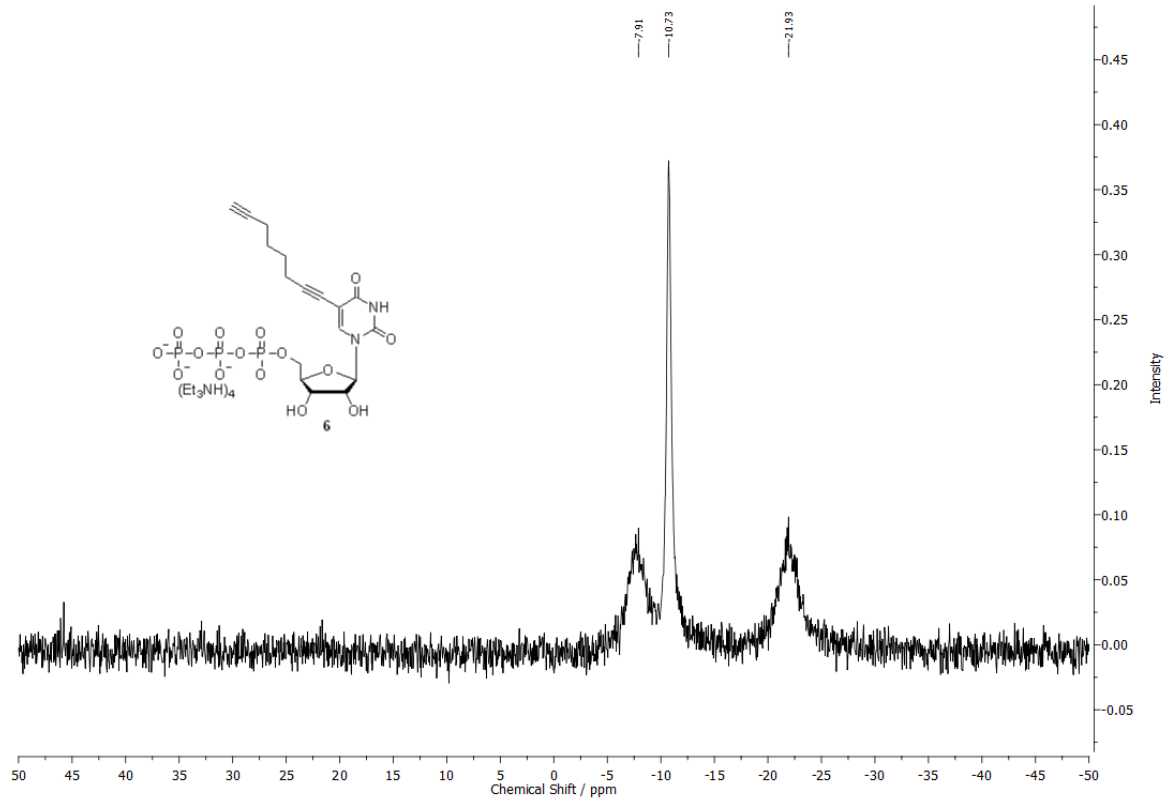

^{1}H-NMR of naphthalimide azide **9** in d_6- DMSO

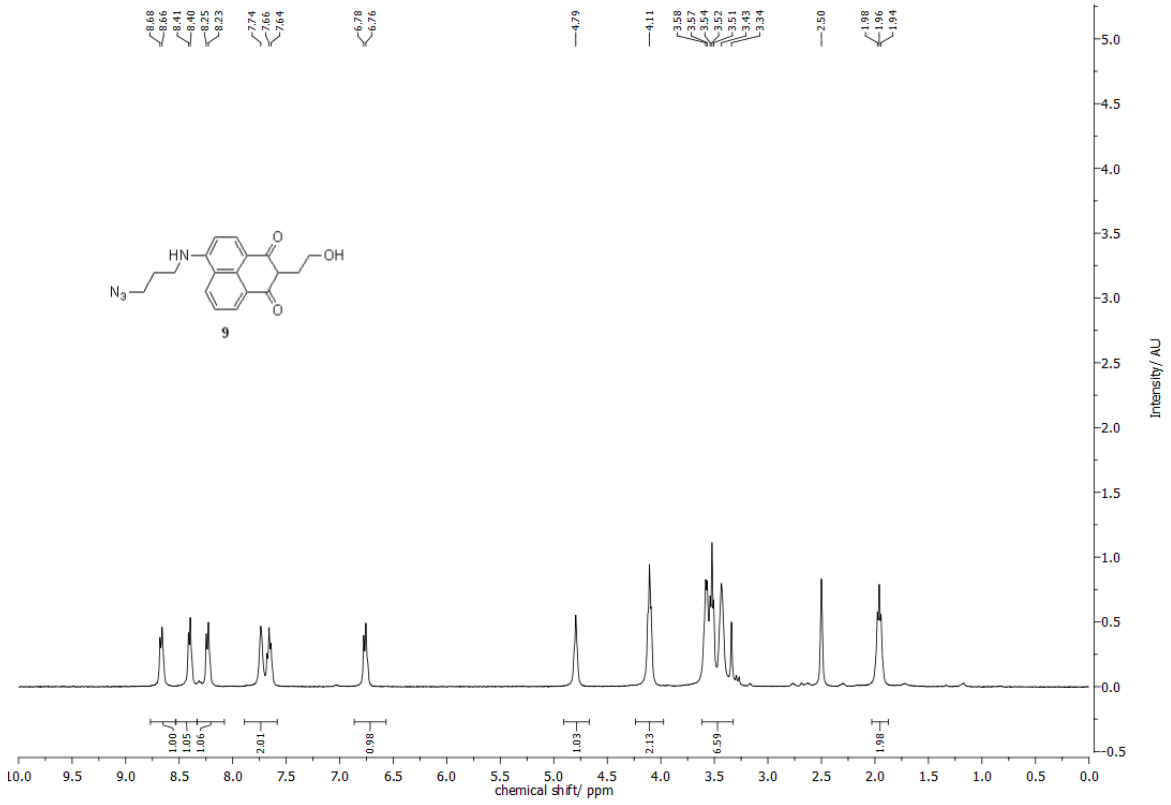

^{13}C-NMR of naphthalimide azide **9** in d_6- DMSO

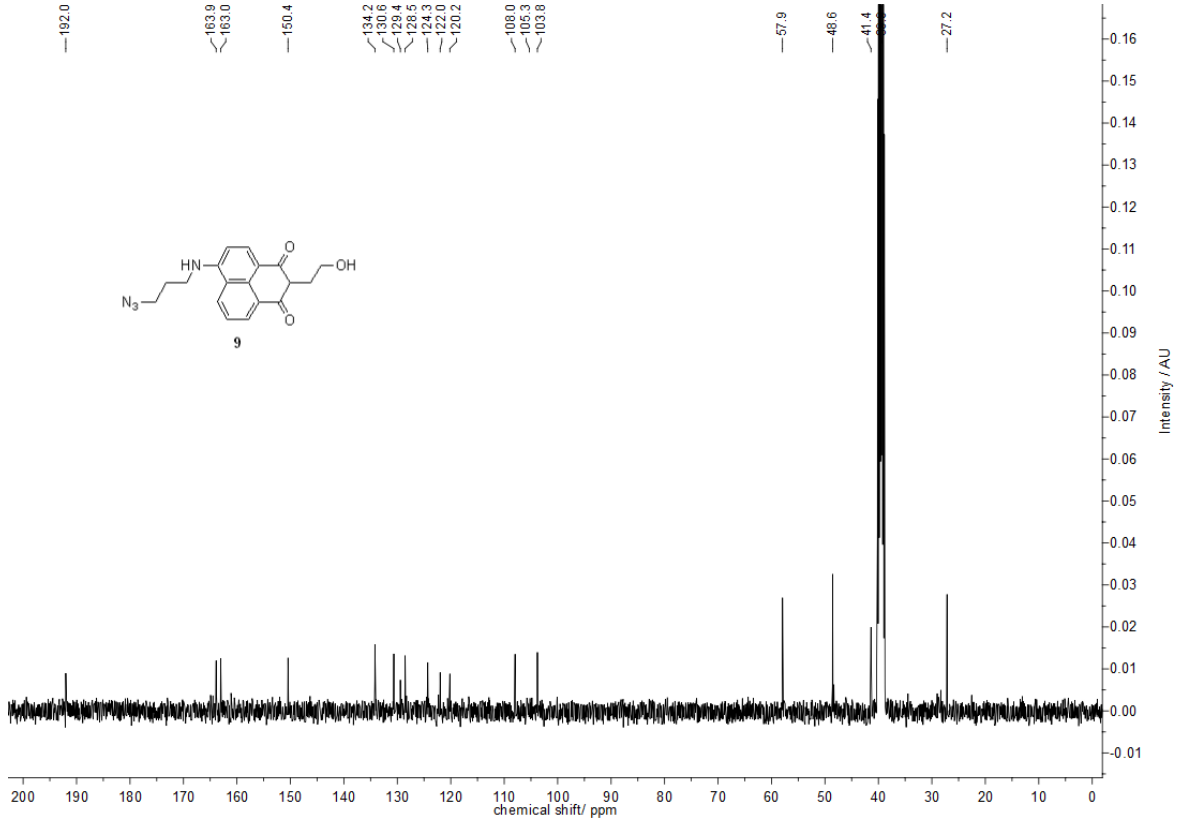

^{1}H-NMR of glucose azide **11** in D_2O

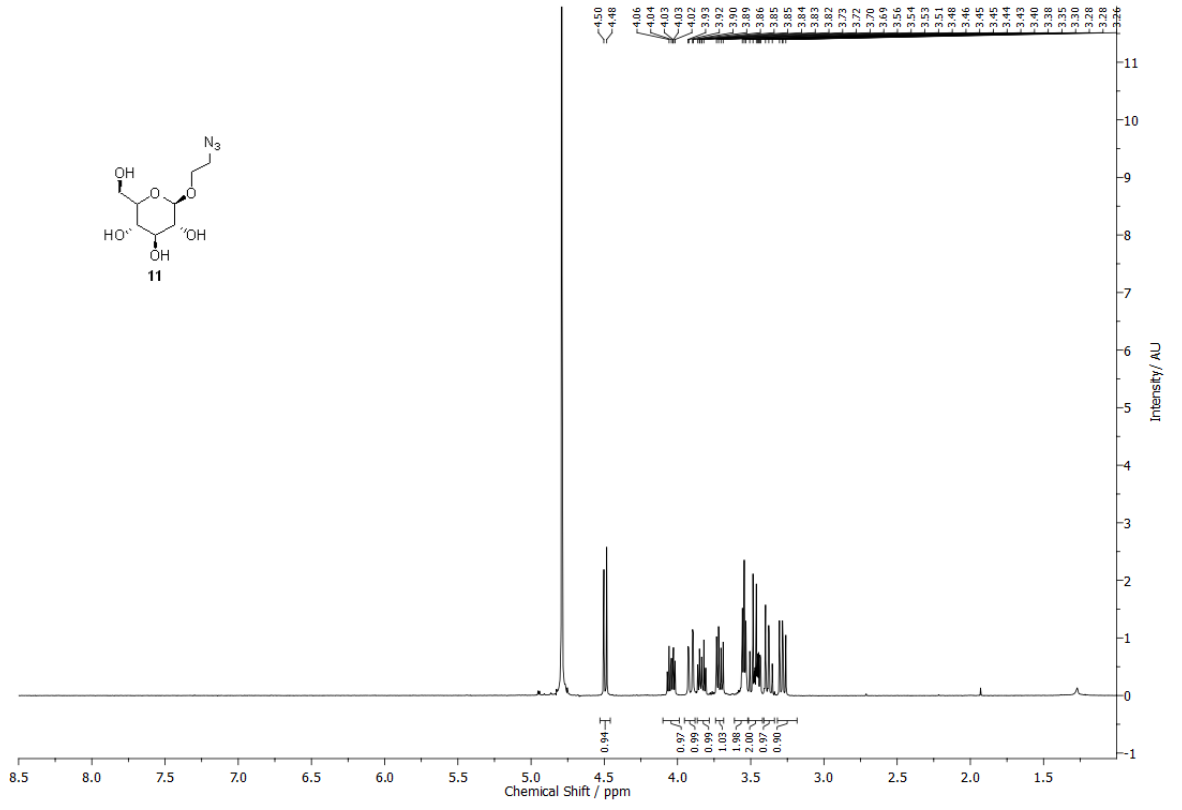

^{1}H-NMR of biotin azide **12** in D_2O

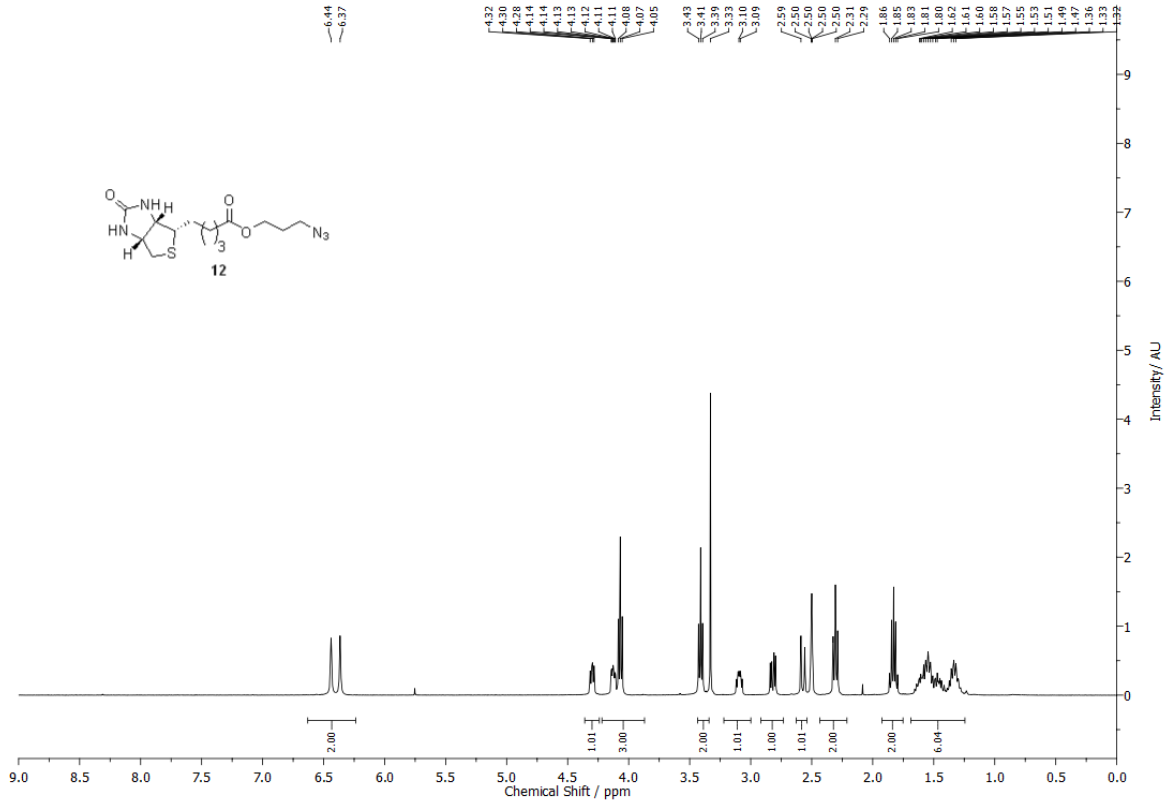

^{1}H-NMR of tryptophan azide **13** in d_6- DMSO

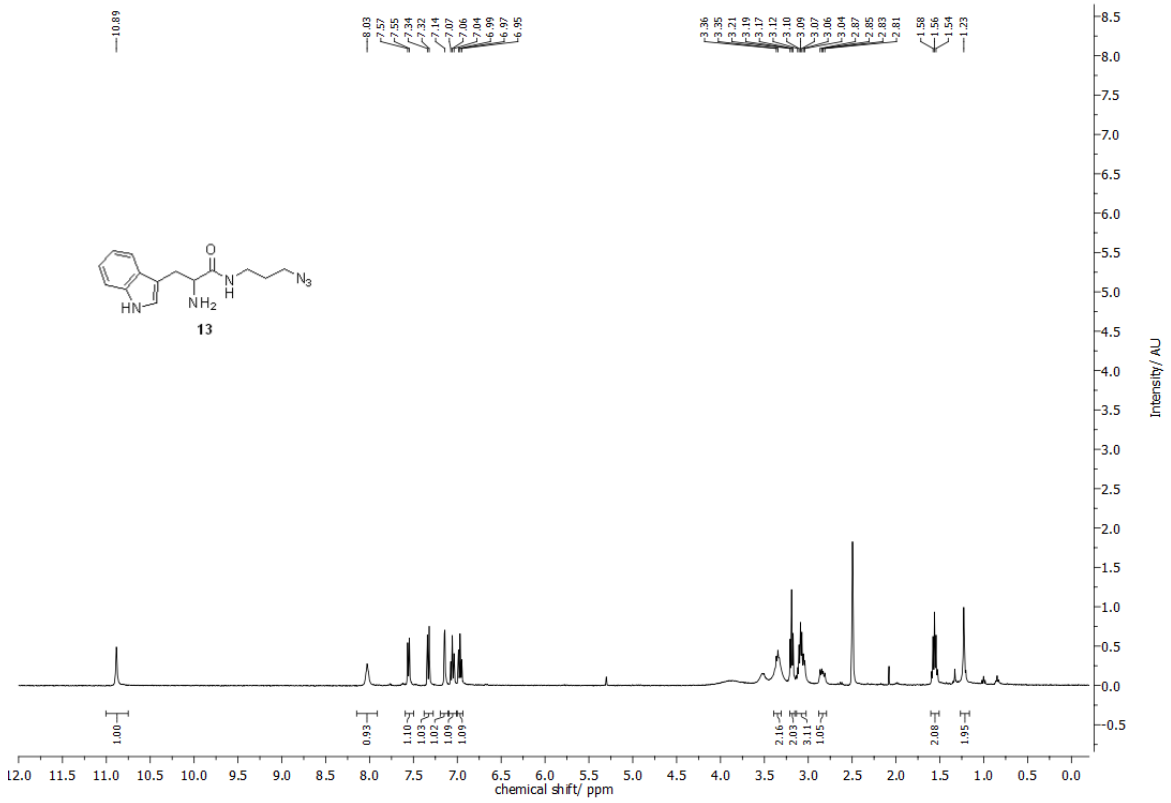

^{13}C-NMR of tryptophan azide **13** in d_6- DMSO

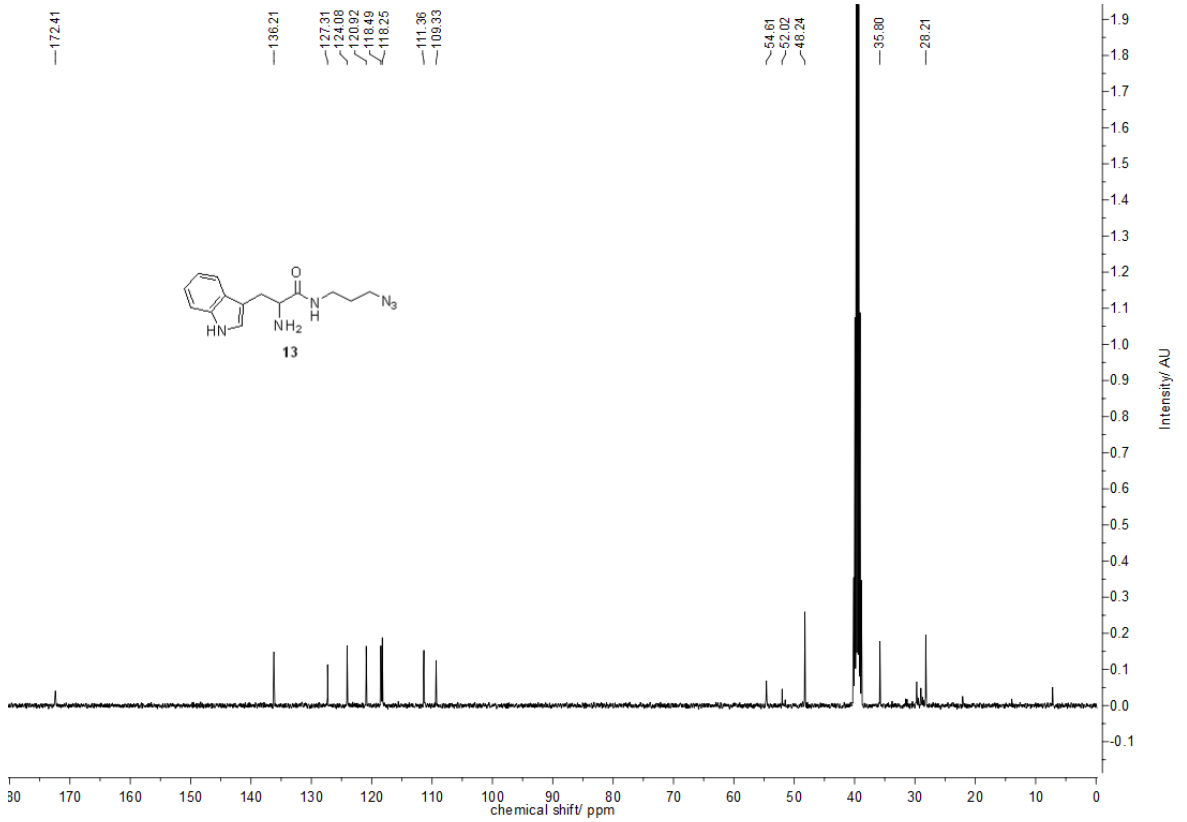

MALDI-TOF mass spectrum of clicked RNA transcript **9a**

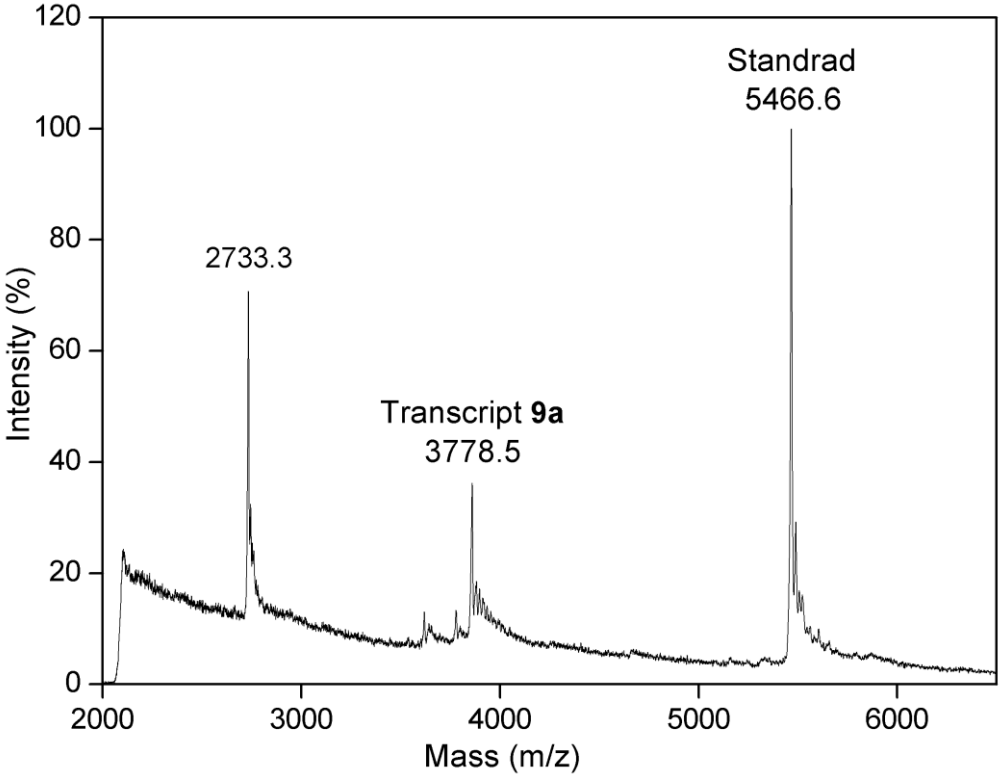

Calcd. mass for clicked RNA transcript **9a**: 3778.3 [M]; found: 3778.5.

MALDI-TOF mass spectrum of clicked RNA transcript **9b**

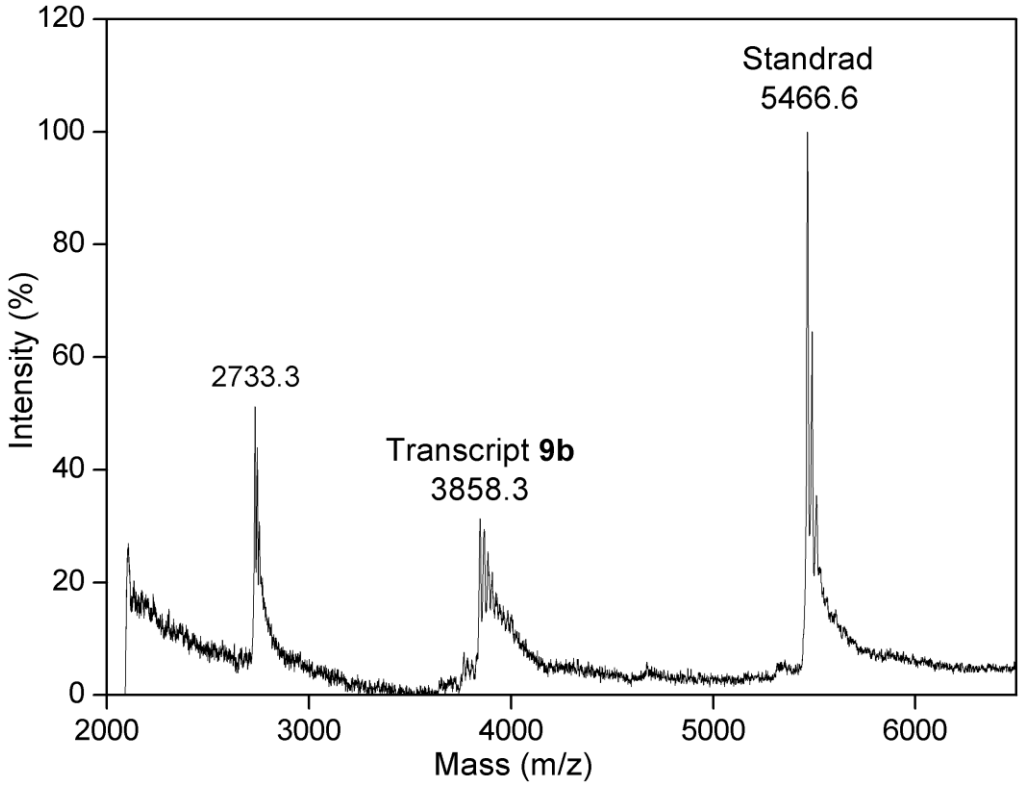

Calcd. mass for clicked RNA transcript **9b**: 3858.6 [M]; found: 3858.3.

MALDI-TOF mass spectrum of clicked RNA transcript **10a**

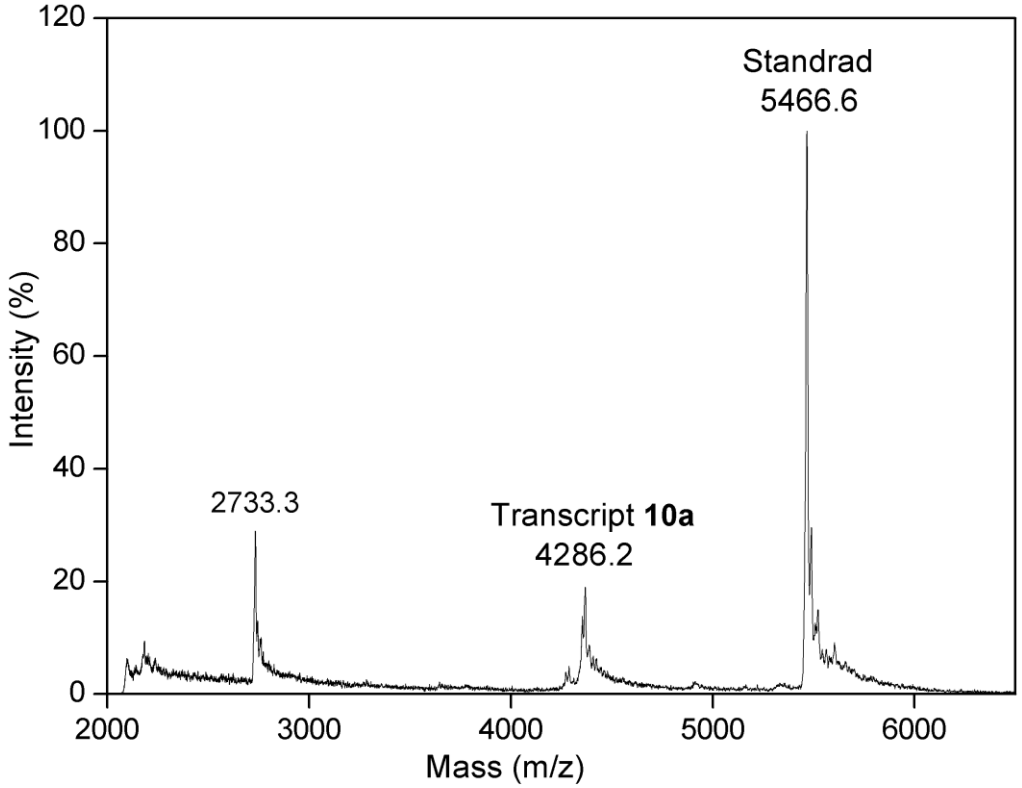

Calcd. mass for clicked RNA transcript **10a**: 4286.9 [M]; found: 4286.2

MALDI-TOF mass spectrum of clicked RNA transcript **10b**

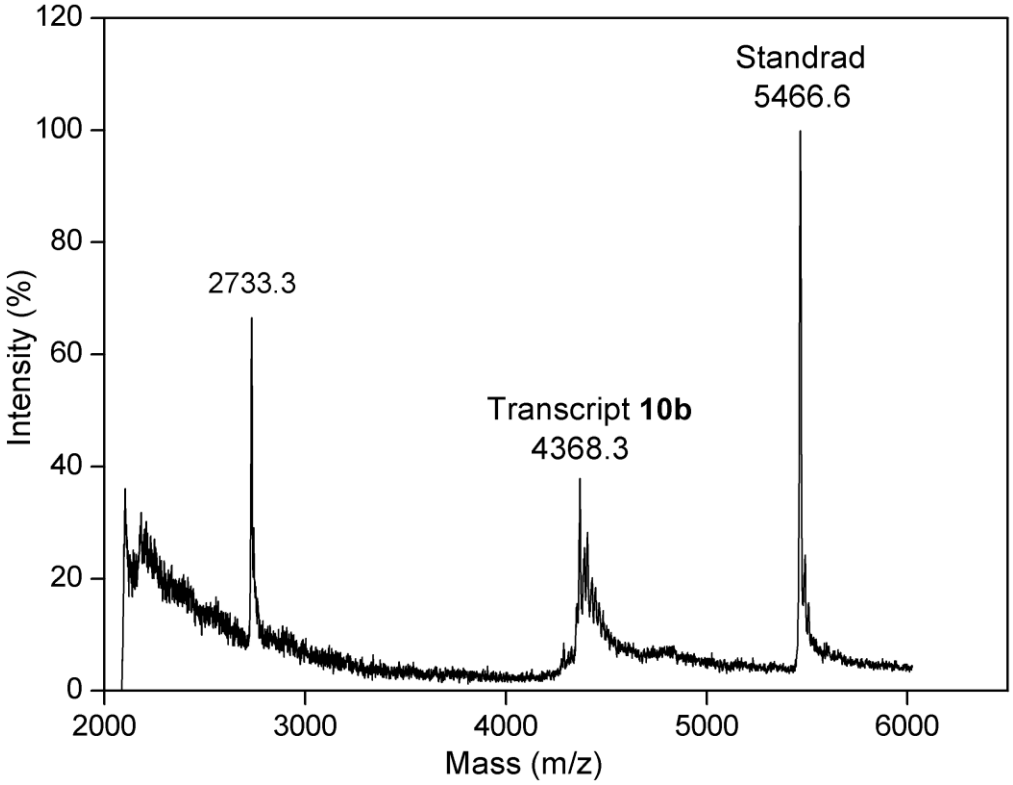

Calcd. mass for clicked RNA transcript **10b**: 4367.0 [M]; found: 4368.3.

MALDI-TOF mass spectrum of clicked RNA transcript **11a**

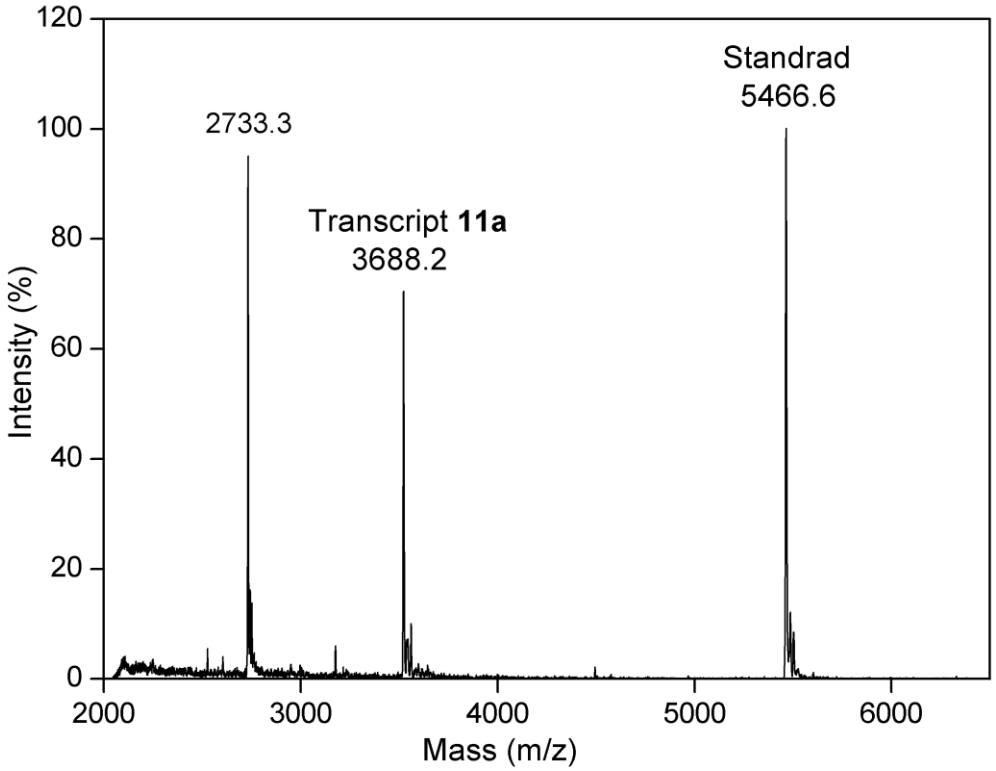

Calcd. mass for clicked RNA transcript **11a**: 3688.2 [M]; found: 3688.2.

MALDI-TOF mass spectrum of clicked RNA transcript **11b**

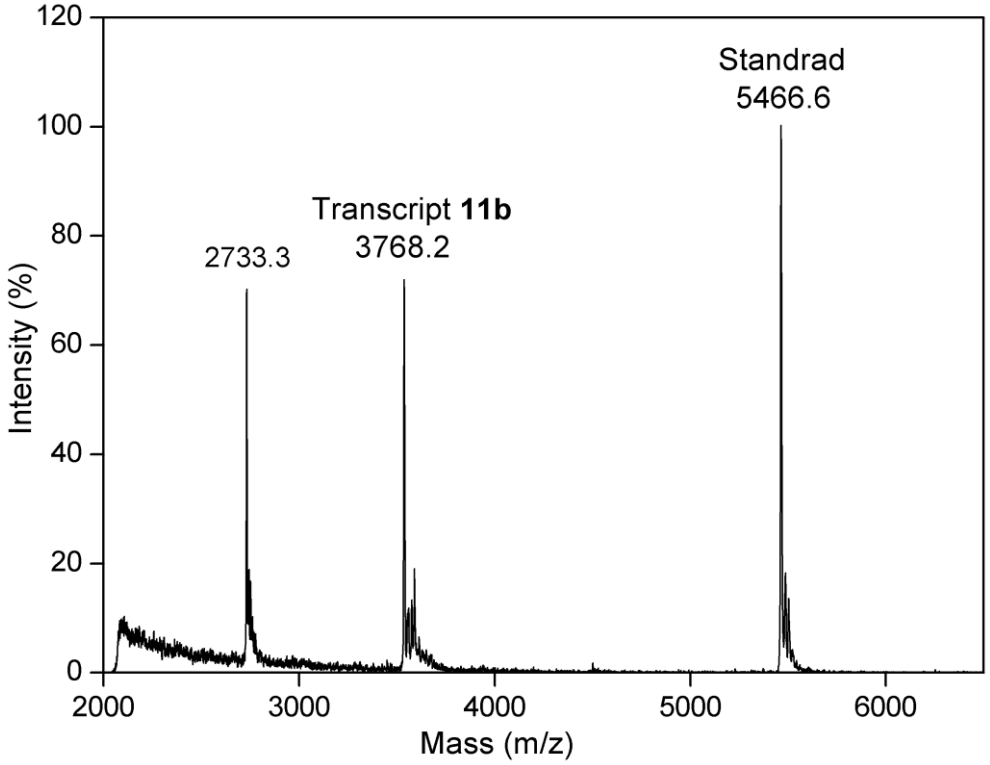

Calcd. mass for clicked RNA transcript **11b**: 3768.8 [M]; found: 3768.2.

MALDI-TOF mass spectrum of clicked RNA transcript **12a**

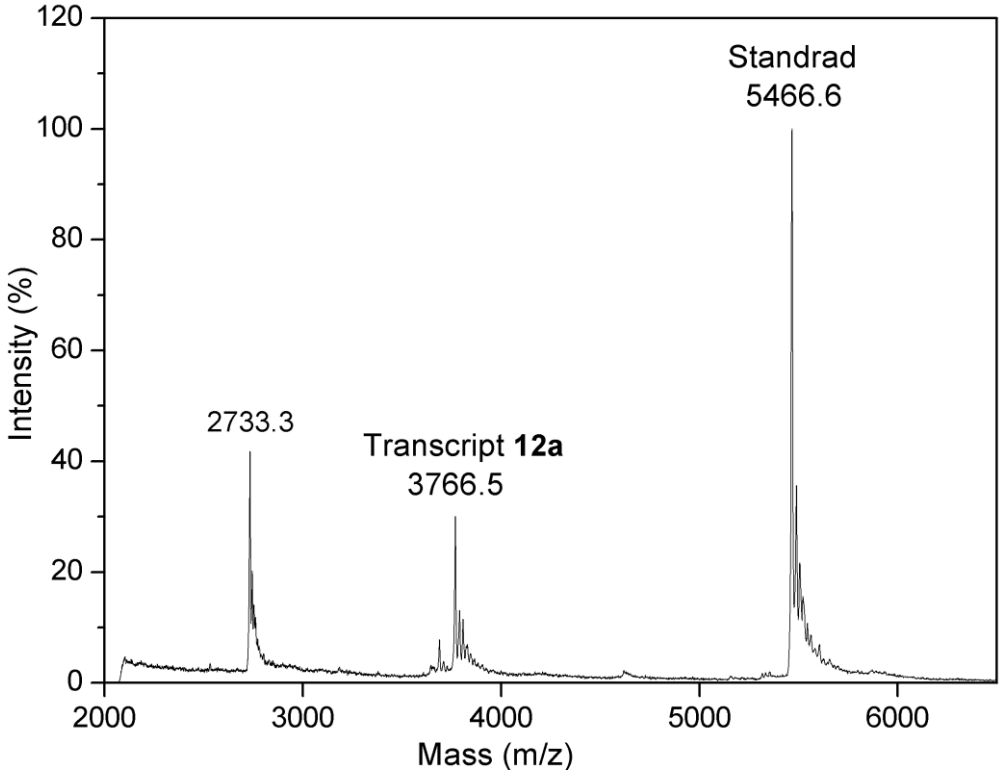

Calcd. mass for clicked RNA transcript **12a**: 3766.8 [M]; found: 3766.5.

MALDI-TOF mass spectrum of clicked RNA transcript **12b**

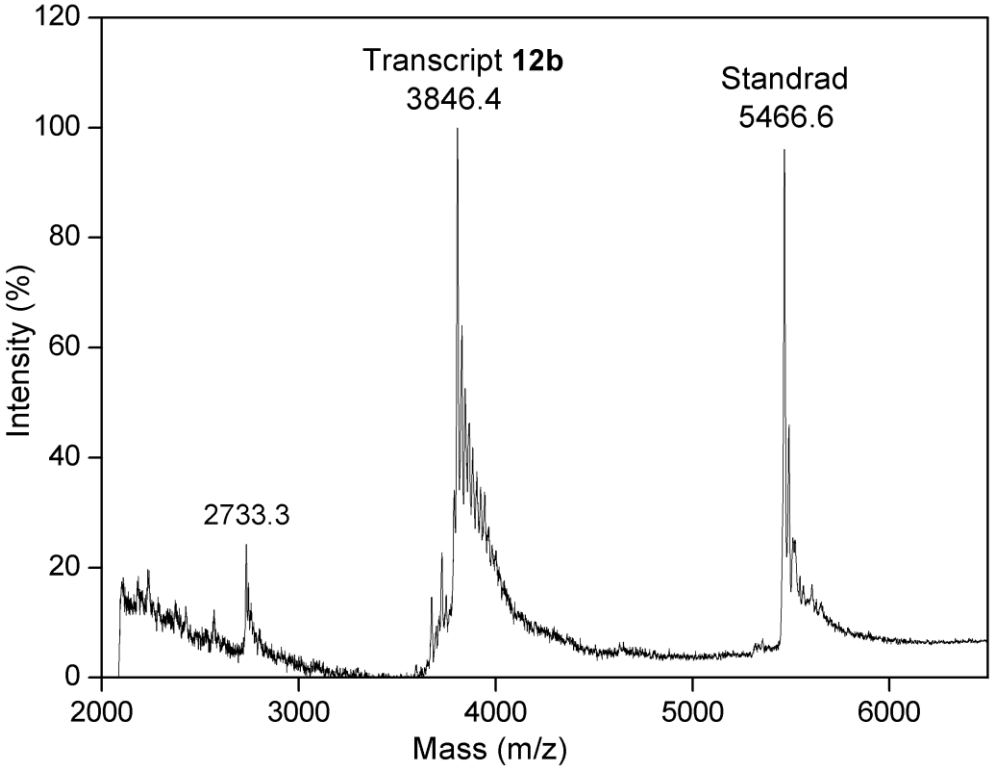

Calcd. mass for clicked RNA transcript **12b**: 3846.8 [M]; found: 3846.4.

MALDI-TOF mass spectrum of clicked RNA transcript **13a**

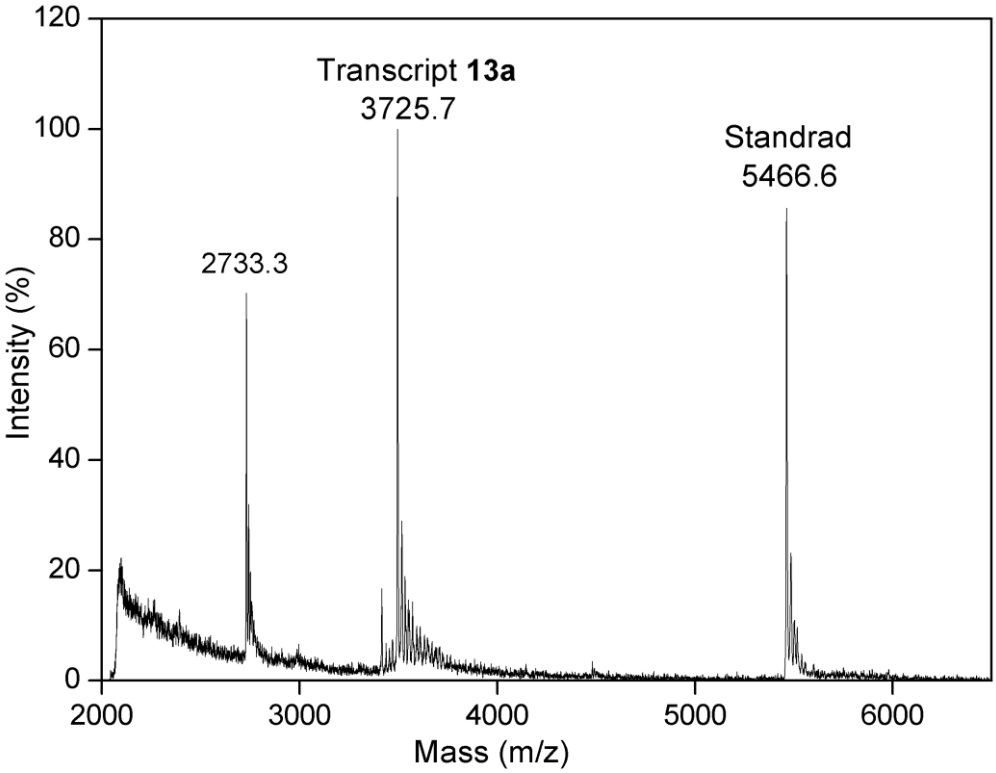

Calcd. mass for clicked RNA transcript **13a**: 3725.3 [M]; found: 3725.7.

MALDI-TOF mass spectrum of clicked RNA transcript **13b**

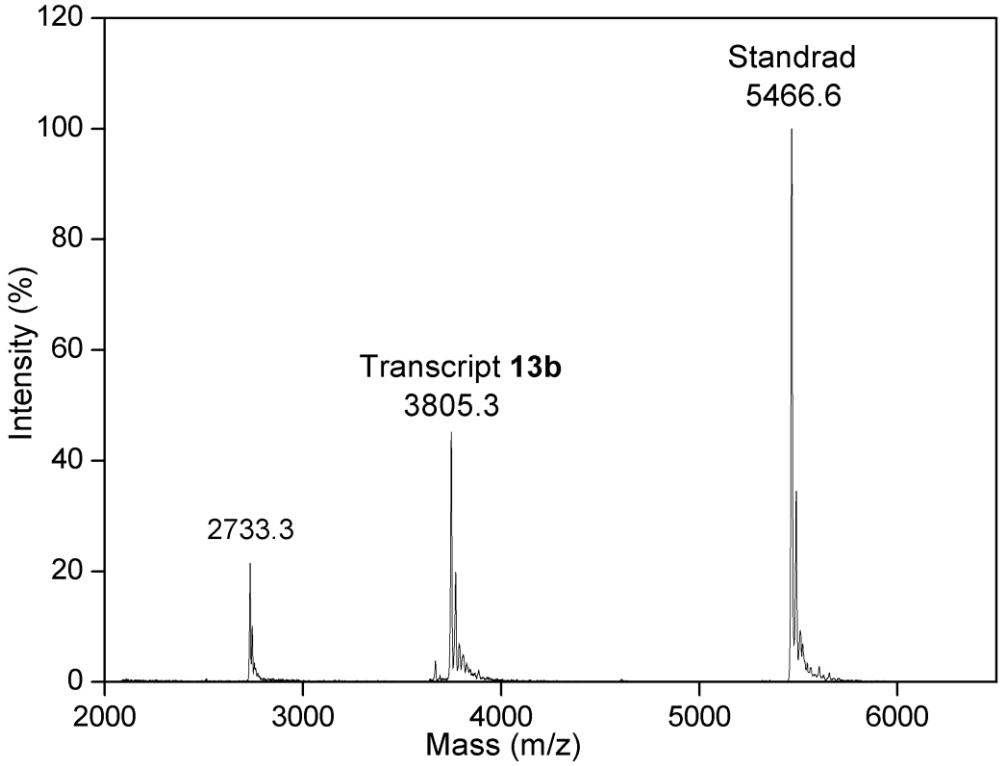

Calcd. mass for clicked RNA transcript **13b**: 3806.1 [M]; found: 3805.3.

Chapter 3

Clickable UTP Analogs for the Posttranscriptional Chemical Imaging of RNA

Chapter 3A

Imaging cellular RNA transcripts using an alkyne-modified UTP analog

3A.1 Introduction

At any given time, cellular RNA levels depend upon highly regulated processes of RNA production, processing and degradation.[1-3] The development of DNA microarrays and deep sequencing technologies for the transcriptome analysis provides snapshots of these differential steady states of cellular RNA.[4-6] Chemically modified RNA that results in the addition of a moiety suitable for visualization, detection, and affinity purification is a powerful tool for understanding cellular RNA processes.[7-9] Noncovalent fluorescence based hybridization approaches have allowed RNA imaging in cells.[10-17] However, these methods do not provide information about RNA synthesis and degradation dynamics in cells.

Early efforts to detect RNA biogenesis in cells relied on metabolic incorporation of modified nucleoside analogs such as radioisotope labeled [3H]-uridine, 5-bromouridine (5-BrU) and 4-thiouridine (4-sU) followed by autoradiography and immunostaining.[18-23] However, the use of radioactivity and antibody staining is cumbersome and or laborious due poor permeability of antibody. Recently, chemical functionalization using bioorthogonal reactions strategy has emerged as a valuable tool for the detection of protein, lipids, glycans and nucleic acids both *in vitro* and in cells.[24-30] Chemically functionalized metabolite precursors with reactive functional groups such as azide, alkyne and alkene serve as useful chemical reporters for protein, lipids, glycans and nucleic acids.[31-51] The success of postsynthetic labeling strategy in cells completely depends upon efficacy of endogenous enzymes to incorporate these modified chemical reporters into nucleic acid in presence of native counterparts. The successful incorporation of chemical reporter into nucleic acids in first step allows selective detection of nascent nucleic acids by chemoselective reactions with fluorescent cognate partners. Therefore, chemically modified nucleosides with small reactive functionality like azide, alkyne and alkene would serve as promising chemical reporters for *in vivo* RNA detection. The combinations of chemical reporters (azide, alkyne and alkene) and chemoselective reactions (Staudinger ligation, SPAAC, CuAAC, tetrazine reaction) are at the disposal for bioorthogonal labeling and imaging of nucleic acids.[45,49,50] However, RNA imaging using alkyne chemical reporter and CuAAC reactions attracted early attention due to accessibility and reaction kinetics.[46]

While methods have been well established for labeling RNA in cell-free environment, tools to label endogenous RNAs are less prevalent. Salic and Jao showed for the first time that an alkyne-modified nucleoside analog, 5-ethynyluridine (EU), could be introduced into

RNA metabolically by the ribonucleoside salvage pathway.[46] Further modification under CuAAC reaction conditions enabled the visualization of cellular RNA synthesis, turnover and localization. In a similar approach, alkyne-containing cytosine and adenosine analogs have been introduced into endogenous RNA transcripts and their synthesis and polyadenylation process have been monitored by fluorescence microscopy.[52-54] More recently, clickable group-containing cosubstrates of nucleotidyltransferase, methyltransferase and tRNA-modifying enzymes have been elegantly utilized in site-specific labeling of eukaryotic and prokaryotic mRNAs, and subsequent click chemistry has facilitated the elucidation of mRNA processing.[55-61]

Encouraged by the results disscussed in previous chapter, we wanted to evaluate the utility of an alkyne modified uridine analog (ODU) as chemical reporter for labeling and imaging cellular RNA transcripts by using CuAAC reactions with fluorescent probe. Rewardingly, we found that triphosphate substrate ODUTP is specifically incorporated into cellular RNA transcripts by endogenous RNA polymerases, which permitted the fluorescence imaging of newly synthesized RNA in cells by using click reaction. Furthermore, literature precedence and our preliminary spectroscopic analysis provide evidence that ODU label could be potentially suitable for dual imaging of RNA by click chemistry as well as by Raman spectroscopy.

3A.2 Results and discussion

3A.2.1 Imaging cellular RNA transcripts using alkyne-modified uridine (ODU) 4

Effective incorporation of ODUTP into RNA ONs by RNA polymerase and compatibility of ODU-labeled RNA to click reaction prompted us to study the usefulness of this analog in labeling and imaging cellular RNA. This would be possible if cellular RNA transcripts could be labeled with ODU metabolically by the biosynthetic machinery of the cell followed by cycloaddition reaction with an appropriate azide-modified biophysical probe. The alkyne labeling of cellular RNA transcripts by ribonucleoside salvage pathway was examined by incubating HeLa cells (human cervical cancer cells) in culture with ODU. The cells were fixed, permeabilized and stained by using click reaction with Alexa594-azide (**10**). The cells were then DAPI-stained and visualized by fluorescence microscopy. Unfortunately, fluorescence signal from the cells was very low indicating that the modified ribonucleoside is not incorporated into RNA (Figure 1). This observation is in contrast to EU, which is effectively incorporated into cellular RNA under similar conditions. It is possible that ODU

having a longer linker is either cell impermeable or a poor substrate for the ribonucleoside processing enzymes (e.g., kinases) that are responsible for the generation of triphosphate substrate required for the transcription reaction.

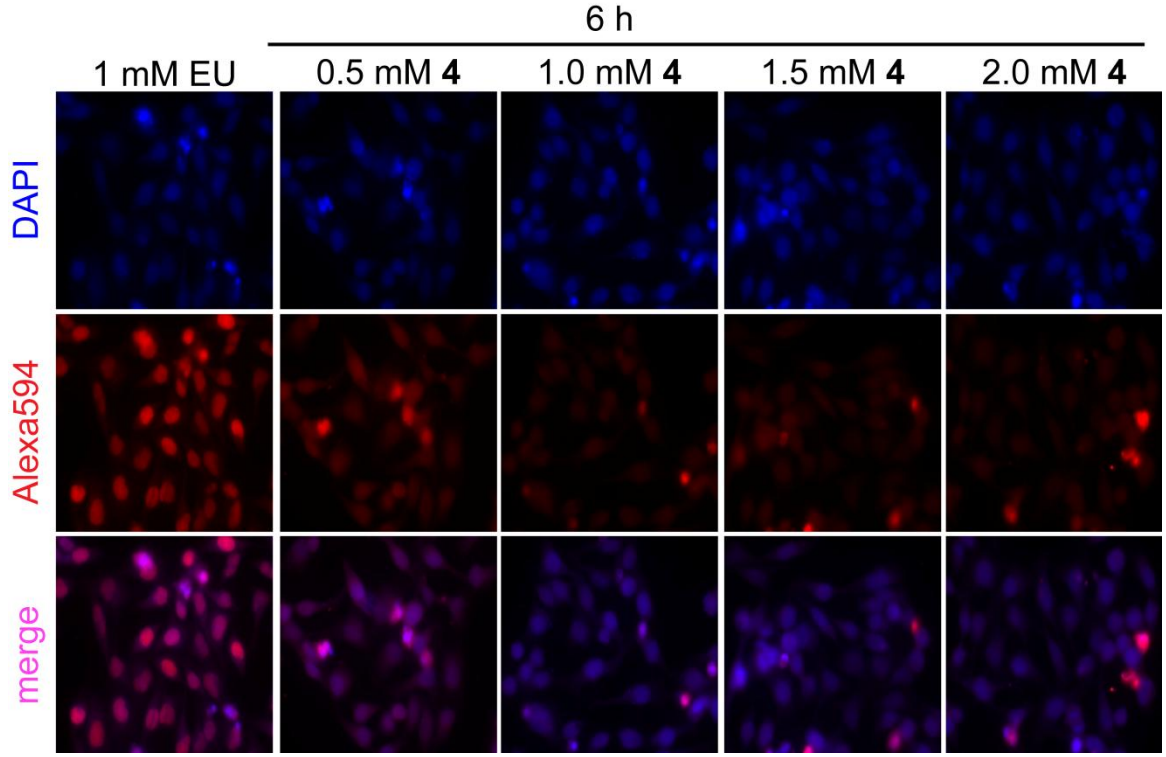

Figure 1. Incorporation of the alkyne-modified uridine analog **4** into cellular RNA transcripts followed by detectetion using CuAAC reactions with Alexa594-alkyne **10**.

3A.2.2 Imaging cellular RNA transcripts using alkyne modified UTP (ODUTP) 6

To circumvent this problem, we decided to transfect the cells with ODUTP **6** such that the modified substrate would be directly available for incorporation into RNA transcripts by endogenous RNA polymerases. The cells in culture were transfected with increasing concentrations of **6** for 3 h using DOTAP (*N*-[1-(2,3-Dioleoyloxy)propyl]-*N*,*N*,*N*-trimethylammonium methylsulfate). As before, fixed and permeabilized cells were stained by means of CuAAC reaction with Alexa594-azide **10**. Rewardingly, we observed dose-dependent increase in nuclear staining wherein more than 90% of the cells were stained at 4 mM of ODUTP (Figure 2). We then monitored the ODU labeling as a function of transfection time. Few cells exhibited nuclear staining within 15 min of exposure to ODUTP (4 mM), which increased with increase in incubation time (Figure 3). Importantly, control experiments in the absence of ODUTP showed no fluorescence signal in the Alexa594 channel when cells were stained under similar conditions (column 1 in Figure 2 and 3).

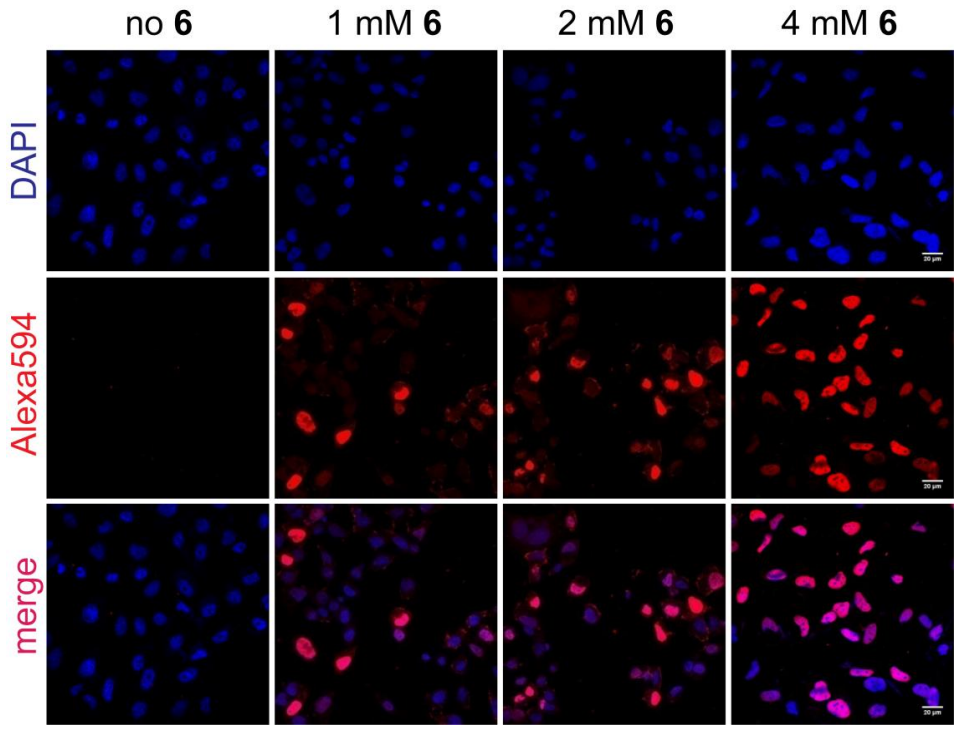

Figure 2. Imaging cellular RNA transcripts using alkyne-modified UTP **6**. HeLa cells were transfected with alkyne-modified UTP **6** (1 mM to 4 mM) for 3 h using DOTAP. The cells were then fixed, permeabilized and the alkyne-modified uridine labeling was detected by performing CuAAC reaction with Alexa594-azide **10**.

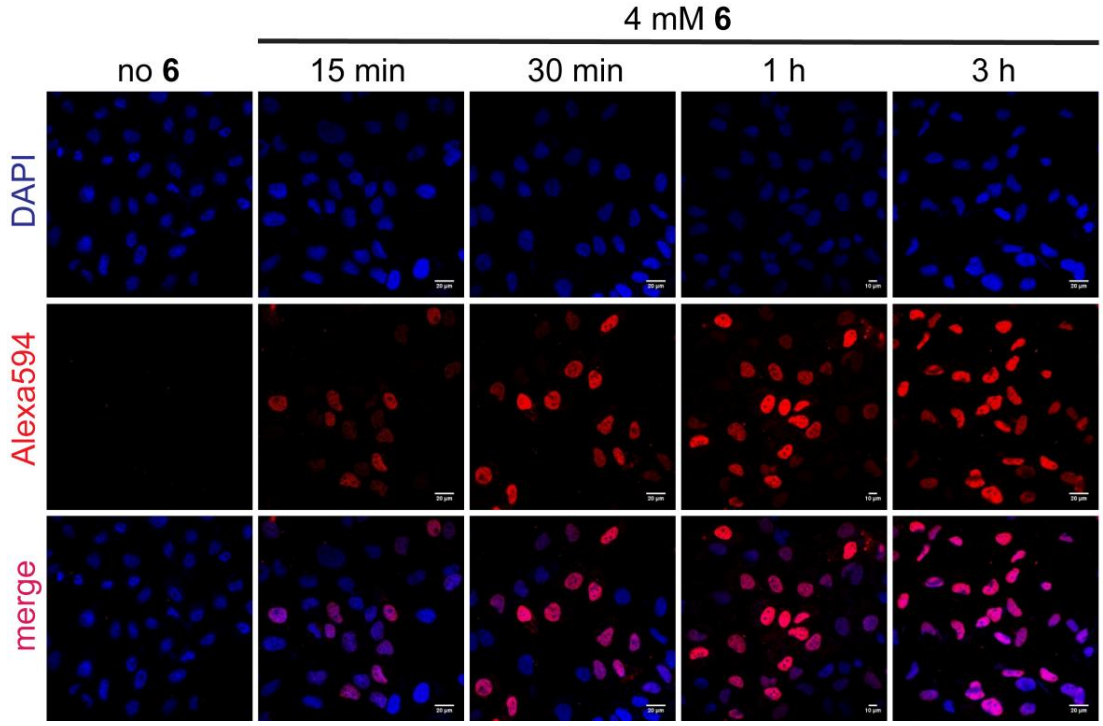

Figure 3. Incorporation of alkyne-modified UTP **6** into RNA transcripts as a function of transfection time. HeLa cells were incubated with **6** (4 mM) in the presence of DOTAP for 15 min to 3 h. The cells were fixed, permeabilized and the alkyne-modified uridine labeling was detected by performing CuAAC reaction with Alexa594-azide **10**. The number of cells showing nuclear staining increased with increasing incubation time.

3A.2.3 ODUTP 6 is a specific biosynthetic label for cellular RNA

The specific incorporation of ODUTP into RNA by cellular RNA polymerase was confirmed by performing the following experiments. ODUTP can be potentially dephosphorylated into ODUDP in cells, which can be converted into ODdUDP by the action of ribonucleoside diphosphate reductase. Further, ODdUDP can be phosphorylated into ODdUTP and then incorporated into replicating DNA by DNA polymerase. Hydroxyurea is an inhibitor of ribonucleoside diphosphate reductase activity, which is known to hamper the DNA replication process by reducing the effective concentration of dNTPs in the cell.[62] Cells treated with ODUTP in the presence and absence of hydroxyurea showed similar subcellular click staining pattern (Figure 4A, column 3). However, in a control experiment addition of hydroxyurea to cells incubated with 5-ethynyl-2'-deoxyuridine (EdU), a metabolic DNA labeling agent,[45] completely inhibited the labeling of EdU into DNA (Figure 4A, compare column 1 and 2). This result indicates that ODUTP is not incorporated into DNA. Next, the influence of RNA polymerases inhibitor on the incorporation of ODUTP into RNA transcripts was studied by using actinomycin D, a potent RNA polymerases inhibitor.[63] Addition of increasing concentrations of actinomycin D to cells incubated with ODUTP abolished the staining throughout the cells (Figure 4B). This is due to the inhibition of endogenous RNA polymerases activity to incorporate ODUTP into newly transcribing RNA.

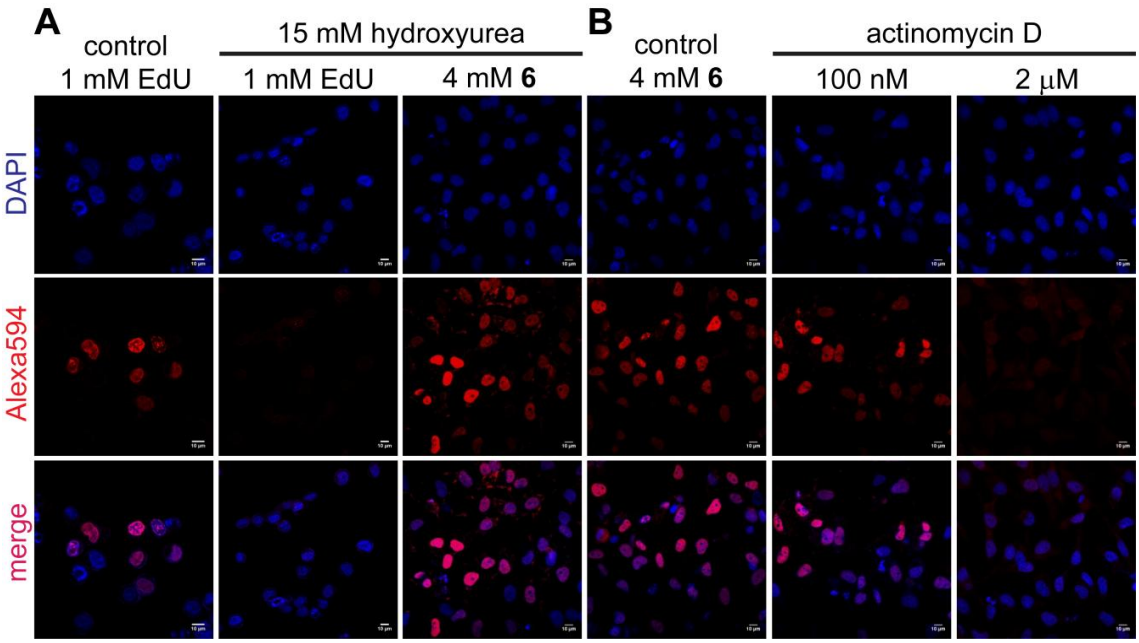

Figure 4. The ODUTP **6** specifically label transcribing RNA in cells. HeLa cells were transfected with **6** in the presence and absence of variable concentrations of **A)** Hydroxyurea and **B)** actinomycin D individually. Progressive reduction in fluorescence signal in cells treated with actinomycin D (Panel **B**) confirms specific labeling of cellular RNA containing ODUTP **6**.

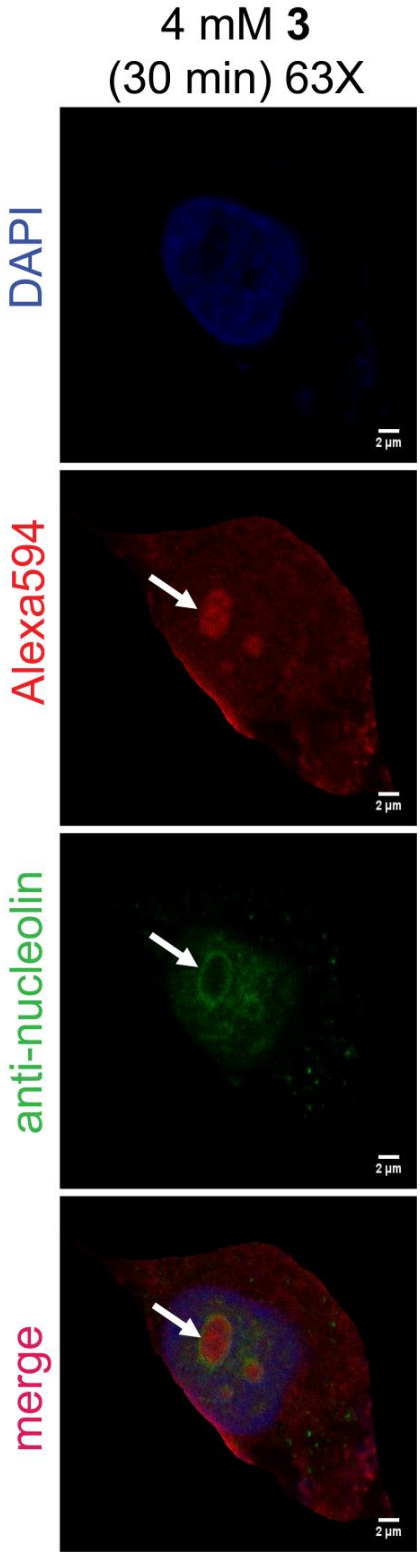

Figure 5. Confocal images (cross section) of HeLa cells transfected with ODUTP **6** showing intense staining in nucleoli (marked using an arrow). Anti-nucleolin (green), which targets nucleolin present at the periphery of nucleoli, was used to confirm the localization of ODU labeling in the nucleoli. Merging the signals obtained after click reaction (red) and anti-nucleolin (green) staining revealed concentrated ODU labeling within the nucleoli.

Additionally, small globular structures, most likely nucleoli where abundant rRNA synthesis takes place, were also visible at a higher magnification in the nuclei stained by click reaction. An antibody against nucleolin, which targets nucleolin present at the periphery of nucleoli, was used to confirm the localization of ODU labeling within the nucleus. Merging the signals obtained after click reaction (red) and anti-nucleolin (green) staining revealed concentrated ODU labeling within the nucleoli (Figure 5).

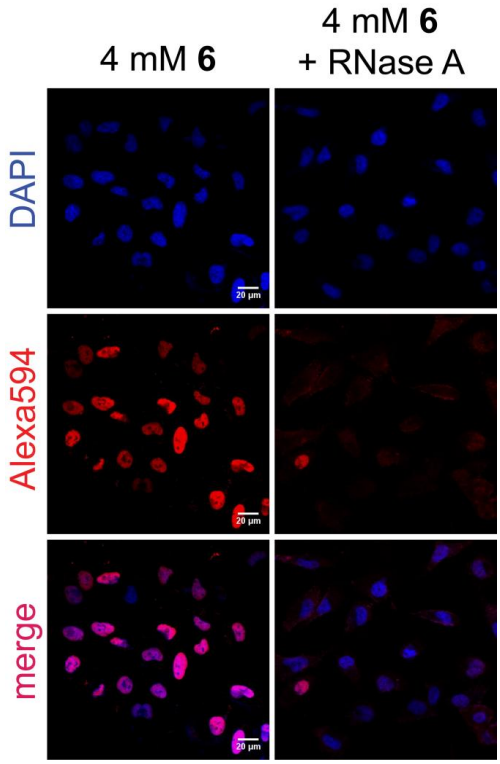

Figure 6. Confocal images of RNases A treatment experiment. HeLa cells were transfected with ODUTP **6** (4 mM) for 3 h, respectively. Fixed cells were then treated with RNase A (200 µg/mL). The cells were stained using Alexa594-azide. Reduced fluorescence signal in cells treated with RNase A revealed the selective labeling of ODU into RNA by endogenous RNA polymerases.

In another experiment, cells incubated with ODUTP were fixed, permeabilized and then treated with RNase A before staining by click reaction. Here also RNase A treatment leads to a dramatic reduction in the fluorescence signal (Figure 6). Together, these results clearly indicate that ODUTP is specifically incorporated into RNA transcripts by endogenous RNA polymerases, which has further allowed the visualization of newly transcribing RNA in cells by click reaction. Further, the cell viability was found to be preserved to a reasonable extent under these labeling conditions (Figure 7).

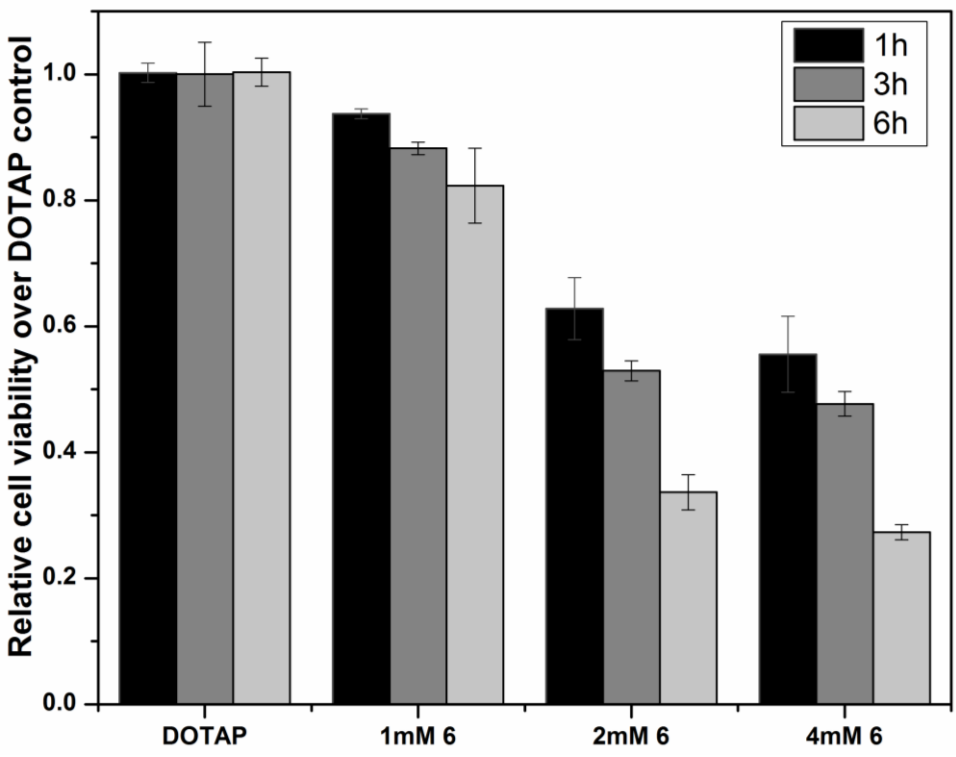

Figure 7. Plot showing the cell viability of HeLa cells in the presence of varying concentrations of ODUTP **6**. Hela cells were seeded in a 96-well plate (10,000 cells per well) and varying concentrations of **6** were transfected using DOTAP as described before. The cell viabilities in the presence of **6** are reported relative to cell viability in the presence DOTAP alone as a control.

3A.3 Conclusion

In summary, alkyne-modified UTP analog (ODUTP) containing a clickable moiety and a Raman active label served as a good substrate for endogenous RNA polymerase present in mammalian cells. The incorporation of ODUTP by endogenous RNA polymerase results in harbouring alkyne label into newly synthesizing cellular RNA transcripts. These alkyne-modified RNA transcripts were then conveniently visualized by performing bioorthogonal CuAAC reaction with fluorescent azide probe. Interestingly, alkynes which are accessible for bioorthogonal labeling using CuAAC exhibit characteristic strong Raman scattering in the range of 2100–2250 cm^{-1} with high contrast, which apparently falls in the Raman-silent region of the cells (1800–2800 cm^{-1}). More recently, alkyne modified EU and EdU with unique alkyne vibrational signature have been aptly employed in imaging DNA and RNA synthesis in living cells using Raman spectroscopy.[64-66] Although EU and ODUTP can be incorporated specifically into cellular RNA, ODU has an added advantage as ODU-modified RNA will contain two Raman scattering alkyne labels. When subjected to click staining, only the terminal alkyne would undergo reaction leaving the internal alkyne intact. Taken

together, compatibility of ODUTP as chemical reporter for posttranscriptional RNA detection by CuAAC reaction and preliminary Raman spectroscopic analysis underscore the usefulness of ODU label as an efficient tool for the investigation of RNA in cellular settings. Hence, both click chemistry (using terminal alkyne) and Raman spectroscopy (using internal alkyne) could be potentially used simultaneously to image RNA synthesis in cells.

3A.4 Experimental Section

3A.4.1 Materials

Sodium azide, sodium ascorbate, $CuSO_4$, triton X-100, actinomycin D, hydroyurea, EdU, DAPI were purchased from Sigma Aldrich. Fluorescent dye Alexa594-azide **10** and MTT (3-(4, 5-dimethylthiazol-2-yl)-2, 5-diphenyltetrazolium bromide) were aquired from Invitrogen and RNase A were obtained from Fermentas Life Science. Dulbecco's Modified Eagle Medium (DMEM), Opti-MEM, fetal bovine serum (FBS), PBS were purchased from Gibco. Transecting agent DOTAP (*N*-[1-(2,3-dioleoyloxy)propyl]-*N*,*N*,*N*-trimethylammonium methylsulfate) was purchased from Roche. Chemicals for preparing all buffer solutions were purchased from Sigma-Aldrich (BioUltra grade). Autoclaved water was used in all biochemical reactions.

3A.4.2 Instrumentation

The cell images have been acquired by a Zeiss LSM710 Confocal Laser Scanning Microscope with oil immersion using 40X and 63X lenses. The channels used for acquiring images are DAPI filter (λ_{ex} = 350 nm and λ_{em} = 470 nm), Alexa594 filter (λ_{ex} = 590 nm and λ_{em}= 617 nm), Alexa488 filter (λ_{ex} = 495 nm and λ_{em}= 519 nm). The Zen 2012 software has been used for image acquisition and z stacking. *Z* dimension has been captured in step sizes of 0.114 um to check existence of nuclear staining in all steps throughout the nucleus of cells and also to check the localization of nucleoli situated at different planes. *Z* dimension has been reconstructed into 3D image by Java ImageJ software. This software has been also used to split multichannel images and also for counting number of stained vs. unstained nuclei. The brightness/contrast of an image has not been modified exceeding the Gaussian values for the line graph through a nuclei.

3A.4.3 Biosynthetic labeling of RNA transcripts in HeLa cells using ODUTP 6

Mammalian (HeLa) cells were cultured in Dulbecco's Modified Eagle Medium (DMEM) supplemented with 10 % fetal bovine serum (FBS). 0.3−0.5 million HeLa cells were plated in 6 well plates on glass cover slips for nearly 24 hours before the experiment. Transfection solution (150 µL) containing varying concentrations of alkyne-modified UTP **6** (1.0−4.0 mM) and DOTAP (30 µL, 1 µg/µL) were prepared in HEPES buffered saline (HBS, 20 mM HEPES, 150 mM NaCl, pH 7.4). Each solution was incubated for 15min at RT, and was mixed with 450 µL of Opti-MEM. The cells were treated with above transfection solution (600 µL) for 3 h (**6**) at 37 ºC. The cells were then washed with PBS (3x1 mL), and subsequently fixed and permeabilized with 3.7% formaldehyde and 0.5% Triton X-100 in PBS, respectively, for 30 min at RT. The cells were washed with PBS (3x5 min) before click reaction. Alkyne-labeled RNA transcripts were detected by performing CuAAC reaction with Alexa594-azide **10**, under the following conditions.

Fixed cells were treated with click reaction mix (500 µL) containing $CuSO_4$(4 mM), **10** (15 µM) and sodium ascorbate (10 mM) in TBS (50 mM Tris, 150 mM NaCl, pH 7.4) for 30 min at RT. After this period, the cells were washed with PBS containing sodium azide (2 mM) for 20 min and rinsed again with PBS. DNA was stained with DAPI (500 µL, 2 µg/mL) in dark for 2 min at RT. The coverslip was then washed with PBS (1 mL) and glued upside-down on microscopy slide using 10 µL of slowfade antifade gold. The cells were imaged using a Confocal Laser Scanning Microscope with an oil immersion using 40X and 63X lenses.

3A.4.4 ODUTP 6 is a specific biosynthetic label for cellular RNA

3A.4.4.1 Hydroxyurea treatment

Cells were incubated in Opti-MEM (600 µL) containing 20 mM hydroxyurea for 3 h after which 150 µL of the media was removed. The cells were then supplemented with a freshly prepared solution of transfection mix (150 µL, mentioned above) containing **6** and incubated for another 3 h. The final concentration of hydroxyurea and **6** in the media was 15 mM and 4 mM, respectively. The cells were washed, fixed and stained by click reaction using Alexa594-azide **10** as mentioned above.

3A.4.4.2 Actinomycin D treatment

Cells were incubated in Opti-MEM (600 µL) containing actinomycin D (150 nM or 2.5 µM) for 3 h after which 150 µL of the media was removed. The cells were then supplemented with

a freshly prepared solution of transfection mix (150 µL) containing **6**, and incubated for another 3 h. The final concentration of actinomycin D and **6** in the media was 100 nM/2.0 µM and 4 mM, respectively. The cells were washed, fixed and stained by click reaction using Alexa594-azide **10**.

3A.4.4.3 RNase A treatment

Cells were incubated in Opti-MEM (600 µL) with ODUTP **6** (4 mM) and DOTAP (30 µg) for 3 h. The cells were washed, fixed and rinsed as before. The cells were treated with RNase A (single-stranded RNA cleaving enzyme, 200 µg/mL) for 45 min at RT. The cells were washed with PBS and stained in the presence of Alexa594-azide **10** as before.

3A.4.4.4 Click and Anti-nucleolin staining

To perform anti-nucleolin staining cells were first transfected with 4 mM **6** for 3 h and labeled by using CuAAC reaction with alexa594-azide **10** as before. Primary antibody staining was performed in closed moist chamber where 50 µL of primary antibody dilution of anti-nucleolin (ab-22758, containing 5% BSA in 1X PBS) was placed on parafilm. Over this solution coverslip was inverted at incubated overnight at 4^{o}C. After incubation cover slip was washed twice with 1X PBS and followed by secondary antibody staining in presence of AF-488 anti-rabbit (A-11034, Life technologies). Secondary antibody staining was performed in closed moist chamber using 50 µL of AF-488 anti rabbit antibody dilution in 1X PBS containing 5% BSA. The coverslip was inverted over this dilution and incubated overnight at 4 ^{o}C. After secondary antibody staining coverslip was washed twice with 1X PBS and DAPI staining is performed and cells were imaged as before.

3A.4.5 Cell viability assay for ODUTP 6

The cytotoxicity of ODUTP **6** on HeLa cells were assessed by the MTT (3-(4,5-dimethylthiazol-2-yl)-2,5-diphenyltetrazolium bromide) method. For the experiment 10^4 cells per well were seeded in 96-well plates and incubated for 12–16 h at 37 °C. Cells were transfected with 100 µL of transfection solution containing varying concentrations of ODUTP **6**. Three time points for ODUTP **8** were chosen for the MTT assay. The transfected cells were treated with 100 µL of MTT solution (final conc. of 0.05 mg/mL to each well) at different time points and incubated in dark at 37 °C for 4 h. Formazon crystals were dissolved by adding 100 µL DMSO to each well and the absorbance was measured at 570 nm on a plate

reader. The % cell viability was normalized to cells transfected with DOTAP alone as a control.

3A.5 References

1. Keene, J. D. Global regulation and dynamics of ribonucleic acid. *Endocrinology.*, **151**, 1391–1397 (2010).
2. Tani, H., Mizutani, R., Salam, K. A., Tano, K., Ijiri, K., Wakamatsu, A., Isogai, T., Suzuki, Y. and Akimitsu, N. Genome-wide determination of RNA stability reveals hundreds of short-lived noncoding transcripts in mammals. *Genome Res.*, **22**, 947–956 (2012).
3. Pérez-Ortín, J. E., de Miguel-Jiménez, L. and Chávez, S. Genome-wide studies of mRNA synthesis and degradation in eukaryotes. *Biochim. Biophys. Acta.*, **1819**, 604–615 (2012).
4. Raghavan, A. and Bohjanen, P. R. Microarray-based analyses of mRNA decay in the regulation of mammalian gene expression. *Brief Funct. Genomic Proteomic*, **3**, 112–124 (2004).
5. Shyu, A. B., Wilkinson, M. F. and van Hoof, A. Messenger RNA regulation: to translate or to degrade. *EMBO J.*, **27**, 471–481 (2008).
6. Ghosh, S. and Jacobson, A. RNA decay modulates gene expression and controls its fidelity. *Wiley Interdiscip. Rev. RNA*, **1**, 351–361 (2010).
7. Qian, X., Ba, Y., Zhuang, Q. and Zhong, G. RNA-Seq technology and its application in fish transcriptomics. *OMICS.*, **18**, 98–110 (2014).
8. Imamachi, N., Tani, H., Mizutani, R., Imamura, K., Irie, T., Suzuki, Y. and Akimitsu, N. BRIC-seq: a genome-wide approach for determining RNA stability in mammalian cells. *Methods*, **67**, 55–63 (2014).
9. Pérez-Ortín J. E., Alepuz, P., Chávez, S. and Choder, M. Eukaryotic mRNA decay: methodologies, pathways, and links to other stages of gene expression. *J. Mol. Biol.*, **425**, 3750–3775 (2013).
10. Dirks, R.W. RNA molecules lighting up under the microscope. *Histochem. Cell Biol.*, **106**, 151–166 (1996).
11. Dirks, R.W., Molenaar, C. and Tanke, H. J. Methods for visualizing RNA processing and transport pathways in living cells. *Histochem. Cell Biol.*, **15**, 3–11 (2001).
12. Dirks, R. W., Molenaar, C. and Tanke, H. J. Visualizing RNA molecules inside the nucleus of living cells. *Methods*, **29**, 51–57 (2003).
13. Silverman, A. P. and Kool, E. T. Quenched probes for highly specific detection of cellular RNAs. *Trends Biotechnol.*, **23**, 225–230 (2005).
14. Santangelo, P., Nitin, N. and Bao, G. Nanostructured probes for RNA detection in living cells. *Ann. Biomed. Eng.*, **34**, 39–50 (2006).
15. Silverman, A. P. and Kool, E. T. Oligonucleotide probes for RNA-targeted fluorescence in situ hybridization. *Adv. Clin. Chem.*, **43**, 79–115 (2007).
16. Tyagi, S. Imaging intracellular RNA distribution and dynamics in living cells. *Nat. Methods*, **6**, 331–338 (2009).
17. Armitage, B. A. Imaging of RNA in live cells. *Curr. Opin. Chem. Biol.*, **15**, 806–812 (2011).
18. Uddin, M., Altmann, G. G. and Leblond, C. P. Radioautographic visualization of differences in the pattern of [3H]uridine and [3H]orotic acid incorporation into the RNA of migrating columnar cells in the rat small intestine. *J. Cell Biol.*, **98**, 1619–1629 (1984).

19. Wansink, D. G., Schul, W., van der Kraan, I., van Steensel, B., van Driel, R. and de Jong, L. Fluorescent labeling of nascent RNA reveals transcription by RNA polymerase II in domains scattered throughout the nucleus. *J. Cell Biol*., **122**, 283–293 (1993).
20. Cmarko, D., Verschure, P. J., Martin, T. E., Dahmus, M. E., Krause, S., Fu, X. D., van Driel, R. and Fakan, S. Ultrastructural analysis of transcription and splicing in the cell nucleus after bromo-UTP microinjection. *Mol Biol. Cell.*, **10**, 211–223 (1999).
21. Wei, X., Somanathan, S., Samarabandu, J. and Berezney, R. Three-dimensional visualization of transcription sites and their association with splicing factor-rich nuclear speckles. *J. Cell Biol.*, **146**, 543–558 (1999).
22. Haukenes, G., Szilvay, A. M., Brokstad, K. A., Kanestrøm, A. and Kalland, K. H. Labeling of RNA transcripts of eukaryotic cells in culture with BrUTP using a liposome transfection reagent (DOTAP). *BioTechniques*, **22**, 308–312 (1997).
23. Sadoni, N. and Zink, D. Nascent RNA synthesis in the context of chromatin architecture. *Chromosome Res.*, **12**, 439–451 (2004).
24. Agard, N. J., Prescher, J. A. and Bertozzi, C. R. A strain-promoted [3 + 2] azide-alkyne cycloaddition for covalent modification of biomolecules in living systems. *J. Am. Chem. Soc*., **126**, 15046–15047 (2004).
25. Prescher, J. A. and Bertozzi, C. R. Chemistry in living systems. *Nat. Chem. Biol.*, **1**, 13–21 (2005).
26. Sletten, E. M. and Bertozzi, C. R. Bioorthogonal chemistry: fishing for selectivity in a sea of functionality. *Angew. Chem. Int. Ed. Engl*., **48**, 6974–98 (2009).
26. Bertozzi, C. R. A decade of bioorthogonal chemistry. *Acc. Chem. Res.*, **44**, 651–653 (2011).
27. Sletten, E. M. and Bertozzi, C. R. From mechanism to mouse: a tale of two bioorthogonal reactions. *Acc. Chem. Res*., **44**, 666–676 (2011).
28. Ramil, C. P. and Lin, Q. Bioorthogonal chemistry: strategies and recent developments. *Chem. Commun*., **49**, 11007–11022 (2013).
29. Schulz, D. and Rentmeister, A. Current approaches for RNA labeling *in vitro* and in cells based on click reactions. *Chembiochem*, **15**, 2342–2347 (2014).
30. McKay, C. S. and Finn, M. G. Click chemistry in complex mixtures: Bioorthogonal bioconjugation. *Chem. Biol*., **21**, 1075–1101 (2014).
31. Ngo, J. T. *et al.* Cell-selective metabolic labeling of proteins. *Nat. Chem. Biol*., **5**, 715–717 (2009).
32. Grammel, M., Zhang, M. M. and Hang, H. C. Orthogonal alkynyl amino acid reporter for selective labeling of bacterial proteomes during infection. *Angew. Chem. Int. Ed. Engl.*, **49**, 5970–5974 (2010).
33. Lang, K. *et al.* Genetic encoding of bicyclononynes and trans-cyclooctenes for site-specific protein labeling *in vitro* and in live mammalian cells via rapid fluorogenic Diels-Alder reactions. *J. Am. Chem. Soc*., **134**, 10317–10320 (2012).
34. Grammel, M., Dossa, P. D., Taylor-Salmon, E. and Hang, H. C. Cell-selective labeling of bacterial proteomes with an orthogonal phenylalanine amino acid reporter. *Chem. Commun*., **48**, 1473–1474 (2012).
35. Saxon, E. and Bertozzi, C. R. Cell surface engineering by a modified Staudinger reaction. *Science*, **287**, 2007–2010 (2000).
36. Laughlin, S. T. and Bertozzi, C. R. Imaging the glycome. *Proc. Natl. Acad. Sci. USA*., **106**, 12–17 (2009).
37. Yarema, K. J., Goon, S. and Bertozzi, C. R. Metabolic selection of glycosylation defects in human cells. *Nat. Biotechnol*., **19**, 553–558 (2001).

38. Laughlin, S. T., Baskin, J. M., Amacher, S. L. and Bertozzi, C. R. *In vivo* imaging of membrane-associated glycans in developing zebrafish. *Science*, **320**, 664–667 (2008).
39. Zaro, B.W., Yang, Y.Y., Hang, H.C.and Pratt, M.R. Chemical reporters for fluorescent detection and identification of O-GlcNAc-modified proteins reveal glycosylation of the ubiquitin ligase NEDD4-1. *Proc. Natl. Acad. Sci.USA.*, **108**, 8146–8151 (2011).
40. Anderson, C. T., Wallace, I. S. and Somerville, C. R. Metabolic click-labeling with a fucose analog reveals pectin delivery, architecture, and dynamics in Arabidopsis cell walls. *Proc. Natl. Acad. Sci. USA.*, **109**, 1329–1334 (2012).
41. Zheng, T. *et al.* Tracking N-acetyllactosamine on cell-surface glycans *in vivo*. *Angew. Chem. Int. Ed. Engl*., **50**, 4113–4118 (2011).
42. Kho, Y. *et al.* A tagging-via-substrate technology for detection and proteomics of farnesylated proteins. *Proc. Natl. Acad. Sci. USA.*, **101**, 12479–12484 (2004).
43. Charron, G., Tsou, L. K., Maguire, W., Yount, J. S. and Hang, H. C. Alkynylfarnesol reporters for detection of protein S-prenylation in cells. *Mol. Biosyst*., **7**, 67–73 (2011).
44. DeGraw, A. J. *et al.* Evaluation of alkyne-modified isoprenoids as chemical reporters of protein prenylation. *Chem. Biol. Drug Des*., **76**, 460–471 (2010).
45. Salic, A. and Mitchison, T. J. A chemical method for fast and sensitive detection of DNA synthesis *in vivo*. *Proc. Natl. Acad. Sci. USA.*, **105**, 2415–2420 (2008).
46. Jao, C. Y. and Salic, A. Exploring RNA transcription and turnover *in vivo* by using click chemistry. *Proc. Natl. Acad. Sci. USA.*, **105**, 15779–15784 (2008).
47. Neef, A. B. and Luedtke, N. W. Dynamic metabolic labeling of DNA *in vivo* with arabinosyl nucleosides. *Proc. Natl. Acad. Sci. USA.*, **108**, 20404–20409 (2011).
48. Guan, L., van der Heijden, G. W., Bortvin, A. and Greenberg, M. M. Intracellular detection of cytosine incorporation in genomic DNA by using 5-ethynyl-2′-deoxycytidine. *ChemBioChem*, **12**, 2184–2190 (2011).
49. Neef, A. B. and Luedtke, N. W. An azide-modified nucleoside for metabolic labeling of DNA. *ChemBioChem,* **15,** 789−793 (2014).
50. Rieder, U. and Luedtke, N. W. Alkene-Tetrazine ligation for imaging cellular DNA. *Angew. Chem. Int. Ed*., **53,** 9168−9172 (2014).
51. Li, Z., Wang, D., Li, L., Pan, S., Na, Z., Tan, C. Y. and Yao, S. Q. "Minimalist" cyclopropene-containing photo-cross-linkers suitable for live-cell imaging and affinity-based protein labeling. *J. Am. Chem. Soc*., **136**, 9990–9998 (2014).
52. Grammel, M., Hang, H. and Conrad, N. Chemical reporters for monitoring RNA synthesis and poly (A) tail dynamics. *ChemBioChem*, **13**, 1112–1115 (2012).
53. Qua, D., Zhou, L., Wanga, W., Wang, Z., Wang, G., Chi, W. and Zhang, B. 5-Ethynylcytidine as a new agent for detecting RNA synthesis in live cells by "click" chemistry. *Anal. Biochem*., **434**, 128–135 (2013).
54. Curanovic, D., Cohen, M., Singh, I., Slagle, C. E., Leslie, C. S. and Jaffrey, S. R. Global profiling of stimulus-induced polyadenylation in cells using a poly(A) trap. *Nat. Chem. Biol*., **9**, 671–673 (2013).
55. Motorin, Y., Burhenne, J., Teimer, R., Koynov, K., Willnow, S., Weinhold, E. and Helm, M. Expanding the chemical scope of RNA: methyltransferases to site-specific alkynylation of RNA for click labeling. *Nucl. Acids Res*., **39**, 1943–1952 (2011).
56. Onizuka, K., Shibata, A., Taniguchi, Y. and Sasaki, S. Pin-point chemical modification of RNA with diverse molecules through the functionality transfer reaction and the copper-catalyzed azide-alkyne cycloaddition reaction. *Chem. Commun*., **47**, 5004–5006 (2011).

57. Tomkuviene, M., d'Orval, B. C., Cerniauskas, I., Weinhold E., and Klimasauskas, S. Programmable sequence-specific click-labeling of RNA using archaeal box C/D RNP methyltransferases. *Nucl. Acids Res.*, **40**, 6765–6773 (2012).
58. Winz, M. L., Samanta, A., Benzinger, D. and Jäschke, A. Site-specific terminal and internal labeling of RNA by poly(A) polymerase tailing and copper-catalyzed or copper-free strain-promoted click chemistry. *Nucl. Acids Res*., **40**, e78 (2012).
59. Schulz, D., Holstein, J. M. and Rentmeister, A. A chemo-enzymatic approach for site-specific modification of the RNA cap. *Angew. Chem. Int. Ed.*, **52**, 7874–7878 (2013).
60. Holstein, J. M., Schulz, D. and Rentmeister, A. Bioorthogonal site-specific labeling of the 5'-cap structure in eukaryotic mRNAs. *Chem. Commun*., **50**, 4478–4481 (2014).
61. Li, F., Dong, J., Hu, X., Gong, W., Li, J., Shen, J., Tian, H. and Wang, J. A covalent approach for site-specific RNA labeling in mammalian cells. *Angew. Chem. Int. Ed*., **54**, 4597–4602 (2015).
62. Koc¸ A., Wheeler, L. J., Mathews, C. K. and Merrill, G. F. Hydroxyurea arrests DNA replication by a mechanism that preserves basal dNTP pools. *J. Biol. Chem.*, **279,** 223−230 (2003).
63. Bensaude, O. Inhibiting eukaryotic transcription: Which compound to choose? How to evaluate its activity? *Transcription*, **2,** 103−108 (2011).
64. Yamakoshi, H. *et al.* Imaging of EdU, an alkyne-tagged cell proliferation probe, by Raman microscopy. *J. Am. Chem. Soc*., **133**, 6102–6105 (2011).
65. L. Wei, *et al.* Live-cell imaging of alkyne-tagged small biomolecules by stimulated Raman scattering. *Nat. Methods*., **4**, 410–412 (2014).
66. Z. Chen, *et al.* Multicolor live-cell chemical imaging by isotopically edited alkyne vibrational palette. *J. Am. Chem. Soc.*, **136**, 8027–8033 (2014).

Chapter 3B

Imaging cellular RNA transcripts using an azide-modified UTP analog

3B.1 Introduction

The alkyne-modified ribonucleosides are widely used as bioorthogonal chemical reporter for cellular labeling and imaging of nucleic acids using CuAAC reactions.[1-6] Although, alkyne-modified nucleosides exhibit photochemical and thermal stability under biological conditions, cell-based staining of nucleic acids has been limited only to the CuAAC reactions. Importantly, CuAAC reactions requires the use of toxic Cu (I) catalysts which is known to cause partial degradation of proteins and nucleic acids leading to cell death.[7] Hence, the use of easily accessible alkyne-modified nucleic acids makes this procedure practically one-dimensional and not useful for live cell imaging.

In comparison to alkyne functionality, azide group can undergo a wider variety of bioorthogonal chemical reactions namely CuAAC, copper-free SPAAC and azide-phosphine Staudinger ligation reactions. Azide-modified biomolecules such as glycans, proteins, and lipids have been detected in live cells and organisms by performing copper free SPAAC reactions in presence of cyclooctynes.[8-13] SPAAC reaction does not require the toxic Cu (I) as catalyst which essentially circumvents many of the practical limitations of CuAAC reactions. Despite the successful use of azide group for labeling and imaging glycans, proteins, and lipids, nucleic acid labeling using azide group remained less prevalent.[14] This is due to the lack of effective methods to incorporate chemically and metabolically stable azide group into nucleic acids. Importantly, intracellular labeling of RNA using azide nucleosides is not very well explored.

Due to practical deficiency of current labeling procedures for efficient RNA imaging, we sought to develop a robust and modular protocol for RNA labeling and imaging in cells. Towards this endeavour, our group has recently reported the effective incorporation of azide functionality into short RNA ONs by *in vitro* transcription reactions using a small series of azide-modified nucleotide analogues.[15,16] These analogs have enabled detailed investigation of the utility of our azide labeling technique to functionalize RNA with biophysical probes by CuAAC, SPAAC and azide-phosphine Staudinger ligation reactions *in vitro*. In this chapter, we show for the first time the specific incorporation of azide groups into cellular RNA transcripts by endogenous RNA polymerases. The azide-labeled cellular RNA transcripts are conveniently visualized in fixed cells and live cells by fluorescence microscopy upon click reaction with fluorescent alkynes in the presence and absence of a copper catalyst. Furthermore, the ability to incorporate azide groups specifically into RNA has enabled us to

devise a simple method to simultaneously image replicating DNA and newly transcribing RNA in cells by using click reactions.

3B.2 Results and discussion

3B.2.1 Biosynthetic incorporation of azide-modified uridine analogs into cellular RNA

Encouraged by these results, we sought to devise a cellular RNA labeling and imaging method using our ribonucleoside toolbox. We hypothesized that azide groups could be metabolically introduced into cellular RNA transcripts by using azide-modified ribonucleosides (**16–18**) or ribonucleotides (**19–21,** Figure 1). The labeled RNA could then be chemically functionalized by click reactions with a variety of probes that could be utilized in the study of cellular RNA by various biophysical techniques. The success of this strategy will depend on (i) the cell permeability of modified nucleoside or nucleotides, (ii) the ability of cell's biosynthetic machinery to incorporate the modifications specifically into RNA transcripts, and (iii) the compatibility of modified cellular RNA to posttranscriptional chemical modification under bioorthogonal reaction conditions.

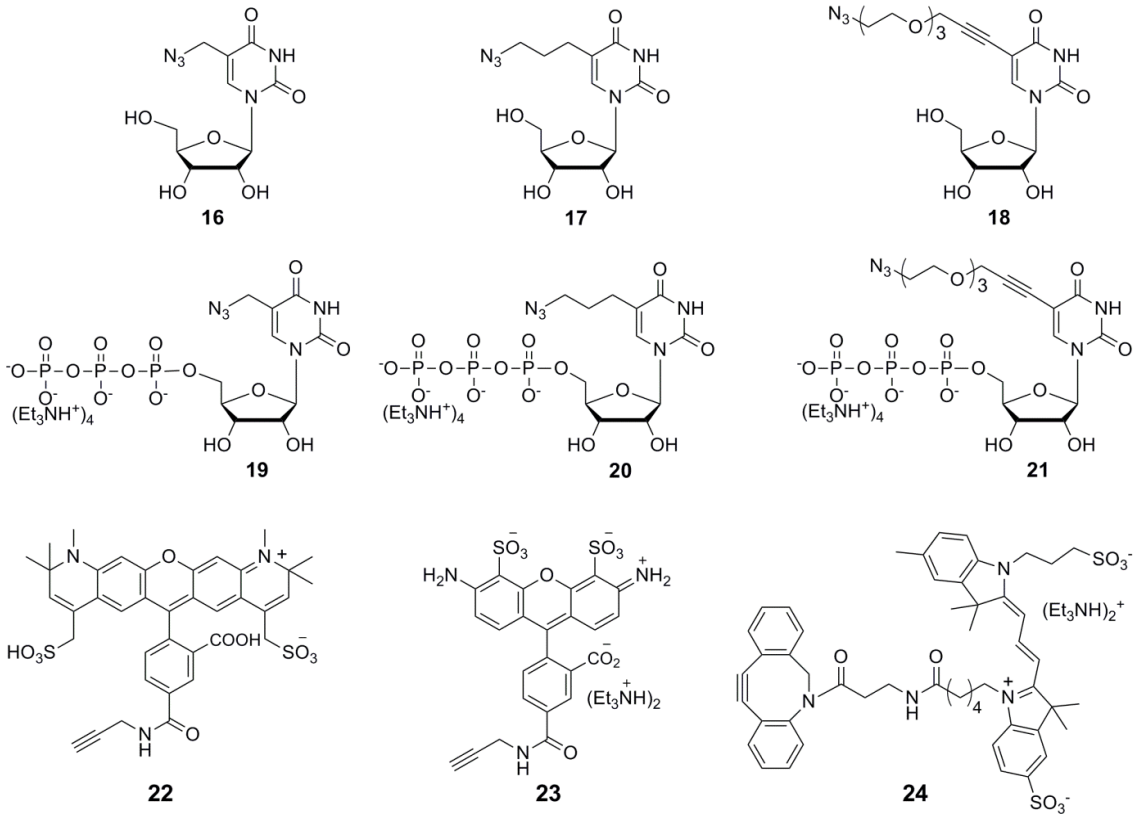

Figure 1. Chemical structures of azide-modified uridine ribonucleosides (**16–18**) and their corresponding triphosphates (**19–21**). Alexa594-alkyne (**22)**, alexa488-alkyne (**23)**, Cy3 (**24)** are used in cellular imaging of RNA by CuAAC and SPAAC reactions.

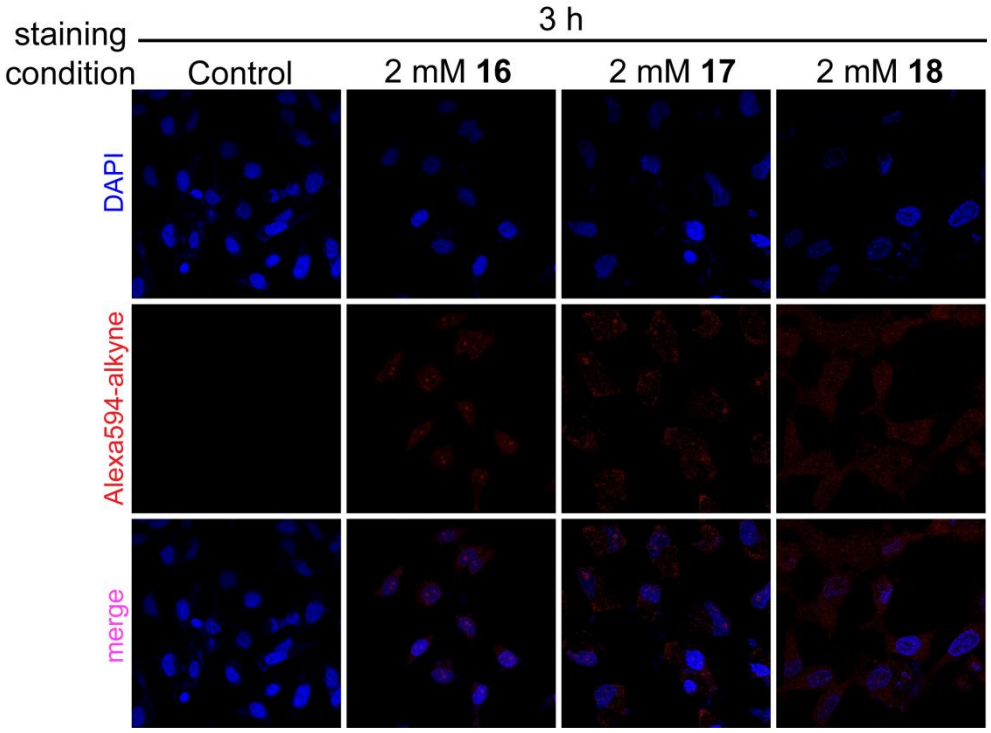

Figure 2. Incorporation of azide-modified uridine analogs (**16**–**18**) into cellar RNA transcritps as detected by CuAAC reactions using Alexa594-alkyne **22**.

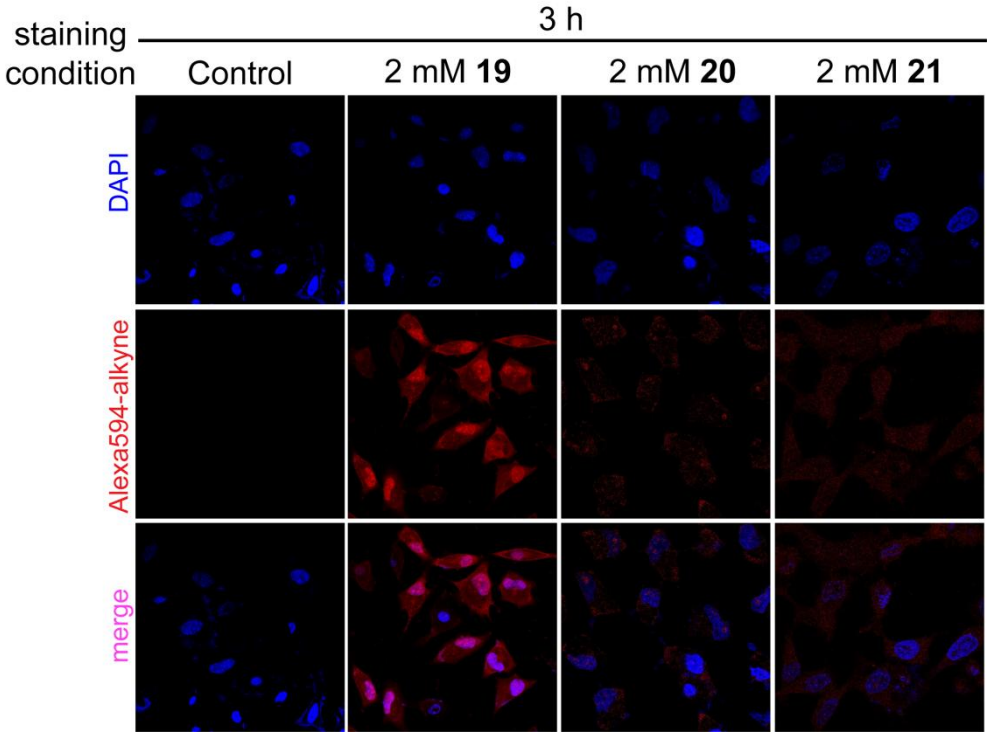

Figure 3. Incorporation of azide-modified UTPs (**19**–**21**) into cellar RNA transcritps as detected by CuAAC reactions using Alexa594-alkyne **22**.

The incorporation of azide functionalities into cellular RNA transcripts was first tested by incubating cultured human cervical cancer cells (HeLa) with ribonucleoside analogs **16**–**18**. The cells were fixed, permeabilized, stained with Alexa594-alkyne (**22**) under CuAAC conditions and imaged by fluorescence microscopy. Unfortunately, the cells did not show appreciable fluorescence signal indicating that the ribonucleoside analogs are probably cell-impermeable and or not good substrates for metabolic labeling by the ribonucleoside salvage pathway (Figure 2). As a result, we decided to bypass the phosphorylation steps involved in the salvage pathway by transfecting the cells with modified UTPs, which could now be directly incorporated into cellular RNA by RNA polymerases. Rewardingly, among the nucleotides, cells transfected with 5-azidomethyl UTP (AMUTP, **19**) resulted in AMU-labeled RNA transcripts, which were detected by click reactions with fluorescent alkyne probes. Transfection of UTP analogs **20** and **21** in which the azide group is linked via a propyl and tetraethylene glycol linker did not result in detectable incorporation of azide groups into cellular RNA (Figure 3). This observation indicates that the endogenous RNA polymerases efficiently incorporate the azide-modified UTP **19** containing a shorter linker into RNA as compared to **20** and **21**.

3B.2.2 Imaging cellular RNA transcripts using azide-modified UTP analog 19

The AMU labeling of RNA by endogenous polymerases was evaluated by transfecting the HeLa cells with increasing concentrations of **19** (50 μM to 1 mM) for 1 h using DOTAP. Upon fixing and staining the cells with Alexa594-alkyne **22** under CuAAC conditions, nuclear and cytoplasmic staining was observed in concentration-dependent manner (Figure 4). As low as 50 μM of AMUTP and incubation time of 15 min produced significant fluorescence signal in all cells (Figure 5). The nucleoli, where abundant rRNA synthesis takes place, stained more intensely indicating higher levels of AMU labeling, presumably in the pre-rRNA (Figure 6). Apparently, longer incubation times (≥ 3 hr) and concentrations of **19** ≥ 2 mM resulted in discernable reduction in staining due to cell death (Figure 5 and Figure 7). Expectedly, cells cultured in the absence or presence of **19** alone (without DOTAP) displayed no detectable fluorescence signal upon fixing and staining under similar conditions.

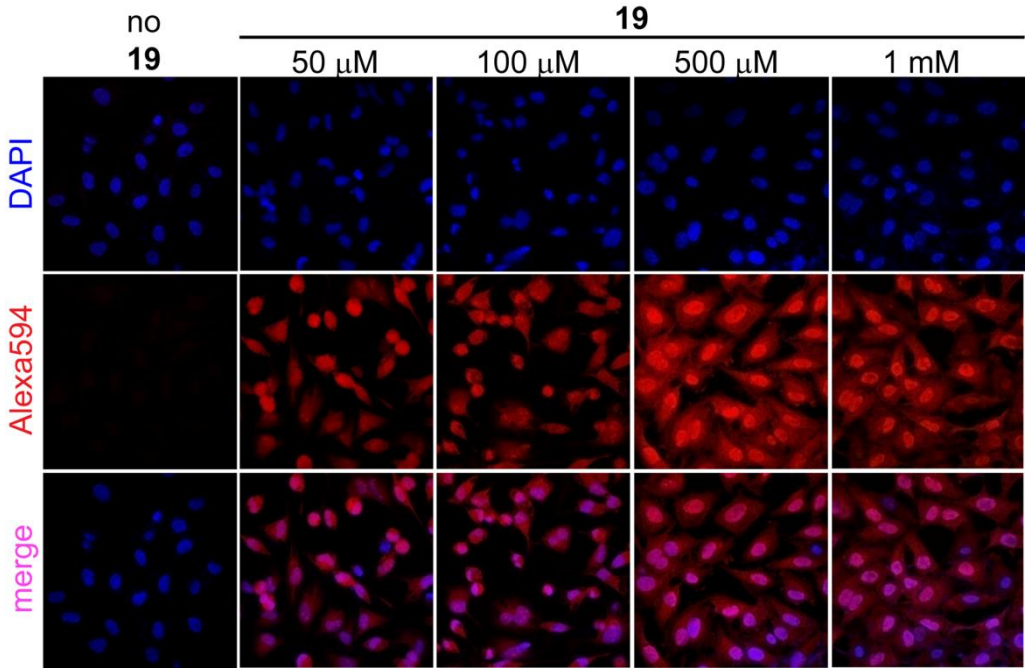

Figure 4. Imaging cellular RNA transcription using AMUTP **19**. Cultured HeLa cells were transfected with **19** (50 μM to 1 mM) for 1 h using DOTAP. The cells were then fixed, permeabilized and the AMU-labeling was detected by performing CuAAC reaction with Alexa594-alkyne **22**.

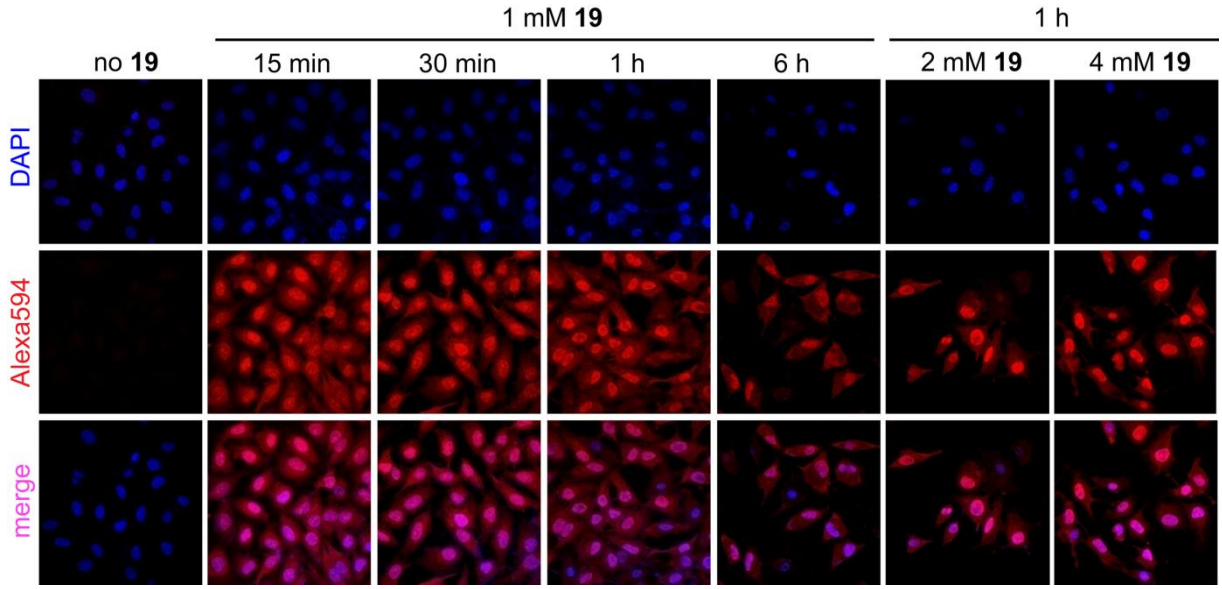

Figure 5. Incorporation of **19** into cellular RNA transcripts as a function of transfection time and concentration of nucleotide. HeLa cells were incubated with **19** (1 mM) in the presence of DOTAP for 15 min to 6 h. Cells were also incubated with higher concentrations of **19** (2 mM and 4 mM) in the presence of DOTAP for 1 h. The cells were fixed, permeabilized and the AMU labeling was detected by performing CuAAC reaction with Alexa594-alkyne **22**. A transfection time of 15 min produced significant fluorescence signal in all cells. Longer incubation times (≥ 3 hr) and concentrations of AMUTP ≥ 2 mM resulted in an appreciable reduction in fluorescence signal.

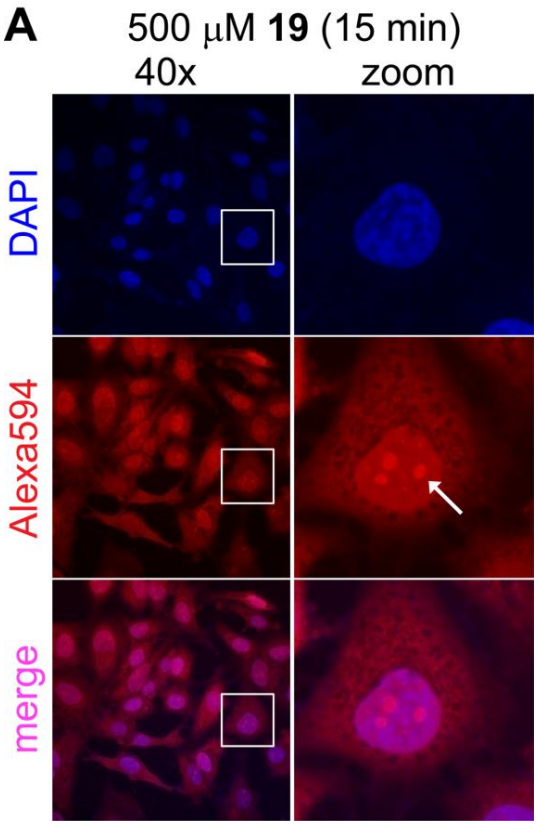

Figure 6. Images of HeLa cells transfected with **19** showing intense staining in nucleoli (marked using an arrow), where abundant rRNA synthesis takes place. The boxed cell has been zoomed-in.

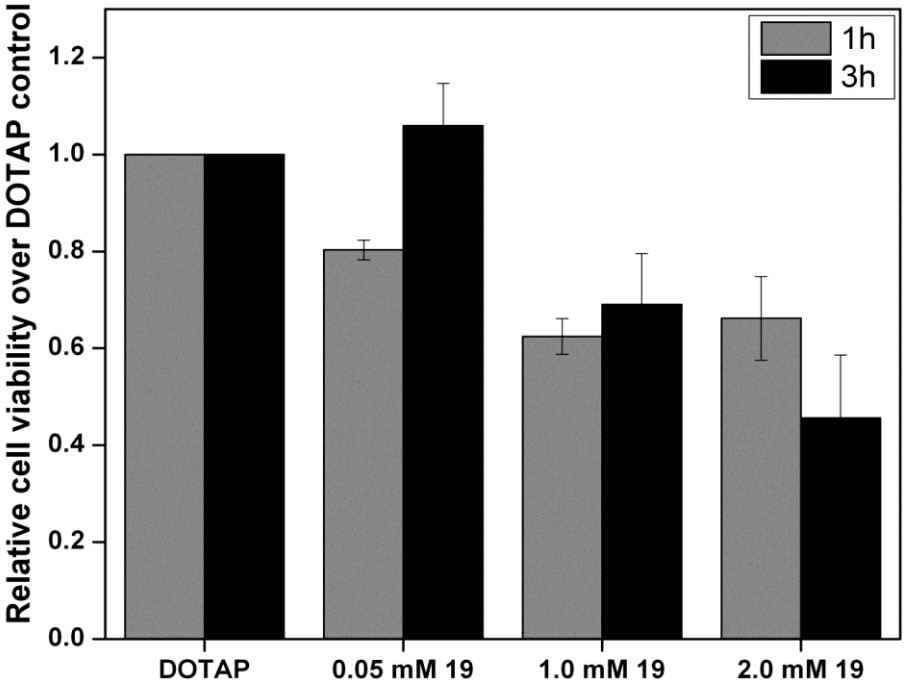

Figure 7. The plot showing the cell viability of HeLa cells in the presence of varying concentrations of AMUTP **19.** Hela cells were transfected using DOTAP and varying concentrations of AMUTP **19** as described before. The cell viabilities in the presence of **19** are reported relative to cell viability in the presence DOTAP alone as a control.

3B.2.3 Azide-modified UTP analog 19 specifically labels cellular RNA

The observed fluorescence signal from the cells could be due to (i) the specific incorporation of AMU into RNA transcripts followed by a click reaction with Alexa594-alkyne, (ii) a click reaction between unincorporated AMUTP and Alexa594-alkyne and or (iii) non-specific labeling of azide moiety into DNA. To determine the specific incorporation of azide functionality into transcripts by endogenous RNA polymerases, the following tests were performed.

AMUTP can be potentially dephosphorylated into AMUDP by cellular phosphatases, which can serve as a substrate for ribonucleoside diphosphate reductase leading to the production of AMdUDP. AMdUDP can be phosphorylated into AMdUTP, which then could get incorporated into replicating DNA. In such a scenario the observed fluorescence staining would not be exclusively due to AMU-labeled RNA transcripts. Hydroxyurea, a known inhibitor of ribonucleoside diphosphate reductase activity, reduces the effective concentration of dNTPs in the cell thereby stalling the DNA replication process. Cells incubated with AMUTP in the presence of hydroxyurea did not show significant changes in the subcellular staining pattern as compared to in the absence of hydroxyurea (Figure 8A). However, control experiments performed in the presence of 5-ethynyl-2'-deoxyuridine (EdU) that incorporates efficiently into DNA, revealed that addition of hydroxyurea abolished the labeling of EdU into DNA. These observations confirm that AMUTP does not label DNA.

Next, we studied the effect of inhibition of RNA polymerases on the AMU labeling. A lower concentration of actinomycin D (100 nM) at which RNA polymerase I is inhibited a significant reduction in fluorescence signal in the nucleus was observed (Figure 8B). Further, higher concentration of actinomycin D (2.0 μM), which blocks RNA polymerase II also abolished the staining throughout the cells. In a parallel experiment, cells incubated with AMUTP for 1 h were fixed, permeabilized and treated with RNase A (single-stranded RNA cleaving enzyme) for 45 min. The cells were then stained by performing cycloaddition reaction with **22**. RNase A treatment resulted in a significant reduction in fluorescence intensity (Figure 9). Collectively, these results demonstrate that AMU is specifically incorporated into RNA transcripts by endogenous RNA polymerases.

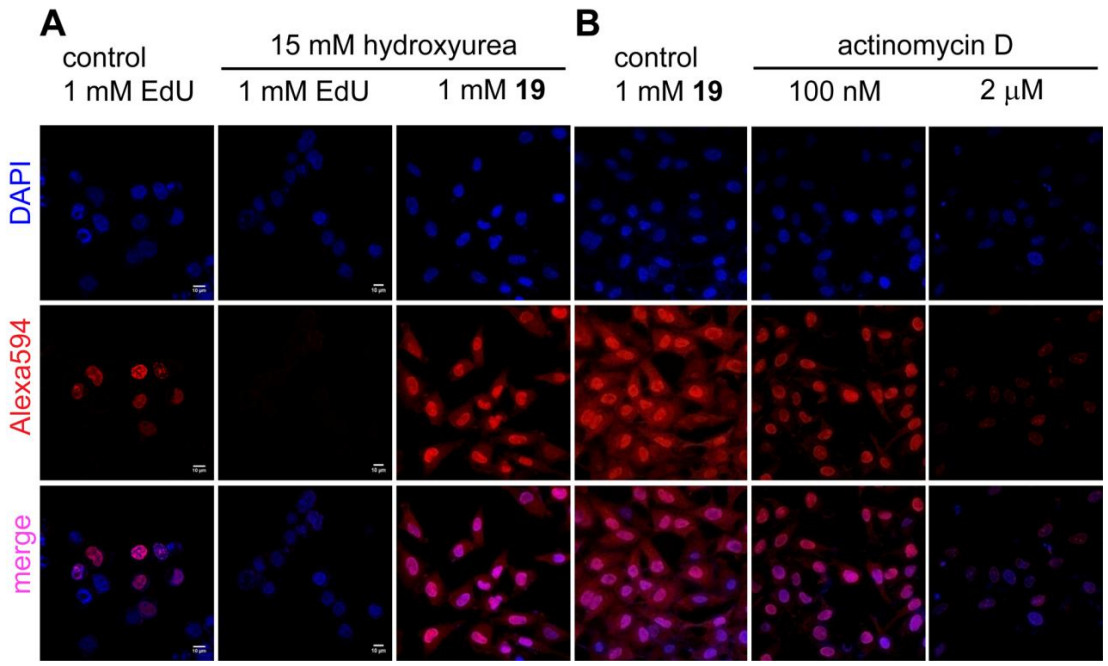

Figure 8. (A) azide-modified UTP**19** is incorporated into RNA and not into DNA. HeLa cells were incubated with 15 mM hydroxyurea (ribonucleotide reductase inhibitor) and EdU/**19**, and were click stained as before using Alexa594-azide (**10**) or Alexa594-alkyne (**22**). DOTAP was used when cells were incubated with **19**. Inhibition of DNA synthesis by using hydroxyurea abolished the incorporation of EdU. No significant change in staining pattern in cells incubated with **19** in the presence of hydroxyurea indicates that **19** is not incorporated into DNA. (**B**) AMUTP **19** specifically labels transcribing RNA in cells. HeLa cells were transfected with **19** in the presence and absence of variable concentrations of actinomycin D, an RNA polymerase inhibitor. Progressive reduction in fluorescence signal in cells treated with actinomycin D confirms specific AMU labeling of cellular RNA.

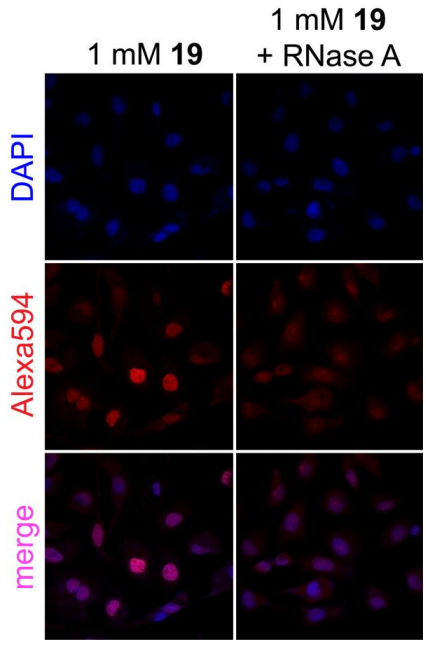

Figure 9. Confocal images of cells treated with RNases A (single-stranded RNA cleaving enzyme). HeLa cells were transfected with **19** (1 mM) for 1h. Fixed cells were then treated with RNase A (200 μg/mL). The cells were stained using Alexa594-alkyne. Reduced fluorescence signal in cells treated with RNase A revealed the selective labeling of AMU into RNA by endogenous RNA polymerases.

3B.2.4 Detection of azide-labeled cellular RNA transcripts by SPAAC reaction

SPAAC reaction using cyclooctyne probes has been widely used in the bioconjugation of azide-modified glycan, protein, lipid and recently, DNA in cells as it avoids copper catalyst, which is toxic to cells.[14,17-19] However, its utility has not been extended to cellular RNA labeling procedures due to lack of efficient methods to label RNA with chemically and metabolically stable azide groups. Now that we have developed a simple method to label cellular RNA with azide functionality using AMUTP, we sought to explore the efficacy of SPAAC reaction in staining RNA posttranscriptionally.

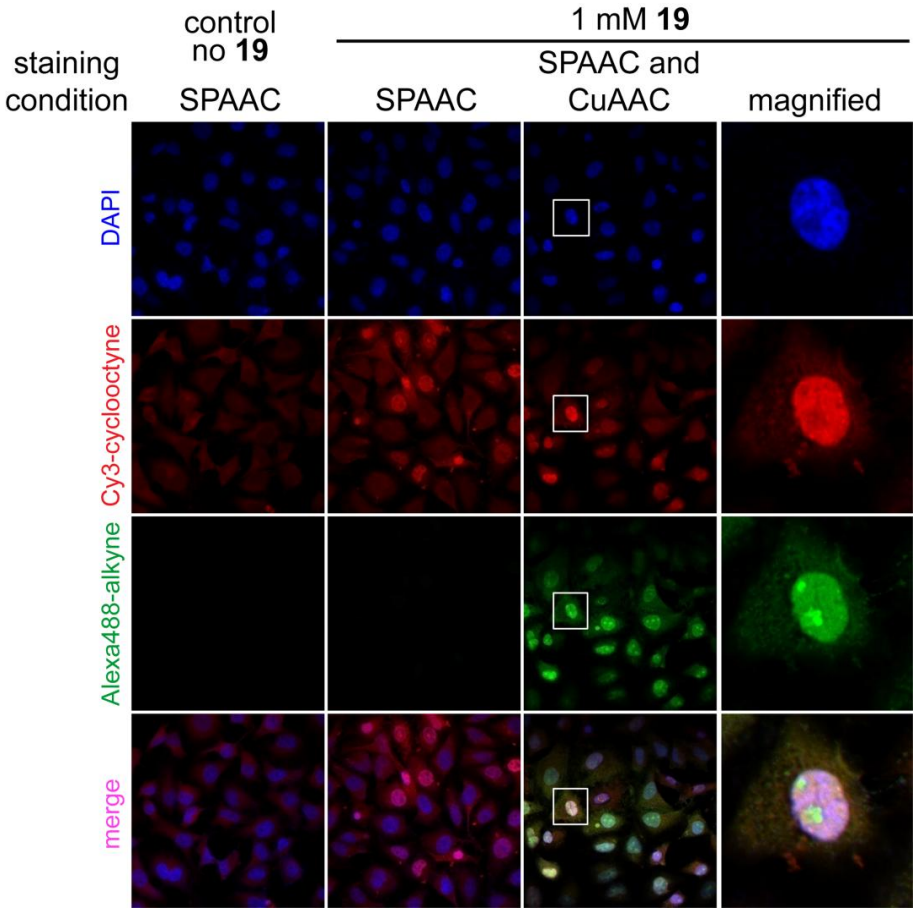

Figure 10. Imaging cellular RNA transcription using **19** under copper-free SPAAC reaction conditions. HeLa cells were transfected with 1 mM of **19** for 1 h. The cells were fixed and stained by SPAAC reaction using Cy3-cyclooctyne substrate **24** (red). In a parallel experiment, cells transfected with AMUTP were stained by first SPAAC reaction using **19** (red) followed by CuAAC reaction using Alexa488-alkyne **23** (green). Bottom panel is a merge of all three channels (blue, red and green). Boxed cell has been magnified.

The cells were incubated with AMUTP for 1 h and then fixed and stained with cyclooctyne-conjugated Cy3 (**24**) for 2 h. Unlike staining under CuAAC conditions, SPAAC staining using cyclooctyne **24** was partial and produced intense fluorescence staining only in

few cells (Figure 10). In order to determine cell to cell comparison of the two staining methods, cells were first stained by SPAAC reaction using **24** and then were washed and stained again by CuAAC reaction using Alexa488-alkyne **23**. Few cells, which were labeled by copper-free SPAAC reaction (red), were also labeled by CuAAC reaction (green, Figure 10). However, the intranuclear staining pattern was different. Apart from staining most cells, CuAAC reaction resulted in intense nucleoli staining as compared to under SPAAC reaction conditions (Figure 10 rightmost panel). Despite the differences in staining efficiency (possibly due to poor cell permeability and bulkiness of the cyclooctyne probe),[20] these results underscore the potential use of SPAAC reaction in detecting RNA in cells.

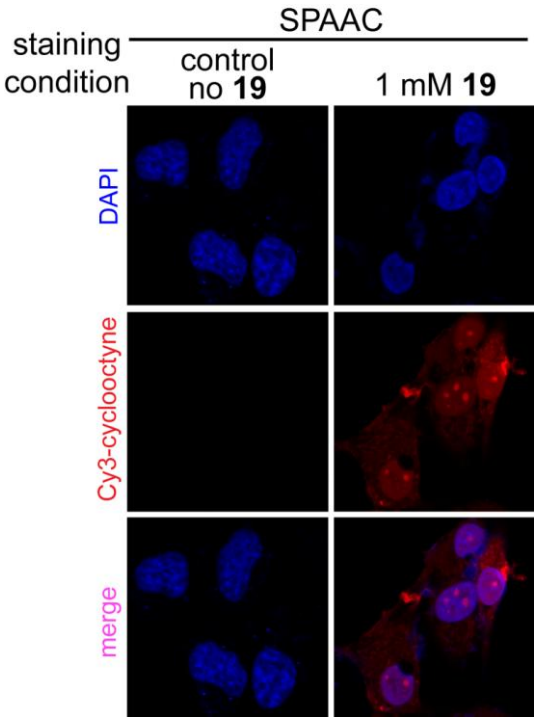

Figure 11. Imaging cellular RNA transcription using AMUTP **19** under copper-free SPAAC reaction conditions in live HeLa cells. The AMU-labeled RNA transcripts in live cells were detected by treating the cells with 40 µM cyclooctyne-conjugated Cy3 **24** at 37 °C for 30 min. Control reaction without AMUTP **19** underwent an identical treatment as the SPAAC stained cells.

The utility of copper-free SPAAC reaction to detect newly transcribing RNA in living cells was studied by first treating the cells with AMUTP for 1 h followed by transiently permeabilizing the cells without fixation using pre-cooled solution of Triton X-100. Subsequently, cells were treated with cyclooctyne **24** for 30 min at 37 °C, and were washed and observed by confocal microscopy. Given the poor cell permeability of currently available cyclooctyne probes, staining of RNA transcripts under SPAAC conditions yielded intense punctuate nucleoli staining and faint nuclear staining in few cells (Figure 11).

Further, cell viability test confirmed the low toxicity of the probe in this staining reaction conditions (Figure 12). This RNA labeling method is advantageous as the selective incorporation of azide groups into RNA using AMUTP and SPAAC staining procedure provides an alternative route to image transcribing RNA in living cells.

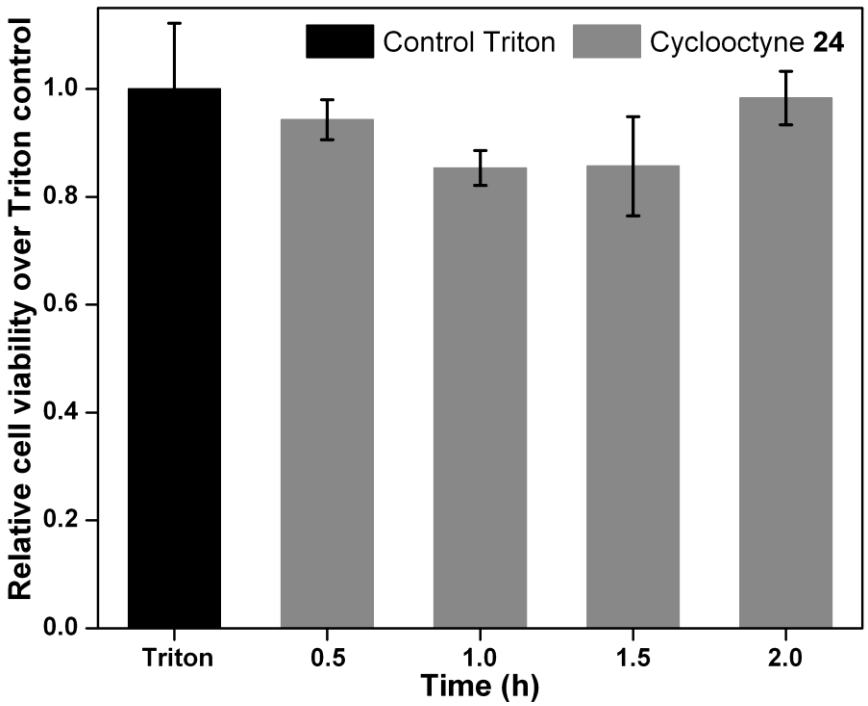

Figure 12. The plot showing the cell viability of HeLa cells in the presence of cyclooctyne-conjugated Cy3 **24** (40 μM) as a function of time. Hela cells were seeded in a 96-well plate (~10,000 cells per well) and treated with Cy3 **24**. Cell viability in the presence of **24** is reported relative to cell viability in the presence Triton X alone.

3B.2.5 Simultaneous imaging of DNA and RNA synthesis in cells

The specific incorporation of EdU into DNA and AMUTP **19** into RNA was further exploited in designing a simple experiment to simultaneously image replicating DNA and newly transcribing RNA in cells. In this experiment, cells in culture were incubated with EdU and then transfected with AMUTP **19**. The fixed cells were sequentially stained with Alexa594-azide **10** to detect EdU labeling in DNA (red) and then with Alexa488-alkyne **23** to detect AMU labeling in RNA (green) under CuAAC conditions (Figure 13). Although alkyne and azide are cognate reactive partners in cycloaddition reaction, selective incorporation of these groups into DNA and RNA by endogenous polymerases uniquely enabled the simultaneous visualization of replicating DNA and newly transcribing RNA by using click reactions.

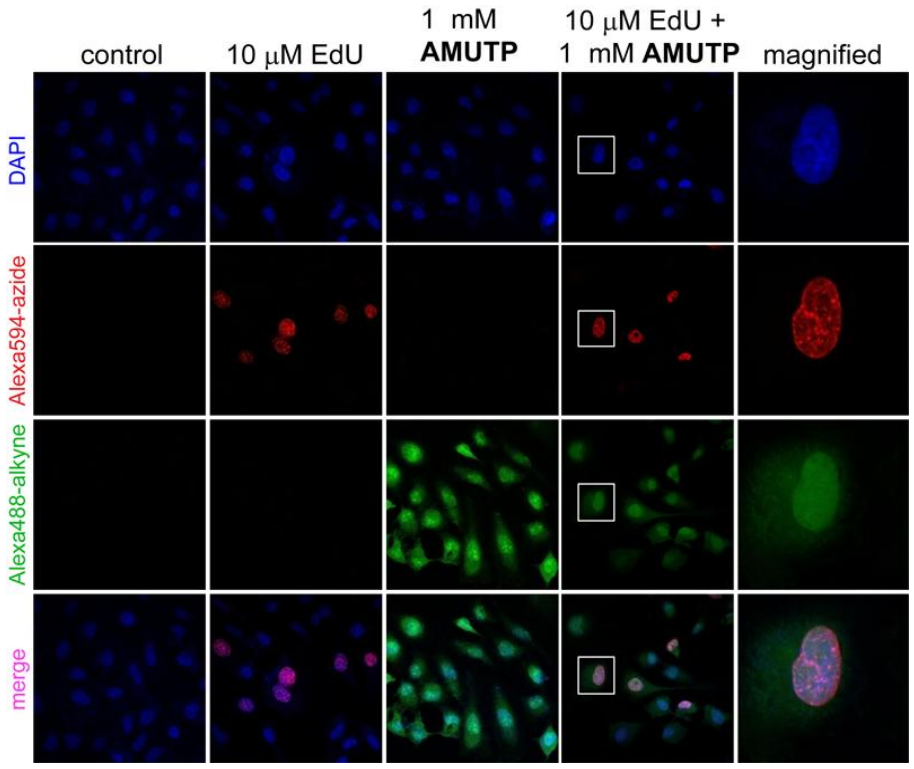

Figure 13. Simultaneous visualization of DNA and RNA synthesis in cells by CuAAC reactions. In separate experiments, HeLa cells were incubated with EdU/AMUTP and a combination of EdU and AMUTP **19**. While EdU labeling in DNA was detected by a click reaction with Alexa594-azide **10** (red), AMU labeling in RNA was detected by a reaction with Alexa488-alkyne **23** (green). Bottom panel is a merge of all three channels (blue, red and green). Boxed cell has been magnified.

3B.4 Conclusion

We have developed a robust and modular posttranscriptional chemical functionalization protocol to label RNA in cells with biophysical probes by using a novel azide-modified UTP analog. Although methods are available to metabolically incorporate the versatile azide functional group into glycan, protein and DNA, incorporation of azide groups into cellular RNA has remained elusive until now. In this context, the incorporation of azide-modified UTP analog (AMUTP) by endogenous RNA polymerases is the first example of selective labeling of cellular RNA transcripts with azide groups. The azide groups in RNA provide an easy handle to image newly transcribing RNA in fixed cells as well as live cells by CuAAC and copper-free SPAAC reactions. Further, the selective labeling of RNA with azide has enabled us to devise a simple method to simultaneously image DNA and RNA synthesis in cells by using click reactions. It is expected that this modular and practical chemical labeling methodology will provide a new platform to study RNA *in vitro* and in cells (e.g., RNA

synthesis, localization and degradation). We are currently investigating the utility of this method to develop pull-down assays.

3B.5 Experimental Section

3B.5.1 Materials

Sodium azide, sodium ascorbate, $CuSO_4$, triton X-100, actinomycin D, hydroyurea were purchased from Sigma Aldrich. Fluorescent dyes Alexa594-alkyne **22**, alexa488-alkyne **23** were obtained from Invitrogen while Cy3 **24** was obtained from Click tools. Dulbecco's Modified Eagle Medium (DMEM), Opti-MEM, fetal bovine serum (FBS), PBS were purchased from Gibco. Transecting agent DOTAP (*N*-[1-(2,3-dioleoyloxy)propyl]-*N*,*N*,*N*-trimethylammonium methylsulfate) was purchased from Roche. RNase A was obtained from Fermentas Life Science. Chemicals for preparing all buffer solutions were purchased from Sigma-Aldrich (BioUltra grade). Autoclaved water was used in all biochemical reactions.

3B.5.2 Instrumentation

The cell images have been acquired by a Zeiss LSM710 Confocal Laser Scanning Microscope with oil immersion using 40X and 63X lenses. The channels used for acquiring images are DAPI filter (λ_{ex} = 350 nm and λ_{em} = 470 nm), Alexa594 filter (λ_{ex} = 590 nm and λ_{em}= 617 nm), Alexa488 filter (λ_{ex} = 495 nm and λ_{em}= 519 nm). The Zen 2012 software has been used for image acquisition and z stacking. *Z* dimension has been captured in step sizes of 0.114 um to check existence of nuclear staining in all steps throughout the nucleus of cells and also to check the localization of nucleoli situated at different planes. *Z* dimension has been reconstructed into 3D image by Java ImageJ software. This software has been also used to split multichannel images and also for counting number of stained vs. unstained nuclei. The brightness/contrast of an image has not been modified exceeding the Gaussian values for the line graph through a nuclei.

3B.5.3 AMU labeling of RNA transcripts in HeLa cells using AMUTP (19)

Mammalian (HeLa) cells were cultured in Dulbecco's Modified Eagle Medium (DMEM) supplemented with 10 % fetal bovine serum (FBS). 0.3–0.5 million HeLa cells were plated in 6 well plates on glass cover slips for nearly 24 hours before the experiment. Transfection solution (150 µL) containing varying concentrations of AMUTP **19** (50 µM–4.0 mM) and DOTAP (*N*-[1-(2,3-Dioleoyloxy)propyl]-*N*,*N*,*N*-trimethylammonium methylsulfate, 30 µL, 1

μg/μL) were prepared in HEPES buffered saline (HBS, 20 mM HEPES, 150 mM NaCl, pH 7.4). Each solution was incubated for 15 min at RT, and was mixed with 450 μL of Opti-MEM. The cells were treated with above transfection solution (600 μL) for 1 h at 37 ºC. The cells were then washed with PBS (3x1 mL), and subsequently fixed and permeabilized with 3.7% formaldehyde and 0.5% Triton X-100 in PBS, respectively, for 30 min at RT. The cells were washed with PBS (3x5min) before click reaction. AMU-labeled RNA transcripts were detected by performing CuAAC reaction with Alexa594-alkyne **22** under the following conditions.

Fixed cells were treated with click reaction mix (500 μL) containing $CuSO_4$ (4 mM), **22** (15 μM) and sodium ascorbate (10 mM) in TBS (50 mM Tris, 150 mM NaCl, pH 7.4) for 30 min at RT. After this period, the cells were washed with PBS containing sodium azide (2 mM) for 20 min and rinsed again with PBS. DNA was stained with DAPI (500 μL, 2 μg/mL) in dark for 2 min at RT. The coverslip was then washed with PBS (1 mL) and glued upside-down on microscopy slide using 10 μL of slowfade antifade gold. The cells were imaged using a Confocal Laser Scanning Microscope with an oil immersion using 40X and 63X lenses.

3B.5.4 AMUTP 19 is a specific biosynthetic label for cellular RNA

3B.5.4.1 Hydroxyurea treatment

Cells were incubated in Opti-MEM (600 μL) containing 20 mM hydroxyurea for 5 h after which 150 μL of the media was removed. The cells were then supplemented with a freshly prepared solution of transfection mix (150 μL, mentioned above) containing **19** and incubated for another 1 h. The final concentration of hydroxyurea and **19** in the media was 15 mM and 1 mM, respectively. The cells were washed, fixed and stained by click reaction using Alexa594-alkyne **22** as mentioned above.

3B.5.4.2 Actinomycin D treatment

Cells were incubated in Opti-MEM (600 μL) containing actinomycin D (150 nM or 2.5 μM) for 5 h after which 150 μL of the media was removed. The cells were then supplemented with a freshly prepared solution of transfection mix (150 μL) containing **19**, and incubated for another 1 h. The final concentration of actinomycin D and **19** in the media was 100 nM/2.0 μM and 1 mM, respectively. The cells were washed, fixed and stained by click reaction using Alexa594-alkyne **22**.

3B.5.4.3 RNase A treatment

Cells were incubated in Opti-MEM (600 µL) with AMUTP **19** (1 mM) and DOTAP (30 µg) for 1 h. The cells were washed, fixed and rinsed as before. The cells were treated with RNase A (single-stranded RNA cleaving enzyme, 200 µg/mL) for 45 min at RT. The cells were washed with PBS and stained in the presence of Alexa594-alkyne **22** as before.

3B.5.5 Detection of AMU labeling in cellular RNA by copper-free SPAAC reaction

HeLa cells were incubated with Opti-MEM (600 µL) supplemented with AMUTP **19** (1 mM) and DOTAP (30 µg). After incubating for 1 h, the cells were washed, fixed and permeabilized as before. For staining under SPAAC condition, fixed cells were first treated with 500 µL of Triton X (0.01% in PBS) solution containing (10 µM) cyclooctyne **24** for 2 h at RT. In a parallel experiment, cells transfected with AMUTP were stained by first SPAAC reaction using **24** (red) as mentioned above. After copper-free click reaction, cells were washed once with 1 mL Triton X (0.01% in PBS) followed by washing with PBS (3 x 5 min). Subsequently, CuAAC reaction was performed using Alexa488-alkyne **23** as mentioned before.

3B.5.6 Live cell imaging using SPAAC reaction

0.3−0.4 million HeLa cells were seeded in 35 mm glass coverslip and cultured for 12 hours at 37 °C. Cells were incubated in Opti-MEM (600 µL) with AMUTP **19** (1 mM) and DOTAP (30 µg) for 1 h. Cells were then washed with fresh medium and 1 mL pre-cooled solution of Triton X-100 (0.01 % in PBS) containing 40 µM of cyclooctyne **24** was added. After 12 min at 4 °C, cells were washed with PBS (3x1 mL) and supplemented with 1 mL of fresh medium containing 40 µM of cyclooctyne 2**4** for 30 min at 37 °C. SPAAC labeling was followed by Hoechst 33342 staining (1 µM in 1 mL growth medium, 30 min at 37 °C). Cells were again washed with live cell imaging medium (Life Technologies) and imaged using confocal microscope with an oil immersion 63X lens.

3B.5.7 Simultaneous imaging of replicating DNA and newly transcribing RNA in cells

HeLa cells were incubated in DMEM supplemented with 10 % FBS and containing EdU (10 µM) for 4 h. The media was removed and immediately supplemented with Opti-MEM (600 µL) containing AMUTP **19** (1 mM) and DOTAP (30 µg). After incubating for 1 h, the cells were washed, fixed and stained under CuAAC conditions as before. The fixed cells were first

stained with Alexa594 azide **10** to detect EdU labeling (red) in DNA. The cells were washed and then stained with Alexa488-alkyne **23** to detect AMU labeling (green) in RNA.

3B.5.8 Cell viability assay for AMUTP 19

The cytotoxicity of AMUTP **19** on HeLa cells were assessed by the MTT (3-(4,5-dimethylthiazol-2-yl)-2,5-diphenyltetrazolium bromide) method. For the experiment 10^4 cells per well were seeded in 96-well plates and incubated for 12–16 h at 37 °C. Cells were transfected with 100 µL of transfection solution containing varying concentrations of AMUTP **19**. Two time points for AMUTP **19** were chosen for the MTT assay. The transfected cells were treated with 100 µL of MTT solution (final conc. of 0.05 mg/mL to each well) at different time points and incubated in dark at 37 °C for 4 h. Formazon crystals were dissolved by adding 100 µL DMSO to each well and the absorbance was measured at 570 nm on a plate reader. The % cell viability was normalized to cells transfected with DOTAP alone as a control.

3B.5.9 Cell viability assay for cyclooctyne 24

The cytotoxicity of cyclooctyne **24** in the presence of Triton X (0.01%) on HeLa cells were assessed by the MTT (3-(4,5-dimethylthiazol-2-yl)-2,5-diphenyltetrazolium bromide) method. For the experiment 10^4 cells per well were seeded in 96-well plates and incubated for 12–16 h at 37 °C. Cells were treated with 100 µL of Triton X (0.01%) solution containing 40 µM of cyclootyne **24**. Further, cells were treated with 100 µL of MTT solution (final conc. of 0.05 mg/mL to each well) at different time points and incubated in dark at 37 °C for 4 h. Formazon crystals were dissolved by adding 100 µL DMSO to each well and the absorbance was measured at 570 nm on a plate reader. Cell viability in the presence of **24** is reported relative to cell viability in the presence Triton–X alone.

3B.6 References

1. Salic, A. and Mitchison, T. J. A chemical method for fast and sensitive detection of DNA synthesis *in vivo*. *Proc. Natl. Acad. Sci. USA* **105**, 2415–2420 (2008).
2. Jao, C. Y. and Salic, A. Exploring RNA transcription and turnover *in vivo* by using click chemistry. *Proc. Natl. Acad. Sci. USA* **105**, 15779–15784 (2008).
3. Neef, A. B. and Luedtke, N.W. Dynamic metabolic labeling of DNA *in vivo* with arabinosyl nucleosides. *Proc. Natl. Acad. Sci. USA* **108**, 20404–20409 (2011).
4. Guan, L., van der Heijden, G. W., Bortvin, A. and Greenberg, M. M. Intracellular detection of cytosine incorporation in genomic DNA by using 5-ethynyl-2′-deoxycytidine. *ChemBioChem*, **12**, 2184–2190 (2011).

5. Grammel, M., Hang, H. and Conrad, N. K. Chemical reporters for monitoring RNA synthesis and poly (A) tail dynamics. *ChemBioChem* **13**, 1112–1115 (2012).
6. Yamakoshi, H. *et al*. Imaging of EdU, an alkyne-tagged cell proliferation probe, by Raman microscopy. *J. Am. Chem. Soc.*, **27**, 6102–6105 (2011).
7. Kennedy, D. C. *et al.* Cellular consequences of copper complexes used to catalyze bioorthogonal click reactions. *J. Am. Chem. Soc.,* **133**, 17993–18001 (2011).
8. Ngo, J. T. *et al*. Cell-selective metabolic labeling of proteins. *Nat. Chem. Biol.,* **5**, 715–717 (2009).
9. Truong, F., Yoo, T. H., Lampo. T. J. and Tirrell, D. A. Two-strain, cell-selective protein labeling in mixed bacterial cultures. *J. Am. Chem. Soc*., **134**, 8551–8556 (2012).
10. Hart, G. W., Slawson, C., Ramirez-Correa, G. and Lagerlof, O. Cross talk between O-GlcNAcylation and phosphorylation: roles in signaling, transcription, and chronic disease. *Annu. Rev. Biochem.,* **80**, 825–858 (2011).
11. Vocadlo, D. J., Hang, H. C., Kim, E. J., Hanover, J. A. and Bertozzi, C. R. A chemical approach for identifying O-GlcNAc-modified proteins in cells. *Proc. Natl. Acad. Sci. USA,* **100**, 9116–9121 (2003).
12. Zaro, B. W., Yang, Y. Y., Hang, H. C. and Pratt, M. R. Chemical reporters for fluorescent detection and identification of O-GlcNAc-modified proteins reveal glycosylation of the ubiquitin ligase NEDD4-1. *Proc. Natl. Acad. Sci. USA,* **108**, 8146–8151 (2011).
13. Rexach, J. E., Clark, P. M. and Hsieh-Wilson, L. C. Chemical approaches to understanding O-GlcNAc glycosylation in the brain. *Nat. Chem. Biol.,* **4**, 97–106 (2008).
14. Neef, A. B. and Luedtke, N. W. An azide-modified nucleoside for metabolic labeling of DNA. *ChemBioChem,* **15,** 789−793 (2014).
15. Rao, H., Sawant, A. A., Tanpure, A. A. and Srivatsan, S. G. Posttranscriptional chemical functionalization of azide-modified oligoribonucleotides by bioorthogonal click and Staudinger reactions. *Chem. Commun*., **48,** 498−500 (2012).
16. Sawant, A. A., Tanpure, A. A., Mukherjee, P. P., Athavale, S., Kelkar, A., Galande, S. and Srivatsan, S. G. A versatile toolbox for posttranscriptional chemical labeling and imaging of RNA. *Nucl. Acids Res*., **44**, e16 (2016).
17. Chang, P. V., Prescher, J. A., Sletten, E. M., Baskin, J. M., Miller, I. A., Agard, N. J., Lo A. and Bertozzi, C. R. Copper-free click chemistry in living animals. *Proc. Natl. Acad. Sci. U.S.A.,* **107**, 1821−1826 (2010).
18. Truong, F., Yoo, T. H., Lampo, T. J. and Tirrell, D. A. Two-strain, cell-selective protein labeling in mixed bacterial cultures. *J. Am. Chem. Soc.,* **134,** 8551−8556 (2012).
19. Haga, Y., Ishii, K., Hibino, K., Sako, Y., Ito, Y., Taniguchi N. and Suzuki, T. Visualizing specific protein glycoforms by transmembrane fluorescence resonance energy transfer. *Nat. Commun.,* **3**, 907 (2012). doi: 10.1038/ncomms1906
20. Dommerholt, J. *et al.* Readily accessible bicyclononynes for bioorthogonal labeling and three-dimensional imaging of living cells. *Angew. Chem. Int. Ed.,* **49**, 9422–9425 (2010).

Chapter 4

Alkyne-and azide-labeled RNA transcripts as potential candidates for *in vitro* selection of nucleic acid aptamers

4.1 Introduction

Combinatorial *in vitro* selection or systematic evolution of ligands by exponential enrichment (SELEX) is a technique used for isolating catalytic nucleic acids,[1-3] such as ribozymes[4] and selective target binding ligands, such as aptamers[5] from a random pool of nucleic acid library. For example *in vitro* selection of RNA begins with the generation of a random DNA library containing constant T7 promoter and primer regions at 5' and 3' end of each DNA sequence (Figure 1).[6,7] In second step random pool of RNA is generated by performing transcription reaction with random DNA pool. Purified RNA transcripts then subsequently set for selection protocol in presence of target molecule of interest. In the next step of selection, strongly binding RNA molecules are eluted and unbound RNA molecules are discarded. RNA population selected in the first round is then subjected to reverse transcription and PCR reaction to again generate enriched DNA pool. These steps are repeated several times to isolate robust RNA binder or catalyst. In each round selection pressure on nucleic acid population is increased to isolate an aptamer with better binding characteristics than the previous cycle. Similar methodology can be used for DNA and RNA aptamer and ribozyme selection.

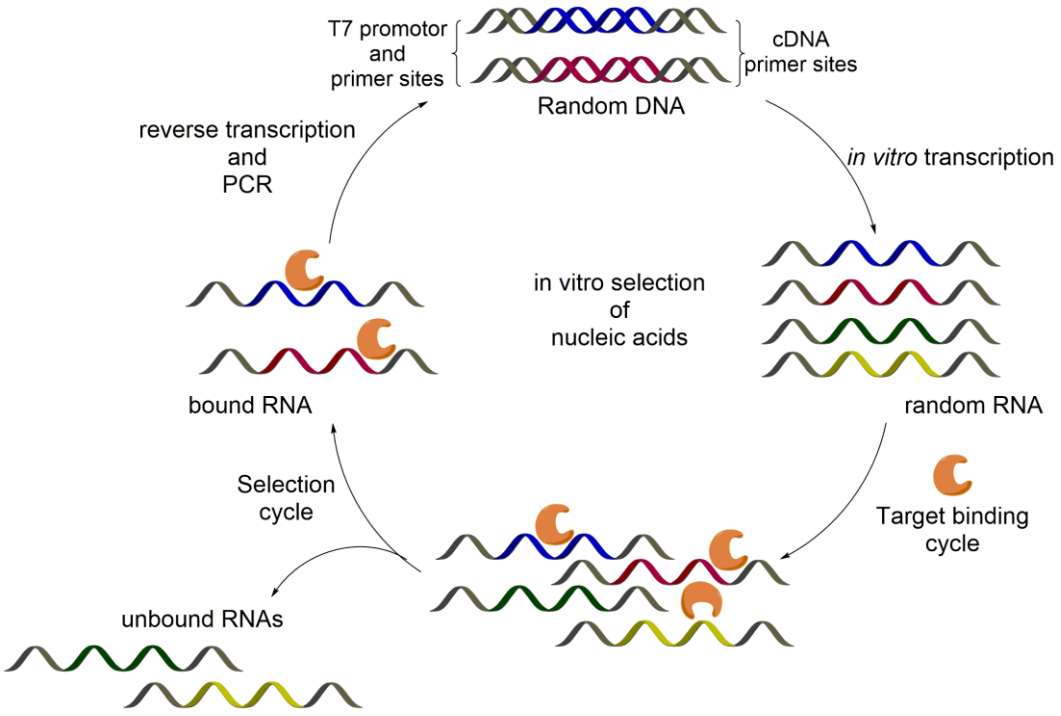

Figure 1. General scheme depicting *in vitro* selection protocol to identify functional nucleic acid motifs. Random DNA library is generated using automated synthesis strategy. All random DNA contains T7 promoter region and primer site at 5' end for *in vitro* transcription and PCR amplification. 3' end of DNA contain cDNA primer site which is used during reverse transcription and PCR reactions.[8]

Over the years, numerous ribozymes have been identified that can catalyze chemical and biochemical reactions such as Diels–Alder reaction,[9] phosphodiester synthesis,[10] peptide bond synthesis,[11] peptidyl transfer[12], aminoacylation[13] and ester hydrolysis.[14] Similarly, numerous RNA aptamers that act as molecular biosensor have emerged as promising tools in therapeutic and diagnostic applications.[15-20] Despite these successes, nucleic acid enzymes and aptamers evolved from selection protocol using natural DNA and RNA impose few challenges (i) aptamers or nucleic acid enzymes are susceptible for nucleases degradation,[21] and (ii) furthermore, restricted presence of functional groups in natural nucleic acids often limit the aptamer binding ability of selected nucleic acids. The lack of functional groups that can improve target binding and provide necessary nuclease resistance to natural nucleic acids encouraged the development of *in vitro* selection using modified nucleic acids.

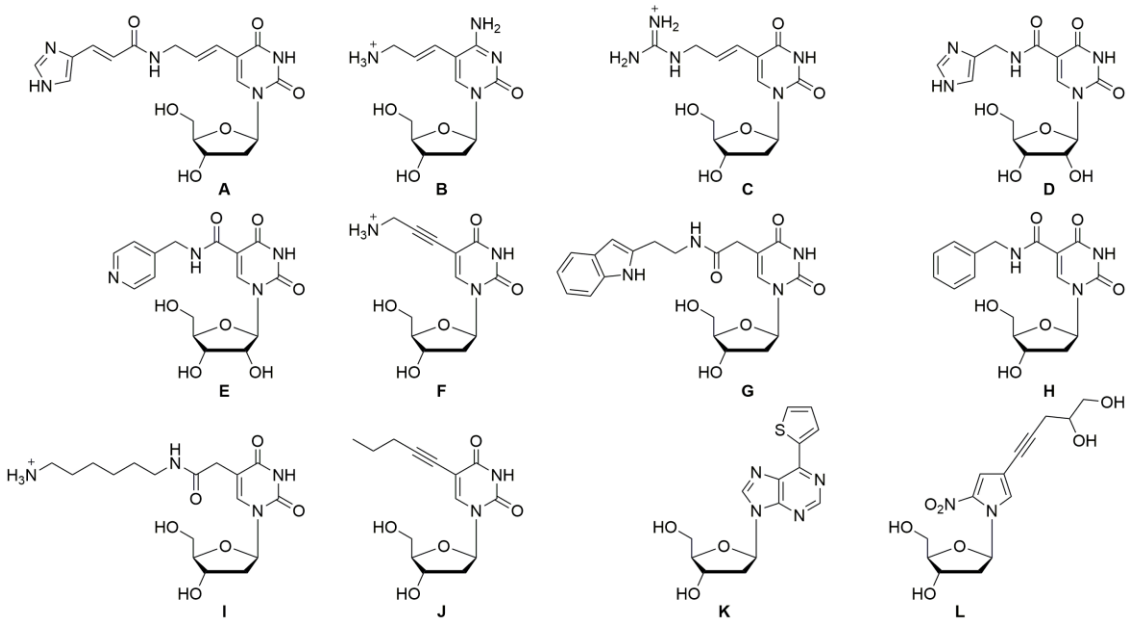

Figure 2. A partial list of desirable functionality that showed potential for isolating nucleic acids with enhance catalytic and binding platform by SELEX protocol.

In recent years, the use of base–modified nucleotide triphosphates (dNTPs and NTPs) in selection protocols has provided alternative avenues to isolate nucleic acids enzymes and aptamers with enhanced catalytic and binding platform.[21-26] Notably, Santoro *et al.* and Perrin *et al.* showed that incorporation of imidazole residues and cationic amine enhances the catalytic activity of DNAzyme (Figure 2A–2C).[27,28] Subsequently, use of a 5-imidazole modified UTP analog (Figure 2D) and a UTP equipped with a pyridiylmethyl unit (Figure 2E) in SELEX protocol allowed the isolation of RNA amide synthetase[29] and a Diels–Alder ribozyme[30] with improved catalytic activity. The first example of an aptamer *in vitro*

selection using a modified dNTP was reported by Benner *et al.* in 1999.[31] They used a 5-modified dUTP analog carrying a cationic amine to select for ATP, ADP, and AMP binding aptamers (Figure 2F). In addition, various carboxyamide–modified dUTP analogs were engaged in selection of human tumor necrosis factor binding aptamers (Figure 2G–2H).[32] Similarly, Sawai group reported the isolation of thalidomide–binding aptamers using base modified cationic amine triphosphates (Figure 2I). Further, Tolle *et al.* showed elegant use of (1-pentynyl)-2'-deoxyuridine triphoshate (Figure 2J) for the *in vitro* selection of aptamers against human thrombin.[33]

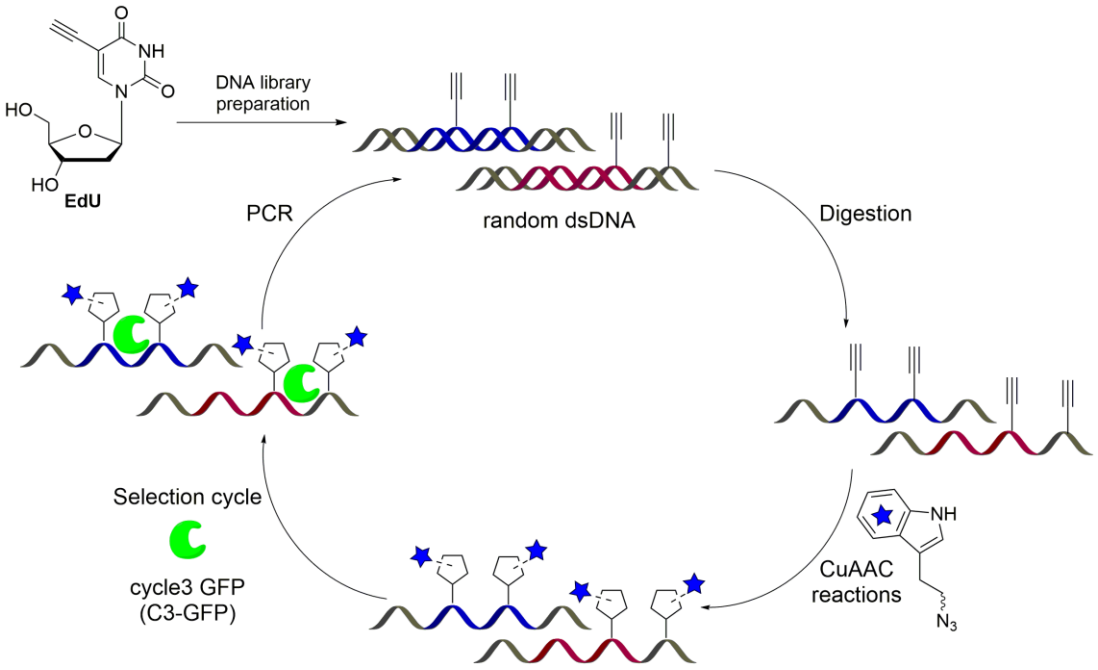

Figure 3. Schematic of click SELEX protocol developed for *in vitro* selection using alkyne–modified DNA aptamers.

Recently, Hirao's group reported the selection of aptamers using nucleotides containing unnatural base–pairs (Ds–Px) system (Figure 2K–2L).[34] Initially, they prepared single stranded DNA library containing hydrophobic unnatural (Ds) base. In selection cycle sequences containing Ds modification showed improved binding to target proteins and therefore selection pressure was further increased by amplifying selected DNA aptamers in presence of dNTPs and PxTP. Their SELEX protocols using unnatural base–pairs allowed the identification of two high affinity aptamers against human proteins. Tolle and Gunter's group developed a practical approach for aptamer selection using pool of alkyne-modified DNA prepared using 5-ethynyl deoxyuridine (5-EdU) building block (Figure 3).[35] In their strategy, alkyne–modified nucleic acid libraries were further expanded by using CuAAC reaction with

azide modified indole moiety. Further, these indole modified nucleic acids showed enhanced recognition and binding to the aptamer target cycle3 GFP. Despite these examples, only few dNTPs and NTPs are compatible with the enzymatic manipulations that are used in SELEX protocols (transcription, reverse transcription, PCR amplification). Therefore, development of new tools that would be compatible to selection cycles and would enhance the chemical space of nucleic acid libraries is highly desired.

In this chapter we have explored the suitability of alkyne and azide modified NTP analogs described in previous chapters (Figure 4) for *in vitro* selection protocols. Modified nucleotides are suitable for *in vitro* selection protocols, if they meet the following requirements: (i) modified nucleotide triphosphate must be compatible to incorporation into RNA by a RNA polymerase with high fidelity and (ii) modified transcripts must be compatible to reverse transcription to produce cDNA with high fidelity prior to PCR amplification. Therefore, to assess the compatibility of these modified nucleotides we performed basic *in vitro* experiments like transcription, reverse transcription, PCR amplification and sequencing in presence of alkyne and azide modified UTP. We found that high density alkyne–labeled RNA was successfully reverse transcribed by using ImProm–II™ reverse transcriptase to generate the cDNA, which was subsequently PCR amplified and sequenced. The sequence analysis of PCR product matched well with the template DNA sequence used for the incorporation of EUTP and ODUTP into RNA by *in vitro* transcription reaction. Additionally, the fidelity of transcription reaction in the presence of AMUTP was further confirmed by reverse transcribing modified transcripts into cDNA, which was then PCR amplified and sequenced. The sequencing data of PCR product showed 100% sequence identity with the template DNA used for the *in vitro* transcription reactions. These results demonstrate that the alkyne-and azide-modified NTPs could be utilized in expanding the chemical and functional diversity of the RNA library used in SELEX protocol.

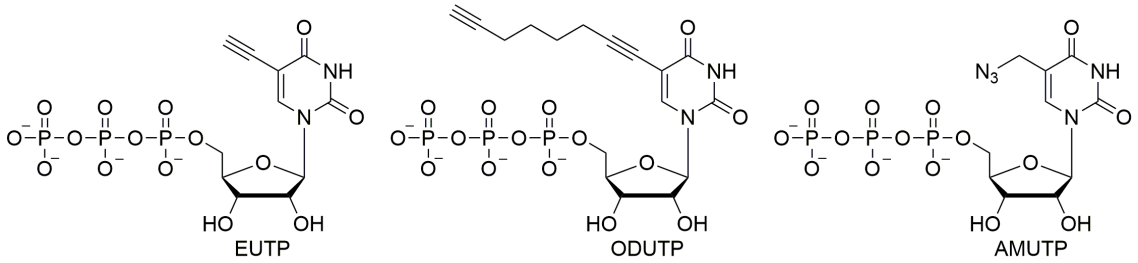

Figure 4. Alkyne-and azide-modified UTP analogs as possible candidates for *in vitro* selection protocols.

4.2 Result and Discussion

4.2.1 Synthesis of high density functionalize RNA by using T7 RNA polymerases

The ability of T7 RNA polymerases to incorporate multiple alkyne modifications into RNA ONs of varying length were tested by performing *in vitro* transcription reactions in presence of EUTP **5** and ODUTP **6**. The DNA templates required for transcription reactions were prepared by restriction digestion of genetically modified plasmid DNA (pDisplay, ZiFiinpDisplay, eGFPinpDisplay, Figure 5). The modified plasmids ZiFiinpDisplay and eGFPinpDisplay were prepared by standard cloning protocol in which two genes (ZiFi and eGFP) were cloned into parent empty vector pDisplay. All three plasmids have a common restriction site for restriction enzyme (RE) XhoI at the downstream of the inserts. Enzymatic digestion of plasmid DNA using RE XhoI resulted in linearized DNA templates, which could be used to synthesize transcripts of length 400, 600 and 1100 bp containing nearly 100–260 modifications.

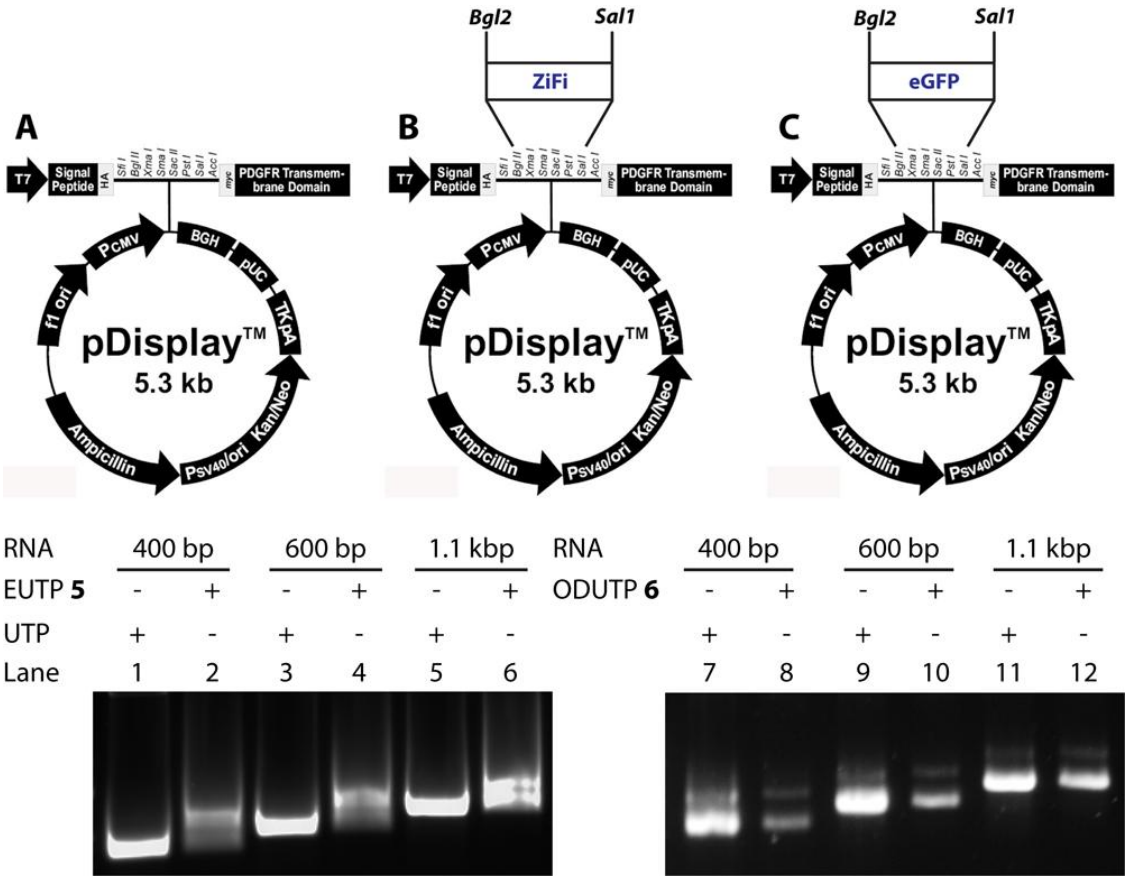

Figure 5. Diagram of pDisplay, ZiFiinpDisplay, eGFPinpDisplay plasmids, which were linearized by using XhoI restriction enzyme (top panel). 1% agarose gel of RNA transcripts obtained after transcription reactions performed in presence of UTP, EUTP and ODUTP will produce 400 bp, 600 bp, and 1.1 kb RNA transcript containing 100–260 uridine or modified uridine residues, respectively.

Transcription reactions with these templates revealed that high density incorporation of EUTP and ODUTP into longer RNA transcripts could be achieved, albeit with reduced efficiency as compared to reactions with UTP (Figure 5). As before the presence of alkyne–modified nucleoside in the longer RNA transcripts was confirmed by subjecting one of the purified transcripts (~1.1 kb long) to enzymatic digestion. HPLC analysis of the digest clearly indicated the incorporation of EUTP and ODUTP in RNA (Figure 6).

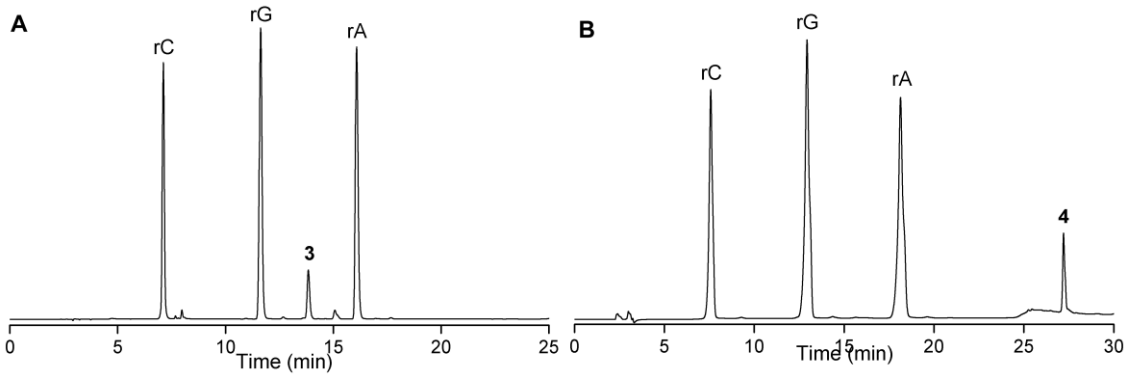

Figure 6. HPLC chromatogram of ribonucleoside products obtained from enzymatic digestion reactions of RNA transcripts, which were prepared by *in vitro* transcription reactions with linearized eGFPinpDisplay plasmid template and in the presence of **A**) EUTP (**5**), **B**) ODUTP (**6**). The presence of modified ribonucleosides **3** and **4** in RNA transcripts was confirmed by comparing the retention times with standard ribonucleoside mix as before.

4.2.2 Reverse transcription and amplification of EU and ODU modified RNA

PCR amplification and sequencing are essential steps to measure fidelity of incorporation of modified UTPs. For this purpose 1.1 kb long eGFP RNA was transcribed by transcription reaction using PCR amplified eGFP gene (Figure 7) in presence of UTP/EUTP/ODUTP and T7 RNA polymerase. High density alkyne-labeled RNA transcripts were subjected for RNase free DNase treatment for 2h at RT. The aliquot from DNase reactions were subjected for reverse transcription by using ImProm–II™ reverse transcriptase and reverse primer to generate the complementary DNA (cDNA). Further, cDNA generated from respective RNAs were subjected for PCR amplification by using high fidelity *Pfx* DNA polymerase in presence of forward and reverse primers. DNase treated RNA aliquots were also PCR amplified which act as negative control to confirm successful reverse transcription of RNA transcripts. PCR product obtained after amplification reactions were directly resolved on 1% agarose gel to confirmed cDNA synthesis (Figure 8).

Importantly, all aliquots from positive reverse transcription reactions (+RT) showed the amplicon band. Whereas absence of band from negative control reaction (–RT) clearly

confirmed the successful conversion of alkyne-modified RNA transcripts into cDNA by reverse transcription reactions. Further to evaluate the fidelity of transcription and reverse transcription reaction, PCR amplicons obtained from amplification of respective cDNA products were sequenced. The sequence analysis of PCR product matched well with the template DNA sequence used for the incorporation of EUTP and ODUTP into RNA by *in vitro* transcription reaction (Figure 9 and 10). Taken together, these results indicate that EUTP and ODUTP are efficiently incorporated into RNA transcripts, which are effectively recognized and copied by reverse transcriptase to produce corresponding cDNA. This ability of alkyne–modified UTP analogs to preserve the sequence information in a cycle of steps namely, transcription, reverse transcription and amplification could be beneficial in introducing new functionalities into RNA libraries for the selection of robust aptamers.

5'GGACCGAAATTAATACGACTCACTATAGGGGTCTATATAAGCAGAGCTGGTTT
AGTAACCGTCAGATCCGCTAGCGCTACCGGTCGCCACC**ATGGTGAGCAAGGGC**
GAGGAGCTGTTCACCGGGGTGGTGCCCATCCTGGTCGAGCTGGACGGCGACGTA
AACGGCCACAAGTTCAGCGTGTCCGGCGAGGGCGAGGGCGATGCCACCTACGGC
AAGCTGACCCTGAAGTTCATCTGCACCACCGGCAAGCTGCCCGTGCCCTGGCCCA
CCCTCGTGACCACCCTGACCTACGGCGTGCAGTGCTTCAGCCGCTACCCCGACCA
CATGAAGCAGCACGACTTCTTCAAGTCCGCCATGCCCGAAGGCTACGTCCAGGA
GCGCACCATCTTCTTCAAGGACGACGGCAACTACAAGACCCGCGCCGAGGTGAA
GTTCGAGGGCGACACCCTGGTGAACCGCATCGAGCTGAAGGGCATCGACTTCAA
GGAGGACGGCAACATCCTGGGGCACAAGCTGGAGTACAACTACAACAGCCACA
ACGTCTATATCATGGCCGACAAGCAGAAGAACGGCATCAAGGTGAACTTCAAGA
TCCGCCACAACATCGAGGACGGCAGCGTGCAGCTCGCCGACCACTACCAGCAGA
ACACCCCCATCGGCGACGGCCCCGTGCTGCTGCCCGACAACCACTACCTGAGCA
CCCAGTCCGCCCTGAGCAAAGACCCCAACGAGAAGCGCGATCACATGGTCCTGC
TGGAGTTCGTGACCGCCGCCGGGATCACTCTC**GGCATGGACGAGCTGTACAAG**
TCCGGACTCAGATCTCGAGCTCAAGCTTCGAATTCTGCAGTCGACGGTACCGCGG
GCCCGGGATCCACCGGATCTAGATAACTGATCATAATCAGCCATACCACATTTGT
AGAGGTTTTACTTGCTTTAAAAAACCTCCCACACCTCCCCCTGAACCTG 3'

Figure 7. PCR amplified template sequence from pEGFPC1 vector used in transcription reactions. T7 promoter sequence is underlined. Primer site for reverse transcription is denoted in red. Regions highlighted in yellow are primer sites for PCR amplification of cDNA.

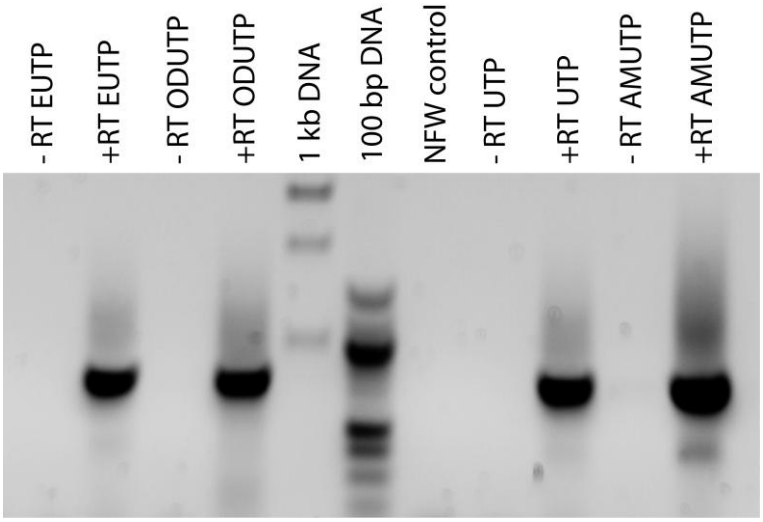

Figure 8. Gel picture depicting PCR amplicons obtained from cDNA. PCR reactions performed with cDNA generated after successful reverse transcription of control RNA containing UTP and modified RNA containing EUTP/ODUTP and AMUTP (+RT) respectively. DNase treated RNA aliquots used as negative reaction control (–RT).

4.2.3 Reverse transcription and amplification of azide modified RNA

Similar to EUTP and ODUTP, we also tested the efficacy of RNA polymerase to incorporate azide groups at multiple sites in eGFP RNA sequences. For this purpose 1.1 kb long eGFP RNA was transcribed by transcription reaction using PCR amplified eGFP gene in presence of AMUTP and T7 RNA polymerase. The fidelity of transcription reaction in the presence of AMUTP was further confirmed by reverse transcribing modified transcripts into cDNA, which was then PCR amplified and sequenced (Figure 8).

The sequencing data of PCR product showed 100% sequence identity with the template DNA used for the *in vitro* transcription reactions (Figure 11). Further, additional experiments were performed where PCR amplified fragment was further subjected to A-tailing using *Taq* polymerase, which was then cloned using TA cloning kit. The individual colonies were sequenced and sequence reads were then aligned to the DNA template sequence. Out of the eight clones, there was 100% identity in five and in the remaining three only one base was different at three different locations (Figure 12). It is very important to note that none of the misincorporated bases are thymines, implying that none of the modified uridines in the original RNA sequence were misread as any other base. These results clearly reveal that (i) the azide-modified UTPs are incorporated into RNA transcripts with high fidelity and (ii) the transcription products are recognized and copied by reverse transcriptase with high fidelity to generate cDNA, which can be PCR amplified and transcribed again in the presence of modified UTPs. This feature of nucleoside analogs could be highly beneficial

in expanding the structural and functional diversity of RNA library used in the *in vitro* selection protocols.

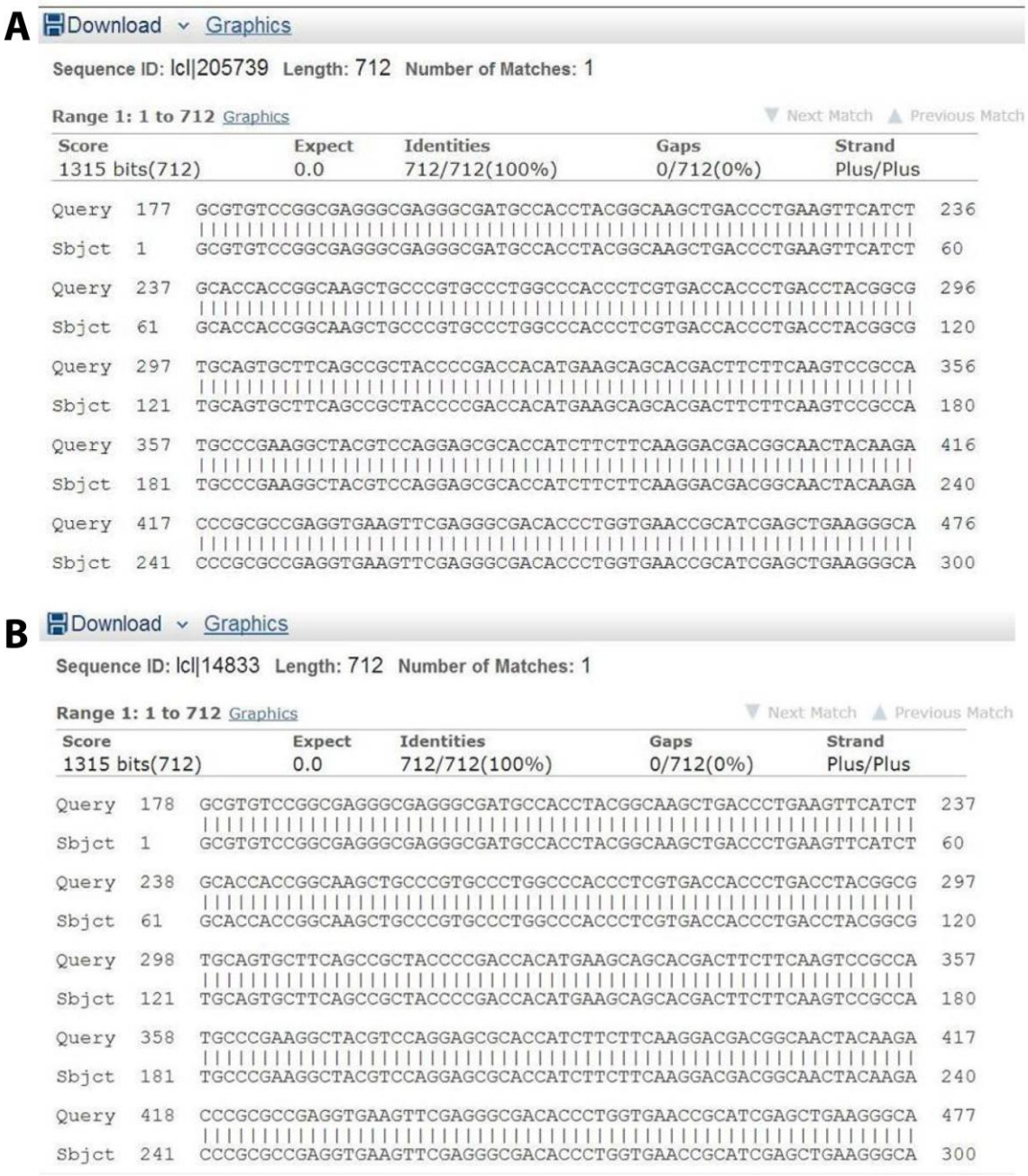

Figure 9. Representative sequence alignment (BLAST) of PCR amplified DNA products obtained from cDNAs, which were in turn synthesized by reverse transcribing EU-(**A**) and ODU-(**B**) containing eGFP RNA transcripts. The sequencing data showed 100% sequence identity with the template DNA used for the *in vitro* transcription reactions.

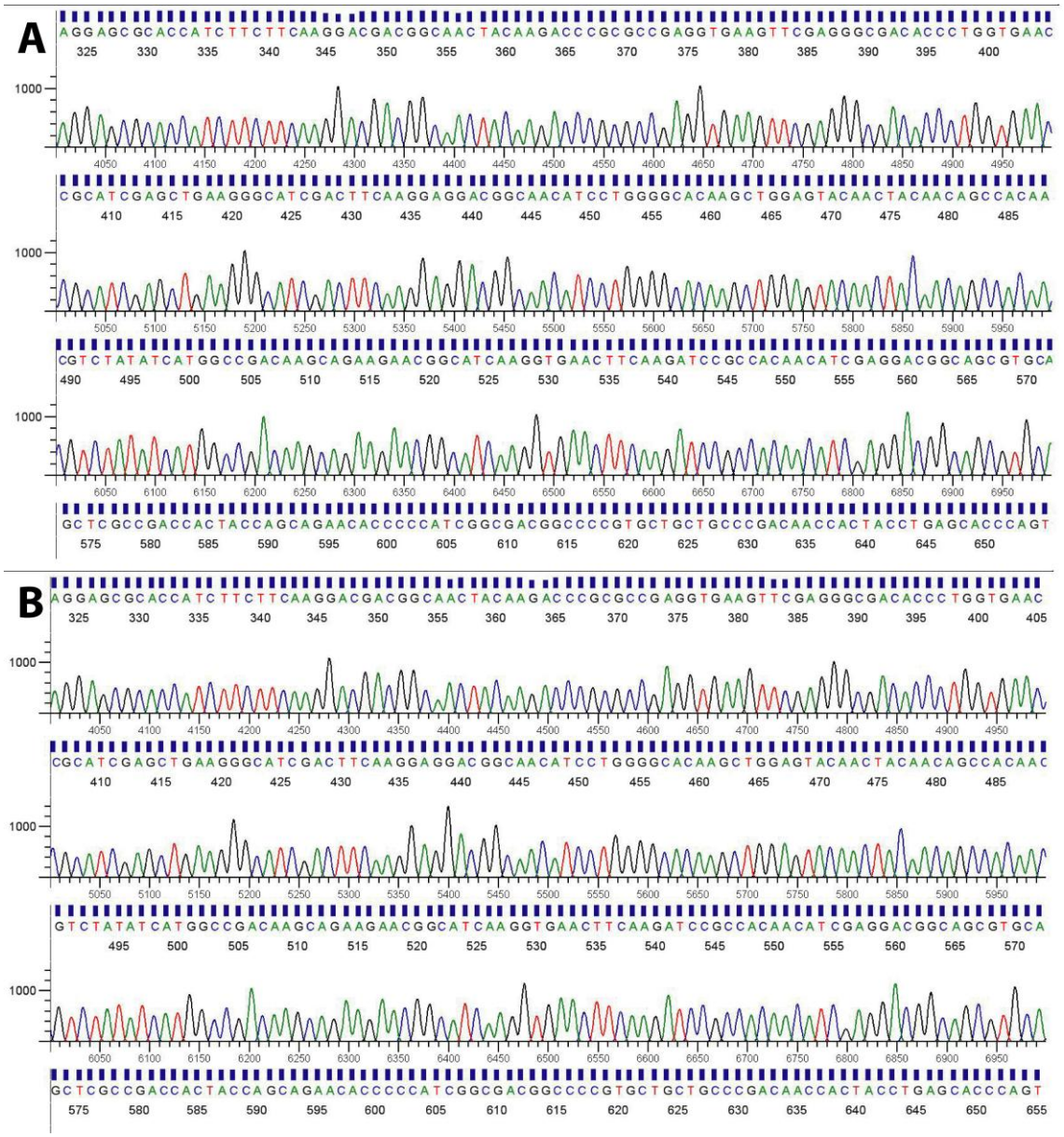

Figure 10. The confidence read of base calling (blue bar above each base) in the sequencing reaction is depicted. The figure (**A**) EU and (**B**) ODU is generated from the raw sequencing data using the software ABI Sequence Scanner V2.0:

(https://products.appliedbiosystems.com/ab/en/US/adirect/ab?cmd=catNavigate2&catID=600583&tab=DetailInfo).

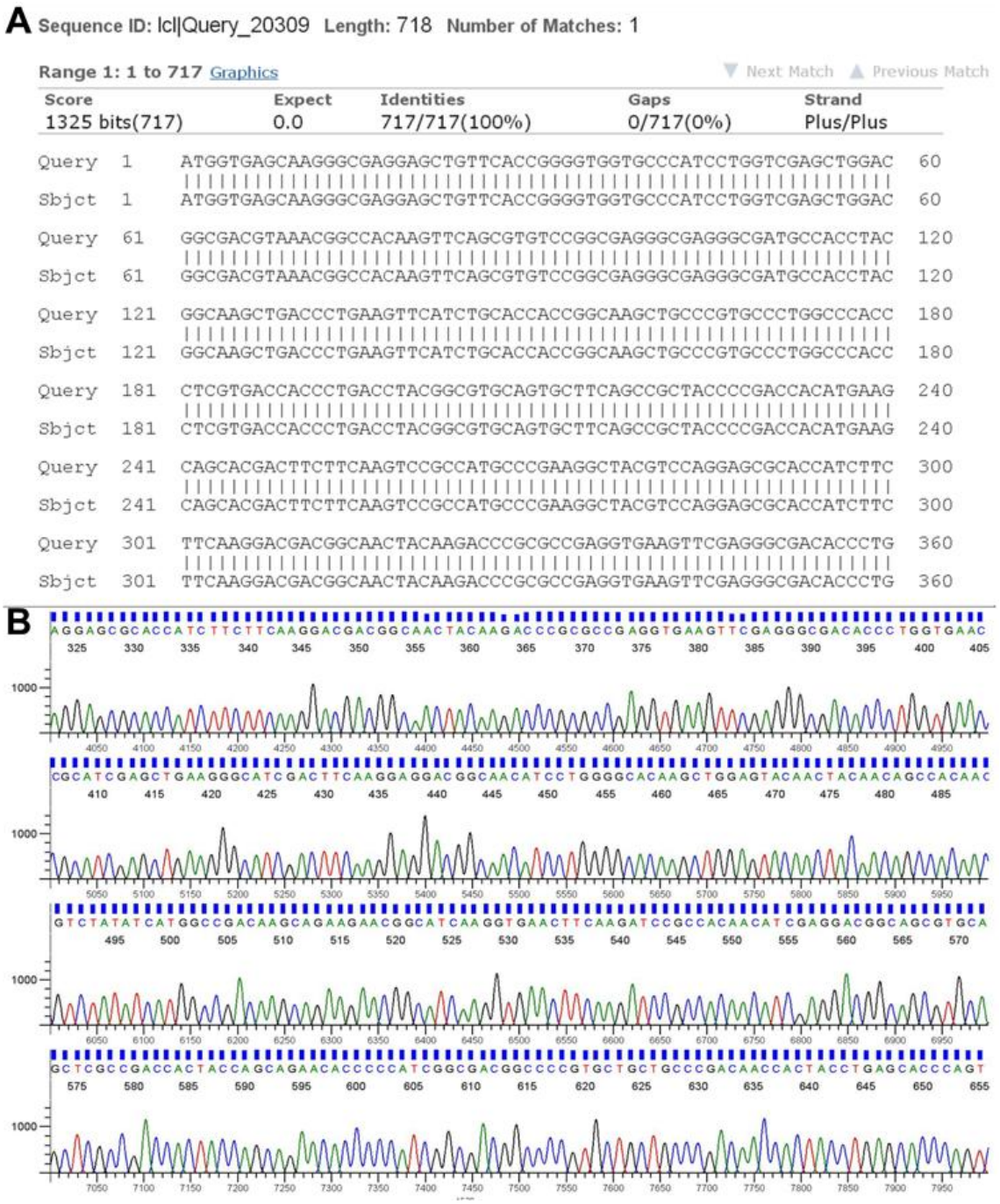

Figure 11. (**A**) Representative sequence alignment (bl2seq) of PCR amplified DNA products obtained from cDNA, which was in turn synthesized by reverse transcribing AMU-containing RNA transcript. The sequencing data showed 100% sequence identity with the template DNA used for the *in vitro* transcription reactions. (**B**) The confidence of base calling (blue bar above each base) in the sequencing reaction is also depicted. The figure is generated from the raw sequencing data using the software ABI Sequence Scanner V2.0:

(https://products.appliedbiosystems.com/ab/en/US/adirect/ab?cmd=catNavigate2&catID=600583&tab=DetailInfo).

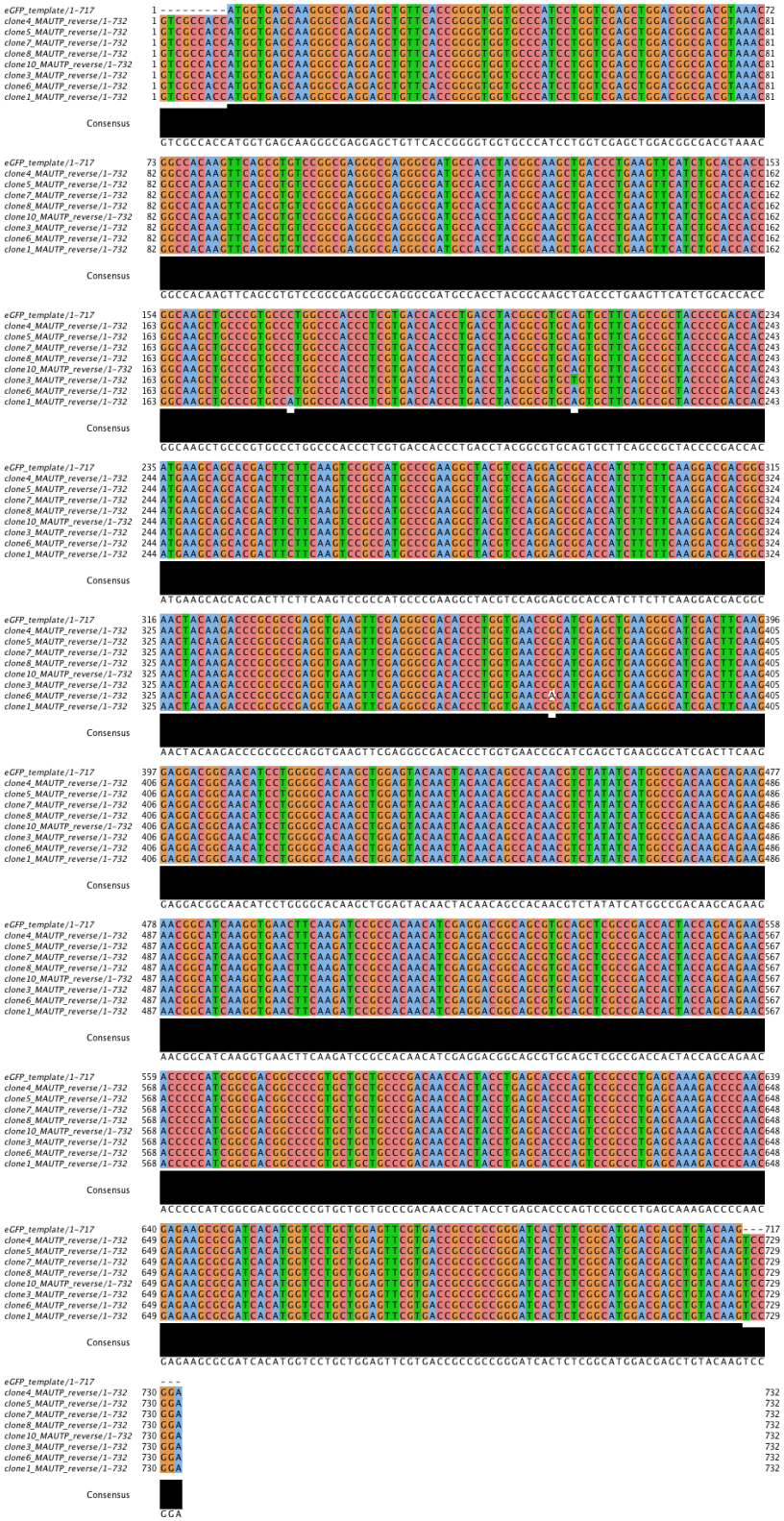

Figure 12. The sequencing reads for each individual clone were aligned to the template eGFP sequence shows that out of the 8 clones, there is 100% identity in 5 clones and in the remaining three only 1 base is different at 3 different non–thymidine locations. It is very important to note that none of the misincorporated bases are thymines, implying that none of the modified uridines in the original RNA sequence were misread as any other base. Thus, AMU does not lead to misreading of uridine in the RNA sequence as any other base.

4.3 Conclusion

In summary, alkyne-modified UTP analogs EUTP and ODUTP which contains active labels for click chemistry and Raman spectroscopic analysis served as a good substrate for T7 RNA polymerase to produce high density modified RNA of varying lengths. Further, EU and ODU labeled RNA transcripts showed high fidelity in transcription and reverse transcription as they are effectively recognized and copied by reverse transcriptase to produce corresponding cDNA. Similar to alkyne we have demonstrated the suitability of azide-modified RNA in selection cycle where fidelity of transcription, reverse transcription is also preserved. Very recently, a clickable alkyne nucleoside has been aptly utilized in expanding the chemical space of nucleic acid libraries in generating nucleobase-modified DNA aptamers with excellent recognition properties. Our results and recent literature reports highlight usefulness of clickable nucleotide analogs in enhancing the functional range of RNA in selection of robust aptamers for various applications.

4.4 Experimental Section

4.4.1 Materials

Platinum® *Pfx* DNA polymerase, Calf intestinal alkaline phosphatase (CIAP), pDisplay vector, SYBR®Safe were acquired from Invitrogen. Restriction endonuclease XhoI was obtained from New England Lab (NEB). RNA polymerase, ribonuclease inhibitor (RiboLock), NTPs, dNTPs RNase A and RNase T1 were obtained from Fermentas Life Science. LiCl, low melting agarose, snake venom phosphodiesterase I were obtained from Sigma–Aldrich. DNA oligonucleotides primers were purchased from Integrated DNA Technologies, Inc. Chemicals for preparing all buffer solutions were purchased from Sigma–Aldrich (BioUltra grade). Autoclaved RNase free water was used in all biochemical reactions and HPLC analysis.

4.4.2 Instrumentation

HPLC analyses were performed using Agilent Technologies 1260 Infinity and Dionex ICS 3000.

4.4.3 *In vitro* transcription with linearized plasmid DNA templates in the presence of EUTP, ODUTP

Linearized plasmid DNA templates were obtained by single restriction digestion of DNA plasmids (pDisplay, ZiFiinpDisplay, eGFPinpDisplay) as follows: 100 µL of digestion reactions were carried out in the presence of 1x CutSmart® Buffer (10 µL, 50 mM potassium acetate, 20 mM Tris–acetate, 10 mM magnesium acetate, 100 µg/mL BSA, pH 7.9) containing 10 µg of plasmid DNA. To each reaction solution 5 µL of restriction enzyme XhoI (10 units/µL) was added and was incubated at 37 °C for 3 h. Linearized plasmid DNA product from respective reaction was then purified using GenElute™ PCR Clean–Up Kit (Sigma Aldrich, Catalog No.NA1020) by following the manufacturer's instructions. Linearized plasmid DNAs pDisplay, ZiFiinpDisplay and eGFPinpDisplay serve as templates for the synthesis of 400 bp, 600 bp and 1.1 kb RNA transcripts, respectively.

The transcription reactions were carried out in 40 mM Tris–HCl buffer (pH 7.9) containing 500 ng of the linearized plasmid DNA template, 1 mM GTP, CTP, ATP, UTP/EUTP/ODUTP, 10 mM $MgCl_2$, 10 mM NaCl, 10 mM of dithiothreitol (DTT), 2 mM spermidine, 1 U/µL RNase inhibitor (Riboblock) and 40 units T7 RNA polymerase in a total volume of 25 µL. Samples were incubated at 37 °C for 3 h. LiCl (7.5 M, 12.5 µL) was added and the reaction solutions were kept at –20 °C for 1 h followed by centrifugation (12000 rpm) at 4 °C for 15 min. The RNA pellet formed from each reaction was washed with 70% aqueous ethanol, dried and dissolved in 20 µL of nuclease free water. Control and modified transcripts obtained after transcription reactions were resolved and detected by 1% agarose gel containing SYBR® Safe (Invitrogen, catalog no. S33102). Further, the presence of EU and ODU labels in RNA transcript was confirmed by enzymatic digestion followed by HPLC analysis of ribonucleoside products obtained from the digestion reaction.

4.4.4 Reverse transcription of alkyne and azide–modified RNA transcript

Standard PCR conditions with Platinum *Pfx* polymerase (Invitrogen) were used to amplify the eGFP gene from pEGFPC1 vector (Clontech) (forward primer: 5' GGACCGA AATTAATACGACTCACTATAGGGGTCTATATAAGCAGAGCTGGTTTG 3' and reverse primer: 5' CAGGTTCAGGGGGAGGTGTG 3',). PCR amplified DNA product purified by phenol–chloroform extraction was used as the template for transcription reactions in the presence of UTP and modified UTP (EUTP, ODUTP, and AMUTP) as described above. Trace amounts of DNA template present in the transcription products were removed

by DNase treatment. The DNase reaction was carried out in Q1 reaction buffer (40 mM Tris–HCl, 100 mM $MgSO_4$, 10 mM $CaCl_2$, pH 8.0) containing 500 ng of unmodified (control) or ODU–modified RNA transcripts, and 1 unit Q1 RNase free DNase (Promega) in a total volume of 10 µL. The reaction mixture was incubated at 37 °C for 3 h. The reaction was stopped by adding 1 µL stop solution (20 mM EGTA pH 8.0) and followed by incubation at 65 °C for 10 min. An aliquot of this reaction was used as a negative control (−RT control) for the PCR after cDNA preparation.

The reverse transcription reaction was carried out in the reaction buffer (Promega, ImProm–II™ 5X reaction buffer, M289A) containing 4 µL of DNase treated unmodified or modified RNA transcript, 0.5 µM reverse primer (5' GCGCGCAGATCTCTTGTA CAGCTCGTCCATGCC 3'), 1 mM $MgCl_2$, 1 mM dNTPs, reverse transcriptase (Promega, ImProm–II™ reverse transcriptase, M314A) in a total volume of 10 µL. (reaction conditions: 25 °C for 5 min, 42 °C for 60 min, 70 °C for 15 min).

4.4.5 PCR amplification of cDNA and sequencing

The PCR reaction was set up in PCR amplification buffer (Invitrogen, *Pfx* amplification buffer, Part # 52806) containing 2 µL of cDNA, 0.25 µM forward primer (5' GCGCGCGTCGACATGGTGAGCAAGGGCGAGGAG 3') and reverse primer (5' GCGCGCAGATCTCTTGTACAGCTCGTCCATGCC 3'), 0.5 mM dNTPs, 1 mM $MgSO_4$, 0.25 units Platinum® *Pfx* DNA polymerase (50 mM Tris–HCl, 50 mM KCl, 1 mM DTT, 0.1 mM EDTA, pH 8.0) in a total volume of 100 µL. [PCR conditions: denaturation at 94 °C for 5 min, 35 cycles (denature: 94 °C for 0.5 min, anneal: 60 °C for 0.5 min, extend: 72 °C for 1 min), final extension at 72 °C for 10 min]. PCR product was purified by phenol–chloroform extraction method. PCR product was sequenced by dideoxy sequencing method (1^{st} Base, Asia) using PCR amplified DNA (40 ng/µL, 10 µL) and reverse primer (10 pmol/µL, 10µL).

4.4.6 Cloning and sequencing

After the PCR reaction A–tailing was performed at 37 °C for 10 min by adding 1 µL of Taq DNA polymerase to the reaction. PCR product was then purified by phenol–chloroform extraction method and was cloned using a pGEM–T Easy Vector System as per the manufacturer‘s instructions (Promega). The resulting plasmid DNA was isolated individually from eight positive colonies and sequenced by automated dideoxy sequencing method using forward and reverse primers.

4.5 References

1. Ellington, A. D. and Szostak, J. W. *In vitro* selection of RNA molecules that bind specific ligands. *Nature*, **346**, 818–822 (1990).
2. Tuerk, C. and Gold, L. Systematic evolution of ligands by exponential enrichment: RNA ligands to bacteriophage T4 DNA polymerase. *Science*, **249**, 505–510 (1990).
3. Robertson, D. L. and Joyce, G. F. Selection *in vitro* of an RNA enzyme that specifically cleaves single–stranded DNA. *Nature*, **344**, 467–468 (1990).
4. Kruger, K., Grabowski, P. J., Zaug, A. J., Sands, J., Gottschling, D. E. and Cech, T. R. Self–splicing RNA: Autoexcision and autocyclization of the ribosomal RNA intervening sequence of tetrahymena. *Cell*, **31**, 147–157 (1982).
5. Que–Gewirth, N. S. and Sullenger, B. A. Gene therapy progress and prospects: RNA aptamers. *Gene Ther.*, **14**, 283–291 (2007).
6. Osborne, S. E. and Ellington, A. D. Nucleic acid selection and the challenge of combinatorial chemistry. *Chem. Rev.*, **97**, 349–370 (1997).
7. Hermann, T. and Patel, D. J. Adaptive recognition by nucleic acid aptamers. *Science*, **287**, 820–825 (2000).
8. Breaker, R. R. *In vitro* selection of catalytic polynucleotides. *Chem. Rev.*, **97**, 371–390 (1997).
9. Stuhlmann, F. and Jäschke, A. Characterization of an RNA active site: interactions between a Diels–Alderase ribozyme and its substrates and products. *J. Am. Chem. Soc.*, **124**, 3238–3244 (2002).
10. Herschlag, D., Piccirilli, J. A. and Cech, T. R. Ribozyme–catalyzed and nonenzymic reactions of phosphate diesters: rate effects upon substitution of sulphur for a nonbridging phosphoryl oxygen atom. *Biochemistry*, **30**, 4844–4854 (1991).
11. Nissen, P., Hansen, J., Ban, N., Moore, P. and Steitz, T. The structural basis of ribosome activity in peptide bond synthesis. *Science*, **289**, 920–930 (2000).
12. Thompson, J. *et al.* Analysis of mutations at residues A2451 and G2447 of 23S rRNA in the peptidyl transferase active site of the 50S ribosomal subunit. *Proc. Natl. Acad. Sci. USA*, **98**, 9002–9007 (2001).
13. Lee, N., Bessho, Y., Wei, K., Szostak, J. W. and Suga, H. Ribozyme–catalyzed tRNA aminoacylation. *Nat. Struct. Mol. Biol.*, 7, 28–33 (2000).
14. Chun, S., Jeong, S., Kim, J., Chong, B., Park, Y., Park, H. and Yu, J. Cholesterol esterase activity by *in vitro* selection of RNA against a phosphate transition–state analogue. *J. Am. Chem. Soc.*, **121**, 10844–10845(1999).
15. Osborne, S. E., Matsumura, I. and Ellington, A. D. Aptamers as therapeutic and diagnostic reagents: problems and prospects. *Curr. Opin. Chem. Biol*., **1**, 5–9 (1997).
16. Jayasene, S. D. Aptamers: an emerging class of molecules that rival antibodies in diagnostics. *Clin. Chem*., **45**, 1628–1650 (1999).
17. Jhaveri, S., Rajendran, M. and Ellington, A. D. *In vitro* selection of signaling aptamers. *Nat. Biotechnol.*, **18**, 1293–1297 (2000).
18. Thiel, K.W. and Giangrande, P. H. Therapeutic applications of DNA and RNA aptamers. *Oligonucleotides*, **19**, 209–222 (2009).
19. Kang, K. N. and Lee, Y. S. RNA aptamers: a review of recent trends and applications. *Adv. Biochem. Eng. Biotechnol*., **13**, 153–69 (2013).
20. Germer, K., Leonard, M. and Zhang, X. RNA aptamers and their therapeutic and diagnostic applications. *Int. J. Biochem. Mol. Biol.*, **4**, 27–40 (2013).
21. Keefe, A. D. and Cload, S. T. SELEX with modified nucleotides. *Curr. Opin. Chem. Biol*., **12**, 448–456 (2008).

22. Hollenstein, M. Expanding the catalytic repertoire of DNAzymes by modified nucleosides. *Chimia*, **65**, 770–775 (2011).
23. Obeid, S., Baccaro, A., Welte, W., Diedrichs, K. and Marx, A. Structural basis for the synthesis of nucleobase modified DNA by *Thermus aquaticus* DNA polymerase. *Proc. Natl. Acad. Sci. USA*, **107**, 21327–21331 (2010).
24. Bergen, K., Steck, A. -L., Strütt, S., Baccaro, A., Welte, W., Diedrichs, K. and Marx, A. Structures of *Klen Taq* DNA polymerase caught while incorporating C5–modified pyrimidine and C–7 modified 7–deazapurine nucleoside triphosphates. *J. Am. Chem. Soc*., **134**, 11840–11843 (2012).
25. Joyce, G. F. Forty years of i*n vitro* evolution. *Angew. Chem. Int. Ed*., **46**, 6420–6436 (2007).
26. Mayer, G. The chemical biology of aptamers. *Angew. Chem. Int. Ed*., **48**, 2672–2689 (2009).
27. Santoro, S. W., Joyce, G. F., Sakthivel, K., Gramatikova, S. and Barbas, C. F. RNA cleavage by a DNA enzyme with extended chemical functionality. *J. Am. Chem. Soc*., **122**, 2433–2439 (2000).
28. Perrin, D. M., Garestier, T. and Hélène, C. Bridging the gap between proteins and nucleic acids: A metal–independent RNAseA mimic with two protein–like functionalities. *J. Am. Chem. Soc*., **123**, 1556–1563(2001).
29. Wiegand, T. W., Janssen, R. C. and Eaton, B. E. Selection of RNA amide synthase. *Chem. Biol*., **4**, 675–683 (1997).
30. Tarasow, T. M., Tarasow, S. L. and Eaton, B. E. RNA–catalysed carbon–carbon bond formation. *Nature*, **389**, 54–57 (1997).
31. Battersby, T. R. Quantitative analysis of receptors for adenosine nucleotides obtained via i*n vitro* selection from a library incorporating a cationic nucleotide analog. *J. Am. Chem. Soc*., **121**, 9781–9789 (1999).
32. Shoji, A., Kuwahara, M., Ozaki, H., Sawai, H. Modified DNA aptamer that binds the (R)–isomer of a thalidomide derivative with high enantioselectivity. *J. Am. Chem. Soc*., **129**, 1456–1464 (2007).
33. Latham, J. A., Johnson, R. and Toole, J. J. The application of a modified nucleotide in aptamer selection: Novel thrombin aptamers containing (1–pentynyl)–2'–deoxyuridine. *Nucl. Acids Res*., **22**, 2817–2822 (1994).
34. Kimoto, M., Yamashige, R., Matsunaga, K., Yokoyama, S. and Hirao, I. Generation of high–affinity DNA aptamers using an expanded genetic alphabet. *Nat. Biotechnol*., **31**, 453–457 (2013).
35. Tolle, F., Brändle, G. M., Matzner, D. and Mayer, G. A versatile approach towards nucleobase–modified aptamers. *Angew Chem. Int. Ed. Engl*., **54**, 10971–10974 (2015).